The Pre-Clinical Evaluation of a Synthetic Fibrin-Alginate Dermal Scaffold – the Smart Matrix™

Raina Zarb Adami
Student number: 05035710

University of Malta

Submitted in partial fulfilment of the requirements for a Doctorate in Philosophy

For my father, the true boffin who lured me into the wonderful world of academia on the promise that I would love it. I missed the chance to tell him he was right.

L-Università ta' Malta

FACULTY/INSTITUTE/CENTRE/SCHOOL SURGERY

DECLARATIONS BY POSTGRADUATE STUDENTS

Student's I.D. /Code 05035710

Student's Name & Surname RAINA ZARB ADAMI

Course DOCTORATE IN PHILOSOPHY

Title of Dissertation
THE PRE-CLINICAL EVALUATION OF A SYNTHETIC FIBRIN-ALGINATE DERMAL SCAFFOLD - THE SMART MATRIX™

(a) Authenticity of Dissertation

I hereby declare that I am the legitimate author of this Dissertation and that it is my original work.

No portion of this work has been submitted in support of an application for another degree or qualification of this or any other university or institution of higher education.

I hold the University of Malta harmless against any third party claims with regard to copyright violation, breach of confidentiality, defamation and any other third party right infringement.

(b) Research Code of Practice and Ethics Review Procedures

I declare that I have abided by the University's Research Ethics Review Procedures.

As a Master's student, as per Regulation 58 of the General Regulations for University Postgraduate Awards, I accept that should my dissertation be awarded a Grade A, it will be made publicly available on the University of Malta Institutional Repository.

Signature of Student

RAINA ZARB ADAMI
Name of Student (in Caps)

16TH JULY 2019
Date

Abstract

Cutaneous wound management remains challenging. A synthetic fibrin/alginate dermal scaffold, Smart Matrix (SM), demonstrated rapid short term vascularisation and skin graft (STSG) integration. Long term healing using SM+STSG was examined in the porcine model. SM+STSG was compared to STSG alone and secondary intention healing in simple wounds, before being compared to commercially available scaffolds - Matriderm and Integra. The value of such adjuncts lies in their ability to heal attenuated wounds. The medical literature revealed few appropriate wound models. The partial excision of a full thickness burn was described and compared with the full thickness excision wound. This model was then used to evaluate SM+STSG and compare it with STSG alone and MD+STSG. SM wounds contracted less than other wound groups with lower levels of contractile markers. Graft take was similar in all simple wounds but increased in attenuated wounds treated with SM and MD. SM wounds showed increased earlier angiogenesis, similar to normal skin in the long term, with lower inflammation than STSG alone and I+STSG wounds. Scaffold persistence was shortest for SM+STSG and prolonged in all groups in the attenuated model. There were no long term differences between SM and MD in acute and attenuated wounds apart from contraction. The attenuated wound healing model displayed delayed epithelialisation and angiogenesis with prolonged oedema and inflammation. Fibrin attenuates α-SMA formation, decreasing myofibroblast differentiation and therefore reducing wound contraction. SM supports long term healing, with reduced wound contraction and inflammation in simple and attenuated wounds.

Keywords: fibrin, dermal scaffold, wound contraction, α-smooth muscle actin, wound healing, attenuated wound healing model, wound model

Acknowledgements

I would like to express my gratitude to Dr Julian F Dye and Prof Godfrey LaFerla, my research supervisors, for their patient guidance, enthusiastic encouragement and useful critiques of this research work. I would also like to thank RAFT and the Kirby Laing Foundation for funding my research and providing the facilities. My grateful thanks are also extended to my predecessors, Miss Sophie Dann, Mr Chris Baldwin and Mr Matthew Potter. Their efforts and contributions towards this project afforded me the substrate on which to embark on my research. I would also like to extend my thanks to the scientists at RAFT laboratory for their assistance with technical issues, namely Dr Khwaja Islam, Mrs Nimesha Patel and Mrs Nirosheeha Ragunathan. In particular, I would like to thank Dr Vaibhav Sharma and Mr Amir Taheri for their help with the photography, Moor FPLI and Eykona 3D imaging and interpretation, Dr Keith Blackwood and Dr Philippa Franke for their help with immunohistostaining techniques. I am grateful to Dr Sorousheh Samizadeh for her significant contribution in the evaluation and scoring of the many histology slides. I am grateful to Mr Jeremy Rodrigues for his assistance with the statistical analysis of the data.

Finally, I wish to thank my parents, my brother and my husband Jeremy for their wonderful support and encouragement throughout my study. Finally thanks go to my beautiful little daughter Safira for making it all worth it.

Table of Contents

List of Figures

List of Tables

List of Abbreviations

α-SMA	alpha smooth muscle actin
B	Burn
CaK	cultured isolated keratinocytes
Coll III	collagen type three
DHEA	dehydroepiandrosterone
DHT5	α-dihydrotestosterone
EC	endothelial cells
ECM	Extra-cellular Matrix
EDA-FN	alternatively spliced domain A fibronectin
EU	European Union
FDA	Food and Drugs Authority
FGF	fibroblast growth factor
GA	general anaesthetic
HBOT	hyperbaric oxygen therapy
I	Integra™
IL	interleukin
INF	interferon
JFD	Julian Francis Dye
MD	Matriderm™
MHC	Major Histo-compatibility Complex
MHRA	Medical Health Regulatory Authority
MMP	Matrix Metallo-Proteinase
NAWCO	Named Animal Worker Welfare Officer
NB	Non-burn
NPIMR	Northwick Park Institute for Medical Research

NVS	Named Veterinary Surgeon
PDGF	platelet derived growth factor
RAFT	Restoration of Appearance and Function Trust
RCN	Royal College of Nurses
RZA	Raina Zarb Adami
TGF	transforming growth factor
SOP	Surgical and Operating Protocol
SM	Smart Matrix™
SML	Smart Matrix™ Limited
STSG	Split thickness skin graft
UK	United Kingdom
US	United States
UV	Ultraviolet
VEGF	vascular endothelial growth factor
vWF	von Willebrand factor

Chapter 1: Background and Introduction

The management of cutaneous wounds remains a pressing challenge across many clinical scenarios. The primary and ultimate goal is to heal these wounds as quickly as possible (Simman *et al*., 2011). Effective treatment requires the patient to engage with a prolonged and disciplined treatment pathway (Sen *et al*., 2009). The integrity of the human integument is key to its protective properties and to its role in homeostasis. While in normal circumstances a breach in the skin is rapidly repaired, often, due to a variety of factors the skin is rendered unable to heal itself in a timely or appropriate manner.

Any therapeutic advance to significantly accelerate tissue reconstruction, and to improve preventative measures and diagnostic techniques, has the potential to achieve significant benefit (Posnett, Franks 2008). The gold standard treatment for full thickness (comprising the loss of the epidermis and dermis) acute cutaneous wounds that cannot be closed directly remains autologous split thickness skin grafting (Simman *et al*., 2012). Various attempts to expedite this healing trajectory or improve the outcome have been made historically, through the advent of various wound healing adjuncts and dressings. The use of artificial or xenograft replacements of various skin components marked a pivotal change in the wound healing armamentarium (Halim *et al*., 2010). The issues encountered in the treatment of large area full thickness wounds are a paucity of availability of donor site skin, a vulnerability to infection secondary to the compromise of the barrier properties of skin – allowing colonising bacteria to invade and become pathogenic, and the risk of hypertrophic, keloid or contracting scars (Otene *et al*., 2011). The last three decades have seen the introduction of dermal replacement matrices as a novel method to aid wound closure in challenging wounds such as large area acute burns and also in the treatment of indolent wounds refractory to conventional

methods of treatment. Dermal replacement scaffolds are still at the heart of much ongoing research, and many new scaffolds with different matrix compositions are currently undergoing experimental *in vitro* and *in vivo* trials.

These scaffolds often required to be placed in a hostile environment, not conducive to wound healing, hence the presence of the challenging wound in the first place. These wounds are intrinsically compromised (attenuated blood supply and oxygenation), vulnerable to infection and biofilm formation, subject to chronic inflammation and oxidant stress and in a proteolytic environment. A successful tissue scaffold should exhibit appropriate physical and mechanical characteristics and provide an appropriate surface chemistry and nano- and microstructures to facilitate cellular attachment, proliferation, and differentiation. Most such scaffolds are of bovine or porcine origin. While very well tolerated by the body, some risks such as those pertaining to immunogenicity and prion or micro-organism transfer, persist, together with some adversity from some religious groups. Surgical experience defines an unmet need: an intrinsically reliable, robust synthetic dermal replacement.

The literature review shows that pre-clinical (animal) studies pertaining to wound healing most commonly involve the use of acute full-thickness wounds. There is a paucity of attenuated wound healing models that can be employed to evaluate the performance of these scaffolds where their use is most indicated.

Smart Matrix™ (SM) was developed by scientists at The Restoration of Appearance and Function Trust (RAFT), in a bid to create a scaffold that would address the shortfalls highlighted, namely a pro-angiogenic, robust scaffold that supports and expedites wound healing with an overlying split thickness skin graft as a single step procedure. Ideally, the resulting scar quality will be an improvement on wounds treated by split thickness grafting alone or with a scaffold ie. less contracture and a decreased incidence of hypertrophic or keloid scarring, with as close a match as possible to native uninjured skin.

1.1 Clinical exigencies

Reported UK data from 2012-3 showed that wound care costs amounted to between £4.5 and 5.1 billion (adjusted for cost of co-morbidities), for an estimated 2.2 million patients (Guest *et al*., 2015). Reported UK data from 2003 showed 200,000 patients were suffering from a chronic wound at any one time, with 20,000 of these being hospital in-patients (Franks, Morgan, 2003). The cost to the National Health Service (NHS) of caring for patients with a chronic wound is estimated at-around 3% of the total estimated out-turn expenditure on health, £89.4 billion (Posnett, Franks, 2008). Sixty-one per cent of all wounds heal within a year. The cost of these wounds ranges between £698 and £3998 per patient, while that of unhealed wounds ranges between £1719 and £5976 (135% that of a healed wound) (Guest *et al*., 2017). With accurate diagnosis, identification of preventative, causative and exacerbating factors and prompt appropriate definitive treatment, much of this burden should be avoidable. Indirect costs through loss of income, psychological morbidity, de-conditioning, social isolation and the negative impact on friends and family (Chin *et al*., 2013).

A chronic wound is defined as one which has not healed spontaneously within 3 months (Harding *et al*., 2002). The commonest causes of chronic wounds are venous leg ulcers, followed by pressure sores. One in 5 long-term hospital in-patients (Clark *et al*., 2004) develop pressure sores and around 400,000 individuals develop a new pressure ulcer annually (UK data). Trends in the structure of the UK population over the next 20 years are likely to lead to a significant increase in the number of patients with chronic wounds and the corresponding rise in associated costs of care (Dowsett *et al*., 2014). This is due to increased longevity and an expected rise in the incidence of type II diabetes. The population of the UK is forecast to increase between 2005 and 2025 by 3.4 million (5.6%) from 60.4 million to 63.8 million. In the same period, the UK population aged 65 and older is forecast to increase by 3.5 million (36%) from 9.5 million to 13.0 million. The annual

cost of wound care in the UK was projected to increase to £2377 million in 2019 (Dowsett *et al*., 2014).

Challenging wounds include full or partial thickness skin breaches that defy cure or do not respond favourably to conventional methods of treatment (Hall *et al*., 2014), and somehow deviate from the natural physiologic course (Han *et al*., 2017), thus often requiring additional procedures and interventions to achieve definitive wound closure. This refers to a wound that has somehow deviated from the previously described natural physiologic course of events and has stalled at some point- Examples include large burns, full thickness wounds, wounds of differing depths and wounds located in functionally or cosmetically sensitive areas such as the face, hands, perineum or over joints. Confounding factors such as diabetes, extremes of age, illicit drug use, lack of appropriate nutrition and fluid intake, apathy towards self care, poor hygiene and other co-morbidities are all possible exacerbating factors in rendering an acute clean wound challenging and possibly chronic. One or more of the following conditions must be present for a wound to be categorised as a "complex" type: extensive loss of the integument, acute or chronic infection, compromised viability of superficial tissues—clear necrosis, localised or more extensive circulation compromise and associated systemic pathology impairing normal cutaneous wound healing. Most chronic wounds exhibit a degree of complexity (Ferreira *et al*., 2006).

1.2 The Smart Matrix™

Smart Matrix™ is a synthetic dermal scaffold whose chief components are fibrin and alginate. Due to patent restrictions, its composition will not be mentioned in detail in this thesis. Furthermore, there are no studies available in the published literature due to this same restriction. As a brief overview, the 3-dimensional scaffold consists of fibrinogen mixed with a bulking agent to create a

porous structure with added calcium chloride as a thrombin cofactor. Sodium alginate was found to be suitable as a calcium-sensitive bulking agent, following the exclusion of a variety of other candidate bulking agents (all research was carried out by RAFT prior to the start of the studies mentioned in this thesis). The primary components, fibrinogen, calcium chloride, thrombin and alginate are mixed at high speed to create a foam, which is then cast and allowed to coagulate. Particular sufactants added to the primary mixture allow control of the formed foam structure.

Exploratory work in RAFT's laboratories investigated the pro-angiogenic potential of various biomaterials through *in vitro* assays of angiogenesis. Initial work generated evidence to suggest that different extracellular matrix proteins control fibroblast behaviour (Dye et *al.*, 2004). Studies of cultured human placental microvascular endothelial cells suggested that specific biomaterial matrices influenced the morphological pattern behaviour, while angiogenic growth factors determined the extent of the behaviour. These observations formed the basis of the rationale to concentrate efforts to find an extracellular matrix material with optimal pro-angiogenic properties, in a controllable porous and stabilised biomaterial and manufacture process. As a result, fibrin was identified as the best available material (Potter et *al.*, 2006).

Prior to the studies described in this thesis, *in vitro* evaluation studies, to assess cytotoxicity were carried out. The biocompatibility of cross-linking processed scaffolds was investigated using *in vitro* toxicological and biocompatibility assays. Adult primary human dermal fibroblasts were used as a relevant cell type to test acute cytotoxicity and subsequent proliferative capacity. No toxicity was detected. Non-cross-linked trial fibrin / alginate prototype scaffold formulations gave poor cell-adhesion and cell spreading *in vitro* with microvascular endothelial cells. Chemical stabilisation (used to control stability and resistance to proteolytic degradation) was achieved using chemical (carboxylic acid/primary amine cross-linking chemistry was achieved using 1-Ethy-3(3-dimethyl-propylamino) carbodiimide / N-hydroxysuccinimide (EDC / NHS) cross-linking. This conferred long-term stability of the fully hydrated material.

The optimal structure for efficiency of cellular ingress and integration requires consistency of porosity and homogeneity through the material (Khademhosseini *et al.,* 2007). This was achieved by iterative modifications of the formulation and manufacture conditions of series of prototypes. Trialling and histological evaluation of the integration of each prototype was conducted in a porcine splinted wound excision healing model (Dann 2009, not published). The material is formed from individual 100 nm diameter fibrin filaments, meshed together to form lamellar sheets 1-2 filaments thick, with a variable mesh density, coated with the alginate component.

Proteolytic digestion and scaffold stability were investigated using an extended trypsin digestion assay. Fibrin is an intrinsically labile protein due to the action of plasmin (Gaffney *et al.,* 1980). It was found that the proteolytic degradation rate of fibrin-alginate scaffolds is determined by the extent of cross-linking. In the absence of cross-linking, substantial breakdown occurs within one hour. Stabilisation to trypsin hydrolysis was achieved by cross-linking. Further *in vitro* studies measuring cell ingress into scaffolds were performed by filling and pre-equilibrating the pore capacity of the scaffold with culture medium, before seeding cells above the scaffold. This created a situation in which cells could only ingress actively. A rapid penetration of microvascular endothelial cells through the depth of scaffolds up to 1 mm thick was demonstrated in a 48 hour assay. Comparatively, other biomaterials were penetrated only partially or not at all, over the same time period (Potter *et al*., 2006).

Long-term fibroblast regulation was measured by the thesis author prior to the *in vivo* experimentation described in this thesis, as the appearance of myofibroblasts in a neodermal wound histology would be an indicator of scar fibrosis response, characterised by a contractile phenotype and α smooth muscle actin expression (Hinz *et al.,* 2001). Long-term scaffold environment influence on fibroblast behaviour was investigated using human dermal fibroblast seeded and cultured within scaffolds in a 3 week assay . No detectable contraction occurred in any of the Smart Matrix™ scaffolds, although cells suspended at the same density in 3D collagen gels as a control caused rapid

contraction. The viability of cells demonstrated by MTS was maintained over three weeks, although little proliferation occurred. The expression of α-SM actin in fibrin scaffolds was lower than in collagen scaffolds or the contractile collagen matrices (Zarb Adami, 2011 -- prevented from publishing by RAFT due to patent filing).

Further to this work, a multi-parameter morphological and functional study comparing HDF cultured in fibrin/alginate, non-cross-linked collagen/elastin or collagen/chondroitin sulphate showed some significant differences in cell morphology and secretory function. The relative expression of IL8 was greatest within the fibrin environment, and the TGF-β1 is greatest in the collagen/chondroitin sulphate environment. (Garcia-Gareta *et al.,* 2013). This study suggested that fibroblasts are not induced to the myofibroblast phenotype by interaction with the fibrin matrices.

Initial *in vivo* evaluation work of the Smart Matrix™ dermal scaffold by Dann *et al.*, in 2009 employed a splinted full-thickness cutaneous porcine wound model. This work demonstrated that Smart Matrix™ accelerates overlying split thickness skin graft integration and contributes to a more rapid vascularisation of the wound bed in the porcine acute wound-healing model (when compared to collagen gels). (Dann 2009 - not published, archives of RAFT). These initial studies examined the *in vivo* integration and neovascularisation of the split thickness skin graft using Smart Matrix™ as a dermal template as a single step procedure. The method for these experiments involved the use of a circular silicon strut that held the wound edges of a 4cm diameter circular full thickness cutaneous wound apart throughout the experiment. In this way, studies of the wound bed only involved the dermal scaffold and overlying graft, without including epidermal creep from the wound edges. This restricts healing to granulation from the wound bed without influence from wound contraction and without cellular ingress from the lateral margins or epithelial overgrowth. Hence, change in wound area and possible contraction could not be evaluated. Additionally, previous experiments were carried out over 21 day time periods. During this time the short term wound-heal-

ing trajectory was evaluated. However no information has yet been available on the long term wound healing properties of Smart Matrix™ in the acute cutaneous injury porcine model.

1.3 Overview of cutaneous wound healing

Integumental injury incites a tightly orchestrated sequence of events to repair the skin and seal the wound. Wound healing is a well understood succession of tightly regulated cellular and molecular responses to injury, with rapid inflammatory responses (Steed, 2003, Broughton *et al.*, 2006, Gurtner *et al*., 2008) Wound severity is generally dependent on the surface area, depth and anatomical site, as well as the nature of injury and the systemic well-being of the patient. This healing response involves the differential regulation of multiple genes and protein expression (Nuutila *et al*., 2012,). No single master control gene or molecule has been identified. However, an important role of mitochondrial RNA in regulating healing and repair responses is under investigation (Gu *et al*., 2006, Zhao *et al*., 2015).

1.3.1 Epidermal wound healing

Wounds in which the full thickness of the dermis is not breached, such as a superficial burn, heal through the recruitment of adjacent adnexal keratinocytes with a quicker regenerative time than full thickness skin defects of a similar surface area (Pastar *et al.*, 2014). Epidermal healing, or epithelialisation, is an essential component of wound healing used as a defining parameter of its success and is dependent upon underlying dermal vasoconstriction and epithelial stem cells and many factors involved in the process of keratinocyte differentiation, activated by multiple stimuli (Pastar *et al.*, 2014). These include calcium influx, epidermal growth factor (EGF), tumour necrosis factor

(TNF) and various protein kinase C (PKC) isoforms (Jost *et al*., 2001). The clotting cascade is initiated when plasma fibrinogen is cleaved to form strands of fibrin to be deposited on the wound bed. In turn, fibrin binds fibronectin, which leads to keratinocyte binding, enhancing their proliferation and migration inward from the wound edges. This occurs through cell proliferation and migration from surviving hair follicles and wound margins with evidence that interfollicular epidermal stem cell niches can be re-established (Ito *et al*., 2008). A single epithelial layer is formed with an immature basement membrane zone with laminin, IV collagen and anchoring fibrils to restore the basement membrane. For this process to occur in a timely fashion, an intact dermis is essential.

1.3.2 Dermal wound healing

The healing of partial or full dermal thickness wounds in which the epidermal basement membrane and dermis are lost is dominated by a repair response resulting in replacement of lost dermis by fibrous scar tissue (Nyugen, 2009). Healing of such defects of a critical size occurs by secondary intention, a process of infilling of the defect with granulation tissue which differentiates into fibroblastic scar tissue, together with superficial epidermal regrowth (Singer *et al*., 1999). Dermal wound healing is partly dependent on re-epithelialisation to maintain a moist clean environment. Chemotactic factors released from the deposition and activation of platelets - platelet-derived growth factor (PDGF) and transforming growth factor-beta (TGF-beta) (Singer *et al*., 1999) attract neutrophils (first 3 days) and monocytes, which engulf contaminants and cellular debris through phagocytosis. Activation of the complement cascade (C3a, C5a) results in vasodilatation and inflammation. Nitric acid is integral to the regulation of cellular activity in the inflammatory and proliferative phases.

Cutaneous healing is orchestrated through a precise sequence of events. It is classically characterised by 3 phases, the inflammatory phase, the proliferative phase and the remodelling or maturation phase (Martin, 1997, Singer *et al*., 1999). Some authorities further divide the first phase into haemostasis followed by inflammation (Guo *et al*., 2010). For wound healing to be successful, it is imperative that all phases occur uninterrupted, in the correct sequence and in a timely fashion.

Haemostasis initiates the process through platelet plug formation of the severed blood vessels (Rivera *et al*., 2009). An established provisional matrix serves to re-establish the barrier function and provide the structural support for migrating cells (Nieswandt *et al*., 2009). Simultaneously, vasoconstriction occurs, typically lasting 5-10 minutes, limiting blood loss under the influence of platelet-mediated vasoactive substances (prostaglandins, epinephrine, serotonins and other platelet-derived factors) (Velnar *et al*., 2009, Rendell *et al*., 2002). Platelet-derived factors are also responsible for the stimulation of the next phase. These include serotonins, histamines, and growth factors (Yates *et al*., 2011). This chemotactic cellular ingress is mediated by resident dendritic cells and macrophages, which in turn recruit neutrophils and later lymphocytes, a process lasting approximately 18-24 hours. Through phagocytosis, neutrophils engulf bacteria and remove debris while releasing inflammatory mediators and bactericidal oxygen free radicals (Theilgaard-Monch e*t al*., 2004). Macrophages perform key regulatory functions in wound repair by releasing cytokines and growth factors (Platelet derived growth factor (PDGF), Transforming growth factor-beta (TGF-b), Interleukin-1 (IL1), fibroblast growth factor (FGF)), which promote immigration, proliferation and survival and also signal the cascade to attract endothelial cells and fibroblasts to the wound to promote angiogenesis and dermal regeneration. Macrophages also produce many of the extra-cellular matrix elements and matrix-remodelling metalloproteinases (Lucas *et al*., 2010). Simultaneously, epithelial cells from wound edges and hair follicles undergo phenotypic changes and migrate across the wound surface to re-establish an intact epithelial barrier from the environment over the underlying denuded surface (Yan *et al*., 2010). Keratinocyte migration occurs in a leapfrog fashion, separ-

ating the overlying eschar from new viable tissue (Kubo *et al*., 2001). Acute inflammation normally lasts up to 3 days.

Dermal repair commences 72 hours post insult with deposition of the extracellular matrix. Local (tissue-resident) fibroblast and mesenchymal stem cells are the main contributors to neo-tissue structure (Hinz, 2006, Driskell *et al*., 2013,). An influx of dermal fibroblasts occurs, which are responsible for collagen synthesis and other extracellular matrix constituents such as elastin. Collagen and fibrin cross-linked fibronectin provide an adhesive matrix scaffold for the migrating cells to be guided across the wound base (Baneyx *et al*., 2002, Clark 1990). Other complex macromolecules promote cell migration and proliferation (Chakravarti *et al*., 1990, Steffensen *et al*., 2001), leading to the formation of granulation tissue. This is present in the wound bed at about three to five days due to the proliferative action of fibroblasts, macrophages, smooth muscle and endothelial cells. These fibroblasts further differentiate into myofibroblasts, characterised primarily by a contractile phenotype and the expression of α-smooth muscle actin (α-SMA). α-SMA is preceded by EDA-fibronectin, present in connective tissue during development but reappears in pathological situations such as granulation tissue and fibrotic lesions (Bochaton-Piallat *et al*., 2016). This is a component of the extra-cellular matrix (ECM) (Brown *et al.,* 1993). This differentiation process marks a transition from granulation tissue, which is sensitive to inflammatory cell infiltration and breakdown, into the third healing phase of scar tissue formation. This involves the remodelling of the extracellular matrix, regression of myofibroblasts and differentiation into mature fibroblasts.

Wound maturation is dependent on the timing of the re-epithelialisation process and the start of fibroplasia (Yates *et al*., 2011). During this phase, fibroblasts increase fibronectin production as the chemotactic inflammatory stimulus decreases. They form the key component of the formation of granulation tissue and are responsible for the production of most of the collagen, fibronectin, tenascin C, and other matrix proteins, including critical remodelling metalloproteases (Trebaul *et al*., 2007). Myofibroblasts assist in *de novo* collagen deposition contributing type III collagen and elast-

in deposition, as well as actin filaments. New blood vessels and further granulation tissue form under the influence of matrix factors (VEGF, TGF-beta, FGF, PDGF, TGF-alpha, and other cytokines) (Singer *et al*., 1999) which in turn stimulate other stromal cells (Werner *et al*., 2003, Roberts *et al*., 1990, Raab *et al*., 1997). The extra-cellular matrix evolves to consist mostly of collagen fibrils. Collagen synthesis and deposition are critical to wound healing, forming the major constituents of scar tissue and influencing scar tensile strength, tissue architecture and ECM interactions. Collagen type I and type III mainly make up scar tissue collagen, while type I collagen is pre-dominant in innate adult skin (Varga *et al*., 1987, Schultz *et al*., 2011). Collagen fibre deposition occurs along the framework of fibronectin and form strong crosslinks because of hydroxylation of lysine residues (Clark *et al*., 2004).

Fibroblasts are also responsible for the production of hyaluronic acid and other proteoglycans, which include dermatan sulphate and chondroitin-4-sulphate. Being hydroscopic in nature, these large molecules absorb water and occupy the bulk of the extracellular matrix. Collagen deposition stabilises and homeostasis is achieved within 21 days. Further dermal strengthening occurs through cross-link-age and organisation of these collagen fibres, rendering the now sealed wound a stable scar matrix. Wound strength increases exponentially for about 6 weeks, finally reaching 80% tensile strength of normal skin. Macrophages, in response to a low level of local tissue oxygenation, are responsible for the initiation of angiogenesis (Tonnesen *et al*., 2000). The evolving ECM, with its above-mentioned factors promote endothelial cell migration and tubular structure formation that form the precursors of patent vessels (Iozzo *et al*., 2010). The regenerative phase is marked by a proliferative response with hyperaemic blood flow, a very cellular dermis and a thick epidermis.

Resolution occurs as collagen synthesis moves to type I (rather than type III) and wound contraction starts. Vascularisation decreases gradually, eventually giving rise to a pale flat mark. Chemokines, expressed by keratinocytes through contact inhibition following wound re-epithelialisation, (Tensen *et al*., 1999, Yate *et al*., 2008) and maturing microvasculature (Bodnar *et al*., 2009) channel the con-

tractility of migrating fibroblasts into ECM contraction (Allen *et al*., 2002). Wound contraction is mediated by myofibroblasts, which contain an abundance of actin filaments.

Simultaneously, these chemokines predispose fibroblasts to apoptosis (Shao *et al*., 2008) and stimulate anoikis of immature vessels and endothelial cells (Bodnar *et al*., 2009).

The immature ECM is gradually replaced by a collagen I-rich dermis, which also suppresses the synthetic properties of the stromal cells. Thus, the skin gradually (up to 18 months) reverts to its unwounded state of relative avascularity, hypocellular dermis, and a defined keratinised epidermis.

1.3.3. Scarring

Scars are areas of dense fibrous tissue that replace injured skin following the wound healing process. All types of tissue heal with a degree of scarring. The only exception to this rule is foetal skin, which is capable of complete regeneration (Yates *et al*., 2012).

Scarring occurs during the final maturation phase of wound healing. It is the longest phase, with the resultant repaired tissue undergoing constant remodelling to approximate normal native skin as much as possible. A scar generally takes up to twelve months to reach its final steady state (Xue *et al*., 2015). A normal scar is generally pale and flat in appearance and regains up to approximately 80% of its original tensile strength (Schilling, 1976). It is rather common for the scar tissue to lack its usual adnexae, such as hair follicles and sebaceous and sweat glands.

Abnormal scarring results from the failure of the wound to properly transition from the regenerative phase to the resolving phase extension of matrix deposition and chronic inflammation pathologies (Harty *et al*., 2003, Wynn 2008). The rate-limiting step in the wound healing process is the balance of granulation tissue formation versus resolution. Excessive granulation tissue results in a fibrotic wound. This is due to fibroblasts and other stromal components that are vital to dermal synthesis

and re-modelling and maturation (Raghow, 1994). The extent of scarring is influenced by a variety of factors, including ongoing infection, allergic reactions, and genetic background. Such factors may contribute to pathological scarring (see below).

1.4 Factors essential to wound healing

The wound healing process is subject to many factors (local, systemic or environmental) that may influence its trajectory or interrupt the normal state of affairs. These include tissue perfusion, growth factors, nutrition and wound dressings.

Dermal oxygenation and venous sufficiency ensure adequate cell metabolism and the provision of energy through adenosine tri-phosphate (ATP), the stimulation of angiogenesis, keratinocyte differentiation and migration, fibroblast proliferation and wound contraction. (Bishop 2008). Superoxide dismutase (key to the oxidative destruction of invading pathogens) produced by polymorphonuclear leukocytes depends critically on oxygen levels. (Guo *et al*., 2010).

Growth factors are responsible for the intercellular signalling that regulates the tightly orchestrated sequence of cellular migration, division, differentiation, and protein expression during the wound healing process (Werner *et al*., 2003). Much research has been carried out in order to identify individual growth factors (these can be broadly divided into seven categories) and elucidate their role, and their possible contribution to wound dressings. Of particular significance are the epidermal growth factor (EGF) family, fibroblast growth factor (FGF) family, transforming growth factor beta (TGF−β) family, vascular endothelial growth factor (VEGF), granulocyte macrophage colony stimulating factor (GM−CSF), connective tissue growth factor (CTGF), platelet−derived growth factor (PDGF), and various chemokine including the interleukin (IL) family, and tumour necrosis factor−α family (TNF) (Barrientos *et al*., 2008). Acute wounds contain the majority of growth factors that

contribute significantly to the initial phases of wound healing. (Komarcevic 2000). IL−1 Is responsible for alerting the surrounding cells to initial epithelial cell damage (Barrientos *et al*., 2008).

An optimal nutritional status has been found to be integral to wound healing (Posthauer 2012). Carbohydrate remains the prevailing source of energy in this repair mechanism, followed closely by fats and fatty acids (Arnold *et al*., 2006). Glucose plays a significant role in angiogenesis and neocellularisation (Shepherd 2003). Proteins, particularly arginine and glutamine, play a key role in capillary angiogenesis, fibroblast proliferation, proteoglycan and collagen synthesis as well as wound contraction and scar maturation. Arginine is a precursor to proline (together with lysine) of pro-collagen and collagen. Glutamine, present in abundance in plasma and represents the major metabolic source for cells undergoing rapid mitotic division during the proliferative phase of wound healing. (Campos *et al*., 2008). Nutritional cofactors play a significant role in the wound healing process. (Ruberg 1984). These include Vitamins Vitamins C, A and E, minerals and trace elements such as iron, zinc, copper, manganese and magnesium. Collagen synthesis is dependent on Vitamin C and ferrous iron as co-factors for the hydroxylation of proline and lysine. (Campos *et al*., 2008). Zinc is a cofactor for procollagen N-Proteinase & procollagen C-Proteinase, whose role is to produce procollagen, the precursor to collagen. (Tengrup *et al*., 1981). It is also a co-factor for DNA and RNA polymerase. Magnesium is a co-factor for a multitude of enzymes involved in the synthesis of collagen and protein. Copper is the co-factor for superoxide dismutase (a cytosolic ant-oxidant), for cytochrome oxidase, and for the optimisation of collagen cross-linking. (Shepherd, 2003; Arnold *et al*., 2006; Campos *et al*., 2008). Vitamin A (retinol) demonstrates anti-oxidant activity and enhances fibroblast proliferation, modulates cellular proliferation and differentiation, increases hyaluronic acid and collagen synthesis, while decreasing MMP-mediated extracellular matrix degradation (Burgess, 2008). Vitamin E (tocopherol), another anti-oxidant, stabilises and maintains the integrity of the cellular membrane through the provision of protection against destruction by

oxidative stress. Due to its anti-inflammatory properties, Vitamin E is also suggested to play a role in decreasing excess scar formation in chronic wounds. (Arnold *et al*., 2006). Vitamin C (L-Ascorbic acid) participates in fibroblast differentiation, collagen synthesis, angiogenesis and capillary stability.

1.5 Compromised wound healing

A thorough understanding of the mechanisms of the wound healing process and the characteristics pertaining to its abnormalities allows causative factors to be addressed and targeted methods of treatment to be designed and employed. Occasionally, owing to the severity or the nature of the trauma, its anatomical location and / or associated co-morbidity, the skin's regenerative capability is compromised, resulting in a non-healing indolent wound, with a portal for infection, risk of fluid loss and ensuing systemic complications. It is often the case that chronicity may be due to multiple pathological factors and additive or compound effects (Mustoe *et al*., 2006).

The pathogenesis of chronic wounds is multifold. Causative factors negatively influencing wound healing may be broadly characterised dichotomously into local and systemic factors. Systemic factors include advancing age, diabetes, stress, gender hormones, immune-suppression, steroid use and suboptimal nutrition, while local factors include peripheral vascular disease and ischaemia, and contaminants, debris and infection. Indolent non-healing wounds are rarely found in individuals not otherwise healthy (Sen *et al*., 2009). Elucidation of precipitating factors has led to improved wound care, and to prophylactic measures being employed to offset their incidence.

Individuals over the age of sixty exhibit temporal delays in wound healing without impairment in terms of the quality of the outcome (Gosain *et al*., 2004). This delay is associated with an altered

inflammatory response, delayed T-cell infiltration, altered chemokine production and reduced macrophage phagocytic capacity (Swift *et al*., 2001). Each phase of wound healing sequence undergoes characteristic changes relating to the skin's ageing trajectory. These include enhanced platelet aggregation and secretion of inflammatory mediators, delayed infiltration of macrophages and lymphocytes, impaired macrophage function, decreased secretion of growth factors, delayed re-epithelialisation, delayed angiogenesis and collagen deposition, reduced collagen turnover and remodelling, and ultimately decreased wound strength. (Gosain *et al*., 2004).

Older male individuals have been shown to exhibit delayed healing of acute wounds when compared to their female counterparts of a similar age. Oestrogens (estrone and 17β-estradiol), androgens (testosterone and 5α-dihydrotestosterone, DHT), and their steroid precursor dehydroepiandrosterone (DHEA) appear to positively significantly influence the wound-healing process (Gilliver *et al*., 2007). Differences in gene expression between elderly male and young human wounds are almost exclusively oestrogen-regulated (Hardman and Ashcroft, 2008) as oestrogen regulates genes associated with matrix production and regeneration, protease inhibition, epidermal function, and inflammation (Hardman *et al*., 2008). Studies are indicative that oestrogen has a beneficial influence of the age-related impairment in cutaneous healing in both men and women, while androgens negatively regulate wound healing. (Gilliver *et al*., 2007).

Patients who smoke show a delay in wound healing (Siana *et al*., 1989; McDaniel *et al*., 2014; Ahn *et al*., 2008) and an increase in a variety of complications such as infection, wound rupture, wound necrosis, epidermolysis, and a decrease in wound tensile strength. (Chan *et al*., 2006; Ahn *et al*., 2008). Over four thousand substances have been identified in tobacco smoke, with many having been shown to negatively influence healing (Ahn *et al*., 2008). The main offenders are nicotine, carbon monoxide, and hydrogen cyanide. Nicotine compromises oxygen supply by inducing tissue ischemia, as it causes decreased tissue blood flow. (Ahn *et al*., 2008; Sørensen *et al*., 2009). This is because nicotine stimulates sympathetic nervous activity, with release of epinephrine, which causes

peripheral vasoconstriction and decreased tissue perfusion. It also increases blood viscosity caused through a reduction in fibrinolytic activity and an augmentation of platelet adhesiveness. Carbon monoxide in also causes tissue hypoxia by aggressively binding to haemoglobin with a much greater affinity than oxygen, with a resulting decreased fraction of oxygenated haemoglobin. Hydrogen cyanide impairs cellular oxygen metabolism.

In the inflammatory phase, smoking impairs white blood cell migration, with a resulting decreased wound presence of monocytes and macrophages, and reduced neutrophil bactericidal activity. There is a depression of lymphocyte function, natural killer cell toxicity and IL-1 production (Ahn *et al*., 2008). These effects increase the risk of opportunistic wound infection while also inhibiting the wound healing process. Fibroblast migration and proliferation are decreased during the proliferative phase of wound healing. This results in reduced wound contraction, hindered epithelial regeneration, decreased extracellular matrix production, and a protease imbalance (Ahn *et al*., 2008).

It has been shown that the cessation of smoking results in an improvement in repair and a reduction in incidence of wound infection. (Sorensen *et al*., 2003). However, contrary to the above theories, there have been recent studies suggesting that low doses of nicotine may actually enhance angiogenesis thereby improving healing (Jacobi *et al*., 2002).

Ischaemia, often resulting from peripheral arterial disease, is a major contributing factor to chronic wounds. It is found more commonly in in diabetic patients. Peripheral arterial disease is the only identifiable aetiology in approximately 10% of leg ulcers (Hafner *et al*., 2000) An impaired blood supply fails to deliver oxygenated blood, nutrients and cellular components in adequate amounts and in a timely manner, hence the impairment in healing.

Diabetes is a very commonly occurring condition affecting up to 25% of the population in the developed world. The lifetime incidence of foot ulcers in diabetes sufferers may be as high as 25% (Singh *et al*., 2005). This is due to many factors. Diabetes is closely associated with peripheral vascular disease (Huysman *et al*., 2009). Additionally, hyperglyacaemia makes a diabetic wound

more favourable to pathogens and hence infection and increases vascular superoxide production (Casqueiro *et al*., 2012). This interferes with nitrous oxide production, a promoter of angiogenesis, endothelial and epithelial cell proliferation and migration. Matrix Metalloproteinases (MMPs) are zinc endopeptidases that potentially degrade all components of the extracellular matrix (ECM) during all stages of normal wound healing. (Vitlianova *et al*., 2016) . Usually, the interaction of MMPs with growth factors maintains the balance of the ECM. In such circumstances, the amount of MMP is increased (Ayuk *et al*., 2016). Hence, the increase in tissue destruction and inhibition of normal repair processes.

Deficiencies in carbohydrates, proteins and essential fatty acids may have a profound detrimental impact on wound healing following trauma and/or surgery. Patients with chronic or non-healing wounds and experiencing nutrition deficiency often require special nutrient supplements. (Guo *et al*., 2010). As collagen synthesis is dependent on the hydroxylation of lysine and proline, a deficiency in co-factors such as ferrous iron and vitamin C results in an impairment of wound healing (Campos *et al*., 2008). Additionally a Vitamin C deficiency reduces fibroblast proliferation, decreases angiogenesis, and increases capillary fragility. It also leads to an impaired immune response and an increased susceptibility to wound infection. Similarly, a deficiency in vitamin A results in a reduction of anti-oxidant activity with a resulting compromise of fibroblast proliferation, negative modulation of cellular differentiation and proliferation, decreased collagen and hyaluronate synthesis, and increased MMP-mediated extracellular matrix degradation (Arnold *et al*., 2006; Campos *et al.*, 2008).

Micronutrient deficiencies have been shown to have a negative impact on wound repair. Deficiencies of the important trace elements, iron, magnesium, zinc and copper deficiencies which act as co-factors for many enzymes involved in protein and collagen synthesis, result in significant impairments in wound healing. (Shepherd, 2003; Arnold *et al*., 2006; Campos *et al*., 2008). Composite nutrition support would benefit both acute and chronic wound healing. (Guo *et al*., 2010)

Obesity represents another state of malnutrition. Obese individuals face a higher incidence of wound complications. These include wound dehiscence, hematoma and seroma formation, pressure ulcers, and venous ulcers (Wilson *et al*., 2004). A relative hypoperfusion occurs in subcutaneous adipose tissue and in surgical wounds, there is an increased tension on the wound edges when compared to leaner individuals. This contributes to wound dehiscence, as such wound tension increases tissue pressure, thereby reducing microperfusion and oxygen availability (Wilson *et al*., 2004; Anaya e*t al*., 2006). Obesity is also often associated with many other co-morbidities which impair healing such as diabetes.

Stress can significantly impair cutaneous wound healing in humans and animals through the activation of the hypothalamic-pituitary-adrenal axis (deAlmeida *et al*., 2016). This occurs through the effects of increased circulating glucocorticoids, and pro-inflammatory cytokines. While a robust systemic inflammatory response is imperative to wound healing, high levels of inflammatory markers are associated with impaired healing (Christian *et al*., 2007).

When the protective physical barrier of skin is breached, microbes and contaminants that would normally be commensal, gain access to normally sterile tissue. The inflammatory phase of wound healing is integral to the removal of contaminating micro-organisms. This phase is prolonged in the absence of effective decontamination and removal of debris such as necrotic tissue and /or foreign bodies. Bacterial endotoxins and some exotoxins may induce the prolonged elevation of pro-inflammatory cytokines such as interleukin-1 (IL-1), TNF-α and MMPs (Guo *et al*., 2010). If this perpetuates to become a steady-state, the wound may enter a chronic state, with further ECM degradation and thus fail to heal. Reduced levels of naturally occurring protease inhibitors also occurs, which results in the rapid degradation of growth factors, which is characteristic of chronic wounds. (Edwards and Harding, 2004; Menke *et al*., 2007).

Biofilms – communities of sessile microbial cells that attach to a surface and secrete a hydrated extracellular polymeric substance matrix – are a common factor invariably present in wounds, and

there is evolving evidence to show that they are also involved in the chronicity of wounds and in abnormal wound healing. Sixty per cent of chronic wounds contain a biofilm on light and scanning electron microscopy (Bryers *et al*., 2008) when compared to 6% in acute wounds. The organisms become embedded in in this matrix which is composed of polysaccharides, proteins, glycoprotein's, glycolipids and extracellular DNA. Most microorganisms in chronic wounds exist in biofilms. The implication is that antimicrobials employed conventionally are unable to eradicate the nidus of infection in biofilms. Hence, many chronic wounds become infected repeatedly with the same microorganisms. Thus, to administer the appropriate treatment to poorly healing wounds, the flora of the lesion must be understood together with the composition of the biofilm (Martin *et al*., 2010).

Systemic factors	**Local factors**
Malutrition	Infection
Increasing Age	Ischaemia
Sex	Peripheral vascular disease
Diabetes	
Stress	
Smoking	
Steroid use	

Table 1.5: Factors detrimental to wound healing

While scar formation is part of the natural wound healing process, occasionally this final process may go awry. Such problems include abnormal pigmentation, excessive contraction, hypertrophic scarring or keloid scarring. Poor scar formation is often characterised by excess and aberrantly-linked collagen deposition that renders the tissue weaker than unwounded skin (Hynes 2009).

Variations in melanin deposition may occur (Chadwick *et al*., 2012). Hypopigmentation is commoner in darker skins, while post-inflammatory hyperpigmentation is rather common in Asian

skins. Scar re-pigmentation depends both on the depth and width of the wound (Chadwick *et al*., 2012). Studies have demonstrated that re-pigmentation occurs when melanocytes migrate into a wound after full re-epithelialisation. In healing human burns, melanocyte travel lags behind the leading neo-epithelial edge by 2-3 mm (Chadwick *et al*., 2012). Post-inflammatory hyperpigmentation is often encountered in clinical practice, observed as wounds darken in colour as they heal. This phenomenon can sometimes be persistent for a considerable amount of time following injury. It is thought that melanocytes may become activated by inflammatory mediators, or reactive oxygen species released by damaged skin (Chadwick *et al*., 2012).

Wound contraction occurs as part of the normal healing process, with the aim of sealing the wound in a timely fashion. Myofibroblast activity in the initial stage generates contractile forces to pull the edges of the wound until it disappears by apoptosis during the final stage. An altered regulation of myofibroblast disappearance would cause their persistence in the dermis and the continuous contraction of the scar, leading to a contracture (Shin *et al*., 2004). This may pose a problem if contraction is either excessive or if the scar overlies a joint or causes traction on a facial feature. (see photo). Scar contractures over joints would disallow full range of movement of the joint.

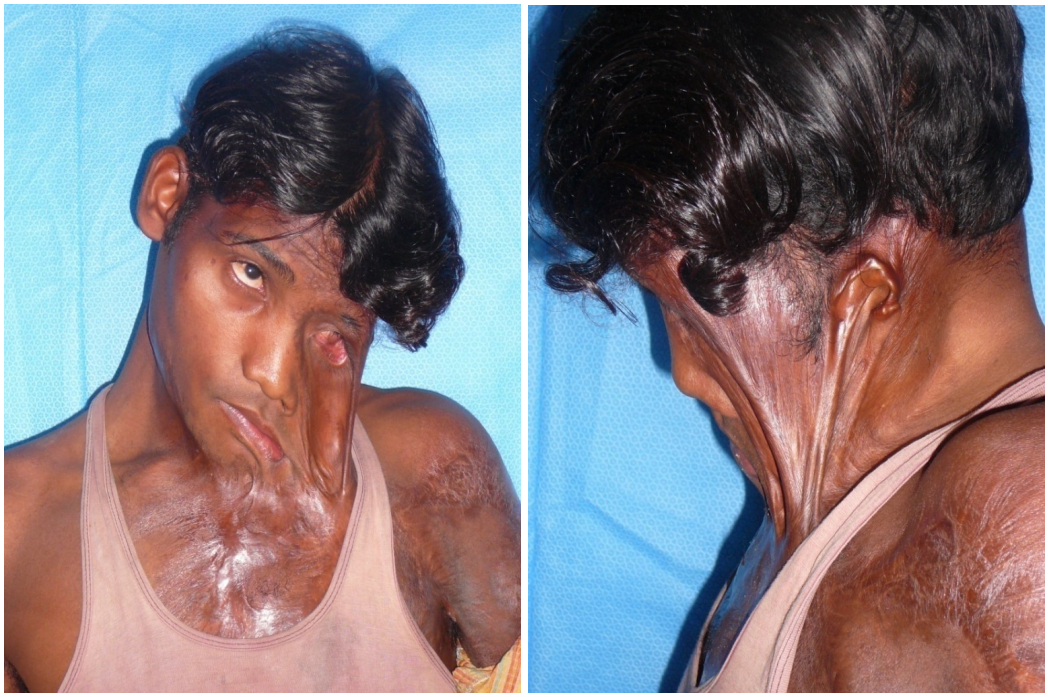

Figure 1.5.1: Scar contractures across the left side of the face and neck following a childhood burn from a kerosene lamp. Source: taken by author (in Scheer Memorial Hospital, Banepa, Nepal, April 2009) and reproduced with the patient's verbal and written consent.

On occasion, fibroblast proliferation is excessive while collagen synthesis is inhibited. The transforming growth factor family (Mainly beta 1 and 2) is largely responsible for excessive scar formation. Contrarily, the TGF-beta 3 may have an inhibitory function on scar formation through its antagonist properties towards TGF-beta 1 and 2 TGF-beta 2. Some cytokines, in particular interferon-alpha (INF-alpha), may also decrease scar formation, as they decrease the fibroblast proliferation and reduce collagen and fibronectin synthesis through reduction of mRNA synthesis (Komarcevic 2000).

Hypertrophic scars primarily contain loosely arrayed type III collagen fibrils oriented parallel to the epidermal surface with many nodules containing collagen filaments, myofibroblasts, and acidic polysaccharides (Hynes 2009, Slemp 2006). Hypertrophic scars stay within the limit of the original wound margins and tend to regress over time due to the gradual reduction of the excessive collagen (Singer *et al*., 1999) secondary to abnormalities in epidermal-dermal crosstalk. They generally oc-

cur within 4 to 8 weeks following wound closure with excess tension, wound infection, or traumatic skin injury (Wheeland 1996) and develop over months. Keloid scars, on the other hand, consist mainly of disorganised type I and III collagen, with pale-staining hypocellular collagen bundles without nodules or excess myofibroblasts (Slemp *et al*., 2006). Both hypertrophic and keloid scars demonstrate a relative overproduction of multiple fibroblast proteins. This is suggestive of either pathological persistence of wound healing signals or a failure of the appropriate down-regulation of stromal cells. This leads to a persistent inflammatory matrix, which attracts macrophages through a sterile inflammatory response, thus accentuating further wound bed turnover. This would suggest that the development of such pathological scars is dependent on the timing of wound resolution (Yates *et al*., 2012).

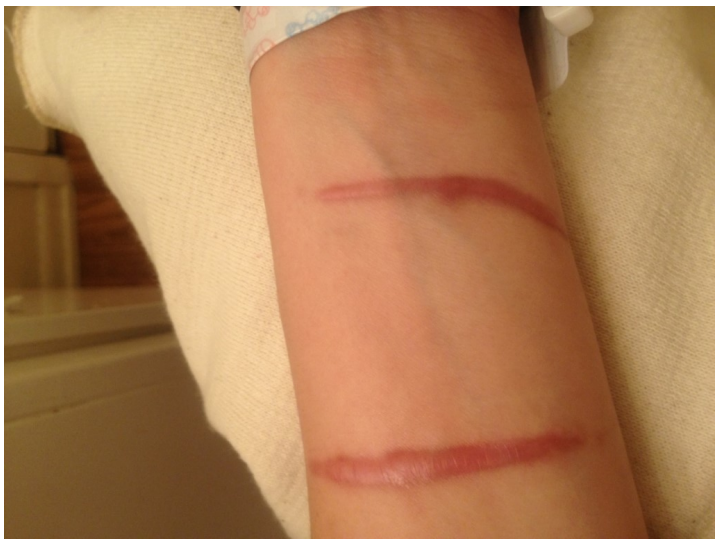

Figure 1.5.2: Hypertrophic Scar. A red raised scar which remains confined to the scar without infiltrating surrounding tissue. Source: taken by author (in Scheer Memorial Hospital, Banepa, Nepal, April 2009) and reproduced with the patient's verbal and written consent.

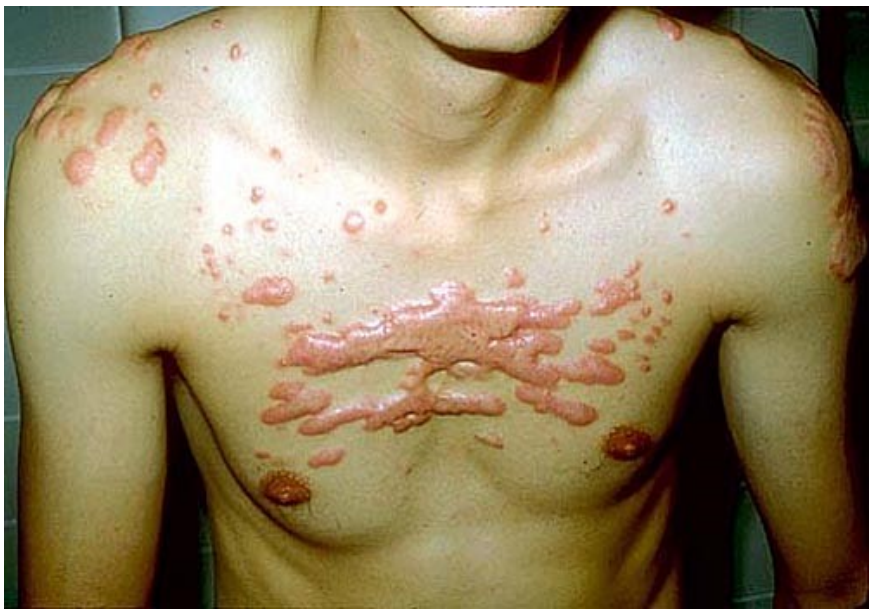

Figure 1.5.3: Keloid scarring over anterior chest wall and shoulders. Keloid scarring is typically raised, pigmented, pruritic and extends beyond the confines of the original injury into uninjured tissue. It is commoner in darker skins and in the distribution of sebaceous glands. Source: RAFT archive.

-

1.6 Adjuncts to wound healing: Dermal Replacement Scaffolds

The adjuncts to cutaneous wound healing are various, ranging from simple wound dressings and local and systemic optimisation of patient parameters to the replacement of skin components. Skin substitutes aim to replace the anatomy and physiology of the skin in order to achieve wound closure (Halim *et al*., 2010). This thesis will concentrate mainly on dermal and extra-cellular matrix substitutes.

Dermal substitutes refer to a heterogenous group of materials used to (permanently or temporarily) cover wounds where extensive areas of skin are missing and to promote healing (Halim *et al*., 2010). Such devices seek to replace the middle layer of the skin, the dermis, so as to facilitate cutaneous wound closure. Such scaffolds or matrices are engineered in such as way as to reliably mimic the dermal structural and functional properties. Although these products are sometimes de-

rived from naturally occurring sources, design, development and manufacture of such adjuncts belong to the discipline of tissue engineering.

1.6.1 Hypothesis

The basic concept of a dermal replacement template is a 3-dimensional biomaterial framework that provides a densely reticulated and protected tissue territory that cells can adhere to, migrate through, and organise around, to form a histological structure (Shahrokhi *et al*., 2014). In order to be effective, cellular ingress from the wound bed into the scaffold must occur, to allow for integration of the material with the body. They refer to bio-matrices that anatomically and physiologically mimic the functions of the cutaneous dermal layer (Shahrokhi *et al*., 2014) and act as scaffolds to promote new tissue growth and enhance wound healing (Zhong *et al*., 2010). The working hypothesis is that pre-vascularised dermal scaffolds will result in better quality scarring when used with split thickness skin grafts (Druecke *et al*., 2004). The exact mechanisms by which such adjuncts support and promote both structural and functional remodelling of injured tissues *in vivo* are being increasingly studied and understood (Turner *et al*., 2015).

1.6.2 History

The concept of replacing skin dates back to the 15th Century BC, where xenografting was described in the Papyrus of Ebers (Halim *et al*., 2010). The Manuscript of Branca in the first half of the 16th Century described the use of allogeneic skin grafts. In 1871, Reverdin first described the concept of autologous skin grafting, as we know it today (Horch *et al*., 2005). Initially skin substitutes were developed as a potentially alternative treatment for burn wounds in the 1980s. Over time, the indic-

ations for such matrices have broadened to include challenging wounds as well as those not curable by conventional treatment methods. This is possibly owing to the fact that there is a much larger incidence of such wounds than burn injuries.

The paradigm of artificial dermal replacement was realised from the experience of long-term results of use of split thickness skin grafts (STSG) onto debrided full thickness wounds being associated with fragile skin and associated occurrence of hypertrophic scarring. Rheinwald and Green were pioneers in substitute skin products almost four decades ago, when they cultured isolated keratinocytes (CaK) and developed them into sheets of cells, two-or three cells thick (Rheinwald *et al*., 1975). In 1981, O'Connor *et al* used cultured autologous epithelium to cover burn defects, creating a "skin equivalent" or "composite culture" over a collagen I based dermal substitute (Ho, 2002). Research into extraction methods improved the removal of immune antigenicity while retaining the extracellular matrix molecular component, architecture and biological activity. These advances contributed to the concept of extracellular matrix as an intrinsic organising structure in cutaneous wound healing (Crapo *et al*., 2011). Its potential continues to be explored and exploited through refined technologies for selective extraction and preservation of residual extracellular matrix-associated biological activity.

Dermal equivalents have since been developed to serve as a template for dermal repair. Parallel developments in synthetic dermal scaffolds, notably with the development of the Integra™ dermal regeneration template, led to the combined use of a dermal template and epidermal reconstruction method, either STSG or CaK sheet. In a bid to improve overall wound healing, dermal scaffolds were either derived xenogeneically and later through bioengineering, and impregnated with dermal fibroblasts and covered with an outer layer of keratinocytes. The concept of a synthetic approach to bio-manufacturing an artificial skin offers potential advantages as synthetic materials can be theoretically defined, engineered and reliably reproduced for mass manufacture. This could lead to more cost-effective realistic products for mass clinical use. This approach is also amenable to at-

tempts to define a minimum physical and chemical requirement for providing a cyto-compatible extra-cellular matrix.

This matrix behaves as a physical and physiological extracellular matrix. Due to different components in different products, the elasticity and pliability of the reconstructed skin is increased. Depending on their components, many of these substitutes were employed as wound dressings or a various skin component replacements, and there exists a continuum of all these adjuncts in the wound healing armamentarium.

1.6.3 Mechanism of action

The scaffold is designed to function as a healthy ECM replacement in the place of the absent or dysfunctional ECM that is unable to support wound healing, providing an inductive microenvironment (Gibson *et al*., 2009, Turner *et al*., 2015). The "journey" of the dermal replacement scaffolds requires a *de novo* synthesis process or the modification of animal derived dermal matrices, followed by adequate preparation, wound bed preparation, implantation into the skin wound, host cell cellularisation, neo-vascularisation and angiogenesis, and scaffold re-modelling and/or degradation (Sun *et al*., 2013). The variation in extra-cellular matrix nature, modification and processing among different bioscaffolds means that the mechanisms of action in tissue repair differs somewhat between one scaffold and another (Ramshaw *et al*., 2007, Sun *et al*., 2013). Some concepts are common to all matrices. Naturally derived ECM scaffold material is subjected to a series of physical, biochemical and radiation processes to rid it of antigenicity, cellular material and micro-organism contamination (Deeken *et al*., 2012). Collectively these processes result in a variation of anatomical and physiological properties, with resulting differences in host responses (Shah *et al*., 2011). A higher degree of similarity of the end product to host ECM, results in a higher degree of

compatibility and therefore a decreased likelihood of eliciting an adverse reaction (MacNeill *et al*., 2007).

The three-dimensional property structure of the scaffold is integral to the processes of cell infiltration and capillary permeation (Loh *et al*., 2013) while providing a degree of biomechanical support. The pores of the ECM are infiltrated by host fibroblasts and capillaries, hence homogeneity in pore size and structure is key to the dependability of a scaffold (Loh *et al*., 2013). This cell-infiltrated membrane is gradually converted into a synthesised vascular connective tissue matrix, similar to innate dermis, as the original network of the substitute scaffold is biodegraded generally by enzymatic degradation or hydrolysis (Badylak *et al*., 2009).

In addition to the native ECM structure, other components are also used in the scaffold in order to simulate the natural skin ECM. This is a stabilisation process referred to as cross-linkage, the degree of which may modify the degradation process (Davidenko *et al*., 2015). Cross-linking agents may have effects on product durability, elasticity and rigidity (Grover *et al*., 2012). Such agents include, polysaccharides such as glycosaminoglycan (GAG), or chemicals such as aldehyde derivatives. Physical methods such as heat application or irradiation have also been employed. Any residual chemicals from the cross-linking process may affect the inflammation process. Among others this may be due to cytotoxicity, calcification and foreign body response (Delgado *et al*., 2015). Ideally inflammation is minimal (Harmsen *et al*. ,2010) and matrix degradation is gradual to complete integration and vasculogenesis with host tissue (de Vries *et al*., 2004). *In vivo* studies demonstrate that the host response to the scaffold is significantly influenced by cross-linking density. Heavily cross-linked collagen-based materials promote a pro-inflammatory response that may result in impaired wound healing or fibrous encapsulation, while those products which are not cross-linked result in a more rapid protease-mediated degradation and thus potentially an increase in scar tissue formation (Delgado *et al*., 2015). These properties determine the extent of cellular infiltration and tissue ingress.

In acute full thickness wounds treated with dermal scaffolds, the vascularisation process is essential to the establishment and survival of the neo-epidermis (Druecke, 2004, Macleod 2005, Haifei, 2014). Neovascularisation is related to formation of granulation tissue (Arbiser, 1996). Activation of the immune system can stimulate angiogenesis (Kwee, 2015). Thus, failure of synthetic graft integration, or time-appropriate vascularisation, have been associated with failure of angiogenesis into graft and implants (Druecke, 2004). These considerations suggest a pro-angiogenic scaffold positively contributes to its overall integration, to that of it overlying skin graft and the subsequent stability of the new tissue. The physical structure of a material such as pore size, homogeneity, interconnectivity and hierarchical structure, is an over-riding determinant of cellularisation and vascularisation relating to scaffold functionality (Hollister 2005, Harley *et al*., 2008).

1.6.4 Criteria for a dermal replacement scaffold

The development of skin substitutes has reduced the incidence of some complications associated with skin grafts, such as donor site morbidity, immune rejection of allogenic skin grafts, pain, adverse scarring, slow healing, and infection (Capo *et al*., 2014). Apart from their mechanically supportive action, successful biocompatible scaffolds should assist the successful engraftment of the overlying skin graft (Bi *et al*., 2013), as they expediently promote granulation tissue formation, fibroblast-driven remodelling, angiogenesis, and re-epithelialisation. Ideal dermal replacement scaffold functions require the translation from clinical needs into key physical, chemical, biological, mechanical and immunological properties (Ruszczak *et al*., 2003). As described above, essential characteristics include appropriate physical and mechanical properties, controlled degradation, sterility, non-toxicity and non-antigenicity, minimal inflammatory reactivity and provision of a vital barrier function. Adherence is considered one of the key properties of the ideal dermal template

(Woodroof *et al*., 2010, Woodroof *et al*., 1984, Demling *et al*., 1995, Demling *et al*., 2000, Pruitt *et al*., 1984, Shahrokhi *et al*., 2014). This facilitates the fixed juxtaposition of the scaffold both to the wound bed and to the overlying epidermal replacement to facilitate the "take" while also reducing the risk of seroma or haematoma formation separating the wound bed and overlying structures.

Angiogenic ECM factors (growth factors) are responsible for capillary infiltration and securing the viability of the overlying dermal and epidermal components. While collagen (the most commonly used ECM material in dermal scaffolds) does exhibit some angiogenic properties, a soluble ECM factor such as fibrin has been shown to demonstrate greater angiogenic potential (Potter *et al*., 2006). Integration must be rapid if the barrier to fluid loss and infection is to be established in a timely manner. It should ideally provide a full thickness replacement while allowing for a single-stage reconstruction procedure, thus reducing the number of trips to the operating theatre (thereby reducing length of in-patient stay and costs of management). There exists a variety of synthetic dermal replacements which has certainly modified the reconstructive ladder helping to cover large area cutaneous defects in less time and effort. This is especially of essence in the elderly, paediatric and multimorbid patients (Koenen *et al*., 2010).

The scaffold should be resorbed by the body within 21 days, the average length of the migration phase of the wound healing process (Van der Veen *et al*.,2010, Demling *et al*., 1995). If shorter, it would not function as the necessary template providing the support and direction for inosculation and vascular and cellular ingress. This is largely dependent on the cross-linking of GAGs. Long-term persistence of the scaffold material longer than three weeks may invoke a foreign body effect with possible ensuing chronic inflammation (Badylak, 2008). The composite material should with-stand sterilisation procedures, without alteration in chemical or structural properties. Ease of hand-ling and application, flexibility of the scaffold to conform to irregular wound surfaces would make the product optimal (Capo *et al*., 2014).

Shelf-life should be long with easy storage and transportation properties with easy maintenance shelf stability. Three factors are paramount in the development of tissue-engineered materials: the safety of the patient, clinical efficacy and convenience of use (Blackwood *et al*., 2008).

Cost-effectiveness is paramount in this economic climate. The determination of the cost-efficiency of a dermal scaffold should take into account all factors surrounding the patient's road to recovery including in hospital stay, use of consumables as well as the cost of the biotechnology product. An ideal dermal scaffold would thus reduce to number of trips to the operating theatre if full thickness skin reconstruction were a single stage procedure, and would expedite recovery and down time. (Langer *et al*., 2009).

1.6.5 Wounds eligible for treatment

Their scope is to either expedite or induce wound healing or to provide a method of improvement of the resulting scar. Challenging wounds satisfy the former criteria, while the latter wound pertain to scar revision procedures carried out in order to improve cosmesis and/or function. The applications for dermal replacement scaffolds are many. See the table below for a list of their indications.

1.6.6 Classification of dermal replacement scaffolds

Dermal substitutes may be classified in various different ways. These may be natural versus synthetic scaffolds, they may contain cells or be acellular and finally they may be temporary or permanent substitutes. Some dermal replacement scaffolds are coupled with an overlying epidermal substitute, and are termed composite grafts, such as Apligraf. In some cases there is a fine line between temporary wound dressings and more permanent dermal replacement substitutes. Most

dermal substitutes are not permanent *per se*, as they are generally reabsorbed or broken down by the body, over varying time scales, depending on the nature of the constituents. Dieckmann *et al* divided skin substitutes broadly into two categories, biomaterial and cellular (Dieckmann *et al*., 2010). The former tends to be acellular and derived either from natural sources, or completely synthetic. Natural sources include human cadaver skin - autologous or allogeneic - or xenogeneic: porcine, bovine, ovine, squaline or derived from the frog (Juhasz *et al*., 2010). Derived dermal components as well as other substances such as collagen may be of organ origin such as small intestine. Synthetic materials are composed of biodegradable polymers. Dermal replacements can also sometimes be categorised according to the number and nature of the different layers comprising the product. However, overlap between classifications does occur, as some dermal substitutes combine both biosynthetic materials with natural occurring ones in the same product.

Natural scaffolds consist of human, porcine or bovine derived dermis. The advantages of biologic scaffolds are that the immunologic response is favourable, especially with human-derived scaffolds (Gock *et al*., 2004). Similarities in dermal porosity and basement membrane to native dermis also lend to their success. However, there remains a risk of (albeit small) of disease transmission (Van der Veen *et al*., 2010). The extra-cellular matrix behaves as a three-dimensional acellular scaffold consisting of varying amounts of collagen and elastin.

1.6.7 Currently available dermal scaffolds

The following is a brief summary of the main commercially available dermal scaffolds. This list is by no means exhaustive.

Human derived dermal scaffolds include Alloderm, Glyaderm, SureDerm, Dermagraft (now marketed as Transcyte), Graft Jacket, Tiscover, Allopatch HDTM, Alloskin, Cymetra, Dermacell,

Arthroflex, Flex HD, GammaGraft, Graft Jacket Regenerative Tissue Matrix, Memoderm, Puros Dermis, Repliform and Theraskin and Matrix HD.

Allogeneic cadaveric dermis is farmed and grown in specialist centres and can be delivered on demand. However it is rather expensive and demand heavily outweighs supply. Its shelf life is extremely short, with cells reaching senescence and therefore rather fragile. Cadaveric dermis also carries the potential risk of transmissible viral contamination such as cytomegalovirus. Human derived dermal substitutes not processed from donated human cadaveric skin are generally derived from human neonatal fibroblasts, most commonly placental (Juhasz *et al*., 2010) or neonatal foreskin. Some dermal substitutes, such as Tiscover are autologous human allografts, taken from the patient's own skin and processed.

Alloderm is a human derived natural biologic dermal substitute. The cadaveric dermis is subjected to a freeze-drying procedure following exposure to high salt content, and the removal of cellular components. This is one of the fist dermal substitutes to be employed, having been used in the treatment of burns and soft tissue defects (Levin *et al*., 2011) since the early nineties. As it is derived from human tissue, it is immunologically inert. AlloDerm may also serve as an alternative method of suitable coverage and provide a temporaneous bridge to permanent reconstruction or as a permanent biologic dressing for the treatment of complex surgical defects (Jansen *et al*., 2013). Glyaderm is the European equivalent of Alloderm – an acellular glycerol preserved collagen-elastin matrix, mainly used in the treatment of burn injuries.

GRAFTJACKET® Regenerative Tissue Matrix (Wright Medical Technology; Arlington, TN), similarly is derived from donated human cadaver skin, which is processed to be bereft of the epidermis and all cellular components. The extracellular matrix and biochemical factors are preserved. Graftjacket is used to treat loss of integumental areas such as diabetic foot ulcers. (Wright Medical Technology Inc., 2008) (Brigido *et al*., 2006). GRAFTJACKET® EXPRESS Scaffold (Wright Medical Technology; Arlington, TN) is the decellularised and micronised equivalent soft tissue scaffold in-

dicated for the repair or replacement of damaged or inadequate skin, specifically deep, dermal wounds that exhibit tunnelling and extension from the wound base that may move into the tendon and bone (Harding *et al*., 2010). GammaGraft is a cadaveric human skin allograft which has undergone irradiation. It is designed as a temporary graft for treating full-thickness indolent wounds on the extremities. Irradiating the graft preserves and sterilises the tissue. It is currently used to cover skin defects such as skull calvarial defects (Sivak *et al*., 2016). Dermagraft is a human fibroblast-derived dermal substitute (Marston *et al*., 2003). Available in the EU and the US, it consists of a collagen and GAG extracellular matrix on a synthetic bio-absorbable cultured scaffold (Biobrane) impregnated with neonatal human fibroblasts. It use is largely limited to full-thickness chronic wounds (of 6 weeks duration or longer) such as diabetic ulcers and pressure sores, where there is no exposure of underlying bone, tendon, joint capsule or muscle. Dermagraft is a nylon mesh fabric covered with a thin layer of silicone rubber membrane. The latter, serves as a temporary epidermal "barrier." It is stored in a frozen condition to be thawed only immediately before application to the debrided, clean wound bed. As it is semitransparent, it facilitates continuous observation of the underlying wound bed (Hansbrough *et al*., 1997). Dermagraft is now marketed as Transcyte It is a useful adjunct in expediting healing time in indeterminate depth wounds typically requiring debridement and would otherwise heal spontaneously (Noordenbos *et al*., 1999). TheraSkin® (Soluble Solutions, Newport News, Va.) is a biologically active cryopreserved human skin allograft with both epidermis and dermis layers; the cellular and extracellular composition provides a supply of growth factors, cytokines and collagen to support the wound healing process. It is an effective treatment adjunct in the management of venous leg ulcers and diabetic foot ulcers (Landsman *et al*., 2011). StrataGraft (Stratatech Corporation, Madison, WI USA) is another bi-layered composite skin substitute. This comprises a dermis and a stratified, functional epidermis generated from pathogen-free, neonatal immortalised human keratinocyte progenitor cells. The performance of this medical

device is comparable to cadaver allograft for the temporary management of burns and other challenging skin defects before autografting (Schurr *et al*., 2009).

Porcine dermal replacement substitutes include EZ-Derm, Oasis, Pelnac and Strattice. EZ-Derm is a glutaraldehyde cross-linked acellular porcine dermis. It has been employed since the mid-1980s as a temporary wound dressing and its application is mainly utilised in partial thickness burn wounds (Lawin *et al*., 2002). Viewed more as a biologic wound dressing rather than a synthetic dermal replacement, it was found to reduce wound pain and provide a local environment more conducive to wound healing (Troy *et al*., 2013). Oasis® wound matrix is a cellular natural occurring dermal replacement, derived from porcine small intestine. It is employed in the management of full and partial thickness cutaneous acute or chronic wounds (Juhasz e*t al*., 2010). This is available in the EU and in the US. Pelnac® is a collagen matrix and silicon bilayer scaffold derived from porcine tendons (Suzuki *et al*., 2000). Following neutralisation and freeze-drying, it is employed in Asia and Japan in sponge form for acute cutaneous dermal defects.

MB-Collage, also marketed as Collagen-Klee (Medical Biomaterial Products GmbH Neustadt-Glewe, BRD), is one of the first resorbable, porcine collagen membranes to reach the market. It is relatively thicker than most other scaffolds at 5mm. It is marketed as a medical device to expedite connective tissue proliferation during cutaneous wound repair (Neumann-Scholz *et al*., 1988). BGC Matrix (Brennen Medical Inc, St. Paul MN, USA) is an example of a complex tissue engineered dermal replacement scaffold. It consists of a porcine collagen hydrocolloid matrix and beta-Glucan, as well as a complex carbohydrate isolated from the cell wall of oats, combined in a multifilament mesh (Delatte *et al*., 2001). Biobrane is a synthetic wound dressing consisting of a silicone sheet bonded to a textured nylon mesh coated with porcine collagen and polypeptides (Hansen *et al*., 2001).

Bovine derived dermal replacement matrices include Integra™, Matriderm™ , and Promogran. Matriderm™ is very commonly used in many UK plastic surgery units while Integra™ is very commonly used for burns and large skin defects. The latter is extremely popular in the US.

A multilayer extracellular matrix with bovine collagen and GAG (Integra™, Integra™ NeuroSciences, Plainsboro, NJ), Integra™, is currently the gold standard dermal replacement method employed in the US, and is used very widely in the UK, Japan and other Asian countries and EU too (Melendez *et al*., 2008). This is a bilayer membrane system for skin replacement. The dermal replacement layer is made of a three-dimensional porous matrix of cross-linked bovine tendon collagen fibres and a GAG (chondroitin-6-sulfate) that is manufactured with a controlled porosity and defined degradation rate. The temporary epidermal substitute layer is made of synthetic polysiloxane (silicone) (Murphy *et al*., 2010). The serves to provide wound homeostasis on application by controlling moisture flux from the dermis. The collagen-GAG dermal layer of Integra™ is biodegradable that induces organised regeneration of dermal tissue ("neodermis") (Compton *et al*., 1998). The pore volume fraction, average pore size, and degradation rate of the collagen-glycosaminoglycan dermal layer are controlled to enable cellular and vascular ingress while inhibiting wound contraction. The dermal portion serves as a template for the infiltration of fibroblasts, macrophages, lymphocytes and endothelial cells that form a neovascular network. As healing progresses, native collagen is deposited by fibroblasts, and the collagen portion is biodegraded over time (Murphy *et al*., 2010). Upon adequate vascularisation of the dermal layer and availability of donor autograft tissue, the temporary silicone layer is removed and a thin, meshed layer of epidermal autograft is placed over this "neodermis" (Kremer *et al*., 2000). Cells from the epidermal autograft grow, forming a confluent stratum corneum, thereby sealing the wound and reconstituting a functional dermis and epidermis. Integra™ is available in two different versions: Integra™ Dermal Replacement template, mainly employed in the management of scar contracture (Figues *et al*., 2007) or in the post-excisional treatment of life threatening full-thickness wounds when sufficient

autograft is not available or the patient's physiological status does not allow for more invasive intervention. Integra™ Bilayer wound dressing is used for both partial and full thickness cutaneous wounds (Singh *et al*., 2001, Stern *et al*., 1990), chronic ulcers, or surgically created wound defects (for example post excision of skin neoplasms) (Stern *et al*., 1990). It is also indicated to expedite donor site healing after free flap harvest (Gravvanis *et al*., 2007). Pre-clinical *in vivo* data was achieved with studies involving female Yorkshire swine and the creation of full-thickness wounds. Wounds treated simultaneously with Integra™ and cell suspension demonstrate that cells remain viable, migrate through the Integra™ template and self-organise into differentiated epidermis (Wood *et al*., 2007). This matrix is a scaffold that is well tolerated by mice, pigs and humans and supports epithelial cell invasion and capillary growth and found its purpose as an immediate wound dressing for coverage to a dermal regeneration template that allows for the transition from an acellular matrix to specific host tissue. Integra™ has also been used extensively to study the *in vivo* kinetics of neo-vascularisation (Shaterian *et al*., 2009, Lindenblatt *et al*., 2008).

Matriderm™ is a native, structurally intact three-dimensional matrix of non-cross-linked bovine collagen I, III, V and elastin hydrolysate based dermal substitute and elastin hydrolysate available in sheets of 1mm or 2mm thickness, which allows for a one-stage reconstructive procedure. The extracellular matrix proteins serve as a scaffold for reconstitution of the skin and the modulation of scar tissue. The matrix serves as a support structure for the ingrowth of cells and vessels. Its elastin component improves the stability and elasticity of the regenerating tissue. As the healing process advances, fibroblasts produce their own extracellular matrix, and Matriderm™ is resorbed. Matriderm™ is currently highly favoured in the UK and the EU due to its one stage application. It has been found to be especially useful in the reconstruction of skin defects on the dorsum of the hand, increasing elasticity and pliability of the skin, when compared to controls with just split-thickness skin grafts (Ryssel *et al*., 2008).

In vitro studies using Matriderm™ show that large numbers of proliferating epidermal cells (keratinocytes and melanocytes) can be generated within 10-14 days and seeded onto the matrix. This enables easy and stable transport of such epidermal cells for up to 24 hours under ambient conditions, thus establishing a transport carrier system to transfer proliferating epidermal cells to human dermis *in vitro* (Ryssel *et al*., 2010). *In vivo* murine studies looked into the use of pancreatic stem cells combined with Matriderm™. These stem cells were found to significantly increase the epidermalisation, vascularisation and healing in full-thickness wounds (Salem *et al*., 2009). *In vivo* studies comparing the efficacy of Matriderm™ and Integra™ in the rat model showed that efficiency and quality of vascularisation expressed by take rate of epidermis, and thickness of resulting neodermis, were identical for both matrices (Schneider *et al*., 2009).

Terudermis® is an acellular multilayer collagen sponge matrix and silicon layer. The collagen sponge is dermis-like tissue made from bovine type I atelocollagen, derived from calf dermis (Tanihara *et al*., 2008). This is available in Asia and Japan where it is used to treat dermal defects secondary to trauma and iatrogenic wounds including mucosal defects such as cleft lip surgery, middle ear surgery and reconstruction after excision of oral mucosal neoplastic lesions and vocal cord scarring (Ohno *et al*., 2010. *In vivo* studies included evaluating the biodegradability of the synthetic polypeptide and its influence on epithelialisation, in the ear pad of the rabbit. Terudermis was compared to a chemically synthesised polypeptide (Pro-Hyp-Gly). This study showed that this chemically synthesized polypeptide may be useful as a scaffold for tissue engineering and tissue regeneration (Tanihara *et al*., 2008).

Renoskin® is a bilayer artificial dermis comprising a purified and stabilised bovine collagen layer with an overlying silicon sheet, the latter acting as a temporary epidermal substitute while providing some control for wound moisture control.

Promogran is a bovine collagen scaffold containing regenerated oxidised cellulose. It is thought that cellulose provides a substrate for binding to the matrix metalloproteases commonly found in chron-

ic wound beds (Juhasz e*t al*., 2010). This binding would lead to the inactivation of such enzymes through a substitution mechanism, thus preventing further degradation of the extra-cellular matrix, and thus facilitating wound repair (Kakagia *et al*., 2007).

Some dermal substitutes cannot be simply categorised as outlined above, due to varying degrees of overlap between the categories. Some of these are mentioned below. Orcel® is a bovine bilayer collagen matrix impregnated with allogeneic human dermal fibroblasts and epidermal keratinocytes cells on opposite sides (Bello *et al*., 2001). It is used in the US in the treatment of acutely excised surgical wounds such as in the release of burn contracture scars. It is particularly effective in the management of donor site wounds after harvest of split thickness skin grafts (Still *et al*., 2003).

Tissue engineering progress has led to the development of synthetic dermal replacements, in the stead of those described above of xenogeneic or allogeneic origin.

Hyalomatrix is comprised of a scaffold dermal replacement of esterified hyaluronic acid beneath a silicone membrane (Longinotti *et al*., 2014,). As hyaluronan is directly delivered to the wound bed, elasticity of the neodermis is improved while the silicone membrane acts as a temporary epidermal barrier (Myers *et al*., 2007). It was found to provide durable skin coverage in full thickness tissue loss (Erbatur *et al*., 2012).

Apligraf is a complex whole skin substitute, with a short shelf-life of 5 days. It is a living skin equivalent comprising type 1 bovine collagen and allogeneic fibroblasts as the dermal component and allogeneic neonatal foreskin-derived keratinocytes as the epidermal component (Zaulyanov *et al*., 2007).

It is worth mentioning that acellular dermal matrices are very often used as adjuncts in other procedures such as Strattice and Surgiderm (porcine acellular dermal matrix) in abdominal wall and hernia repair (Guerra *et al*., 2014) and breast reconstruction surgery (Spear et al., 2013). Cymetra and Surederm can be used to repair cartilage and vocal cords, and is available in an injectable form as a dermal filler in cosmetic procedures (Juhasz *et al*., 2010, Karpenko *et al*., 2003). Allopatch is a

minimally processed acellular human dermal scaffold which is used to treat tendinous injuries such as rotator cuff tears (Barber *et al*., 2009).

1.6.8 Limitations of dermal replacement scaffolds

Currently available skin substitutes for wound healing unfortunately fall short of the ideal dermal replacement scaffold as they exhibit a range of problems including wound contraction, scar formation, and poor integration with host tissue. Bioengineered dermal substitutes possess a similar structure that imitates the natural extra-cellular matrix. However, such replacement scaffolds still lack those structures and functions necessary to the skin's anatomy and physiology, leading to a compromise of form and function when compared to innate undamaged skin. Candidate scaffolds should allow surrounding cells to migrate fully into the scaffolds, enabling vasculogenesis and remodelling without invoking a chronic inflammatory response (Blackwood *et al*., 2008).

The number of dermal regeneration templates available is increasingly on the rise. The use of artificial dermis in surgery prolongs the length of time in theatre per visit only marginally (by a few minutes). Integration of the overlying split-thickness skin graft may take slightly longer than that with split thickness skin grafting alone (Greenwood *et al*., 2010). A porcine study examining the long-term outcome of 5 different dermal substitutes concluded that there was no scar difference in scar quality between the different scaffolds ((Integra™), ProDerm(®), Renoskin(®), Matriderm™ 2mm and Hyalomatrix(®) PA) and the control group. Further to this it speculated that the real only value of dermal replacement scaffolds might lie in the reduction in operating theatre time and inpatient stay in a one-stage reconstruction (Philandrianos *et al*., 2012) but there is no real advantage to a two-stage procedure. Many resources are currently invested into the research of the creation of the scaffold which will satisfy all essential and desirable criteria. Their immediate availability, stor-

age and long shelf life make it possible for large areas of skin loss to be treated in a timely manner, thus enabling more efficient and appropriate wound cover.

Advantages using human derived products include that fact that the resulting transplants do not contain animal ingredients and therefore less immunological rejection occurs than with xenografts. This is reduced further if the dermis is an allograft and less so if autologous to the patient. However, this then introduces a time lapse disadvantage until the skin is processed from the biopsy. It was also noted, in a murine comparative study (Truong *et al*., 2005), that human skin-derived products, produced the least contraction and the thickest neodermis in the healed full thickness cutaneous wounds, when compared to control or synthetically engineered dermal substitutes.

The added benefit of synthetic tissue-engineered and decellularised scaffolds, as opposed to those bearing cellular components, lies in the avoidance of antigenic eiptopes (Macadam *et al*., 2012). Infection and prion transfer potential remain small risks in naturally occurring dermal substitutes (Halim *et al*., 2010). Some religious groups find opposition to the use of animal-derived tissue being implanted into their bodies, with a resulting limitation and conflict over treatment options and surgical procedures. Abrahamic religions including Judaism and Islam find strong opposition against porcine products, while the Hindus consider the cow sacred and avoid beef products. It is now considered acceptable for members of the Jewish faith to undergo surgery using porcine products (Jenkins *et al.*, 2010). Followers of the Muslim faith are only permitted to use porcine surgical products in exceptional circumstances when all other options have been exhausted. Hindu religious leaders do not condone the application of bovine surgical implants (Easterbrook *et al*., 2012). Jehovah's witnesses believe that the Bible prohibits the transfusion of blood and the internment of human derived products, though this is usually reserved to cellular components of blood and some plasma-derived products (Jenkins *et al*., 2010).

The evolution of the dermal regeneration template has come a very long way since its inception. However, preferably, the new skin will exhibit all the features and functions of naturally occurring native un-injured skin, similar to its immediately surrounding skin. At present, dermal substitutes only partially address functional skin prerequisites (Shakespeare *et al*., 2005). These properties are largely inherent to the dermis and include pigmentation, and adnexae such as sensation, sweat glands and hair follicles, all of which are usually absent in skin grafts. Any wound typically contracts, and especially grafted wounds tend to contract and often have a snake or crocodile-skin appearance (due to commonly practiced meshing procedures) (Shevchenko *et al*., 2010). The ideal dermal regeneration template will reduce the inherent contractile property of scar tissue to a minimum and leave the skin texture as close to that of normal skin as possible. Another avenue for improvement is to reduce the 'seams' between normal skin and treated skin, thus rendering the transition less apparent. Animal-derived dermal replacements may represent other potential pitfalls. These include low thermal stability, nonspecific cell attachment, and susceptibility to contamination by infectious pathogens, such as prions, which may transfect humans inflicting deleterious conditions (Tanihara *et al*., 2008).

Synthetic creation of dermal templates using methods such as electrospinning is seen as advantageous due to the possibility to determine and tailor scaffold pore size and uniformity (Rnjak-Kovacina *et al*., 2011). Hyaluronan also appears to be a very promising component of scaffolds, as it significantly enhances *in vitro* cell infiltration and *in vivo* tissue ingrowth, as well demonstrating interactions with cell surface receptors to activate signalling pathways conducive to cell migration (Li *et al*., 2012).

1.6.9 Conclusions

In summary, in order for Smart Matrix™ to be "fit for purpose", it needs to fulfil the following requirements:

- Suitable long-term graft survival with adequate or improved scarring parameters
- Superiority to the current gold standard (split thickness skin grafting alone) and to the alternative of allowing a wound to heal by secondary intention
- Non-inferiority to the dermal scaffolds currently most commonly used (Integra™ and Matriderm™).
- Improvement of the wound healing trajectory in the challenging wound

1.7 A review of the literature of the pre-clinical compromised wound healing models to evaluate dermal replacement scaffolds

1.7.1 Introduction

As research into regenerative skin technologies continues to evolve, more products make their way to patients. The translation from bench to bedside is a long and arduous multi-step journey, in which multiple *in vitro* and *in vivo* studies are required. The real value of wound healing adjuncts lies in their ability to heal a refractory wound. In the planning of this research project, it was thought to be of value to examine the healing trajectory of Smart Matrix™ in both the acute wound setting as well as the challenging wound setting. While the acute full thickness excisional porcine wound is standardised, a literature review was carried out to find a reliable reproducible pre-clinical model of attenuated cutaneous wound healing.

The animal model chosen depends heavily on the research topic in question, the product to be tested, as well as the clinical scenario to be simulated (Middelkoop *et al*., 2004). Currently the gold standard utilises full thickness excision wounds to evaluate experimental materials and advanced therapies (Middlekoop *et al*., 2004). The most commonly accepted and widely used model is the porcine skin, as this most closely bears semblance to the wound healing physiology and anatomy of human skin. (Philandrianos *et al*., 2012). (Kangesu, 2002, Sullivan *et al*., 2001, Ramos *et al*., 2008). Rodent skin anatomy and physiology bears the next closest semblance to human skin (Gallant-Behm *et al*., 2009, Wang *et al*., 2010). Pig studies showed 78% agreement in wound healing with human skin, while small mammal studies showed 53%, and *in vitro* studies showed 57% agreement (Sullivan *et al*., 2001). Less frequently, other models such as the rabbit model are used too. The impact of these differences on wound-healing studies has been recognised since at least 1915 (Spain 1915). It stands to reason, that an accurate model of human wound healing should use an animal that similarly reflects human skin characteristics.

The creation of wounds in animals seeks to reproduce specific clinical scenarios. Simulation of attenuated wound healing requires modulation of wound repair rates. This may be achieved at either systemic or local levels, - by modifying the host response through the use of genetically modified animals or by local alteration of the insult or anatomical site. To date, few animal models simulate such challenging wounds in a reliable, reproducible and cost-effective manner. This means that our ability to simulate or predict the outcome of advances wound healing and reconstruction treatments and biomaterials is very limited. Common challenging wounds occurring in humans include venous and arterial ulcers, decubitus ulcers, diabetic wounds and those resulting from complex trauma or iatrogenic events such as radiation. Aetiologies in different species pertain to differences in habitat, in cutaneous sensitivity, genetics and immunology among other contributing factors (Swaim *et al*.,1993).

Furthermore, the American FDA (Food and Drug Administration) guidelines advocate the use of multiple relevant (ie selected species should exhibit a biological responsiveness to the test product) animal models to assess the effectiveness of wound treatments, to help establish pharmacological responses, as well as assess potential toxicities of wound-treatment products (www.fda.gov.us, 2006).

1.7.2 Aims of review

This review aimed to catalogue the laboratory mammal *in vivo* attenuated wound healing models used. Its objectives included considering how challenging wounds are created, and appraising different models' advantages, disadvantages, reproducibility and reliability, and their application and extrapolation to clinical scenarios. The aim of this review was to determine the optimal pre-clinical compromised wound healing model.

1.7.3 Methods

A systematic review was conducted using PRISMA principles. This was initially carried out in May 2011 and revised for contemporaneity for the writing of this thesis in December 2016. A sensitive search strategy was built in conjunction with an information scientist, then applied to AMED, PUBMED, MEDLINE, EMBASE, Web of Science and the Cochrane Library (including CENTRAL as a source of grey literature from inception) until December 2016. A MESH index and free text terms were used with no language restrictions (google translate was used where necessary). Abstracts for search results were screened using pre-specified stepwise criteria. Data were extract-

ed and if appropriate, meta-analysis would be performed. Otherwise, narrative synthesis was performed. The search strategy included the following terms: animals, disease models, attenuated, chronic, ischaemic, delayed (in conjunction with wounds and animals), skin dermis, epidermis, cutaneous, cicatrix and biofilms (duplicates were removed). Risk of bias was assessed using the Cochrane risk of bias tool for randomised control studies, the ROBINS-I tool for observational studies, and AMSTAR for systematic reviews.

1.7.4 Results

Four hundred and twenty five articles were included after screening 1751 results. No systematic reviews or multi-centre trials were found. There were 11 articles which reviewed the literature pertaining to animal models for challenging skin wound healing. In 2003, Sisco and Mustoe reviewed animal models for cutaneous ischaemic wound healing, particularly in the rabbit and in the rat (Sisco *et al*., 2003). Middelkoop *et al* reviewed porcine wound models for skin substitution and burn treatment in 2004 (Middelkoop *et al*., 2004). Salcido *et al* reviewed animal models for pressure ulcer research in 2007 (Salcido *et al*., 2007), while in 2008, Olerud reviewed models for diabetic wound healing and healing into percutaneous devices (Olerud, 2008). In the same year, Perez *et al* discussed the relevance of animal models for wound healing (Perez *et al*., 2008). A review of external traumatic infected animal wound models was published in 2011. This reviewed experimental infections created in animal models of surgical wounds, skin abrasions, burns, lacerations, excisional wounds and open fractures (Dai *et al*., 2011). More recently, Ansell *et al* published a review article titled “Animal models of wound repair: are they cutting it?” This article reviewed commonly applied models and their limitation, in a bid to provide direction for the future development of new models (Ansell e*t al*., 2012). King reviewed animal models for type 1 and type 2 dia-

betes in 2012 (King, 2012). Avci *et al* published a review of animal models of skin disease for drug discovery in 2013 (Avci *et al*., 2013). This included chronic wounds. In 2014, Nunan *et al* discussed the challenges researchers face to re-capitulate the clinical complexity of a cutaneous chronic wound in an animal model. Again, the most commonly employed models and their limitations were discussed (Nunan *et al*., 2014). In the same year, Abdullahi et al discussed the various animal models used in burn research. (Abdullahi *et al*., 2014). In 2015, Seaton *et al* reviewed porcine wound models for cutaneous healing (Seaton *et al*., 2015).

Studies included description and / or validation of a model, or the use of different models of compromised wound healing to evaluate the use of drugs or medical devices. Employing an attenuated wound model, 312 articles used rat and mouse models, 8 articles used guinea pig models, 42 articles used rabbit models, 3 articles used dogs and 1 article used sheep and 36 articles used pigs. Methodological quality varied. Three papers describes comparative studies, 17 included technical descriptions of methods, while the remainder mentioned the use of techniques to compare different treatment modalities.

Various techniques to compromise cutaneous wound healing were identified. These can be categorised according to the animal used, according to whether the modification was local, systemic or genetic, or according to the pathology being simulated. There appears to be considerable variation in what was considered “compromised” or “attenuated” wound healing based on inferences from studies. Many methods of creating wounds in animals have been described, in both the acute and compromised wound settings. These include abrasions, full thickness incisions, partial thickness (epidermis and varying amounts of dermis) excision wounds, full thickness excision (entirety of dermis) wounds and varying degrees of burns (Davidson 1998). In the studies reviewed, burns were created through the application of a heated metal (brass, steel or copper) rod (Sheu *et al*., 2014) or flask filled with hot liquid (Cuttle *et al*., 2006) and applied to the anaesthetised pigs’ flank or to anaesthetised mice. Scalds (Brans e*t al*., 1994) and flame burns were also described, with con-

trol of the total body surface area and depth of the burn wound. Burning of smaller mammals such as mice, rats and rabbits, involves shaving the area to be burnt (to ensure uniformity of depth and distribution). The animal is then placed on its back in a template constructed of a flame resistant mould with the window exposing a predetermined surface area of skin, which is then immersed in a water bath set to a pre-determined temperature (600-800C) for the necessary amount of time to inflict a partial or full thickness burn (Abdullahi *et al*., 2014). The larger the animal, and the thicker the skin, the longer then amount of time needed to inflict the desired injury (Mitsunaga *et al*., 2012). All these procedures are carried out with appropriate sedation, anaesthesia and pain relief.

1.7.5 Animal models

1.7.5.1 The murine model

The murine model refers to mice and rats interchangeably. As the literature review revealed, this has been used extensively. Wistar and Sprague-Dawley rats were the breeds found to be most commonly used in this literature review.

Modulation of local tissue to attenuate the wound healing response

Ischaemia

In 2005, Gould *et al* described a validated model of an ischaemic wound, using a dorsal bipedicled skin flap. A wound was later created in the central area of this flap (Gould *et al*., 2005). This wound demonstrated reduced vascularisation, with increased inflammation and delayed wound closure. This model was later modified by Trujillo *et al* through the placement of a silicone sheet immediately beneath the flap, thus preventing re-vascularisation and reducing wound contraction, as wound healing takes place (Trujillo *et al*., 2015).

The creation of an ischaemic limb was described by Niiyama *et al* in 2009, as a model for peripheral arterial disease in order to test new therapies. The hind limb of a rat is rendered ischemic through the ligation of the common femoral artery (Niiyama *et al*., 2009). Brenes *et al* further described high femoral artery ligation and total excision of the superficial femoral artery to render the limb severely ischaemic (Brenes *et al*., 2012).

Pressure ulcers

Sadler *et al* described the *in vivo* replication of pressure ulcers using 2 magnets on a pinch of dorsal skin of anaesthetised mice. As pressure ulcers are thought to form due to an ischaemia–reperfusion cycle, 3 12 hour cycles of ischaemia were used to create a pressure sore: full thickness skin loss with necrosis and damage of the underlying subcutaneous tissue (Stadler *et al*., 2004). A similar method involves implanting a metal plate subcutaneously, followed by periodic compressions using an external magnet. These model is advantageous as it does not limit the mobility of the animal (Peirce *et al*., 2000 and Wassermann *et al*., 2009).

Maldonado *et al* described the placement of human full thickness skin grafts onto the dorsum of male, non-obese, diabetic/severe combined immunodeficient mice, which were later subjected to pressure similar to the method described by Stadler, but using a pinch device (similar to a clothes peg) that delivered a constant pressure of 150mmHg in 3 cycles of 8 hours clamping with 16 hour release breaks. This resulted in irreversible tissue ischaemia which in turn led to tissue necrosis, observed as an ulcer on the edges of the compression device and in the underlying deep dermal and subcutaneous tissue(Maldonado *et al*., 2014).

Radiation

In humans, it is known that skin that has undergone treatment with radiation exhibits a delayed and compromised healing response (Hopewell *et al*.,1990, Gu *et al*., 2002). A rat model of impaired

wound healing was established and described by Schwentker *et al* in 1998, where a random-pattern dorsal skin flap was created in an area exposed to a single radiation exposure of 20 Gy. The resulting wound showed diminished scar formation and wound breaking strength, when compared with controls (Schwentker *et al*., 1998). In 2011, Takikawa *et al* described the effect of different radiation doses on mice. Exposure of 15 Gy led to de-pigmentation and depilation, exposure of 20 Gy resulted in minor skin erosions or ulcers in most rats, while exposure to 30 Gy resulted in non-healing wounds. Additionally, full thickness wound defects were created in skin exposed to 20 Gy. These wounds demonstrated delayed wound healing when compared to non-irradiated skin (Takikawa *et al*., 2011). However, a more recent study showed that that irradiation of the mouse lower limb at ~ 15 Gy might be a more appropriate model for basic research into wound healing in irradiated skin, than higher doses on the dorsum, as wounds showed delayed healing with lower inflammation and no necrosis. One study that utilised whole body gamma irradiation. Full thickness wounds were created on the dorsum of Swill Albino mice, to study wound healing parameters. Wound contraction and healing were delayed in the mice that underwent whole body irradiation (El Hamoly *et al*., 2015).

Ultraviolet (UV) damage

UV radiation-induced connective tissue damage in murine models started in the 1960s, when normal mice were used. Hairless mice were adopted in the 1980s as their skin was more similar to human skin (Benavides *et al*., 2009). Currently, the most commonly used hairless mouse for studying photoageing is the albino Skh-hairless-1 (Kligman, 1996). UV induced damage is used to study both the ageing skin and the delayed wound healing responses associated with sun damage and high doses of irradiation (Davidson *et al*., 1991).

Chemical insult

Necrotic skin ulcers have been induced in mice using a single intradermal injection of doxorubicin (0.05 mg; 1 mg/ml). The ulcers reached maximum size between 5 and 10 days after injection (Rudolph *et al.*, 1976). This model has been used to examine various wound treatments and dressings. In 2016 Maeda *et al* described the use of the accepted bleomycin-induced scleroderma model as a model for wound healing retardation. A full thickness wound was created in the sclerosed skin of nude mice following locally injected bleomycin (Maeda *et al*., 2016).

Infection

Infection may prolong the inflammatory phase of wound healing, such that it renders the wound chronic (Guo, *et al*., 2010). Various forms of wound infection are used, ranging from plain wound inoculation to the creation of biofilms. Wounds are most commonly inoculated with *Pseudomonas aeurginosa*, *Staphylococcus aureus* or *Escherichia coli*. Many types of wounds can be infected. These include linear incisions, burn wounds, partial thickness wounds and full thickness excisions. The most common mouse strains used are BALB/c, CD-1, CF-1, C57/BL, as well as mutant diabetic mouse, SCID bg mouse. The major strains of rat used are Sprague-Dawley, Lewis and Wistar (Dai *et al*., 2011).

<u>Systemic modulation to attenuate the wound healing response</u>

Diabetes

Diabetes mellitus sufferers are more prone to developing indolent lower limb wounds. The most commonly used animal model of human diabetes is the chemotherapeutic agent streptozotocin (STZ)-induced type 1 diabetes in the rat (Wei *et al*., 2003). This is a relatively simple and cheap model, that can sometimes also be used in higher animals (Dufrane *et al*., 2006). In this review, this was also found to be the most commonly employed model of compromised cutaneous wound healing. Alloxan is also a commonly used agent. Both these agents compete competitively with

glucose for insulin-secreting pancreatic β-cells due to similar structures (Bansal *et al*.,1980). The substances are injected subcutaneously, intra-peritoneally or intravenously (Szkudelski, 2001), either as a single dose or as multiple low doses. Hyperglycaemia usually occurs a few days following injection. Limitations with these models include the relatively narrow diabetogenic dosing and the toxicity to other organs, especially the kidney (Szkudelski, 2001).

Steroids

In 1999, Gupta *et al* described the validation of a delayed full-thickness excision wound-healing model. Systemic immunocompromise was achieved through the injection of intra-muscular hydrocortisone (40mg/kg) in male rats. 8mm full thickness excision wounds were later created, and their healing parameters evaluated. The immunocompromised state was confirmed through the observation of splenic and adrenal gland atrophy, significantly reduced of circulating lymphocytes and increased neutrophils. The wound edges contracted less than controls and took significantly longer to epithelialise (Gupta *et al*., 1999).

Stress

Chronic stress impairs wound healing through the activation of the hypothalamic-pituitary-adrenal axis, and subsequent elevated levels of circulating glucocorticoids, which have been shown to delay wound closure (deAlmeida *et al*., 2016). Chronic stress can be induced in the murine models in one of several ways: rotational stress, restraint stress, shaking, social defeat, tilted cage, hot air stream, overnight illumination and inverted light cycle (Monteiro *et al*., 2015). Restraint, rotational stress has been employed quite frequently in the study of impaired cutaneous wound healing, where the subject is stressed over a number of days both pre and post-wounding (Padgett *et al*., 1998).

Ageing

In 2012, Soybir *et al* published literature stating that wound healing progressed at a slower rate in aged rats following a cutaneous incisional wound, when compared to their younger counterparts (Soybir e*t al*., 2012). Ageing in mice was associated with lower tensile strength in the initial stages of the wound healing process, but greater tensile strength later on, while ageing in rats was associated with early lower tensile strength difference between young and old rats later in healing wounds (Kim *et al*., 2015).

Malnutrition and metabolic disease

Tanaka *et al* described a delayed healing model of by creating a full-thickness skin wound on the dorsum of rat with induced malnutrition secondary to restricted food intake. Wound healing was prolonged compared to that of well-nourished animals (Tanaka *et al*., 1994). Otranto *et al* studied the effects of various degrees of protein restriction on cutaneous healing in Wistar rats. This study showed that animals exposed to slight protein restriction present disturbed wound healing, but animals exposed to severe protein restriction present impaired wound healing. (Otranto *et al*., 2009). Buck *et al* described inoculating nude mice with Chinese hamster ovary cells secreting TNF-alpha to induce cachexia. These mice showed a decrease in collagen synthesis, and displayed impaired healing of incisional and excisional skin wounds, compared with control animals (Buck e*t al*., 1996).

As obesity can impair wound healing, Eo *et al* described a study examining a therapeutic measure using obese mice. Obesity was induced using a high fat diet for 10 weeks (Eo *et al*., 2016).

<u>Genetic modulation to attenuate the wound healing response</u>

The use of transgenic and knockout animal models allow for the creation of wounds which resemble in behaviour chronic wounds such as diabetic wounds, due to the action and/or absence of certain proteins which are critical to normal wound healing (Martin *et al*., 1997).

Diabetes

Rodent models for diabetes include spontaneous NOD mice, BB rats or LEW.1AR1/-iddm rats, where pancreatic beta-cell destruction occurs due to an auto-immune process or genetically induced AKITA mice.

Genetically diabetic mice have been extensively used to improve understanding of diabetic and compromised wounds and to examine the effects of various wound dressings and wound healing adjuncts (including acellular dermal matrices) dressing on the compromised wounds, on the basis that the diabetes would mirror human compromised wound healing behaviour. One shortfall of diabetic mice is their inability to thermoregulate, which could lead to increased mortality during studies.

Immunocompromise

MMP9-null mice as well as athymic mice have been used to study the effects of wound healing adjuncts. This is because matrix metalloproteinases have been shown to positively participate in the wound healing response, in particular the inflammatory phase, extracellular matrix remodelling, angiogenesis and epithelial remodelling (Kyriakides *et al*., 2009). Genetic murine models also include (among others) models for metabolic syndrome, skin tight mice, various skin pathologies, sickle cell athymic mice and immunocompromise (athymic, nude and SCID mice).

Limitations of the murine model

The murine model has not been found to be truly representative of the human cutaneous situation, due to the distinct physiologic and anatomical differences. These animals also have a thinner dermis and epidermis and an increased number of hair follicles, the presence of a *panniculus carnosus* muscle and an innate ability to heal infected wounds (Sullivan *et al*., 2001, Trujillo *et al*.,

2015). Their wounds heal mainly through contraction rather than epidermal cell migration (Schierle *et al*., 2009).

1.7.5.2 The guinea pig model

In addition to the burn methods described above, sulphur mustard has been used in the hairless guinea pig to create both superficial and deep cutaneous burn defects in the guinea pig. As the reaction is dose-dependent, this model can be used to simulate long-term injuries (Dachir *et al* .,2012). Experimental hypertrophic scars were created using an excision of the panniculus carnosus and treating the resulting wound with coal tar. This wound model remains to be validated (Aksoy *et al*., 2002). The guinea pig belongs to the rodent family and hence limitations are as described above.

1.7.5.3 The rabbit model

<u>Modulation of local tissue to attenuate the wound healing response</u>

Ischaemia

Ahn and Mustoe described using the rabbit ear model to attenuate healing using delayed epithelialisation, thus resulting in prolonged inflammation and hypertrophic scarring (Said *et al*., 2005). Ischemia is induced through the ligation of the caudal and central arteries and dermal circulation circumferentially, so both ears are perfused only by the rostral artery, preserving the caudal, central, and rostral veins. Wounds were then created in the ear. The ischaemic ear was found to more truly represent the compromised wound healing model (Ahn *et al*., 1990). This was then used to research various treatment modalities for hypertrophic scarring (Kloeters *et al*., 2007, Kryger *et al*., 2007).

Infection

Further to this work, another study was carried out by Seth *et al*., in 2012, introducing bacterial biofilms into the ischaemic rabbit ear model. Through blood supply modulation prior to wound creation, a host-related variable was introduced into the interaction between the wound bed and bacterial inoculum. This is otherwise rather difficult to appropriately simulate in other published *in-vivo* models. The biofilm wound model for wound chronicity and complexity simulation has been studied quite extensively to evaluate different wound treatment modalities such lavage, silver sulfadiazene application and debridement on established *Pseudomonas aeruginosa* biofilm wounds (Seth *et al*., 2012). This is due to the fact that biofilms are thought to be a major (65-80%) contributing factor to human non-healing wounds undergoing anti-microbial treatments (Metcalf *et al*., 2013).

The persistent hind limb ischaemia model in rabbits has been used to examine treatment modalities for ischaemic ulcers and for purposes pertaining to vascular surgery. The distal external iliac artery is ligated and the common and superficial femoral arteries are excised. These rabbits then go on to develop superficial necrotic wounds on the foot, while some others are wounded in order to create a specific defect (Pu *et al*., 1994).

Hypertrophic scarring model

A hypertrophic scarring model was described in which 6mm wounds were created on the dorsal or ventral surfaces of the rabbit ear. Seventy per cent of these wounds formed excess dermal scarring similar macroscopically and microscopically to human hypertrophic scars (Li *et al*., 2001)

<u>Systemic modulation to attenuate the wound healing response</u>

Diabetes

Wang *et al* created create a long-term model of diabetes by injecting a single dose of alloxan monohydrate (100 mg/kg) intravenously to New Zealand White rabbits. Hyperglycaemia is confirmed

within 10 days of injection and biopsies of multiple organs showed diabetic change (Wang *et al*., 2010) while skin wound showed a delay in healing.

The rabbit ear ischaemic model was also used in alloxan–induced hyperglycaemia in rabbits (with no vascular compromise) to study the effects of fibrin scaffolds on (Breen *et al*., 2008) gene transfer from adenovirus encoding endothelial nitrous oxide synthase. This study was used to provide insight into improving wound healing in diabetic foot ulcers.

1.7.5.4 The canine model

The greyhound dog has been used in an attempt to recreate decubitus ulcers, as its hind leg is covered by relatively thin skin and a paucity of subcutaneous fat (Swaim *et al*., 1993). The ulcer was created using a cast with increased pressure areas over the bony prominences. Type 1 diabetes can be induced in the dog using streptozocin or a partial or total pancreatectomy procedure (King *et al*., 2012). The use of clinical companion animals (such as dogs and cats) as translational models for cutaneous wound healing has yet to be established. (Volk *et al.*, 2013)

1.7.5.5 The porcine model

Different breeds of pig exhibit responses to wounding that parallel those observed among humans of different ethnicities. As such, porcine models serve as excellent experimental models to study various aspects of human wound healing (Middelkoop *et al*., 2004).

The wound healing mechanism of porcine skin closely resembles that of humans in that it heals through epidermal cell migration and has a similar cutaneous vascular supply (Hadad *et al*., 2010). Like humans, they have a relatively thick epidermis with distinct dermal papillae, rete pegs, and a dense dermal elastin and collagen fibre network. Porcine skin adheres to underlying structures, similar to human skin (Davidson *et al*., 1998). Like the human epidermis, the pig's skin turnover time is approximately 30 days and the immune cells in pig skin include dendritic cells similar to

those in human skin (Seaton *et al*., 2015). Hence this animal has become the gold standard for pre-clinical studies pertaining to skin wounds and their treatments. It also remains the most commonly applied wound model due to similarities in size of wound and animal (Debeer *et al*., 2013). However, porcine skin heals with a lower tendency to form abnormal scars (Rittie *et al*., 2016).

Modulation of local tissue to attenuate the wound healing response

Many articles describe the modulation of local areas of tissue to simulate a compromised wound healing environment. These include rendering tissue ischaemic, creating localised pressure to mimic pressure ulcer pathology, induction of infection, irradiaton, chemical burn creation and foreign body insertion.

Ischaemia

Bipedicled myocutaneous flaps measuring 5 x 15cm (ratio 1:3) were created on the dorsum of pigs (Roy *et al*., 2009, Kerrigan *et al.*, 1986). The skin and muscle were then separated to prevent cutaneous revascularisation. These skin areas were thus rendered ischaemic. The decreased blood supply was confirmed through Laser Doppler. Full-thickness wounds were created in the most vascularly compromised areas of this tissue (Roy *et al*., 2009). These wounds showed delayed macrophage infiltration and epithelialisation, and hence were confirmed as a reproducible wound model for ischaemic ulcers (Seaton *et al*., 2015).

Pressure

The leading cause of pressure ulcers is believed to be the prolonged pressure on the skin overlying a bony prominence, with various other contributing factors such a poor nutrition, immobility, moisture, lack of sensation and shearing forces amongst others (Maklebust *et al*., 1987). Many local and systemic methods have been employed in the porcine model to reproduce decubitus ulcers.

Initial studies described complete spinal cord transection, rendering the pigs immobile and insensate (Dinsdale 1974, Daniel *et al*., 1981. In a subsequent study, pigs were rendered monoplegic through the unilateral transection of the first lumbar nerve root. Some time later, disks were applied to the affected dermatome with constant pressure for 48 hours. This resulted in relatively uniform full-thickness pressure sores extending to bone (Hyodo *et al*., 1995). This latter wound model was associated with significantly decreased morbidity and mortality when compared with the initial models describes (Seaton *et al*., 2015).

Radiation

The effects of radiation have been studied in some depth to assess and characterise the reaction of porcine skin to different doses (Kim *et al*., 2013). In 1998, Bernatchez *et al*, described the validation of a delayed porcine wound healing model that using single dose (1500Rad) irradiation of the dorsal skin (under general anaesthesia) prior to creation of the surgical wounds. Histological examination confirmed a delay in formation of granulation tissue, angiogenesis and filling out of the wounds. Newly formed blood vessels were larger and more irregular than controls. (Bernatchez *et al*., 1998). Hadad *et al* employed electron beam radiation to create a delayed wound healing response in the porcine model to study the capacity of adipose derived stem cells to improve healing rates of perfusion-depleted tissue (Hadad *et al*., 2010).

Infection

An infective inoculum was introduced to porcine partial and full thickness wounds to model burn wound sepsis. *Staphylococcus aureus* was used to inoculate burn wounds sealed and incubated in watertight chambers. Other burn wounds similarly treated but without the infective inoculum were used as controls. Infection (with pus, inflammation and necrosis) occurred in the inoculated group,

while only contamination with *Staphylococcus epidermidis* occurred in the control group (Brueing *et al*., 2003).

Foreign bodies

In 2013, Jung *et al* described the placement of silicon struts subcutaneously and into wounds created in pigs' flanks for varying amounts of time, up to 21 days. Findings consistent with human chronic wounds, suggested that this may be a suitable wounds model. These included elevated TNF-α, IL-1β, and IL-6 expression and decreased tissue perfusion (as measured by Laser Doppler) at the wound edges compared with control wounds (Jung *et al*., 2013).

Burns

Andrews *et al* described a scald burn model in 2016 using Large White Pigs, allowing for the the pathophysiology of scald burn wound creation and progression to be examined. Differeing degrees of hot fluid for different durations of time were applied and the wounds were then examined macroscopically and microscopically. This model was created to simulate the burn injuries children often present with: partial thickness burns secondary to scalding (Andrews *et al.*, 2016).

Chemical burns

Various chemicals such as sulphur mustard burns have been employed to induce wound compromise. Sulfur mustard [bis(2-chloroethyl)sulfide] is a potent incapacitating chemical warfare agent (Graham *et al*., 2002) which causes cutaneous lesions that take several months to heal. This prolonged healing process is due to cells at the margin that cannot replicate because of DNA damage, and due to compromise of the dermis that fails to provide a satisfactory matrix over which epidermal cells can ingress and seal the wound. Graham *et al* reproduced sulphur mustard burns in the porcine wound model to study the effects of various wound treatments. Chemical burns including cal-

cium, Brown recluse spider venom or doxorubicin to create dermonecrotic lesions have also been used historically. Chemical burns are mainly limited to larger animals as in smaller animals, the toxicity caused by these relatively small doses, would disallow further studies.

Systemic modulation to attenuate the wound healing response

Diabetes

The type 1 diabetic porcine model has been used quite frequently. Grussner *et al* described inducing long-lasting diabetes using 150 mg/kg Alloxan in female Yorkshire Landrace pigs (Grussner *et al*., 1993). A compromised porcine wound-healing model was established by Velander *et al* in 2008 using this method. Full-thickness wounds created on the pigs' dorsum were examined. Wound fluid showed significantly lower IGF-1 and TGF-β concentrations, when compared to non-diabetic pigs. Epithelialisation was also much slower in the diabetic group (Velander *et al.*, 2008). This model has been subsequently employed many times, to evaluate various wound dressings (Velander *et al*., 2009) and in combination with other methods of wounds compromise, such as burns (Singer *et al*., 2009) and sepsis (Hirsch *et al*., 2008). Type 1 diabetes can also be established in the pig through pancreatectomy (Morel *et al*., 1991, Mellert *et al*., 1998). This procedure however, is associated with considerable morbidity due to the complexity of the procedure, ensuing hypoglycaemia and pancreas exocrine insufficiency. The latter can be off-set by isolated islet autotransplantation. This results in a very representative model of human type 1 diabetes (Matsumoto, 2010).

Genetic modulation to attenuate the wound healing response

Porcine transgenic models are less commonly employed than murine ones. Research into the breeding of transgenic pigs that represent human disease has progressed over the last three decades. The results have been fruitful in diseases such as Alzheimer's and amyloidosis, but representative models for challenging wound healing are yet to be elucidated. Novel genetic engineering technologies

allowing the incorporation of transgenes into specific genomic target sites (Whitworth *et al*., 2014) appear promising, and may make transgenic pigs an increasingly useful tool for studying wound healing (Seaton *et al*., 2015).

Hypertrophic scarring models

Though not technically employed as attenuated wound healing models, it is worth mentioning that the Red Duroc pig is used as a model to study hypertrophic scarring – raised vascular inflexible scars confined to the wound margins (Mancini *et al*., 1962, Peacock, 1970). This was first described in 1976 and the model validated in 2004 (Zhu *et al*., 2004). The Red Duroc pig was found to more closely resemble human scarring, than the Yorkshire pig, which is more commonly used for cutaneous wound healing studies. While the Yorkshire and large white strains heal relatively scarlessly, the Red Duroc pig, exhibits a tendency for hypertrophic scarring similar to that seen in human skin (Zhu *et al*., 2004, Gallant-Behm *et al*., 2008). This difference is attributed to intrinsic differences in key aspects of the fibroblast response to injury (Harunari *et al*., 2006, Sood *et al*., 2015).

Limitations associated with the porcine wound model

While the porcine wound model has been established as the gold standard, its limitations as a truly representative cutaneous wound healing model must be acknowledged. The skin-associated appendages such as eccrine glands are not found in most laboratory animals including rodents, rabbits or pigs, as they are unique to some primates including humans (Rittie *et al*., 2013). The importance of other appendages such as hair bearing follicles, melanocytes and sebaceous glands are present for their distribution varies widely between subspecies and from human skin. On the basis of the known importance of other skin appendages (hair follicles, apocrine glands, and sebaceous glands)

for wound repair in humans, animal models are not yet truly representative. Hair distribution and/or density differ between mammalian species as does the sweating mechanism.

Another limitation to using the porcine model is the financial implication. Porcine animal models are associated with substantially more expensive purchasing, housing and feeding costs (Middelkoop *et al*., 2004), as well as the necessity for professionally trained staff to anesthetise and look after the animals. It is also more difficult to breed transgenic pigs, than it is other smaller animals (Seaton *et al*., 2015).

1.7.5.6 The primate model

Similar to domestic and companion animals, the use of primates for experimental purposes is met with much adversity due to ethical issues and human affinity towards these animals. Diabetes may be induced using partial or total pancreatectomy sometimes associated with concomitant use of streptozocin (King, 2012, Thomson *et al*., 2010) or through alloxan or streptozocin administration alone (Wei *et al*., 2011). The value of the primate model would lie in its concordance with hair distribution, epidermal thickness and melanocyte deposition to human skin (Montagna 1966), with variation between species.

1.7.6 Discussion

Despite intensive research into understanding challenging wound healing and pathophysiology, developing wound care strategies remains a formidable challenge in human health care. While *in vitro* investigations and *in vivo* studies performed in laboratory animal models provide valuable fundamental information, the lack of concordance with human pathophysiology has been identified as a major impediment to translational research in human wound care. Hence, the identification of

superior clinical models for challenging wounds remains a high priority for human wound healing research. A successful, translational wound healing model should function as a bilaterally flowing intellectual ecosystem between basic science and clinical investigators. The porcine skin model remains the gold standard as it shares many similarities in hair follicle and blood vessel patterns, with slight hair distribution and density discrepancies. Biochemically, the porcine dermis has a collagen and elastin content that is more similar to humans than the other mammal models (Heinrich *et al*., 1971). Additionally, pigs survive long enough to be functional for long term studies into wound healing and are of sufficient size to provide multiple samples. It is true that as yet, no mammal has been found to be truly representative of human skin. As porcine skin exhibits the closest semblance, with a concordance of 78% (Sullivan *et al*., 2001) it is the superior *in vivo* pre-clinical model available.

Animal models have been used quite successfully to provide insight into cutaneous wound healing and the to examine the efficacy of wound healing adjuncts. Many endeavours to create and simulate a challenging wound in large mammals have made significant contributions to the characterisation of such wounds as well as to the assessment of healing adjuncts. However, to date, such a model which is cost-effective and easily reproducible while conforming to ethical guidelines remains to be elucidated.

1.7.7 Conclusion

This review revealed a paucity of pre-clinical animal wound models that reliably represent the human challenging wound. The ideal chronic wound model would use the pig in a cost-effective, reliable safe and easily reproducible manner.

Chapter 2: Aims of research

The aim of this research is to evaluate the wound healing behaviour of Smart Matrix™ in in a range of applicable contexts.

This will be achieved through:

1 The investigation of the long-term (six weeks and six months) healing trajectory and survivability of a split thickness skin graft (STSG) applied as a single stage procedure onto the Smart Matrix™ scaffold in a porcine acute wound healing model, and the comparison with that of STSG alone and wounds allowed to heal by secondary intention.

2 The comparison of wound healing of SM + STSG with that of Matriderm™ + STSG and Integra™ + STSG in the acute wound.

3 The evaluation of a novel porcine wound model of attenuated wound healing – the partial thickness excision of a full thickness burn.

4 The evaluation of the wound healing trajectory of SM + STSG in the attenuated wound model and its comparison to that of MD + STSG.

Chapter 3: Methods and Materials

The majority of methods and materials are common to the four experiments reported in this thesis. To avoid repetition they are described in detail in this chapter.

3.1 Smart Matrix™ manufacture

The production of porous dermal scaffolds from human fibrin/alginate for pre -clinical assessment was performed in sterile conditions in RAFT's laboratory. While exact formulation details are confidential, fibrinogen and alginate were blended together with thrombin, and then incubated at 37C for 30 minutes. Cross-linking of scaffolds was achieved by glutaraldehyde. Scaffolds were then washed with sodium borohydride for 12 hours, followed by water and finally soaked in sorbitol then freeze dried.

3.2 The *in vivo* porcine model

Pre-clinical evaluation of tissue scaffolds was performed in the porcine full thickness wound healing model for experiments 1 and 2, and in the porcine partial thickness excision of a full thickness burn model in experiments 3 and 4.

3.2.1 Regulatory Guidelines

The UK Home Office controls scientific procedures on animals in the UK and does so by the issue of licences under the Animal (Scientific Procedures) Act 1986. The regulations conform to the European Convention for the protection of Vertebrate Animals Used for Experimental and Other Scientific Purposes (Strasbourg, Council of Europe).

3.2.2 Species

Large White/Landrace female crossbred pig (Sus *scrofa domestica*) were used, weighing approximately 50-55kg on arrival. These were supplied by Hygene Pigs, Redwood Farm, Caxton Road, Great Gransden, Sandy, Bedfordshire, SG19 3BQ.

3.2.3 Site

All porcine *in vivo* studies were carried out at Northwick Park Institute for Medical Research (NPIMR), Harrow, UK.

3.2.4 Justification of test system

The current state of scientific knowledge did not provide acceptable alternatives, *in vitro* or otherwise, to the use of live animals to accomplish the purpose of this study. Pigs are the most representative species of humans (Sullivan *et al*., 2001) in which to undertake this work and for regulatory purposes it was essential that data were comparative to those produced in porcine models by other workers. Furthermore, the pig is a recognised species for the assessment of wound repair materials (Middelkoop *et al*., 2004) and enabled the assessment of wound healing parameters and the evaluation of Smart-Matrix™ on the same scale as would have been used in the human application.

3.2.5 Justification of number of animals for study

The studies were designed to use the lowest number of animals possible, consistent with the objective of the study, the scientific needs of the Sponsor (RAFT and SML Limited) and contemporary scientific standards. Therefore this study was designed to use the lowest number of animals possible that allowed sufficient group sizes for meaningful statistical analysis of data.

The Home Office Licence governing this study and the personal licences of the author (Raina Zarb Adami) and her then supervisor (Dr Julian Dye) directly specified the limits of severity of effects on the animals. Unless otherwise specified, all animal procedures described were the subject of detailed standard operating procedures (SOP) which are contained in the SOP manuals of the operating departments of RAFT and NPIMR. PROJECT LICENCE under Dr Julian Dye filed with the UK Home Office in May 2010 PPL no. 80/2215, and Personal Licence obtained for Raina Zarb Adami in May 2010.

3.2.6 Selection for Study

All animals were examined for general health status by the Named Animal Care and Welfare Officer (NACWO) on arrival and by the Named Veterinary Surgeon (NVS) before inclusion into the study.

3.2.7 Method of Identification

The animals were housed at NPIMR and identified by a unique number tattooed on the outer aspect of both ears .The individual animal number and the NPIMR study number comprised a unique iden-

tification for each animal. Each animal pen at NPIMR was identified by a pen label containing study number, animal number, group and sex.

3.2.8 Acclimatisation, housing and diet

Prior to assignment to the study, all animals completed an acclimatisation period of at least 1 week prior to surgery. Animals were singly housed for the whole period of the study. Accommodation was in concrete pens with straw and woodchip/straw bedding and metal bar gates. The ambient temperature range was 15.7 - 21.0 degrees Celsius in the animal housing area and the humidity range was 42 - 67%. Light cycles were natural and artificial except when procedures were taking place at which time artificial light was used for the duration of the procedure.

Super Grow Pig Pellets (Manufacturer: Attlee Diets; Supplier: William Lillico & Son; Batch Number: 60542P3) were provided to all animals once daily as their diet. Water was available ad libitum to all animals. The water for NPIMR was sourced from a potable water supply by Three Valleys Water.

3.2.9 Surgery

The first day of surgery for each animal was considered as day 0. The surgical procedure was performed in the operating theatres of NPIMR (see photo) as follows:

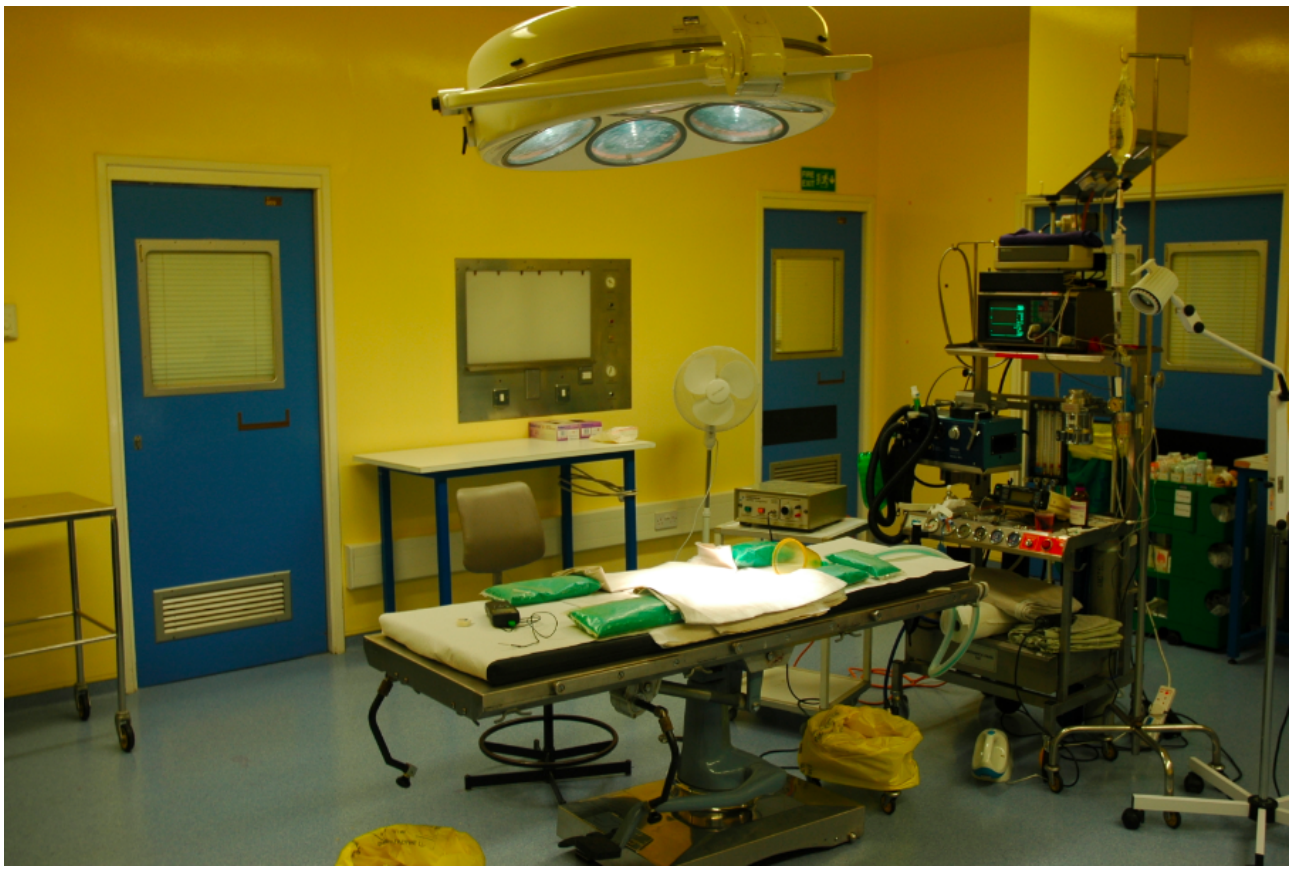

Figure 3.2.9: The operating theatre at NPIMR in which the porcine experiments took place.

3.2.10 Pre-medication and anaesthesia

Pigs were appropriately pre-medicated with Ketamine (Pfizer or Vetoquinol) 5 mg/kg / Xylazine (Bayer) 1 mg/kg intramuscularly. General anaesthesia (GA) was induced with isoflurane over oxygen and nitrous oxide delivered via a close fitting face mask. Pigs were transferred to the operating suite on a trolley, and intubated with a cuffed endotracheal tube. Following intubation, anaesthesia was maintained with isoflurane over oxygen and nitrous oxide, and respiration was controlled via a ventilator. Oxygen saturation, pulse rate, core/rectal temperature and respiratory rate were measured and recorded. Intramuscular antibiotic ampicillin long acting (Amfipen LA, Intervet) 25 mg/kg, subcutaneous analgesia Carprofen (Rimadyl, Pfizer) 4 mg/kg and subcutaneous anthelmintic

(Ivermectin, Merial) 1 mL standard dose were given. Hartmann's fluid (Baxter) was administered intravenously throughout the procedure.

3.2.11 Operative site marking

Once anaesthetised, the flanks of each animal were shaved. Six circles with a 4cm diameter to define the selected wound were marked on each flank using a silicon strut as a template and surgical marker. Two circles were marked on the more dorsal surface of either flank and another wound was created between these two wounds and placed more inferiorly on the flank, so that the arrangement was triangular. These wounds were numbered 1-6. A further circle was tattooed on the right shoulder using the same silicon strut as a template, in order to measure the pig's growth.

3.2.12 Tattoo procedure

The marked circle was re-marked using black tattoo ink. An electrical tattoo machine (property of NPIMR) was then used to embed the pigment into the dermis.

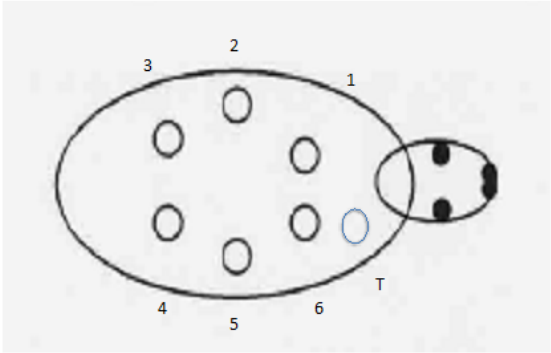

Figure 3.2.12: Line drawing depicting wound distribution on the pig's flanks. Wounds are numbered 1 to 6, T=tattoo.

3.2.13 Skin preparation

The tattoo sites were cleaned with an isopropyl alcohol soaked swab. After the surgeons gloved and gowned, the flanks were then cleaned with alcoholic povidone iodine (Ecolab Ltd) and chlorhexidine 20% (Ecolab Ltd) solutions and the animal draped with sterile cotton drapes held together using surgical towel forceps. Aseptic technique was used from this point on.

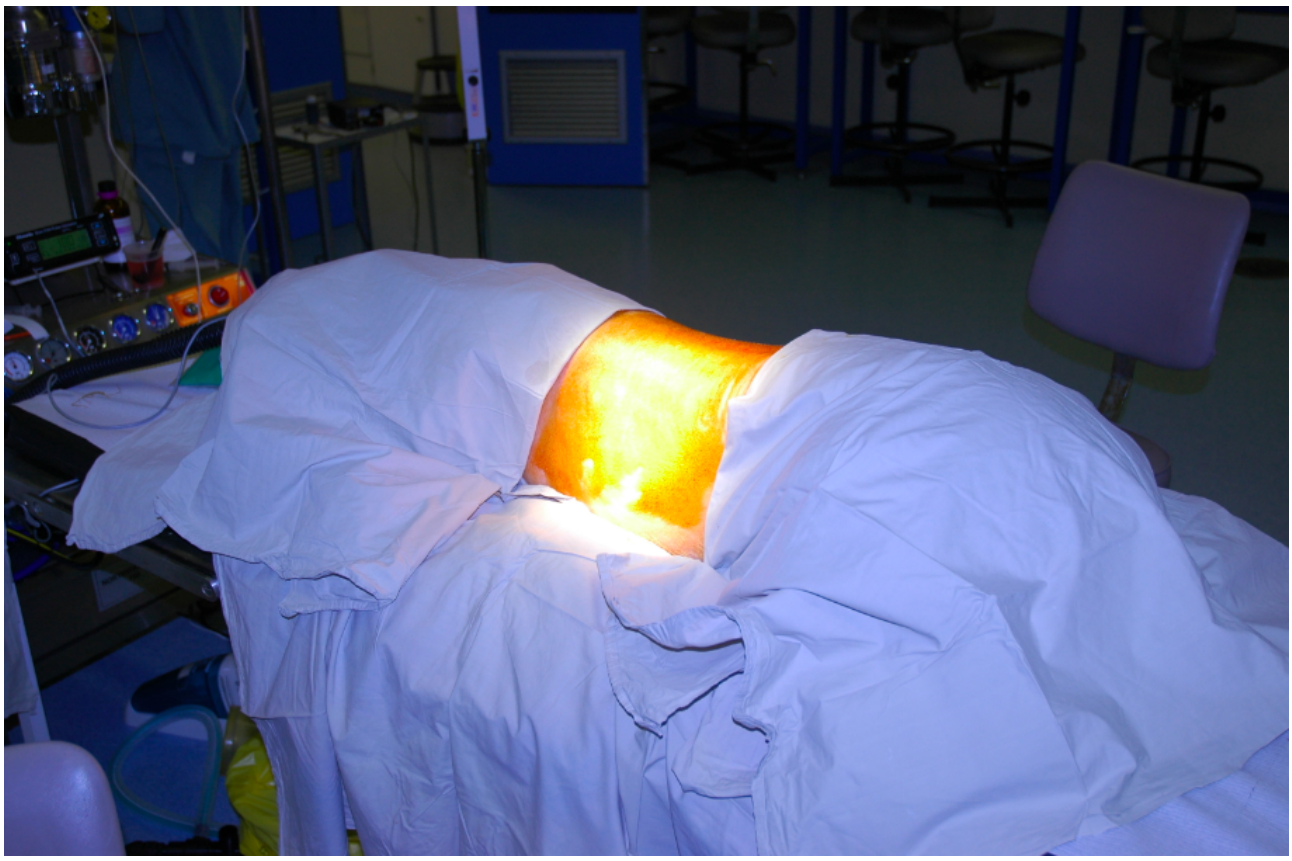

Figure 3.2.13: The anaesthetised pig after skin preparation and sterile draping in preparation for surgery.

3.2.14 Acute wound creation: full thickness excision wound

Three circular full-thickness wounds of 4 cm diameter down to muscle fascia were made on the flank of the animal. A full-thickness excision wound (down to muscle fascia) was surgically created within the dimension of each of the tattooed circles. The wounds were made by scalpel incision demarcating the wound margin following a skin marking, through the depth of dermis, followed by dissection at the tissue plane at the dermal base. Each wound was identified by a wound number which was recorded on the anaesthesia and surgical report form. Meticulous haemostasis was achieved using saline –soaked gauze swabs and bipolar diathermy.

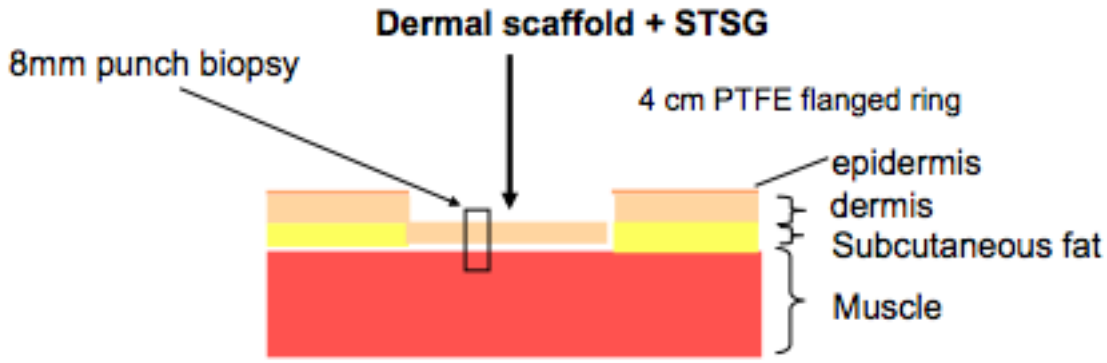

Figure 3.2.14.1.: A schematic representation of the acute full thickness excision wound created on the animal's flank without using a silicon strut to splint to wound edges.

Silicon strut insertion

A silicon strut was inserted into the wounds of half the pigs in Experiment 1. Four small full thickness incisions (approximately 1 cm) were made at 90 angles to the strut and to each other (see figure)

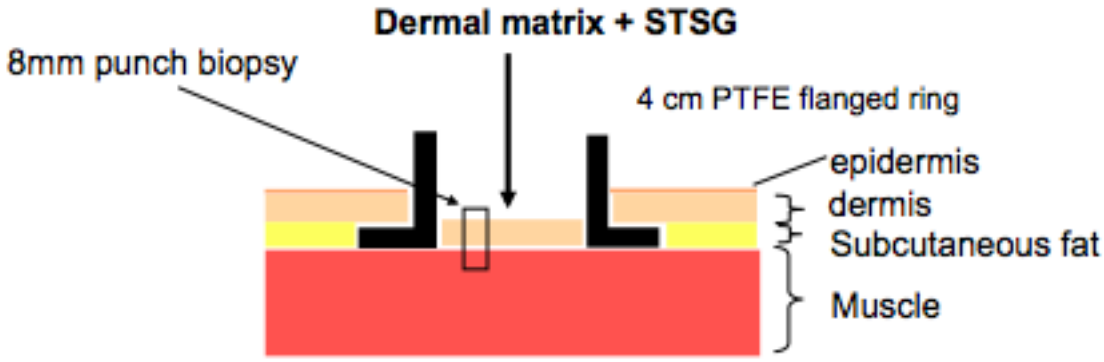

Figure 3.2.14.2: A schematic representation of the acute full thickness excision wound created on the animal's flank using a silicon strut to splint to wound edges.

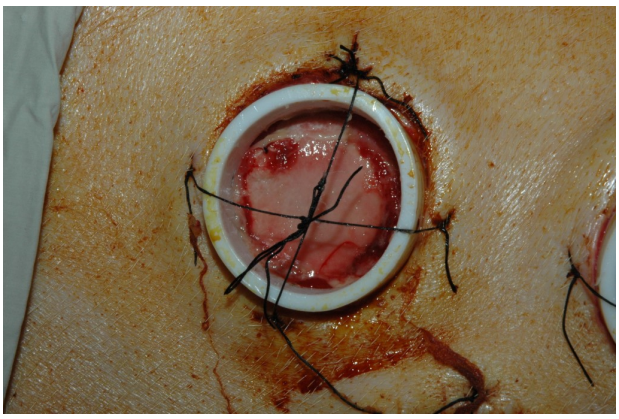

Figure 3.2.14.3: The use of a circular silicon strut to hold open the wound edges.

3.2.15 Burn wound creation

At the end of experiment 2, just prior to termination, the last 2 pigs were used to verify the uniformity and depth of burn to be used for experiment 3. Immediately prior to euthanasia, a burn was created on the pigs' flank using a cylindrical solid stainless steel metal block with a diameter of 4cm (specifically created for tis purpose) that had been heated in vegetable oil to 150 degrees Celsius for 60 seconds. 4 burns were made, each varying the length of time of contact with the pig's skin (30 seconds, 60 seconds, 90 seconds and 120 seconds. The pig's life was immediately terminated thereafter, and the 4 wounds were excised. A full thickness burn down to superficial fascia but not including subcutaneous tissue, was created by the 60 second contact burn. (the 30 second contact burn did not produce a full thickness burn, while the 90 second and 120 second burns burnt underlying muscle and fat).

3.2.16 Attenuated wound healing model creation

(used in experiments 3 and 4)

Six full thickness burns were created under aseptic techniques as described above on day -1, in pigs that were anaesthetised and their skin shaved. They were recovered from anaesthesia (as described below). On day 0 of the experiments, the pigs were anaesthetised again and underwent similar skin preparation and sterile draping. The central necrotic (obviously burnt) plug of skin was excised, leaving the zone of stasis intact (see figures 3.2.16.1-5). This was identified as the zone that was not obviously congealed but had very sluggish blood flow when cut into. This was confirmed using the Moor FPLI system.

Skin grafts were harvested and wound treatments and dressings were applied as described below.

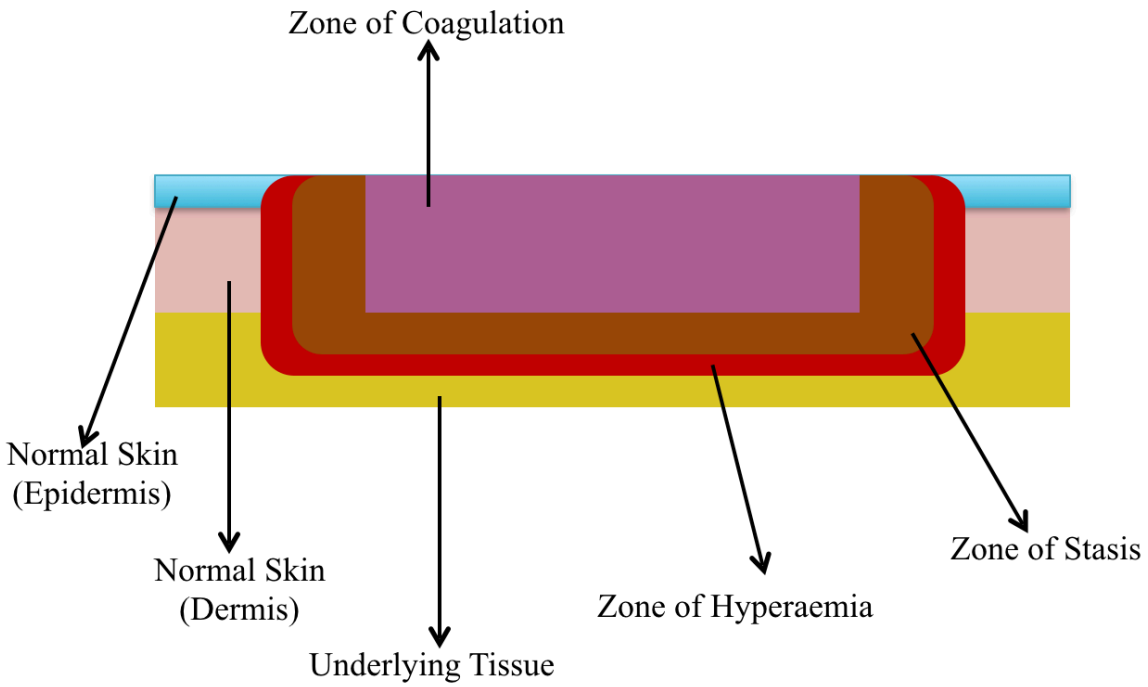

Figure 3.2.16.1: A schematic diagram showing Jackson's model of zones of a burn injury.

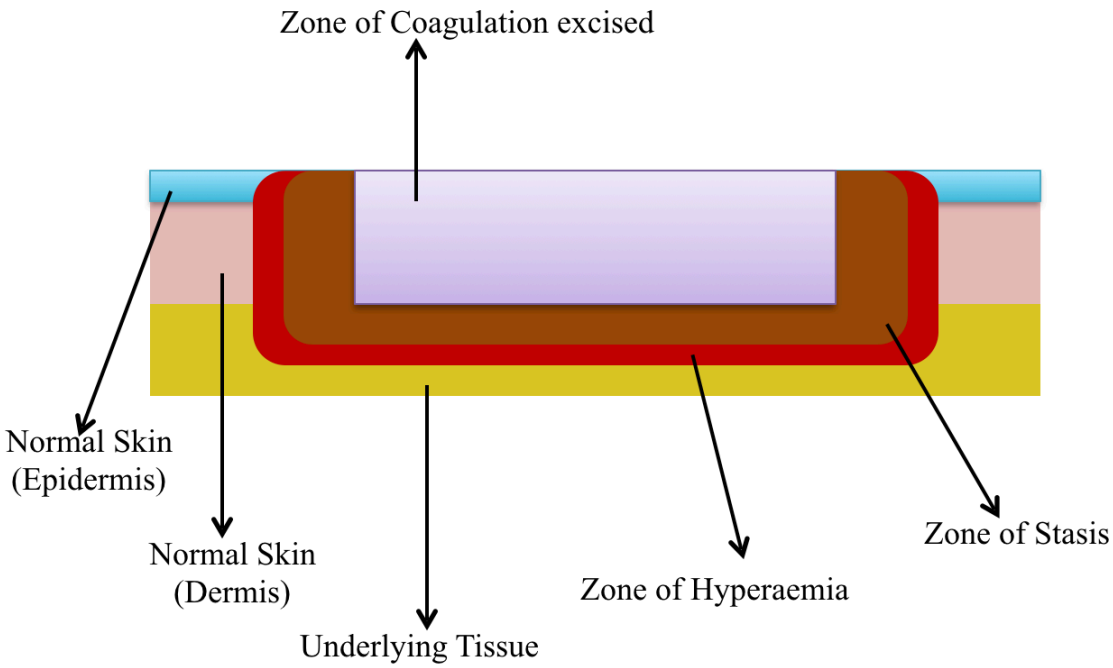

Figure 3.2.16.2: A schematic diagram showing the partial thickness excision of a full thickness burn model

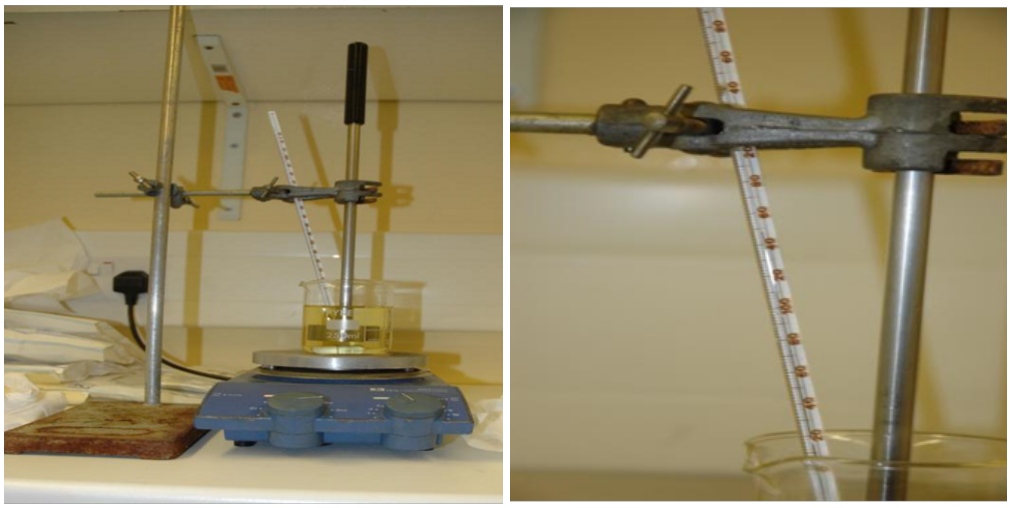

Figure 3.2.16.3: The cylindrical solid stainless steel metal block vegetable oil being heated to 150 degrees Celsius for 1 minute, confirmed using a mercury thermometer

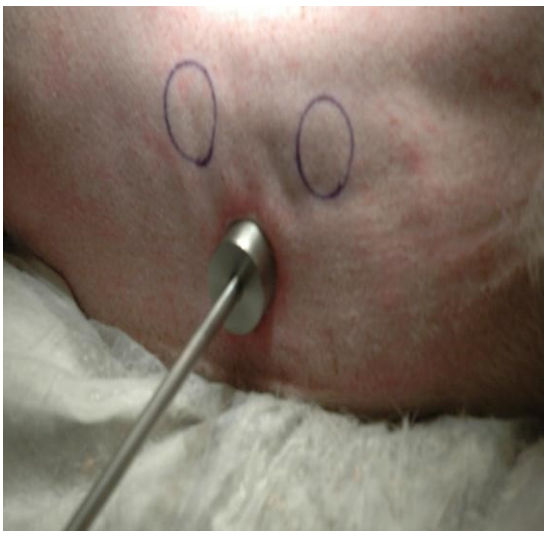

Figure 3.2.16.4: The heated cylindrical solid stainless steel metal block applied to the aseptic anaesthetised pig's flank and held for 60 seconds.

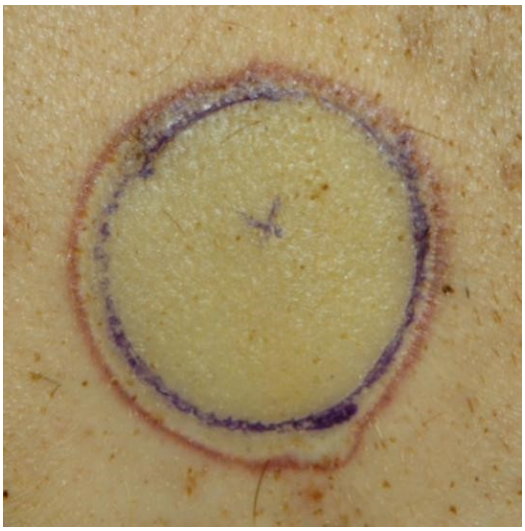

Figure 3.2.16.5: The resulting burn wound after the application of the heated cylindrical solid stainless steel metal block.

3.2.17 Split thickness skin graft harvest

Split thickness (130μm to 1300μm) skin grafts were harvested from the paravertebral and gluteal areas, using the Zimmer air dermatome under aseptic conditions. Sufficient skin was taken to provide cover for a maximum of six 4cm diameter chambers. Split thickness skin grafts (STSG) were prepared by harvesting thin (Zimmer air dermatome set on 0.01" setting; giving approximately 0.2

mm STSG) epidermal autografts from the paravertebral dorsal skin. The harvested STSG was identified for orientation (epidermal side down, dermal side up), spread out onto saline saturated sterile gauze and covered with a second saline soaked gauze swab until use. Puncture incisions, approximately 1-5 mm long, were made with a scalpel tip at approximated 1 cm intervals to allow wound fluid transudation. When Integra™ (I) was used (in Experiment 2), sufficient STSG was harvested for 4 wounds on day 0, and further STSG for another 2 wounds was harvested when the wounds treated with I were ready for grafting at day 14.

The wounds were then treated as per the experiment in question.

3.2.18 Wounds allowed to heal by secondary intention

Wounds allowed to heal by secondary intention received no dermal matrix or skin graft and were simply dressed as described below.

3.2.19 Grafting procedure

Split thickness skin grafting was carried out at Day 0 for all wounds, (as a single stage procedure when used with Matriderm™ and Smart Matrix™) except when used with Integra™ when it was carried out on day 14. The STSG was overlaid directly on to the wound bed or onto the applied dermal scaffold. Any excess was graft trimmed off. The STSG was placed with dermis facing down, i.e. in direct contact with the wound bed or the scaffold. The epithelial surface of the graft was in direct contact with the wound dressing.

The STSG (together with the dermal matrix, when used) was secured to the wound edges using absorbable 3/0 Vicryl (Ethicon) sutures. Additional sutures and staples (Skin Stapler, Covidien) were used, at 2 cm spacings to quilt the construct to the wound bed for secure anchorage.

3.2.20 Wounds treated with Smart Matrix™ and split thickness skin graft

After removal from its secondary packaging, SM was rehydrated in its tray for 5 minutes with generous amounts of sterile saline (approximately 60 mL/scaffold), and transferred to the wound bed using a sterile gauze swab as a carrier. Orientation of SM into the wound was such that the lower surface of SM in the packaging was in direct contact with the wound surface (although the orientation of the scaffold does not actually influence wound healing). Once in place, SM was cut to fit the recipient wound bed, as necessary. Details of scaffolds used for each wound were recorded. The STSG was then applied as detailed above.

3.2.21 Wounds treated with Matriderm™ and split thickness skin graft

After removal from its secondary packaging, Matriderm™ (MD) was rehydrated in its tray for 5 minutes with generous amounts of sterile saline (approximately 60 mL/scaffold), and transferred to the wound bed using a sterile gauze swab as a carrier. Orientation of MD into the wound was such that the lower surface of MD in the packaging was in direct contact with the wound surface (although the orientation of the scaffold does not actually influence wound healing). Once in place, MD was cut to fit the recipient wound bed, as necessary. Details of scaffolds used for each wound were recorded. The STSG was then applied as detailed above.

3.2.22 Wounds treated with Integra™ and split thickness skin graft

After removal from its secondary packaging, Integra™ (Integra™ LifeSciences, Plainsboro, NJ (I) was transferred to the wound bed using a sterile gauze swab as a carrier. Orientation of I into the wound was such that the silicon backing layer (evident by its black line running through it) was on the external surface, while the dermal matrix itself was in contact with the wound bed directly. Once in place, it was cut to fit the recipient wound bed, as necessary. Wounds treated with I did not undergo STSG as a single stage procedure, but as per the package insert directions (and accepted clinical practice), at day 14, the silicon backing was removed, leaving the dermal matrix in place, and STSG was applied. Details of scaffolds used for each wound were recorded.

3.2.23 Wound dressings

When dressing the wounds, and subsequent nursing, prolonged pressure on the wound site was avoided. The wounds were dressed with 'Mepilex Border™' (Molnlycke) 15 x 17 cm self-adhesive foam absorbent dressing, which was secured around the wound margins by stapling. On the second dressing change at day 14, wounds were dressed with 'Mepitel One™' (Molnlycke) perforated silicone in place of 'Mepilex Border', secured around the wound margins by stapling. Wound sites were covered by Velband (S&N 10 cm x 2.75 m), Mefix (Molnlycke 10 cm x 10 m) and Elastoplast (10 cm x 4.5 m), and protected by a rigid jacket with integral foam padding. This was secured in place with Velcro straps (see figure) Dressings were changed weekly until sacrifice, for the first 42 days of the experiment. At day 42 (for the animals that weren't sacrificed) the final dressing was removed.

3.2.24 Recovery

Animals were recovered from anaesthesia following each procedure and returned to the animal accommodation. Post-operative pain relief Carprofen (Rimadyl, Pfizer) 4 mg/kg was given as required.

3.2.25 Sacrifice

At the end of each study, the animals were pre-medicated and induced to GA as for the original surgical procedure. At the end of the procedure, the animals were then euthanised using intravenous Sodium Pentobarbitone (JML) 200 mg/mL (as per Home Office Guidelines).

3.2.26 Change of dressings and observations

Wounds were inspected and re-dressed on post op day 7, 14, 21, 28, 35 and 42, in the six week studies and at days 84 and 180 in the 6 month studies. The pig was anaesthetised and dressings were removed. At each time point, the wounds were observed for graft take and photographed. Wound area was measured using the Eykona system and vascularity was measured using the Moor FPLI system. An 8mm punch biopsy (down to fascia) sample was taken for histology at each of these inspections, before dressings (as above) were re-applied. In Experiment 1, the wound chamber in wound 6 was removed after the dermal scaffold was partially or completely integrated, at day 21.

3.2.27 Punch biopsy

A standard 8mm punch biopsy (see figure 3.2.27) was used to sample the healing tissue. Another biopsy was taken from the tattooed area to sample normal skin, as a control. This was done at each dressing change under aseptic surgical conditions. The biopsy was taken from the centre or just off the centre (but not from the wound seam) and was a full thickness sample (down to, and including wound bed). It was ensured that subsequent biopsies were not taken from previous biopsy site, in order to be sure that the actual sample did consist of the regenerative skin (and not the granulation tissue which formed from healing previous biopsies. Haemostasis was achieved afterwards using compression with a gauze swab soaked in saline or when necessary, using bipolar diathermy.

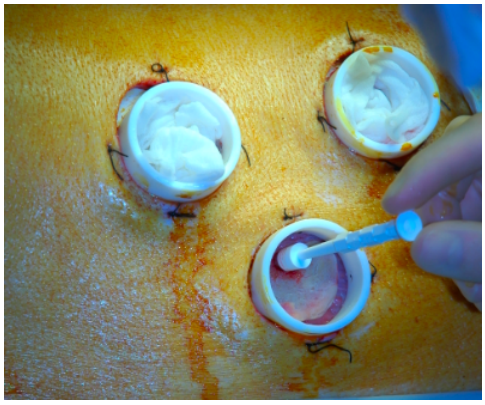

Figure 3.2.27: The 8mm punch biopsy being taken from a wound

3.2.28 Photography

Digital photographs of each wound of each animal at surgery were taken and digitally filed (stored at RAFT).

3.2.29 Graft take observation

Graft take manifests macroscopically as the adherence of the split thickness skin graft to the underlying wound bed with signs of vascularity in the graft, ie pink in colour. (Richards, 2002). Graft take was assessed by the surgeon (RZA) and her assistant (JFD). This was a measure of the percentage wound area of the skin graft adherent to the wound bed and of a similar pinkish-red colour to the wound bed (due to inosculation and vascularisation) (Converse *et al*., 1975). A skin graft was deemed successful if greater than 80% of the wound area showed "take" on examination (Reddy *et al.,* 2014). Graft take refers to the skin graft adherent to the wound bed and of a similar pinkish-red colour to the wound bed (due to inosculation and vascularisation) (Converse *et al.,* 1978, Pope 1988, Swaim 1990).

3.2.30 Wound area measurement

The Eykona Wound Measurement System (Eykona Medical Ltd, Oxford , UK) is a 3D imaging system used to create a digital image of each study wound. This system allowed the measurement of wound area, curved volume and volume (see Figure 3.2.30). Data analysis was carried out as follows: the images from the Eykona were downloaded on to the computer. Measurements of the area were performed by selecting the full perimeter of the wound on the computer image and the software then calculated the above parameters. These measurements were taken after the wound dressings were taken down, and after the wound areas (and tattoo) were cleaned and draped, and before the biopsies were taken. As the surgeons were in sterile gown and gloves at this point, these images

were taken by the other RAFT scientists: Amir Taheri and Viabhav Sharma. The mean values of these measurements were calculated and plotted in a graph.

Figure 3.2.30: A photographic image of the wound area measurement on a pig flank using the Eykona camera. The wound area measured in this example is highlighted in red and outlined in white. The central white disc with a black rectangle is the target needed for recognition by the device.

3.2.31 Wound contraction measurement

In order to assess wound contraction, wound area measurements were calculated as a percentage of the wound area of the tattoo per time point in each pig. The mean values of these measurements were calculated and plotted in a graph.

3.2.32 Vascularity measurement

Moor FPLI)Moor Instruments Ltd, Axminster, UK) is a full-field blood flow imager that uses the laser speckle contrast technique to deliver real-time, high-resolution blood flow images. Differences in flow from different regions are assessed, or flow changes expressed as a percentage change from baseline over a period of time. The contrast image is processed to produce a colour-coded image that correlates with blood flow in the tissue. When there is a high level of movement (fast flow) the changing pattern becomes more blurred and the contrast in that region reduces accordingly. Therefore low contrast is related to high flow, high contrast to low flow. A blue colour denotes a low blood flow and conversely, red denotes a high blood flow (see figure 3.2.32). As the surgeon was in sterile gown and gloves at this point, these images were taken by the RAFT scientists, Amir Taheri and Viabhav Sharma.

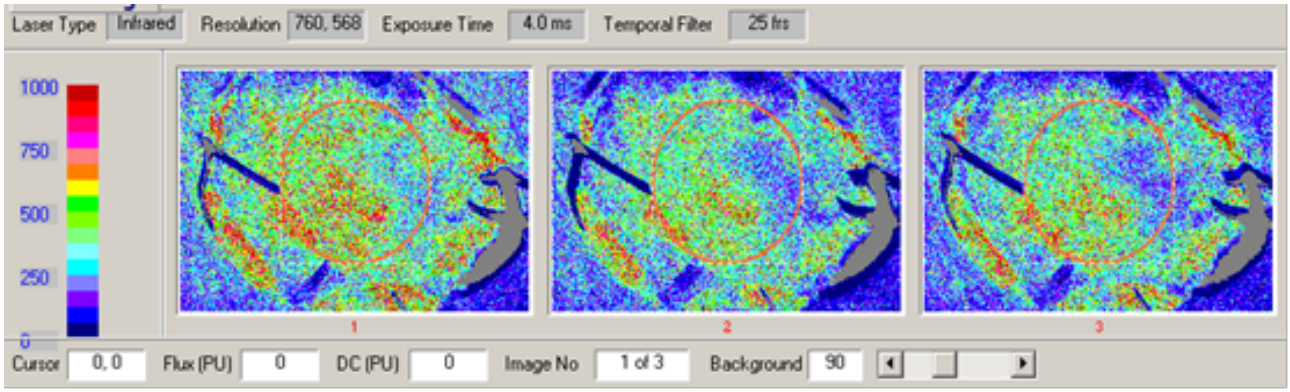

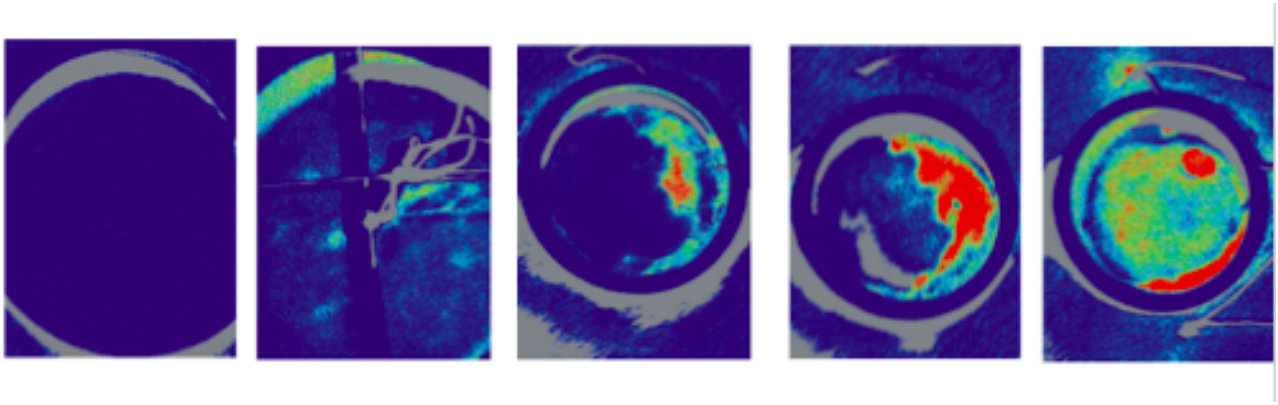

Figure 3.2.32: A representative scale for vascular perfusion, using the Moor FPLI laser Doppler machine, where red denotes increased perfusion and blue denotes a paucity of perfusion. This colour scale is then automatically translated into numerical values.

3.2.33 Histopathology and immunohistostaining

Tissue samples from the 8mm punch biopsies were placed into 10% NBF for a minimum of 48 hours. These were then processed and embedded to paraffin wax by routine automated procedures, with excised skin, STSG and wound tissue oriented for cross-section microtomy. H&E staining was mainly carried out at NPIMR by their staff, while all other immunohisto-staining was carried out at RAFT's laboratories by the author of this thesis (RZA) and other RAFT scientists (Dr Keith Blackwood, Nirosheeha Ragunathan and Nivedita Ravindran, with the help of Philippa Franke and Nimesha Patel). Sequential fragments of each specimen were cut at 5 μm intervals. Representative

sections of each sample were prepared for immunohistochemical staining by deparaffinisation with xylene and rehydration through a graded ethanol series. Slides were first treated with antigen retrieval buffer (Bullseye) at 115C under 1 atmosphere pressure for 10 seconds before being washed with PBS and treated with the Novolink polymer kit. Immunohistostaining was performed via the Shandon Sequenza staining system, following which, the endogenous peroxide activity was blocked with 3% hydrogen peroxide for 30 minutes followed by a block with 10% PBS and an incubation with primary antibodies. One section per batch of slides was incubated with 1% PBS instead of the primary antibody to provide a negative control for the reaction. After washing, the sections were incubated with a secondary antibody (Shandon Sequenza, Thermo Scientfic, US). Finally, the sections were washed in distilled water and counterstained with haematoxylin. To assess neovascularisation and to count the number of blood vessels, sections were stained for von Willebrand factor (vWB) (see figure 3.2.33.1.1). Pico Sirius red was combined with Miller's elastin for collagen, Voerhoff-van Gieson staining for elastin, Extra Domain A-fibronectin (EDA-FN) and α-Smooth Muscle Actin (α-SMA) for myofibroblast activity to help assess wound contractile markers. See figures 3.2.33.1-5.

Figure 3.2.33.1: von Willebrand staining of capillaries. (purple stain). Black arrows point to capillary lumina.

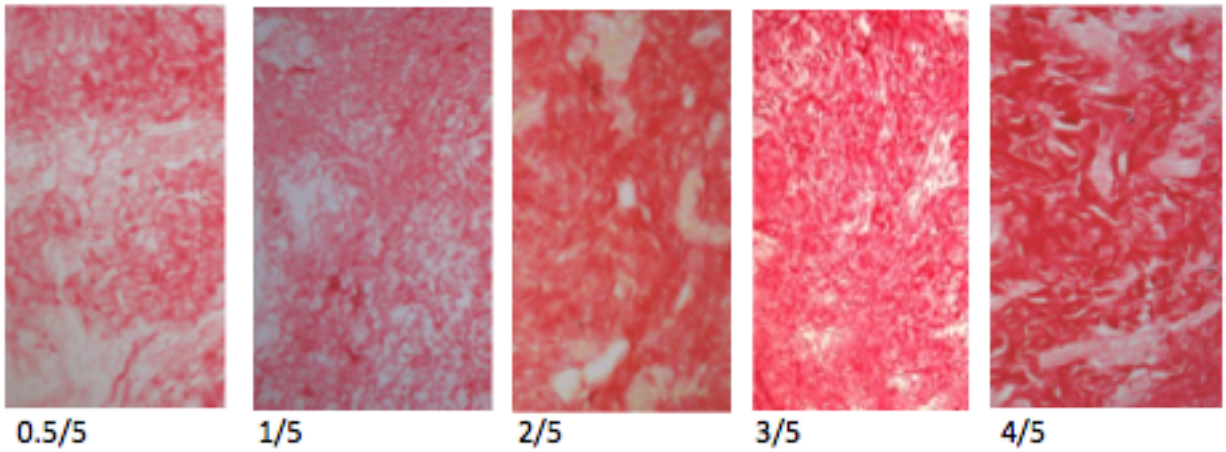

A

Figure 3.2.33.2: A representative scale for pico-Sirius red staining for collagen, with scores out of 5, where 0/5 would represent no staining whatsoever, and 5/5 would represent 100% of the slide showing staining, at x10 magnification.
Red staining denotes fibrillar collagen fibres.

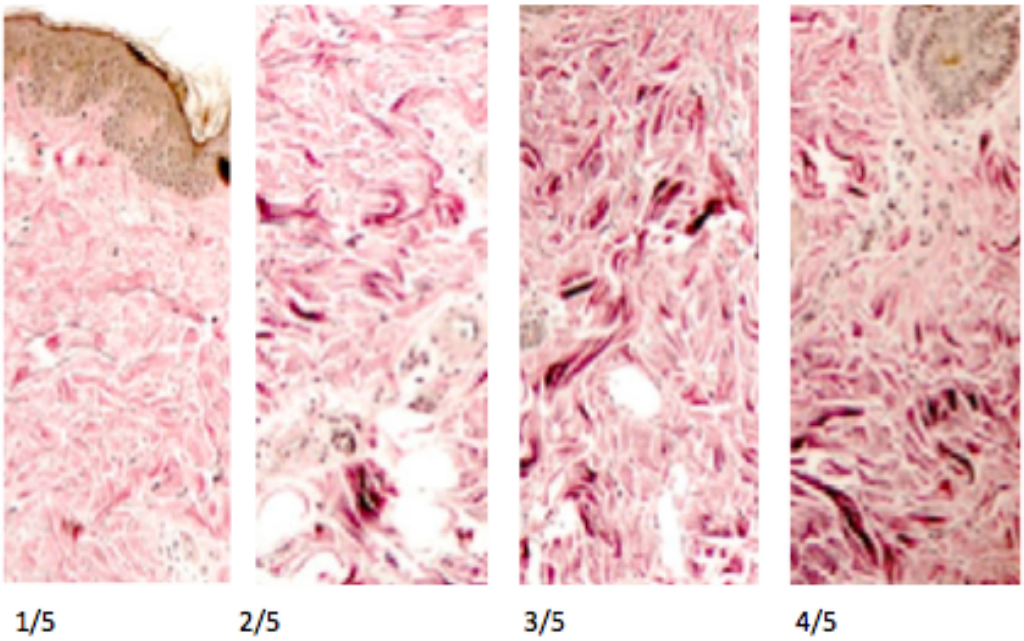

Figure 3.2.33.3: A representative scale for van Gieson staining for elastin, with scores out of 5, where 0/5 would represent no staining whatsoever, and 5/5 would represent 100% of the slide showing staining, at x10 magnification.

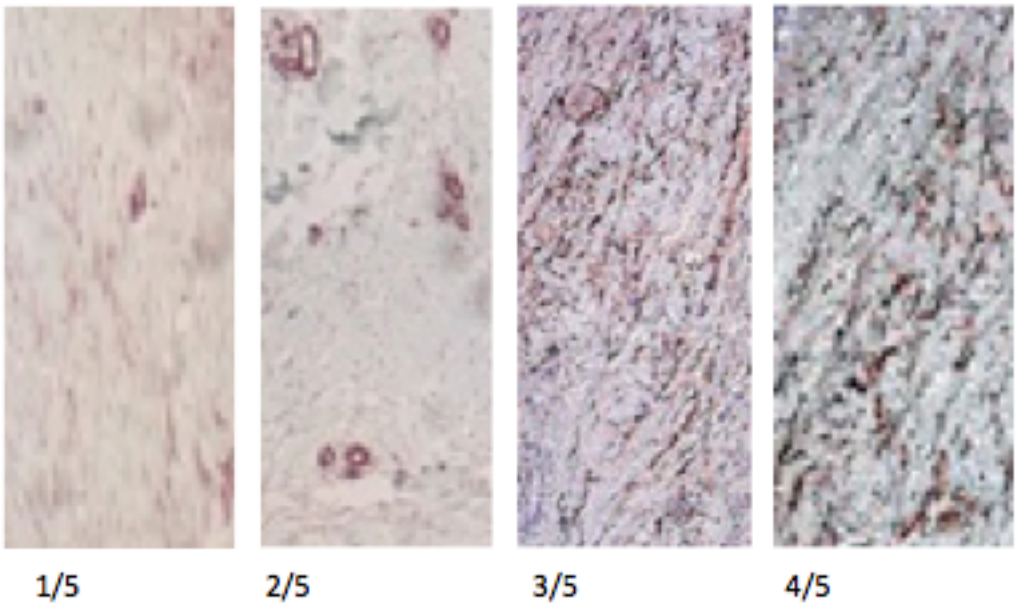

Figure 3.2.33.4: A representative scale for EDA-fibronectin staining, with scores out of 5, where 0/5 would represent no staining whatsoever, and 5/5 would represent 100% of the slide showing staining, at x10 magnification.

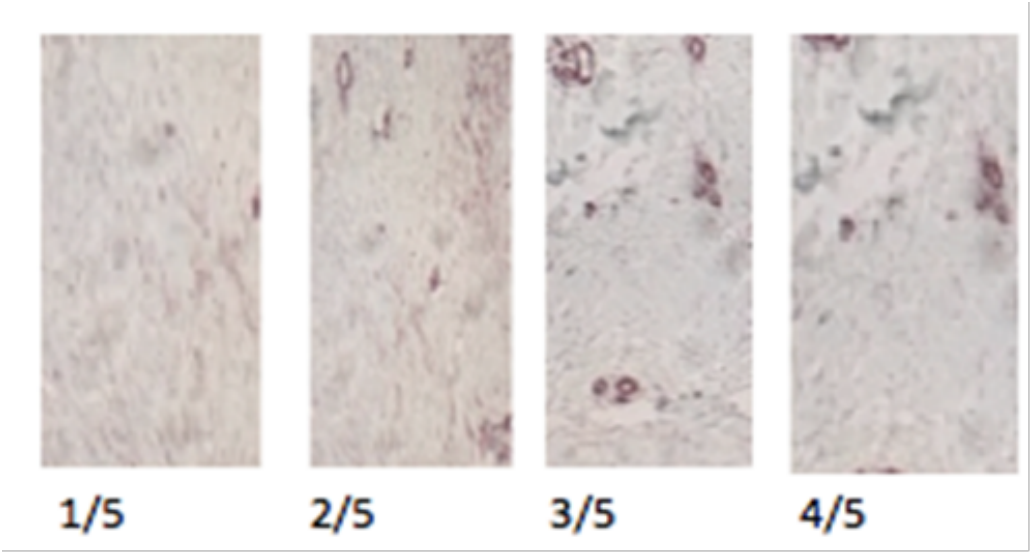

Figure 3.2.33.5: A representative scale for α-SMA staining, with scores out of 5, where 0/5 would represent no staining whatsoever, and 5/5 would represent 100% of the slide showing staining, at x10 magnification.

3.2.34 Measurement of wound vascularity

Wound vascularity was measured using 3 different methods. Moor FPLI was used (as described above) and vWF factor staining was used to delineate blood vessels and capillaries. VWF staining density was measured as a score out of 5 similar to other staining measurements) and capillary lumina counted per visual field.

For the purpose of this thesis, some of the histology slides were photographed using the Microsoft Research Image Composite Editor (ICE).

3.2.35 Macroscopic observations

Microscopic observations were carried out by twice, once each by 2 individuals separately. These were the author (RZA), and a suitably qualified and experienced scientist (Dr Sorousheh Samizadeh) who were both blinded to the subject, time point and wound treatment method of the histology slide, through coded labelling by a third individual (NPIMR staff). Three observations were made per slide, in different areas of the sample. Thus each slide underwent 6 readings. After the values were documented, the origin of the slides was revealed and the mean of each treatment method at each specific time point was calculated (for example: in order to calculate the mean collagen staining density of wounds treated with SM + STSG at day 14, 6 readings were taken from all 48 wounds in experiment, and the mean value was then calculated.) The slides were analysed using an Axioskop 2-Mot Plus Microscope (Carl Zeiss, Jena, GR).

3.2.36 Scaffold presence

On H+E staining, wounds were observed for the presence of the dermal scaffold. (See figure 3.2.36). Scaffold persistence was observed, as in the optimal acellular dermal matrix, the scaffold would persist in the wound for a time period sufficient to redirect neodermal tissue formation while being recognised as living tissue, and not persist as a foreign body and its associated immune response (deVries *et al*., 1993). The dermal scaffold was considered to be present if a reddish-orange pattern of structures, dissimilar to cellular and ECM structures was present between the wounds bed and overlying skin graft and parallel to the wound bed was present.

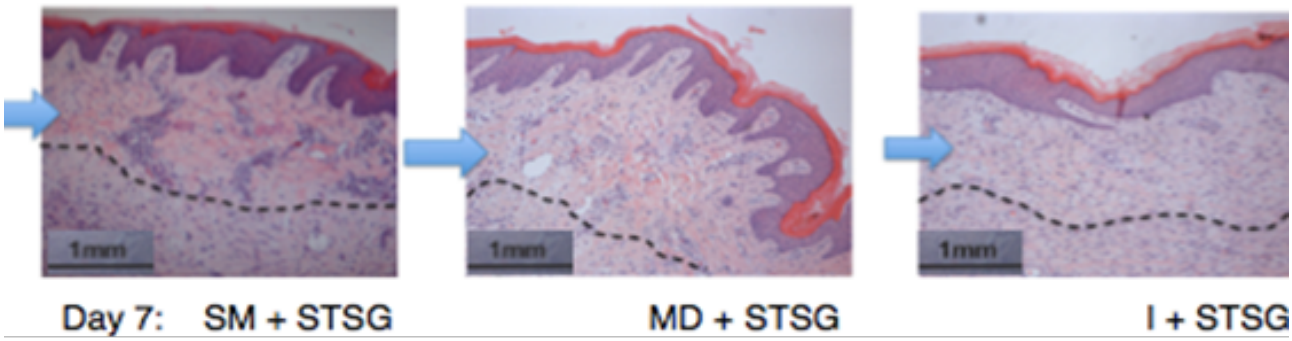

Figure 3.2.36: Photographic images showing examples of the presence of the dermal scaffold (blue arrow) on H&E staining at x10 magnification, for different reconstructive options at day 7. The dashed black line shows the interface of the wound bed and dermal scaffold.

3.2.37 Wound cellular density, neodermal thickness and inflammatory cell density

Neodermal (wound thickness) (micrometers) and cellular density were measured as indicators of formation of neodermis and neo-cellularisation. Wound depth was measured using a graticule inserted into the eyepiece of the light microscope at x10 magnification. Measurements were made from the superficial aspect of the subcutaneous fascia (or underlying muscle or fat) to the epidermal surface. H&E staining was used.

Cellular density was measured in terms of cellular structure density (score out of 5) in the extracellular matrix, in the same slides, at the same magnification (x10). All cells were included (see figure 3.2.37.1).

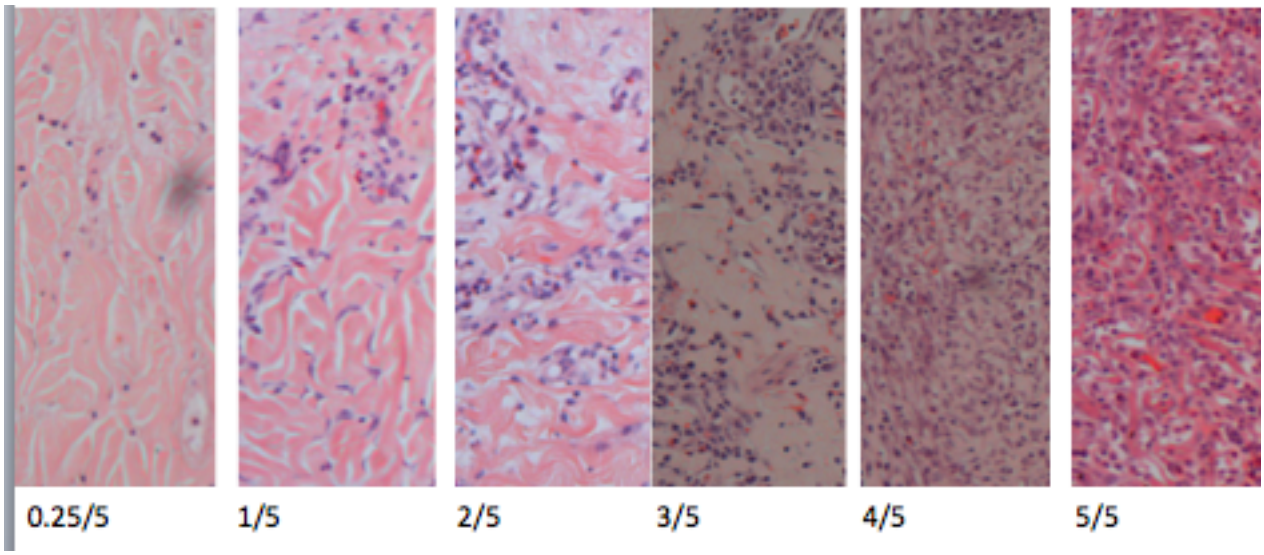

Figure 3.2.37.1: A representative scale for wound dermal cellular density (H&E staining), with scores out of 5, where 0/5 would represent no cells seen whatsoever, and 5/5 would represent 100% of the slide populated by cells, at x10 magnification.

Wound inflammation was measured in terms of neutrophil (identified by large dark staining nuclei) density (score out of 5 of all cellular structures in the field) in the extracellular matrix, in the same slides, at the same magnification (x10). (See figure 3.2.37.2).

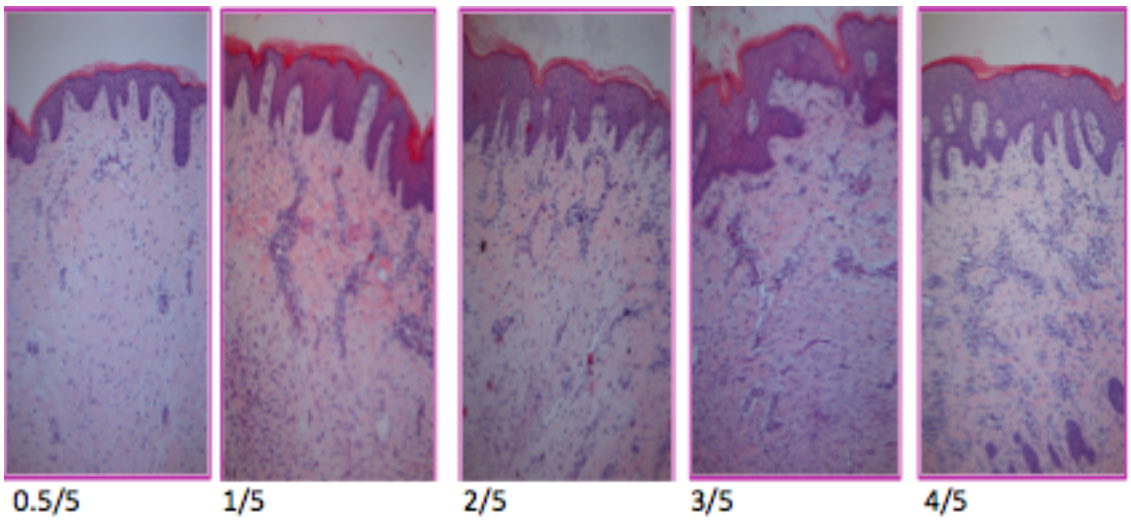

Figure 3.2.37.2: A representative scale for wound inflammatory cell density (H&E staining), with scores out of 5, where 0/5 would represent no cells seen whatsoever, and 5/5 would represent 100% of the slide populated by cells, at x10 magnification.

3.2.38 Analysis of data: statistics

Analyses were performed using GraphPad PRISM version 6.0 for Mac. Analysis of variance (ANOVA) was performed with Tukey's multiple comparison test. This was used to account for multiple post-hoc comparisons between wound treatments. Where matched data analyses were not appropriate ordinary one way ANOVA was performed. Where data sets were matched by animal, repeated measures ANOVA was performed. Statistical significance was defined as $p < 0.05$. The values reported in the brackets following the means refer to the standard error of the measurement (SEM). Where p values were deemed significant the actual p value was quoted, unless it was less than 0.0001, where it was documented as $p<0.0001$. A subset of the data (Experiment 1) was tested for normality and homogeneity of variance using the Shapiro-Wilk and the Kolmogorov-Smirnov tests. This revealed a violation of the assumption of normality in ($p>0.05$) in 55% and 53% respectively. As the variables measured represent complex natural processes, an *a priori* normal distribution of

the means (rather than of the data) of the underlying population mean was assumed (Frank 2009, Norman 2010). Given this, the First Known Property of the normal distribution is expected to be valid for the samples analysed here (Mordkoff, 2016). With large (>30 observations) the distribution of the data can be ignored (Altman *et al.*, 1995) as the violation of the normality assumption should not cause major problems (Ghasemi *et al*., 2012). Additionally, the Central Limit Theorem shows that, for sample sizes greater than 5 or 10 per group, the means are approximately normally distributed regardless of the original distribution. Hence, parametric methods examining differences between means, for sample sizes greater than 5, do not require the assumption of normality, and will yield correct answers even for manifestly non-normal and asymmetric distributions like exponentials (Norman 2000). Given the above facts, an *a priori* decision was made to use parametric statistics studies. Furthermore, using parametric statistics allowed Tukey's Honest Significant Difference test to be used for post-hoc analysis of multiple comparisons, which is less prone to alpha slippage than non-parametric alternatives such as Duncan's test as the latter is based on the Newman-Keuls method. (Jaykaran 2010). As a result, non-parametric tests may have a greater risk of type 1 error in the post-hoc analyses performed here.

Chapter 4: Experiment 1: The Long-term Evaluation of the Smart Matrix™ fibrin-alginate scaffold in the acute full thickness porcine wound

4.1 Hypothesis

Smart Matrix™ supports the long-term survival of the overlying split thickness skin graft when applied to the acute full thickness porcine wound as a single stage procedure.

4.2 Aims

The aim of this study was to evaluate the long term wound healing trajectory of Smart Matrix™ applied in tandem with split thickness skin graft as a single stage procedure to an acute porcine wound healing model, while comparing it to wounds allowed to heal by secondary intention and those treated with the current gold standard, split thickness skin grafting alone.

Specifically this study aimed to examine the quality of the resulting skin in terms of wound area and contraction, and to establish long-term evidence of graft integration and neovascularisation of Smart Matrix™ in an *in vivo* acute wound healing porcine model.

This study aimed to objectively quantify the differences in healing outcome through histological and macroscopic observations.

4.3 Methods and materials

Please refer to Chapter 3: Methods and Materials for further detail.

Six acute full thickness excision wounds were created on the flanks of anaesthetised pigs. Three circular full-thickness wounds of 4 cm diameter (using a silicon template) down to muscle fascia were made on either flank of the animal. The wounds of 9 pigs (in the 42 day study) were fitted with a silicon strut to splint the wound edges, in order to observe wound bed healing without lateral

epidermal creep. The other 9 subjects (3 in the 42 day study and 6 in the 180 day study) did not have silicon struts, in order to observe wound contraction (see figure 6.2). Hence for the wound area and contraction observations in the 42 day study, n=54 with 18 per wound group and in the 180 days study n=36, with 12 per wound group.

4.4 Study outline

For this study, a total of 18 animals were used (and therefore 108 wounds). All animals monitored for a period of 42 days. Of these, 12 pigs were sacrificed after day 42, while the remaining 6 pigs were monitored up to day 180 (therefore 36 wounds). The surgical procedures were carried out by the same surgeon (RZA) and senior project licence holder, JFD. Two wounds per animal were treated with SM+STSG, another two wounds by STSG alone and another two wounds allowed to heal by secondary intention. The wounds were randomly assigned. The minimum number of pigs sufficient to yield statistically significant results was used for this study, as per Home Office regulations and project license restrictions.

<u>42 day Study:</u>

Eighteen pigs were used in the 42 days study with 6 wounds per subject. One hundred and eighteen wounds were created with 36 wounds per wound group. (See table 4.4.1).

subjects = 18

wounds (n) = 108, 36 per wound group

Treatment method	Number of wounds
Healing by secondary intention	36
STSG alone	36
SM + STSG	36

Table 4.4.1: Wound treatment distribution in a 42 day study (n=108, 36 per wound group)

180 day Study:

Six pigs were used in the 42 days study with 6 wounds per subject. Thirty six wounds were created with 12 wounds per wound group. (See table 4.4.2).

subjects = 6

Wounds (n) = 36

Treatment method	Number of wounds
Healing by secondary intention	12
STSG alone	12
SM + STSG	12

Table 4.4.2: Wound treatment distribution in a 180 day study (n=36, 12 per wound group)

Two wounds per animal were allowed to heal by secondary intention and two were treated with split thickness skin graft alone. The Smart Matrix™ scaffold was applied to the remaining two wound beds with overlying split thickness skin grafts applied as a single stage procedure. Macroscopic and microscopic observations were made at five short term time points, day 7, day 14, day 21, day 28 and day 35 three long term time points: day 42, day 84 and day 180. Macroscopic observations included colour, texture and adnexal observations, graft take, wound area and contraction and wound vascularity. Microscopic studies included Haematoxylin and Eosin (H&E) staining to

assess wound depth, cellular ingress and the presence of inflammatory cells. Microscopic observations included parameters pertaining to contractile preoperties (Extra-Domain A-fibronectin (EDA-FN) and α-smooth-muscle actin (α-SMA)), collagen and elastin, neodermal thickness, cellular density and inflammatory cells and parameters pertaining to vascularity (capillary lumen count and von Willlebrand factor staining).

4.5 Results

4.5.1 Graft take

Please see figures 4.5.2.1-3 and figures 4.5.3.1-3.

Wounds treated with Split thickness skin graft alone

Of the 36 wounds, 4 showed 100% (of the total wound surface area) graft take, 6 showed 95% graft take, 8 showed 90% graft take, 6 showed 85%, 4 showed 80% , 2 showed 75% , 4 showed 60% , 1 showed 45% graft take and 1 showed complete graft failure (0%take). This gives a total of 28 wounds showing 80% graft take or more and 8 wounds showing less than 80% graft take. The wound of the skin graft that was completely lost (at day 7) was allowed to heal by secondary intention. For statistical reasons this wound was then evaluated with the wound group ”wounds allowed to heal by secondary intention”. No further grafts were lost thereafter.

Wounds treated with Smart Matrix™ and Split thickness skin graft.

Of the 36 wounds, 6 showed 100% (of the total wound surface area) graft take, 9 showed 95% graft take, 2 showed 90% graft take, 9 showed 85%, 7 showed 80% 1 showed 75% and 2 showed 60% graft take. This gives a total of 33 wounds showing more than 80% graft take, and 3 wounds show-

ing less than 80% graft take. No total graft loss occurred in this group.

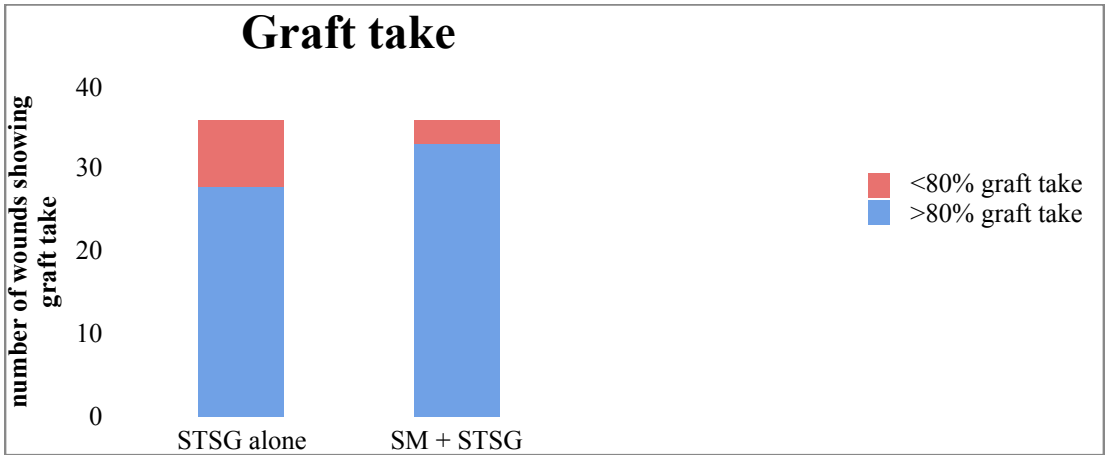

Figure 4.5.1: Wounds showing more than 80% graft take and wounds showing less than 80% graft take (n=72, 36 per wound group) for different reconstructive options.

4.5.2 Macroscopic observations

Please see figures 4.5.2.1-3

Wounds allowed to heal by secondary intention

Wounds allowed to heal by secondary intention showed signs of granulation tissue at day 7. Granulation tissue is identified macroscopically as moist pink vascular (Bhat *et al*.,2013). Granulation tissue was most proliferative at day 14 (in 31% of wounds) and day 21 (in 36 wounds) and persisted in the wound bed until day 28 in all wounds. The area of granulation tissue decreased from the periphery towards the centre of the wound between days 14 and 28. Epithelialisation (a dry wound bed) occurred thereafter. 64% of the wounds were completely epithelialised by day 35 and 100% were epithelialised by day 42, and remained so thereafter. Between days 42 and 180, the wound colour became gradually paler (from dark red-pink) to pale pink, but was still slightly darker than surrounding skin at day 180. No adnexal structures were present in this wound group. Adnexal

structures include hair follicles, sebaceous glands, apocrine and eccrine glands. (Alsaad *et al.,* 2007) No infection was observed in any of the wounds at any of the dressing changes or at termination. The area of the punch biopsy taken the previous week was not included in the macroscopic assessment.

Wounds treated by split thickness skin graft alone

At day 7, all the wounds treated by STSG alone (except for the wound that suffered graft loss, which was then included in the "allowed to heal by secondary intention" wound group) showed a pink vascularised graft on a bed of granulation tissue. At day 14, 18 wounds were still moist, while 18 were dry. All wounds were dark pinkish–red in colour. At day 21, 31 of wounds were dry. The remainder showed small moist patches. The dark pinkish-red colour persisted. At day 35, all wounds in this groups were dry and epithelialised, but a slightly paler pink. At day 42, the colour was a paler pink. By day 84 all wounds were healed and fully epithelialised with full apparent graft integration. The scars became paler in colour from day 42 until day 180. At day 180, the colour closely resembled that of neighbouring native skin. At day 180, the wounds were completely healed and epthelialised. No adnexae were present at any time point. No infection was observed in any of the wounds at any of the dressing changes or at termination. The area of the punch biopsy taken the previous week was not included in the macroscopic assessment.

By day 180 the only slight difference apparent in the macroscopic appearances of wounds allowed to heal by secondary intention and those treated with STSG alone was that the former wound group was a slightly darker pink than the latter.

Wounds treated by Smart Matrix™ and split thickness skin graft

At day 7, all the wounds treated by SM + STSG alone showed a pink vascularised graft adherent to a bed of granulation tissue. At day 14, 6 wounds were still moist, while 30 were dry. All wounds

were dark pinkish–red in colour. At day 21, all wounds were largely dry with occasional very small patches of moist granulation tissue (less than 10% of wound area). The dark pinkish-red colour persisted. At day 35, all wounds in this groups were dry and epithelialised, but a slightly paler pink. At day 42, the colour was a much paler pink, paler than the surrounding native skin. The wound colour approximated that of surrounding skin at day 84, and remained so until day 180, when the wounds were completely healed and epithilialised. No adnexae were present at any time point. No infection was observed in any of the wounds at any of the dressing changes or at termination. The area of the punch biopsy taken the previous week was not included in the macroscopic assessment.

When compared to wounds allowed to heal by secondary intention, wounds treated with SM + STSG epithelialised earlier and became the colour of normal skin earlier.

When compared with wound treated with STSG alone, these wounds were macroscopically similar to the two above groups but a slightly lighter pink than surrounding skin.

Interpretations of macroscopic wound observations and graft take

Wounds treated by secondary intention appeared to heal through the formation of granulation tissue – moist, red, velvet-like texture - apparent from day 7, most proliferative at day 14 through to day 21 and then by epithelialisation, which started peripherally and moved towards the centre of the wound thereafter. The wounds were dry from day 28 onwards, though darker and more red in colour than both the two other wound groups. By day 42 all wounds were epithelialised. Wounds allowed to heal by secondary intention were slightly darker in colour than wounds in the other groups.

By days 84 and 180 there were no macroscopic differences between all wound groups. No adnexal structures were observed in any of the wound groups.

Macroscopic appearances of the wounds in a 42 day study

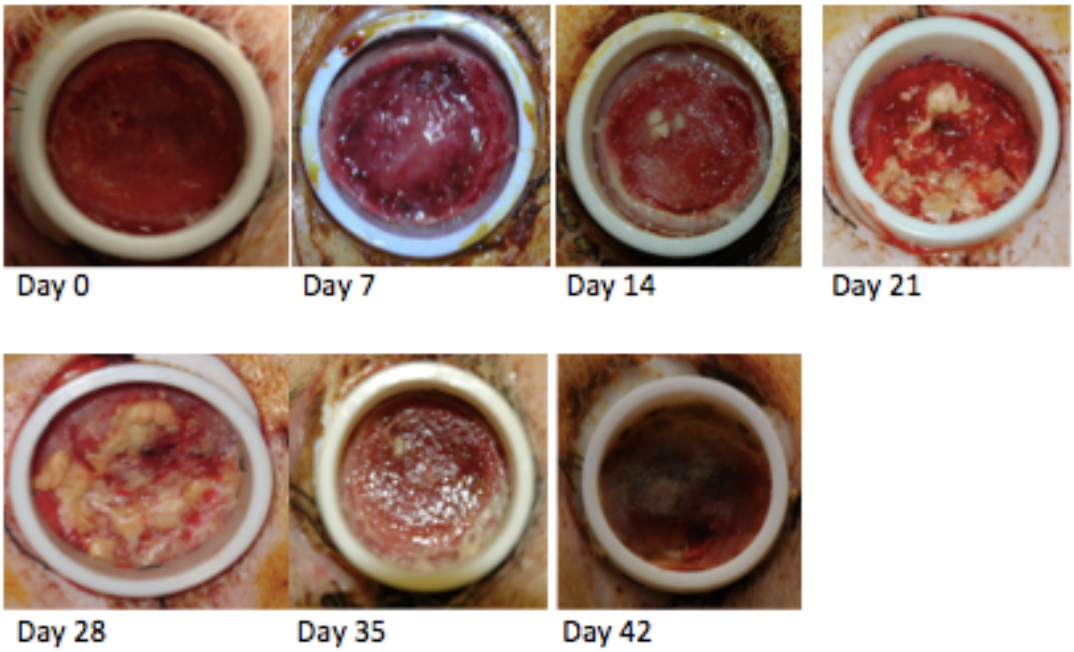

Figure 4.5.2.1:An example of the macroscopic appearances of the full thickness excision wounds allowed to heal by secondary intention in a 42 day study.

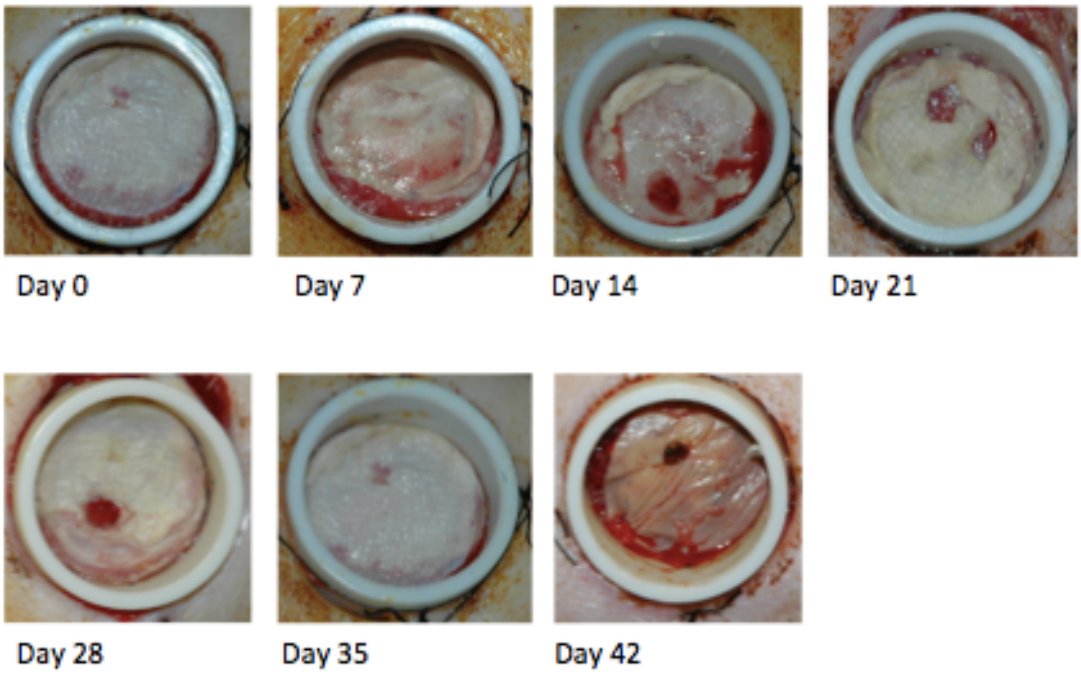

Figure 4.5.2.2: An example of the macroscopic appearances of the full thickness excision wounds treated by split thickness skin graft alone in a 42 day study.

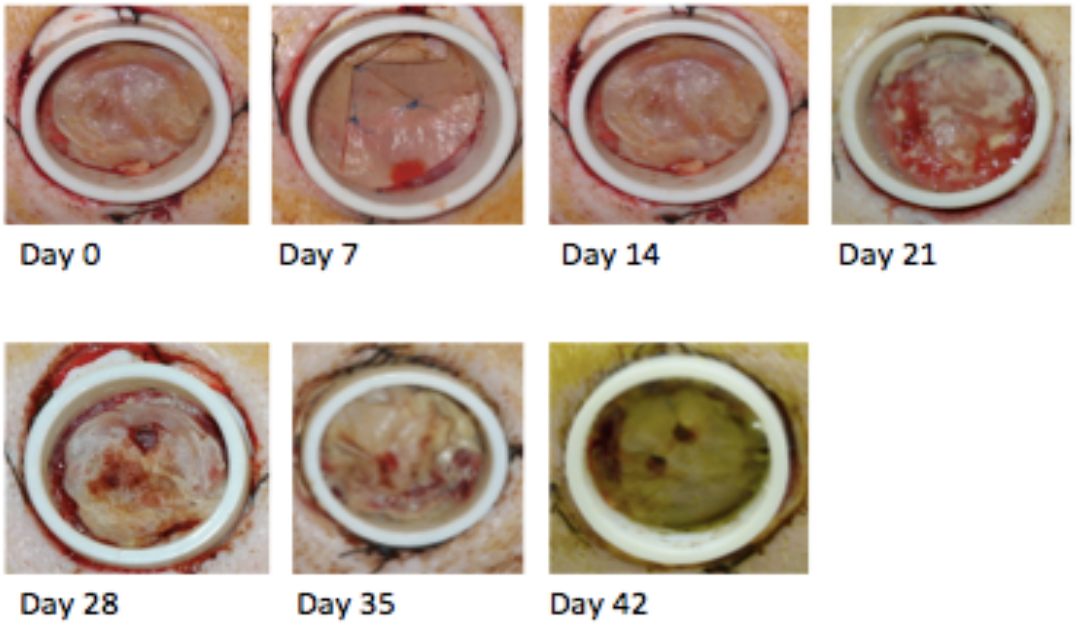

Figure 4.5.2.3: An example of the macroscopic appearances of the full thickness excision wounds treated by Smart Matrix™ split thickness skin graft in a 42 day study.

4.5.3 Wound area and contraction

Please see table 4.5.3 and figures 4.5.3.1-7

Tattooed area

The tattoo area measurements showed a statistically significant difference in wound area ($p<0.0001$) increase from each time point to the next, except between days 21 and 28 and days 21 and 28. The mean wound area difference was an increase of 2.92cm^2 from day 0 to day 7, 3.00cm^2 from day 7 to day 14, 1.93cm^2 from day 14 to day 21, 0.16cm^2 from day 21 to day 28, 0.16cm^2 from day 28 to day 35, 2.13cm^2 from day 35 to day 42, 3.80cm^2 from day 42 to day 84 and 6.93cm^2 from day 84 to day 180.

Wounds allowed to heal by secondary intention

From day 7 through to day 180, wounds allowed to heal by secondary intention decreased in size over time overall. Statistically significant ($p<0.0001$) decreases in wound area occurred between day 0 and day 7 (mean difference of 3.19cm^2) days 14 and 21 (mean difference of 1.49cm^2), days 28 and 35 (mean difference of 0.49cm^2) and days 35 and 42 (mean difference of 7.61cm^2). The differences between remaining consecutive time points were not significant.

At day 7, wounds allowed to heal by secondary intention were 61% of the tattooed area, 54% at day 14, 41% at day 21, 39% at day 28, 37 % at day 35, 30% at day 42, 23% at day 84 and 15% at day 180. The wounds allowed to heal by secondary intention were significantly smaller ($p<0.0001$) at each post-operative time point.

Wounds treated by STSG alone

These wounds showed an initial decrease in size from 12.56^2 cm at day 0 to 11.48cm^2 at day 7, 10.71cm^2 at day 14, and 11.07cm^2 at day 21. All differences were statistically significant

($p<0.0001$), except between days 14 and 21. Wound area increased in from day 21 onwards to 12.48cm^2 at day 28, 14.73cm^2 at day 35, 17.75cm^2 day 42, 23.9cm^2 at day 84 and 27.41cm^2 at day 180.

When compared to the tattooed areas, wounds treated with STSG alone were significantly smaller at each post-operative time point ($p<0.0001$). At day 7, these wounds were 74% of the tattooed area, 59% at day 14, 54% at day 21, 61% at day 28, 71% at day 35, 78% at day 42, 90% at day 84 and 82% at day 180. The mean wound area difference was 3.99cm^2 at day 7, 7.76cm^2 at day 14, 9.34cm^2 at day 21, 8.09cm^2 day 28, 5.96cm^2 at day 35, 5.07cm^2 at day 42, 2.73cm^2 at day 84 and 6.14cm^2 day 180.

When compared to the wounds allowed to heal by secondary intention, wounds treated by STSG alone were significantly larger ($p<0.0001$) at every time point. This difference in size increased over time and was greatest after day 21. The mean wound area difference was 2.11cm^2 at day 7, 0.88cm^2 at day 14, 2.75cm^2 at day 21, 4.39cm^2 day 28, 7.13cm^2 at day 35, 10.93cm^2 at day 42, 17.77cm^2 at day 84 and 21.82cm^2 day 180.

Wounds treated with SM + STSG

All differences between consecutive time points were statistically significant ($p<0.0001$) except between days 7 and 14. When compared to the tattooed areas, wounds treated with SM + STSG were significantly smaller at each post-operative time point ($p<0.0001$). At day 7, these wounds were 89% of the tattooed area, 69% at day 14, 65% at day 21, 74% at day 28, 79% at day 35, 85% at day 42, 91% at day 84 and 85% at day 180. The mean wound area difference was 2.38cm^2 at day 7, 5.84cm^2 at day 14, 7.06cm^2 at day 21, 5.35cm^2 day 28, 4.37cm^2 at day 35, 4.36cm^2 at day 42, 2.50cm^2 at day 84 and 5.05cm^2 day 180.

Wounds treated with SM+STSG were larger than those allowed to heal by secondary intention at each post-operative time point. The mean wound area difference was 3.73cm^2 at day 7, 2.81cm^2 at

day 14, 5.00cm^2 at day 21, 7.12cm^2 day 28, 8.72cm^2 at day 35, 11.64cm^2 at day 42, 18cm^2 at day 84 and 22.91cm^2 day 180. These differences were statistically significant ($p<0.0001$) at each post-operative time point.

Wounds treated with SM + STSG were larger in area than those treated with STSG alone at each time point. The mean wound area difference was 1.61cm^2 at day 7, 1.93cm^2 at day 14, 2.26cm^2 at day 21, 2.74cm^2 day 28, 1.59cm^2 at day 35, 0.71cm^2 at day 42, 0.26cm^2 at day 84 and 1.09cm^2 day 180. These differences were statistically significant ($p<0.0001$) at each time point except at day 84 ($p=0.225$).

Macroscopic appearances of the wounds in a 42 day and 180 day study

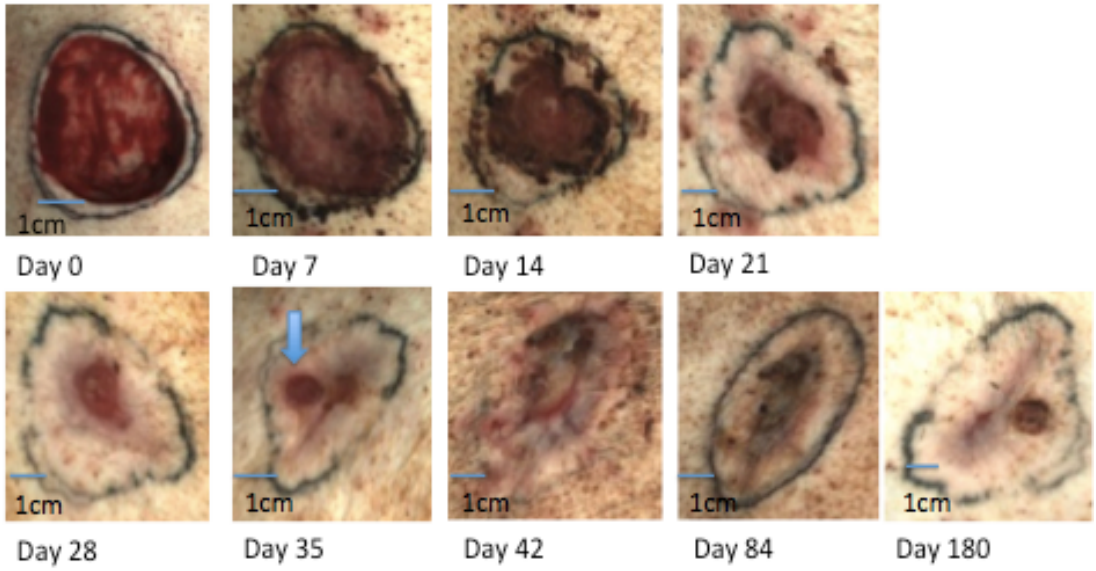

Figure 4.5.3.1: An example of the macroscopic appearances of the full thickness excision wounds allowed to heal by secondary intention in a 42 day and 180 day study. The "nodule" apparent in the pictures (blue arrow) is the scar resulting from the 8mm punch biopsy.*

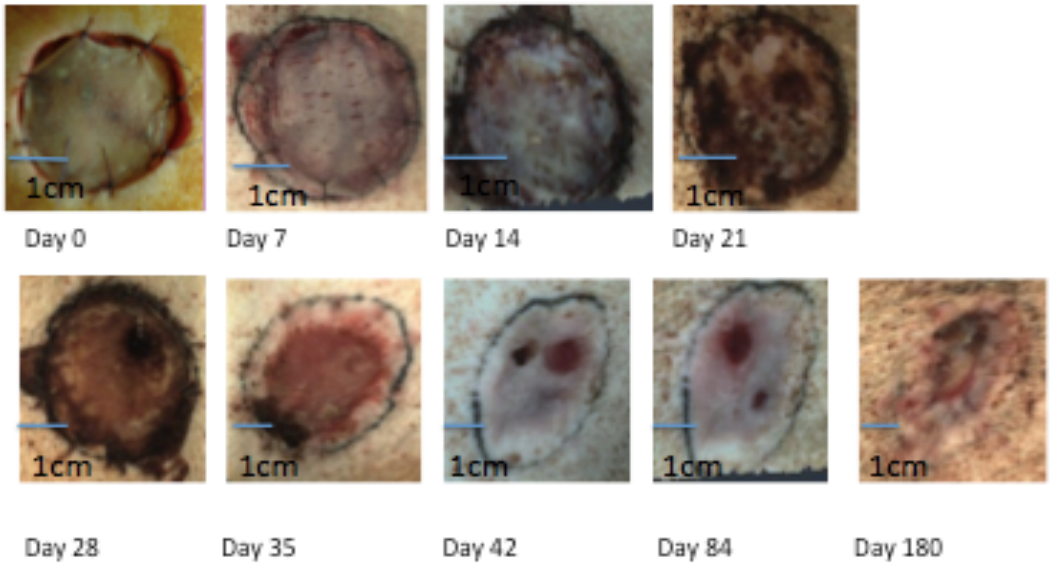

Figure 4.5.3.2: An example of the macroscopic appearances of the full thickness excision wounds treated with split thickness skin graft alone in a 42 day and 180 day study.*

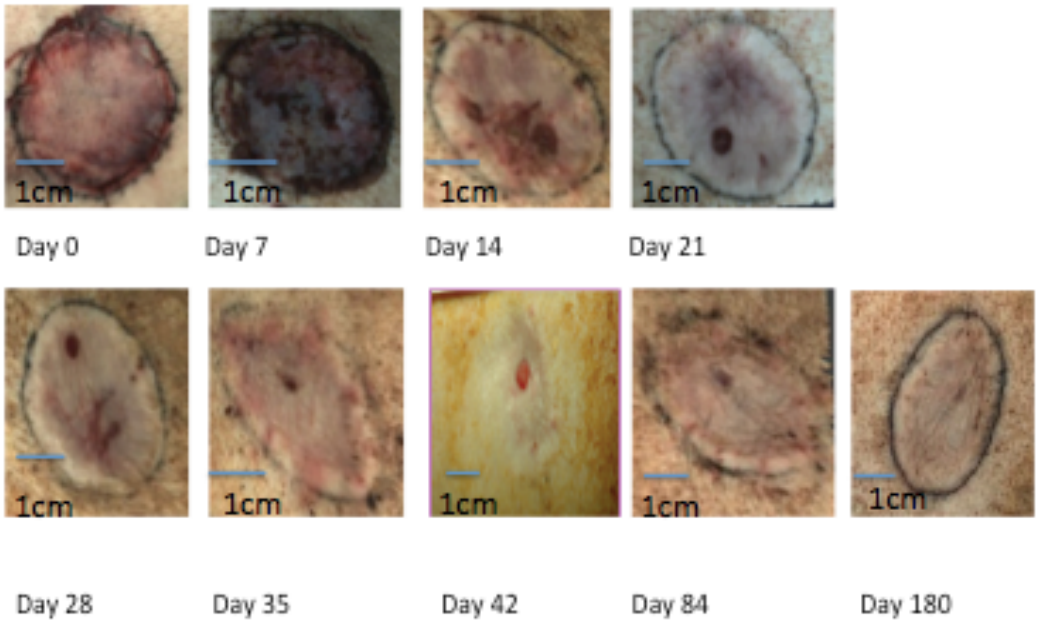

Figure 4.5.3.3: An example of the macroscopic appearances of the full thickness excision wounds treated with Smart Matrix™ + split thickness skin graft in a 42 day and 180 day study.*

*Wound area was measured quantitatively using Eykona. For the purpose of this illustration, approximate scale bars have been added to aid interpretation of the images which have been scaled differently (according to camera zoom).

	Day 0	Day 7	Day 14	Day 21	Day 28	Day 35	Day 42	Day 84	Day 180
SM+STSG	13 (±0)	13 (±0.05)	13 (±0.08)	13 (±0.11)	15 (±0.08)	16 (±0.11)	18 (±0.08)	24 (±0.21)	28 (±0.40)
STSG alone	13 (±0)	15 (±0.08)	11 (±0.08)	11 (±0.08)	12 (±0.09)	15 (±0.09)	18 (±0.11)	24 (±0.28)	27 (±0.34)
secondary intention	13 (±0)	9 (±0.10)	10 (±0.12)	8 (±0.11)	8. (±0.11)	8(±0.10)	7 (±0.10)	6 (±0.16)	5 (±0.16)
normal skin	13 (±0)	13 (±0.12)	13 (±0.10)	13 (±0.08)	15 (±0.10)	16 (±0.09)	18 (±0.11)	24 (±0.24)	28 (±0.40)

Table 4.5.3: Mean wound area (cm^2) as a percentage of the tattooed area versus time (n=54, 18 per wound group) for different reconstructive options, in a 180 day study.

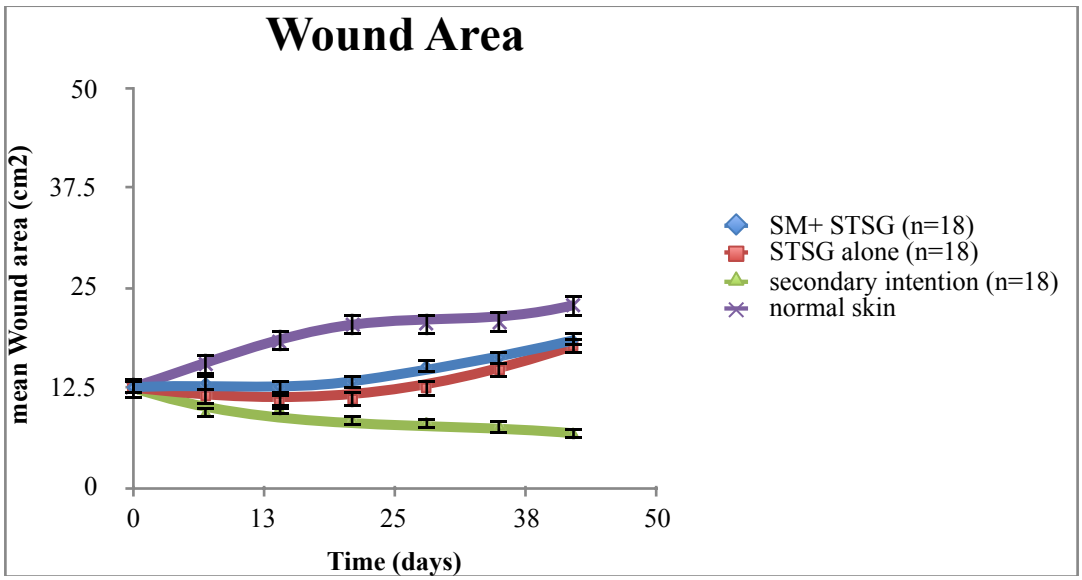

Figure 4.5.3.4: mean wound area versus time (n=54, 18 per wound group) for different reconstructive options, in a 42 day study.

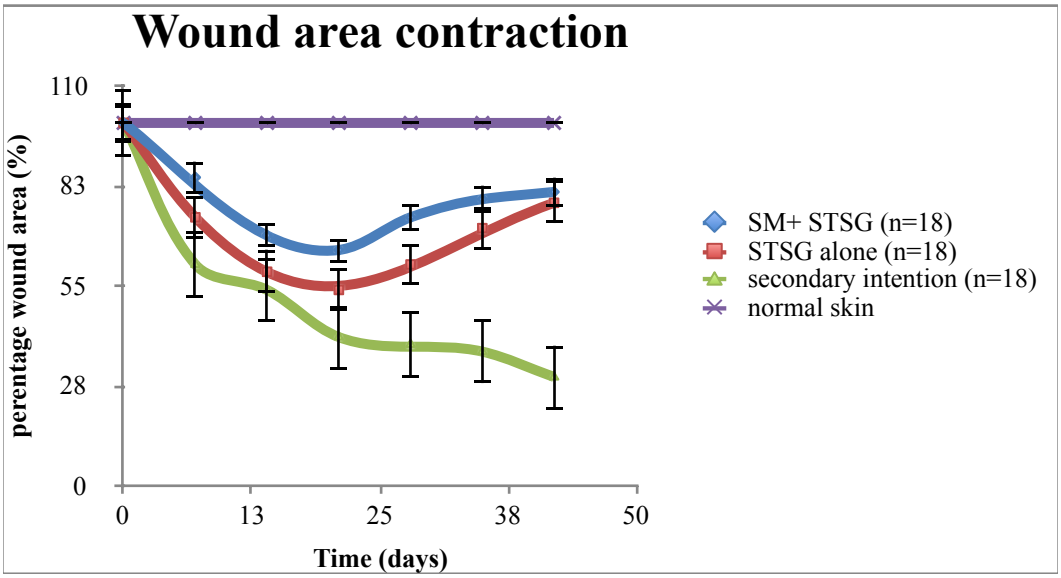

Figure 4.5.3.5: Mean wound area as a percentage of the tattooed area versus time (n=54, 18 per wound group) for different reconstructive options, in a 42 day study.

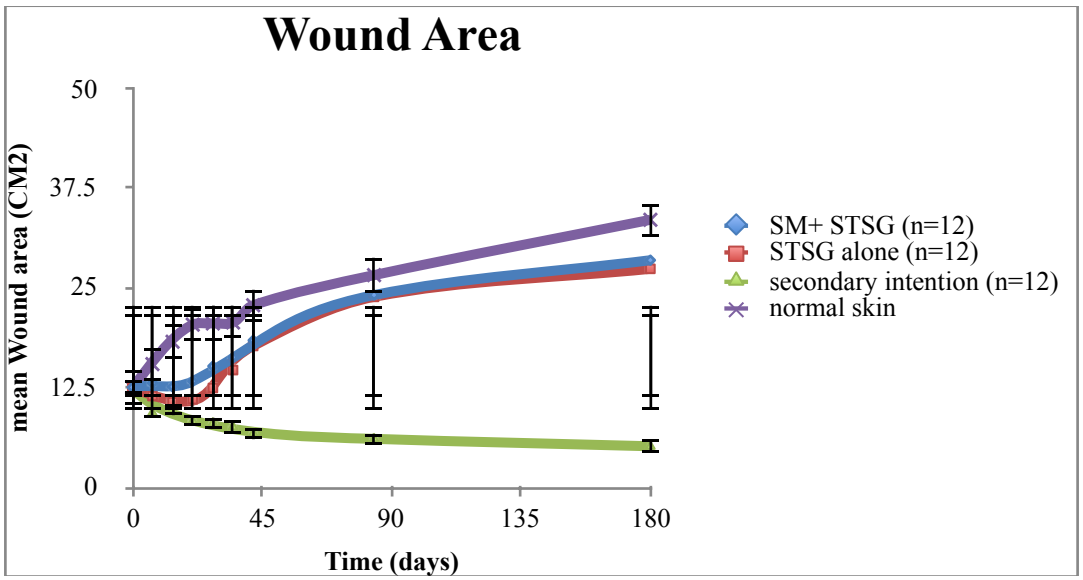

Figure 4.5.3.6: mean wound area versus time (n=36, 12 per wound group) for different reconstructive options, in a 180 day study.

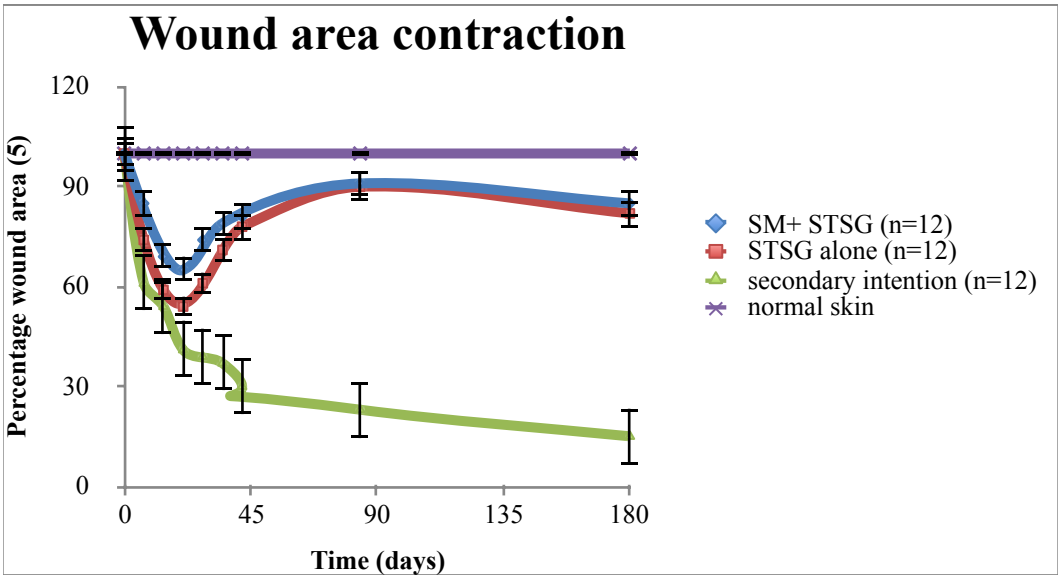

Figure 4.5.3.7: mean wound area as a percentage of the tattooed area versus time (n=36, 12 per wound group) for different reconstructive options, in a 180 day study.

Interpretations for mean wound area and contraction

The tattooed area increased in size over time. Wounds treated with SM+STSG showed the smallest degree of contraction throughout the study. Wounds treated with STSG alone contracted less than those allowed to heal by secondary intention and more than those treated by SM+STSG. All

wounds were smaller at each post-operative time point than the tattooed area. These area differences were all statistically significant ($p<0.0001$).

4.5.4 EDA-Fibronectin (EDA-FN) staining

Please see Table 4.5.4 and Figures 4.5.4.1-2

Normal skin

EDA-FN content of normal skin showed no significant changes over time.

Wounds allowed to heal by secondary intention

The changes in density between individual time points from days 7 to 84 were not statistically significant. Statistically significant ($p<0.0001$) changes occurred between days 42 to 84 (mean difference of 0.19) and days 84 to 180 (mean difference of 1.51).

Wounds allowed to heal by secondary intention showed higher levels of EDA-FN than normal skin throughout the entire study. The mean difference was 2.41 at day 7, 2.36 at day 14, 2.76 at day 21, 2.52 at day 28, 2.52 at day 35, 2.42 at day 42, 2.21 at day 84 and 0.92 day 180. These differences were statistically significant ($p<0.0001$) at each time point.

Wounds treated by STSG alone

These changes were statistically significant ($p<0.0001$) between days 7 and 14 (mean difference of 0.184) and days 28 and 35 (mean difference of 0.644).

Wounds treated with STSG alone showed statistically significantly ($p<0.0001$) higher levels of EDA-FN staining than normal skin throughout the entire study. The mean difference was 1.42 at day 7, 2.46 at day 14, 2.64 at day 21, 2.94 at day 28, 2.62 at day 35, 1.93 at day 42, 1.74 at day 84

and 1.53 at day 180.

Wounds treated with STSG showed lower levels of EDA-FN staining compared to wounds allowed to heal by secondary intention, at day 7, which then increased to similar levels throughout the rest of the study before decreasing after day 28. The mean difference was 0.98 at day 7 (statistically significant, $p<0.0001$), 0.095 at day 14 (not statistically significant) 0.13 at day 21 (not statistically significant), 0.42 at day 28 (statistically significant, $p=0.0004$), 0.76 at day 35 (not statistically significant), 0.49 at day 42 (statistically significant, $p<0.0001$), 0.46 at day 84 (not statistically significant) and 0.61 at day 180 (statistically significant, $p=0.0002$).

Wounds treated with SM + STSG

The changes in EDA-FN staining between consecutive time post-operative time points were statistically significant only between days 42 and 84 (a difference of 0.42, $p=0.0197$).

Wounds treated with SM+STSG showed higher levels of EDA-FN staining than normal skin throughout the entire study. These differences were statistically significant at each time point except days 84 and 180. The mean difference was 1.12 at day 7 ($p<0.0001$), 0.8 at day 14 ($p<0.0001$), 0.83 at day 21 ($p<0.0001$), 0.81 at day 28 ($p<0.0001$), 0.52 at day 35 ($p=0.0003$), 0.51 at day 42 ($p=0.0006$), 0.07 at day 84 and 0.06 at day 180.

Wounds treated with SM+STSG showed lower levels of EDA-FN staining than wounds allowed to heal by secondary intention throughout the entire study. These differences were statistically significant ($p<0.0001$) at days 7, 28, 42 and 84. The mean difference was 0.98 at day 7, 0.09 at day 14, 0.13 at day 21, 0.42 at day 28, 0.26 at day 35, 0.49 at day 42, 0.46 at day 84 and 0.61 at day 180.

Wounds treated with SM+STSG showed lower levels of EDA-FN staining than wounds treated with STSG alone throughout the entire study. The mean difference was at 0.30 day 7, 1.65 at day 14, 1.81 at day 21, 2.13 at day 28, 1.74 at day 35, 1.42 at day 42, 1.67 at day 84 and 1.47 at day 180.

These differences were statistically significant ($p<0.0001$) at each time point except at day 7.

	Day 7	Day 14	Day 21	Day 28	Day 35	Day 42	Day 84	Day 180
SM+STSG	1.81 (±0.05)	1.64 (±0.06)	1.56 (±0.05)	1.54 (±0.05)	1.29 (±0.05)	1.32 (±0.04)	0.90 (±0.05)	0.61 (±0.05)
STSG alone	2.11 (±0.04)	1.81 (±0.05)	3.37 (±0.09)	3.67 (±0.03)	3.03 (±0.05)	2.74 (±0.12)	2.57 (±0.10)	2.14 (±0.07)
secondary intention	3.09 (±0.11)	3.20 (±0.05)	3.49 (±0.04)	3.25 (±0.04)	3.29 (±0.04)	3.24 (±0.06)	3.04 (±0.07)	1.53 (±0.06)
normal skin	0.69 (±0.5)	0.84 (±0.5)	0.73 (±0.06)	0.73 (±0.05)	0.76 (±0.05)	0.82 (±0.05)	0.83 (±0.05)	0.61 (±0.05)

Table 4.5.4: Mean EDA-Fibronectin staining density (score out for 5), where n=108 (36 per wound group) for the 42 day study and n=36 (12 per wound group) for the 180 day study

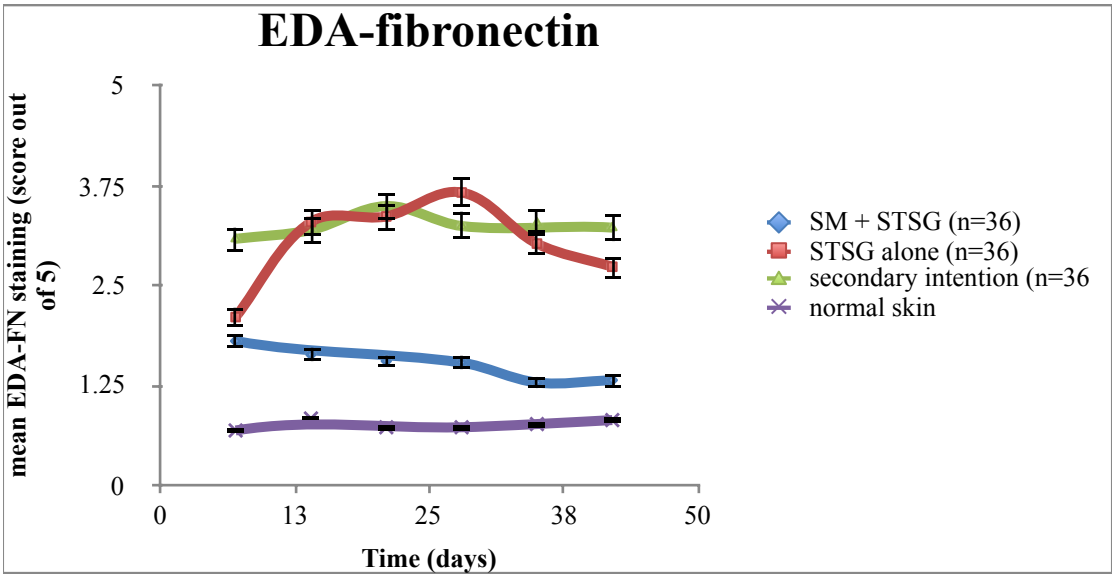

Figure 4.5.4.1 : mean EDA-Fibronectin staining density versus time (n=108, 36 per wound group) for different reconstructive options in a 42 day study.

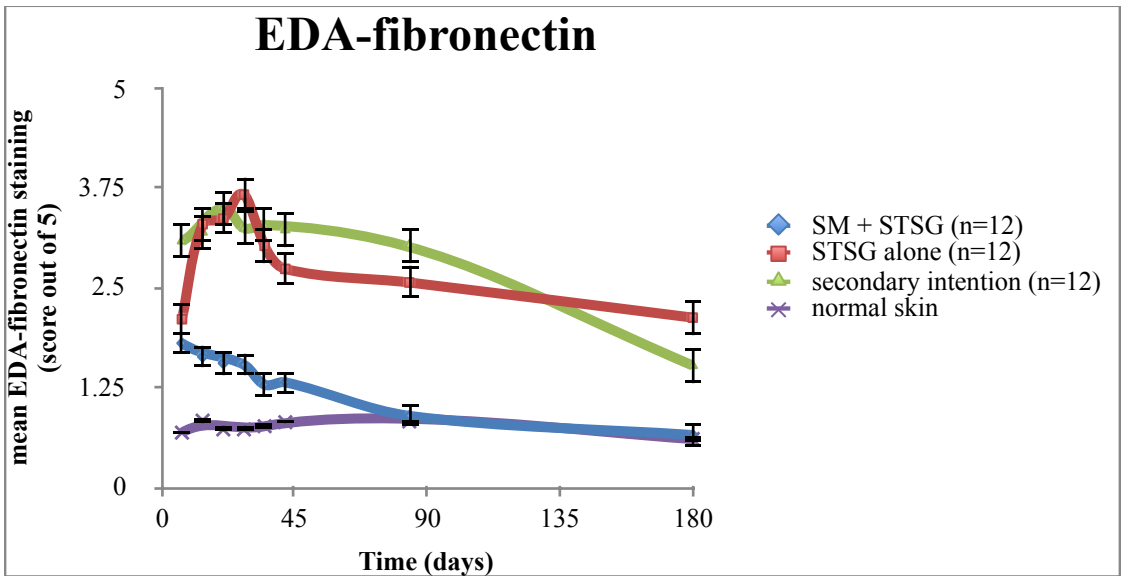

Figure 4.5.4.2: mean EDA-Fibronectin staining density versus time (n=36, 12 per wound group) for different reconstructive options in a 180 day study.

Interpretations of mean EDA-fibronectin staining

EDA-fibronectin staining was lowest in normal skin (the tattooed area), followed by wounds treated by SM+STSG. In this group, an initial peak occurred at day 7 which gradually reduced over time and reached that of normal skin by day 84. Wounds treated with STSG alone exhibited significantly higher levels of staining than wounds treated with SM+STSG with a peak at day 21, which the gradually decreased over time but remained significantly higher than wounds treated with SM+STSG and normal skin. Wounds allowed to heal by secondary intention showed the highest levels of EDA-fibronectin staining throughout the study, peaking at day 28.

4.5.5 Alpha-smooth muscle actin (α-SMA)

Please see table 4.5.5 and figures 4.5.5.1-2

Normal skin

α-SMA content of normal skin showed no significant changes over time ($p>0.999$ at each time interval).

Wounds allowed to heal by secondary intention

The changes in density between individual time points throughout the entire study were statistically significant between days 7 and 14 (mean difference of 0.58, $p<0.0001$), days 14 and 21 (mean difference of 0.37, $p<0.0001$), days 35 and 42 (mean difference of 0.29, $p=0.0125$), 42 and 84, (mean difference of 0.48, $p<0.0001$) and day 84 and 180 (mean difference of 0.6, $p<0.0001$).

Wounds allowed to heal by secondary intention showed significantly ($p<0.0001$) higher levels of α-SMA than normal skin throughout the entire study. The mean difference was 1.96 at day 7, 2.56 at day 14, 2.96 at day 21, 2.94 at day 28, 2.95 at day 35, 2.73 at day 42, 2.19 at day 84 and 1.66 at day 180.

Wounds treated by STSG alone

The changes in α-SMA staining were statistically significant between days 7 and 14 mean difference of 1.02, $p<0.0001$), days 28 and 35 (mean difference of 0.92, $p<0.0001$), days 35 and 42 (mean difference of 0.37, $p<0.0001$), days 42 and 84 (mean difference of 0.43, $p=0.0002$) and days 84 and 180 (mean difference of 0.94, $p<0.0001$).

Wounds treated with STSG alone showed higher levels of α-SMA staining than normal skin throughout the entire study. The mean difference was 1.97 at day 7, 0.45 at day 14, 0.22 at day 21, 1.97 at day 28, 2.11 at day 35, 1.81 at day 42, 1.31 at day 84 and 0.44 at day 180. These differences were statistically significant ($p<0.0001$) at each time point, except at days 28 and 180.

The mean differences between wounds treated with STSG compared to wounds allowed to heal by secondary intention were 0.02 at day 7, 0.45 at day 14, 0.22 at day 21, 0.03 at day 28, 0.85 at day 35, 0.49 at day 42, 0.88 at day 84 and 1.22 at day 180. These differences were significant ($p<0.0001$) at days 14, 35, 42, 84 and 180.

Wounds treated with SM + STSG

The changes in α-SMA staining between consecutive time post-operative time points were statistically significant ($p<0.0001$) between days 21 and 28 (a mean difference of 0.68) and days 35 and 42 (a mean difference of 0.75).

Wounds treated with SM+STSG showed very slightly higher levels of α-SMA staining when compared to normal skin at days 7 and 14. The mean differences were 0.01 at day 7, 0.02 at day 14, 0.17 at day 21, 0.78 at day 28, 0.88 at day 35, 0.20 at day 42, 0.10 at day 84 and 0.01 at day 180. These differences were only significant at day 35 ($p<0.0001$).

Wounds treated with SM+STSG showed lower levels of α-SMA staining than wounds allowed to heal by secondary intention throughout the entire study. The mean difference was 1.93 at day 7, 2.67 at day 14, 2.78 at day 21, 2.17 at day 28 at day 35, 2.07 at day 42, 2.30 at day 84 and 1.67 at day 180. These differences were statistically significant ($p<0.0001$) at each time point.

Wounds treated with SM+STSG showed lower levels of α-SMA staining than wounds treated with STSG alone throughout the entire study. The mean difference was at 1.98 day 7, 3.01 at day 14, 2.9 at day 21, 2.19 at day 28, 1.23 at day 35, 1.60 at day 42, 1.42 at day 84 and 0.45 at day 180. These differences were statistically significant at each time point ($p<0.0001$ at each point except day 180, significant at 0.0021).

	Day 7	Day 14	Day 21	Day 28	Day 35	Day 42	Day 84	Day 180
SM+STSG	0.53 (±0.04)	0.51 (±0.04)	0.66 (±0.03)	1.34 (±0.06)	1.39 (±0.03)	0.64 (±0.03)	0.40 (±0.04)	0.42 (±0.04)
STSG alone	2.51 (±0.05)	3.52 (±0.05)	3.66 (±0.15)	3.53 (±0.03)	2.67 (±0.04)	2.24 (±0.05)	1.81 (±0.07)	0.87 (±0.06)
secondary intention	2.49 (±0.05)	2.07 (±0.05)	3.44 (±0.05)	3.51 (±0.04)	3.46 (±0.04)	3.17 (±0.06)	2.69 (±0.04)	2.04 (±0.07)
normal skin	0.53 (±0.05)	0.51 (±0.05)	0.49 (±0.05)	0.57 (±0.05)	0.51 (±0.05)	0.44 (±0.05)	0.50 (±0.05)	0.43 (±0.05)

Table 4.5.5: Mean Alpha- Smooth Muscle Actin staining density (score out for 5), where n=108 (36 per wound group) for the 42 day study and n=36 (12 per wound group) for the 180 day study

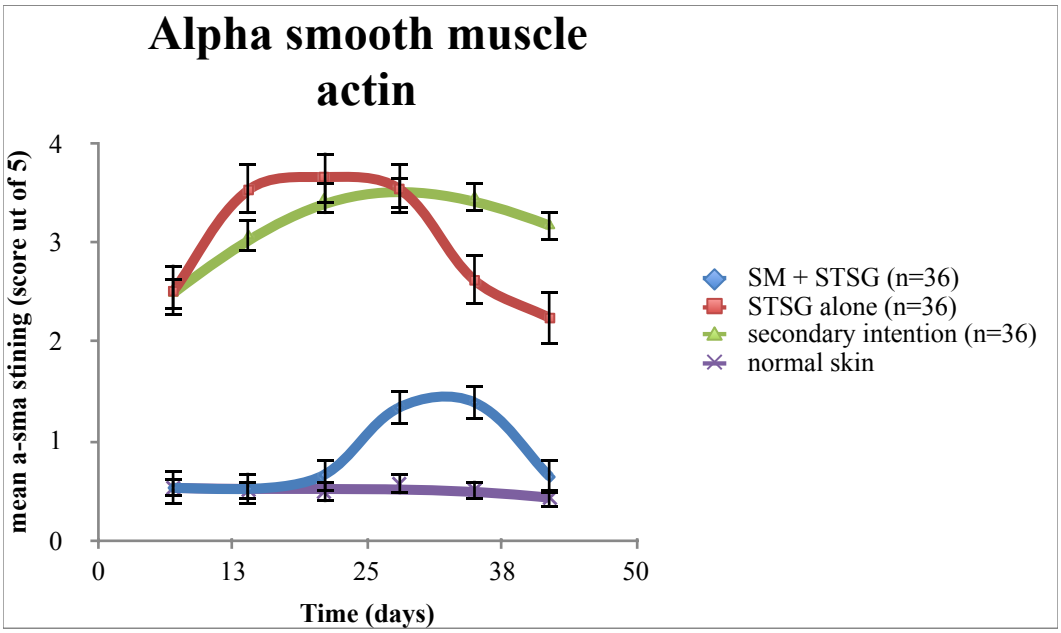

Figure 4.5.5.1: mean α-smooth muscle actin staining density versus time (n=108, 36 per wound group) for different reconstructive options, in a 42 day study.

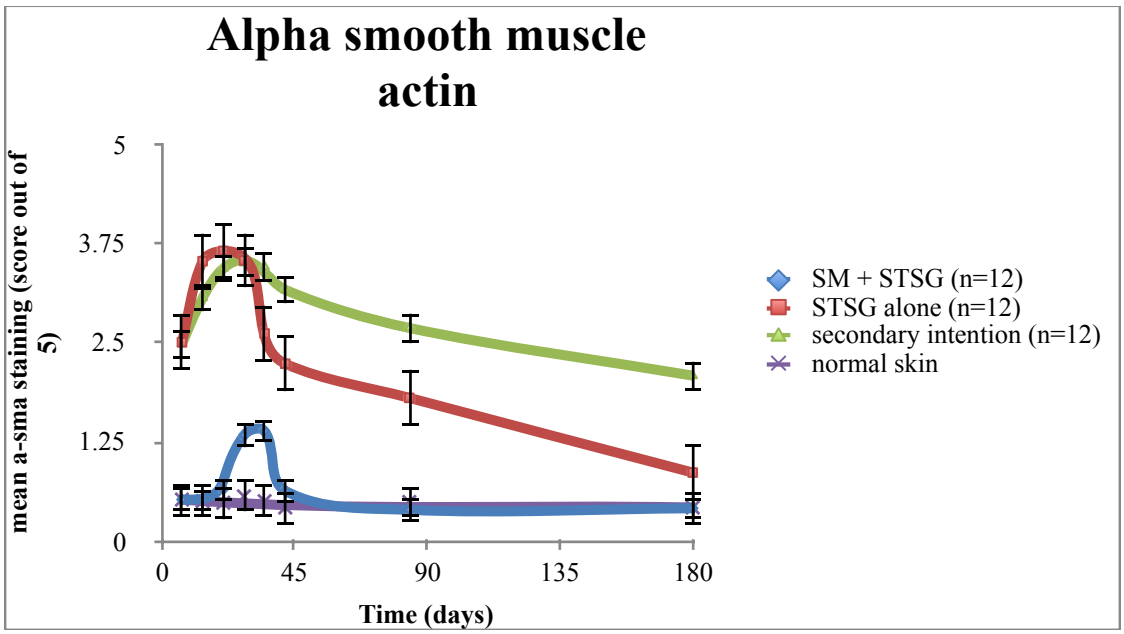

Figure 4.5.5.2: Mean α-smooth muscle actin staining density versus time (n=36, 12 per wound group) for different reconstructive options in a 180 day study.

Interpretations for mean EDA-Fibronectin and Alpha Smooth Muscle Actin staining density

Alpha Smooth Muscle Actin staining followed that of EDA-fibronectin temporally, with a lag phase of about 7 days, in all the wounds. EDA-FN and α-SMA staining was lowest in normal skin, followed by wounds treated by SM+STSG. These wounds approached staining levels of normal skin by day 84. Wounds treated with STSG alone exhibited higher levels of EDA-FN and α-SMA staining than wounds treated with SM+STSG. Wounds allowed to heal by secondary intention showed the highest levels of both EDA-FN and α-SMA staining. In wounds treated with SM + STSG, α-SMA and EDA-FN staining appeared closer to the wound bed (in the reticular dermis) investing pericytes, than to the wound surface.

4.5.6 Collagen

Please see table 4.5.6 and Figures 4.5.6.1-2

Normal skin

Collagen content of normal skin showed no significant changes over time between days 7 and 180.

Wounds allowed to heal by secondary intention

The changes in density between individual time points throughout the entire study were statistically significant ($p<0.0001$) between days 14 and 21 (mean difference of 0.75), days 28 and 35 (mean difference of 0.84) and days 35 and 42 (mean difference of 1.03).

Wounds allowed to heal by secondary intention showed lower levels of collagen than normal skin from throughout the study. These differences were statistically significant at all consecutive post-operative time point between days 7 and 42 ($p<0.0001$). The mean difference was 3.11 at day 7, 2.88 at day 14, 2.23 at day 21, 2.44 at day 28, 1.56 at day 35, 1.02 at day 42, 0.67 at day 84 and 0.58 at day 180.

Wounds treated by STSG alone

The changes in collagen staining were statistically significant ($p<0.0001$) between days 14 and 21 mean difference of 0.75), days 28 and 35 (mean difference of 0.84,) and days 35 and 42 (mean difference of 10.3).

Wounds treated with STSG alone showed levels of collagen staining than normal skin throughout the entire study. The mean difference was 3.11 at day 7, 2.88 at day 14, 2.23 at day 21, 2.44 at day 28, 1.56 at day 35, 1.02 at day 42, 0.67 at day 84 and 0.58 at day 180. These differences were statistically significant ($p<0.0001$) at each time point, except at days 84 and 180.

Wounds treated with STSG showed higher levels of collagen staining compared to wounds allowed

to heal by secondary intention, throughout the study. The mean difference was 0.87 at day 7, 0.75 at day 14, 0.91 at day 21, 1.2 at day 28, 0.81 at day 35, 0.04 at day 42, 0.41 at day 84 and 0.36 at day 180. These differences were statistically significant ($p<0.0001$) at each time point, except at days 42, 84 and 180.

Wounds treated with SM + STSG

The changes in collagen staining between consecutive time post-operative time points were statistically significant only between days 7 and 14 ($p<0.0001$), days 14 and 21 ($p=0.01$), days 21 and 28 ($p<0.0001$) and days 28 and 35 ($p=0.0015$).

Wounds treated with SM+STSG showed lower levels of collagen staining when compared to normal skin throughout the entire study. The mean differences were 1.99 at day 7, 1.12 at day 14, .88 at day 21, 0.25 at day 35, 0.5 at day 42, 0.06 at day 84 and 0.15 at day 180. These differences were significant ($p<0.0001$ at each time point except at day 42 where $p=0.0007$) at each time point except at days 35, 84 and 180.

In wounds treated with SM+STSG, collagen fibrils appeared more organised into a fibril formation after day 28 closer to the surface, and slightly more haphazard closer to the wound bed. Over time, the collagen fibrils appeared more organised into a fibrillar structure homogenously throughout the wound. This was similar in wounds treated by STSG alone. Wounds allowed to heal by secondary intention showed an initially homogenously disorganised network with subsequent signs of organisation by day 84.

Wounds treated with SM+STSG showed higher levels of collagen staining than wounds allowed to heal by secondary intention throughout the entire study. The mean difference was 1.12 at day 7, 1.76 at day 14, 1.35 at day 21, 1.77 at day 28, 1.36 at day 35, 0.54 at day 42, 0.61 at day 84 and 0.47 at day 180. These differences were statistically significant ($p<0.0001$) at each time point except at day 180 ($p=0.06$).

Wounds treated with SM+STSG showed higher levels of collagen staining than wounds treated with STSG alone throughout the entire study. The mean difference was at 0.25 at day 7, 1.00 at day 14, 0.43 at day 21, 0.57 at day 28, 0.51 at day 35, 0.51 at day 42, 0.20 at day 84 and 0.07 at day 180. These differences were statistically significant ($p<0.0001$) at each time point except at days 7, 84 and 180.

	Day 7	Day 14	Day 21	Day 28	Day 35	Day 42	Day 84	Day 180
SM+STSG	1.49 (±0.03)	2.25 (±0.04)	2.59 (±0.05)	3.22 (±0.04)	3.60 (±0.04)	3.86 (±0.03)	3.92 (±0.03)	3.91 (±0.03)
STSG alone	1.24 (±0.03)	1.24 (±0.03)	2.15 (±0.04)	2.65 (±0.05)	3.09 (±0.04)	3.36 (±0.04)	3.72 (±0.05)	3.84 (±0.04)
secondary intention	0.37 (±0.03)	0.49 (±0.03)	1.24 (±0.03)	1.45 (±0.04)	2.29 (±0.03)	3.32 (±0.11)	3.37 (±0.23)	3.49 (±0.05)
normal skin	3.48 (±0.06)	3.37 (±0.06)	3.45 (±0.03)	3.89 (±0.04)	3.84 (±0.04)	4.34 (±0.03)	3.99 (±0.01)	4.26 (±0.08)

Table 4.5.6: Mean Collagen staining density (score out for 5), where n=108 (36 per wound group) for the 42 day study and n=36 (12 per wound group) for the 180 day study

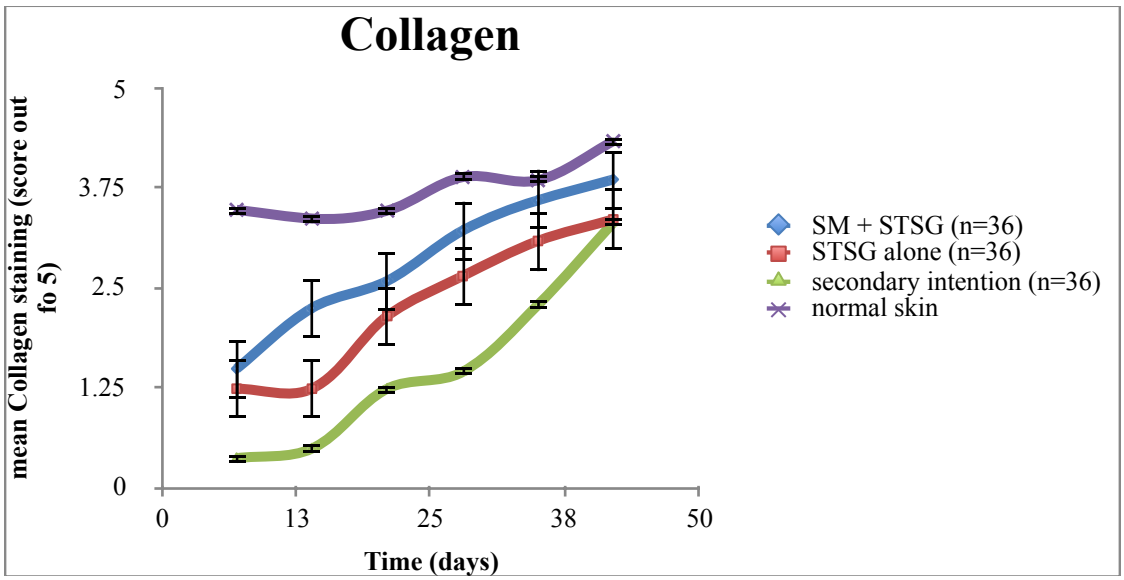

Figure 4.5.6.1: A graph showing mean collagen staining density versus time (n=108, 36 per wound group) for different reconstructive options in a 42 day study.

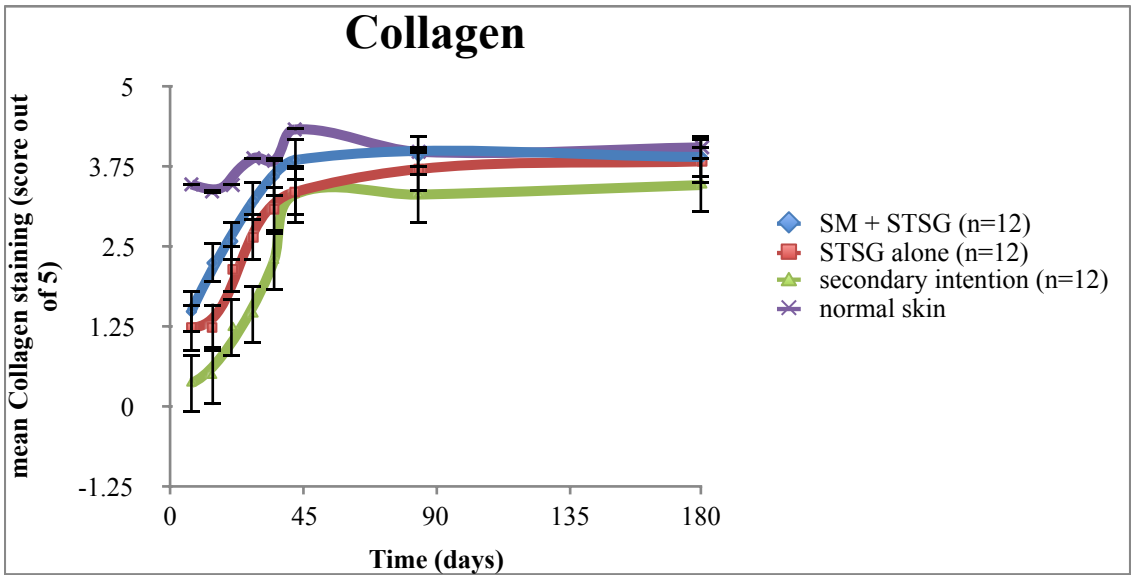

Figure 4.5.6.2: A graph showing mean collagen staining density versus time (n=36, 12 per wound group) for different reconstructive options in a 180 day study.

Interpretations for mean collagen staining density

Wounds treated by SM + STSG showed an increase in staining levels for Collagen from day 7. This trajectory was similar to wounds treated with STSG alone. Wounds treated with SM+STSG showed higher levels of collagen staining than those treated with STSG alone. Wounds allowed to

heal by secondary intention followed by a lag phase of 14 days (at day 21). By day 42, all wounds had reached their mature state of collagen quantity. Total staining was similar for all wounds with wounds treated by SM+STSG exhibiting similar amounts to that of normal skin (the tattooed area), followed closely by those treated with STSG alone, with smaller scores for wounds allowed to heal by secondary intention.

4.5.7 Elastin

Please see table 4.5.7 and Figures 4.5.7.1-2

Normal skin

Elastin content of normal skin showed no significant changes over time except between days 14 and 21 (mean difference of 0.36, $p=0.0002$) and days 28 and (mean difference of 0.31, $p=0.0047$).

Wounds allowed to heal by secondary intention

The changes in density between individual time points were statistically significant ($p<0.0001$) between days 35 and 42 (mean difference of 0.34), days 42 and 84 (mean difference 0.74) and days 84 and 180 (mean difference 0.42).

Wounds allowed to heal by secondary intention showed statistically significant ($p<0.0001$) lower levels of elastin than normal skin from throughout the study. The mean difference was 1.90 at day 7, 2.20 at day 14, 1.70 at day 21, 1.62 at day 28, 1.81 at day 35, 1.63 at day 42, 1.06 at day 84 and 1.15 at day 180.

Wounds treated by STSG alone

The changes in elastin staining density were statistically significant between days 14 and 21 (mean difference of 0.2, p=0,0156), days 21 and 28 (mean difference of 0.71, p<0.0001) and days 42 and 84 (mean difference of 0.53, p<0.0001).

Wounds treated with STSG alone showed lower levels of elastin staining than normal skin throughout the entire study. The mean difference was 2 at day 7, 2.20 at day 14, 1.70 at day 21, 1.62 at day 28, 1.81 at day 35, 1.63 at day 42, 1.06 at day 84 and 1.15 at day 180. These differences were statistically significant (p<0.0001) at each time point.

Wounds treated with STSG showed no significant difference in elastin staining levels compared to those allowed to heal by secondary intention at equivalent time points between days 7 and 21. Statistically significant (p<0.0001) higher levels were seen in wounds treated with STSG alone compared to wounds allowed to heal by secondary intention, throughout the study thereafter. The mean difference was 0.07 at day 7, 0.10 at day 14, 0.18 at day 21, 0.88 at day 28, 0.93 at day 35, 0.59 at day 42, 0.80 at day 84 and 0.92 at day 180.

Wounds treated with SM + STSG

The changes in elastin staining between consecutive time post-operative time points were statistically significant only between days 7 and 14 (mean difference of 0.98, p<0.0001), days 14 and 21 (mean difference of 0.65, p=0.01) and days 35 and 42 (mean difference of 0.34, p<0.0001).

When comparing wounds treated with SM+STSG to normal skin, the mean differences were 1.8 at day 7, 1.03 at day4, 0.02 at day 21, 0.09 at day 28, 0.22 at day 35, 0.03 at day 42, 0.24 at day 84 and 0.05 at day 180. These differences were only significant (p<0.0001) at days 7 and 14.

Wounds treated with SM+STSG showed higher levels of elastin staining than wounds allowed to

heal by secondary intention throughout the entire study. The mean difference was 0.15 at day 7, 1.17 at day 14, 1.67 at day 21, 1.71 at day 28, 1.60 at day 35, 1.60 at day 42 , 0.82 at day 84 and 1.19 at day 180. These differences were statistically significant ($p<0.0001$) at each time point except at day 7 ($p=0.4152$).

Wounds treated with SM+STSG showed higher levels of elastin staining than wounds treated with STSG alone throughout the entire study. The mean difference was at 0.22 at day 7, 1.06 at day 14, 1.50 at day 21, 0.83 at day 28, 0.66 at day 35, 1.01 at day 42, 0.44 at day 84 and 0.28 at day 180. These differences were statistically significant ($p<0.0001$ for all except day 180, where $p=0.0324$) at each time point except at day 7 ($p=0.0058$).

	Day 7	Day 14	Day 21	Day 28	Day 35	Day 42	Day 84	Day 180
SM+STSG	0.54 (±0.03)	1.52 (±0.03)	2.16 (±0.04)	2.20 (±0.04)	2.22 (±0.04)	2.56 (±0.04)	2.52 (±0.04)	2.48 (±0.04)
STSG alone	0.32 (±0.03)	0.45 (±0.03)	0.33 (±0.04)	1.37 (±0.03)	1.55 (±0.03)	1.55 (±0.04)	2.08 (±0.06)	2.20 (±0.06)
secondary intention	0.39 (±0.03)	0.36 (±0.03)	0.48 (±0.03)	0.50 (±0.04)	0.62 (±0.04)	0.96 (±0.04)	1.70 (±0.05)	1.30 (±0.06)
normal skin	2.32 (±0.05)	2.54 (±0.05)	2.18 (±0.06)	2.12 (±0.05)	2.43 (±0.06)	2.59 (±0.06)	2.76 (±0.11)	2.43 (±0.11)

Table 4.5.7: Mean Elastin staining density (score out for 5), where n=108 (36 per wound group) for the 42 day study and n=36 (12 per wound group) for the 180 day study

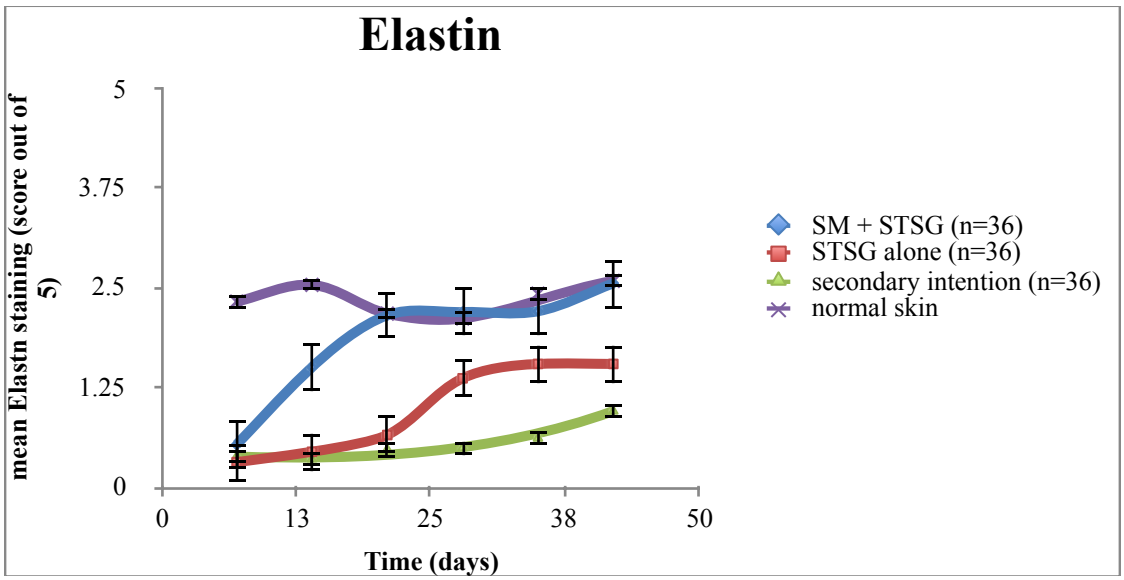

Figure 4.5.7.1: Mean elastin staining density versus time (n=108, 36 per wound group) for different reconstructive options in a 42 day study.

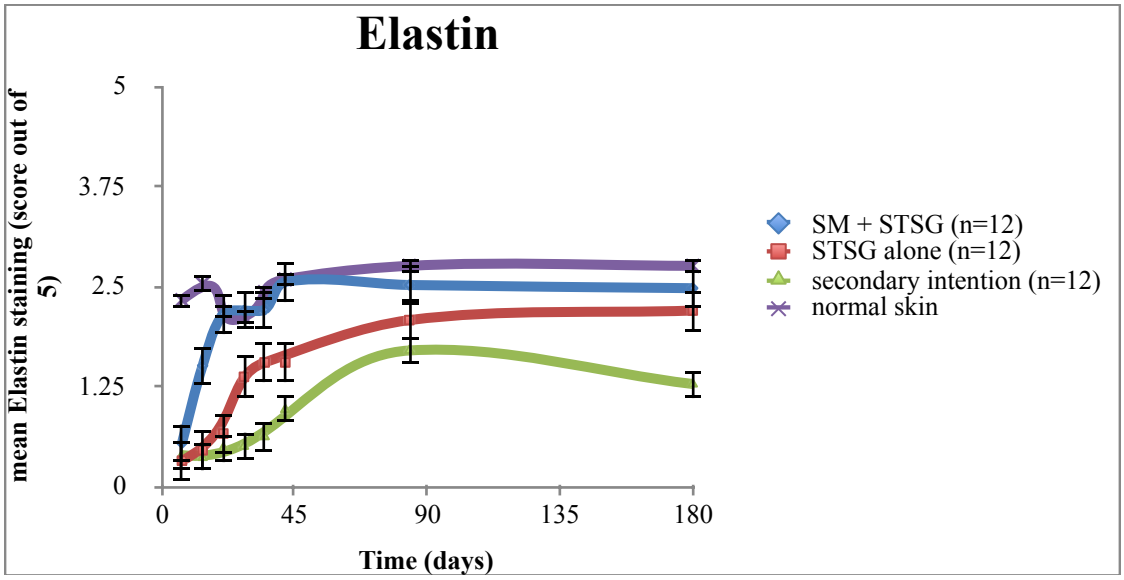

Figure 4.5.7.2: Mean elastin staining density versus time (n=36, 12 per wound group) for different reconstructive options in a 180 day study.

Interpretations for mean elastin staining density

Wounds treated with SM + STSG showed a rapid increase in elastin staining over the first 42 days.

This remained at a similar level thereafter, which was higher than wounds treated with STSG alone

and those allowed to heal by secondary intention. Wounds treated with STSG alone showed a less steep increase over 84 days, which continued to increase slowly up to day 180. Wounds allowed to heal by secondary intention showed the least increase in elastin staining which peaked at day 84 with a small decline thereafter.

4.5.8 Neodermal thickness

Please see table 4.5.8 and figures 4.5.8.1-2

Normal skin

These measurements showed no significant changes over time except between days 28 and 35 (mean difference of 45.22µm, $p=0.0181$).

Wounds allowed to heal by secondary intention

The increases in wound thickness between individual time points were statistically significant ($p<0.0001$) between all consecutive time points except between days 42 and 84 and days 84 and 180.

Wounds allowed to heal by secondary intention were less thick than normal skin between days 7 and 28. These differences were statistically significant ($p<0.0001$). The mean difference was 394.21µm at day 7, 299.14µm at day 14, 255.42µm at day 21 and 91µm and day 28. Between days 35 and 180, wounds allowed to heal by secondary intention were thicker than normal skin. These differences were statistically significant ($p<0.0001$ at each time point except at day 3 where $p=0.0171$). The mean difference was 39.71µm at day 35, 100µm at day 42, 132.21µm at day 84 and

122.04μm at day 180.

Wounds treated by STSG alone

The changes (increasing between days 7 and 35 and decreasing thereafter) in neodermal thickness between consecutive time points were statistically significant at each reading ($p<0.0001$).

Wounds treated with STSG alone were less deep than normal skin between days 7 and 21. These differences were all statistically significant. The mean differences were 325.05μm at day 7 ($p<0.0001$), 90.22μm at day 14 ($p<0.0001$) and 45.45μm at day 21 ($p=0.0009$). Between days 28 and 84, wounds treated with STSG were thicker than normal skin. These differences were statistically significant ($p<0.0001$). The mean differences were 193.08μm at day 28, 248.76μm at day 35, 206.00μm at day 42 and 104.92μm at day 84. At day 180, wounds treated with STSG were less deep than normal skin. The mean difference was 84.03μm. This difference was statistically significant (p=00006).

Wounds treated with STSG were thicker than those allowed to heal by secondary intention throughout the entire study. These differences were all statistically significant ($p<0.0001$) except at day 84. The mean difference was 70.23μm at day 7, 208.60μm at day 14, 210.93μm at day 21, 284.32μm at day 28, 287.74μm at day 35, 90.23μm at day 42, 28.07μm at day 84 and 206.11μm at day 180.

Wounds treated with SM + STSG

The changes in wound depth between consecutive time post-operative time points were statistically significant throughout the study, $p<0.0001$), except between days 21 and 28. The mean difference was 330.05μm between days 7 and 14, 242.24μm between days 14 and 21, 16.5μm between days 21 and 28, 42.23μm between days 28 and 35, 53.57μm between days 35 and 42, 65.22μm between days 42 and 84 and 228.65μm between days 84 and 180.

Wounds treated with SM+STSG were less thick than normal skin at day 7, but then thicker from

days 14 to 180. All these differences were statistically significant ($p<0.0001$), except at day 180. The mean difference was 222.24µm at day 7, 120.54µm at day 14, 332.27µm at day 21, 389.14µm at day 28, 302.78µm at day 35, 278.43µm at day 42, 218.46µm at day 84 and 3µm at day 180.

Wounds treated with SM+STSG were thicker than those allowed to heal by secondary intention throughout the study, except at day 180. All these differences were statistically significant at the same post-operative time points ($p<0.0001$). The mean difference was 173.27µm at day 7, 419.43µm at day 14, 587.2µm at day 21, 480.67µm at day 28, 341.24µm at day 35, 176.56µm at day 42, 87.15µm at day 84 and 119.83µm at day 180.

Wounds treated with SM+STSG were deeper than those treated with STSG alone throughout the study. All these differences were statistically significant at the same post-operative time points ($p<0.0001$). The mean difference was 103.21µm at day 7, 211.54µm at day 14, 378.26µm at day 21, 196.34µm at day 28, 51.06µm at day 35, 88.24µm at day 42, 115.67µm at day 84 and 87.22µm at day 180.

	Day 7	Day 14	Day 21	Day 28	Day 35	Day 42	Day 84	Day 180
SM+STSG	321.13 (±1.37)	650.08 (±0.98)	892.98 (±3.05)	908.63 (±1.17)	866.47 (±0.99)	813.22 (±1.09)	748.64 (±1.63)	519.26 (±1.48)
STSG alone	218.12 (±6.25)	439.31 (±0.94)	514.22 (±1.71)	712.29 (±3.85)	811.14 (±2.61)	725.64 (±1.05)	633.08 (±1.29)	432.87 (±1.23)
secondary intention	147.15 (±5.27)	231.76 (±7.10)	305.23 (±1.47)	428.81 (±1.77)	525.53 (±0.86)	635.67 (±1.09)	661.32 (±1.40	638.73 (±1.17)
normal skin	542.24 (±0.06)	530.18 (±3.62)	560.62 (±1.75)	520.23 (±3.31)	564.42 (±5.83)	535.33 (±3.39)	530.17 (±1.29)	516.23 (±1.23)

Table 4.5.8: Mean neodermal thickness (micrometers) where n=108 (36 per wound group) for the 42 day study and n=36 (12 per wound group) for the 180 day study

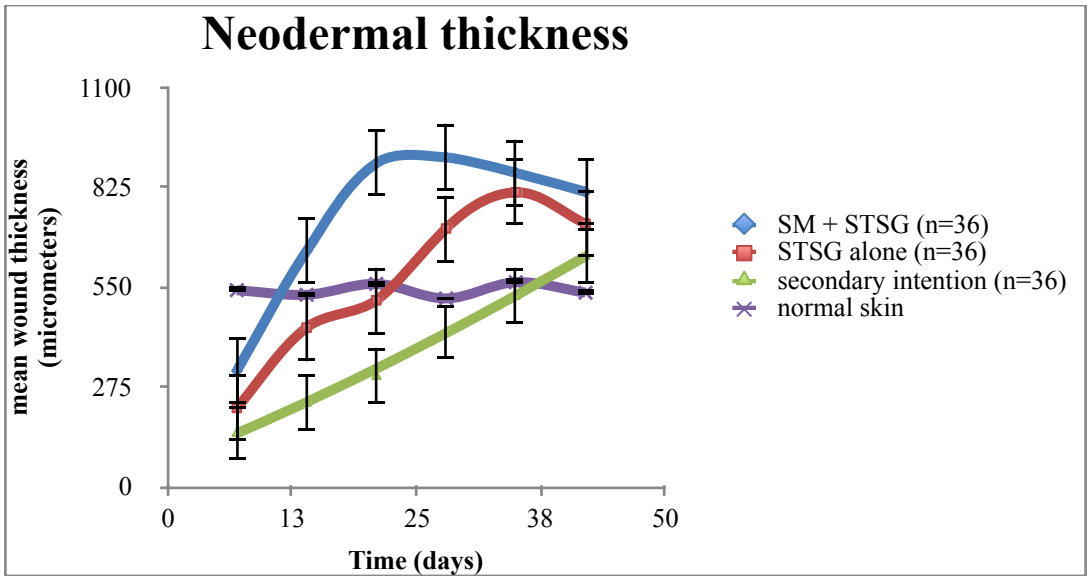

Figure 4.5.8.1: Mean wound thickness versus time (n=108, 36 per wound group) for different reconstructive options in a 42 day study.

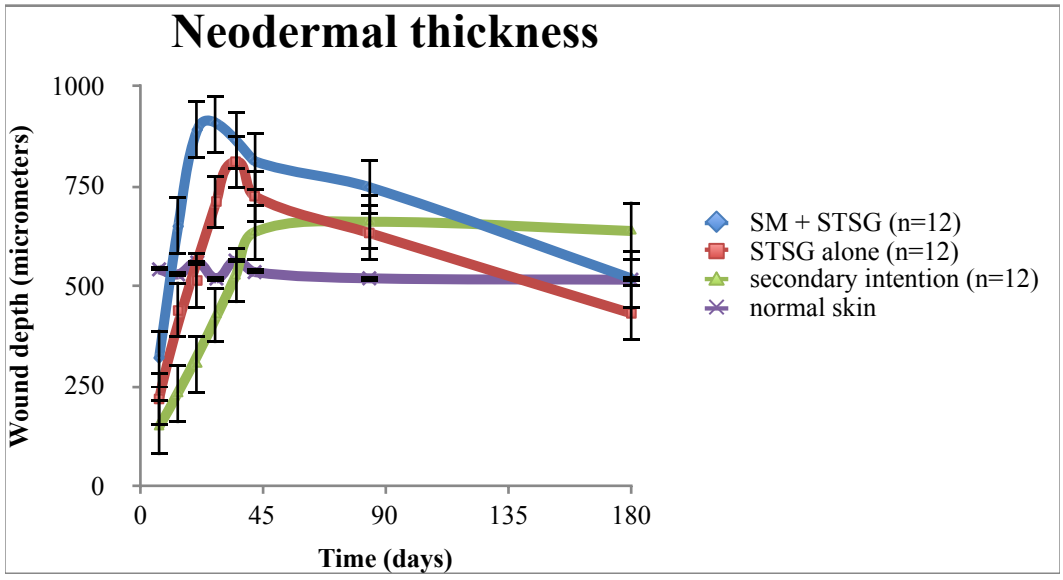

Figure 4.5.8.2: Mean wound thickness versus time (n=36, 12 per wound group) for different reconstructive options in a 180 day study.

Interpretations for mean neodermal thickness

Wounds treated with SM + STSG showed a rapid increase in wound depth peaking at days 14 and

21. This gradually decreased to the level of that of normal skin by day 180. Wounds treated with STSG alone showed a less steep increase over 42 days, which then decreased until the end of the study. Wounds treated by SM+STSG were significantly thicker than those treated by STSG alone ($p<0.0001$). Wounds allowed to heal by secondary intention showed the least increase in wound depth, which peaked at day 42 and remained at a steady state thereafter. This depth was significantly larger than the other wound groups and normal skin at day 180.

4.5.9 Wound cellular density

Please see table 4.5.9 and figures 4.5.9.1-2

Normal skin

Cellular density of normal skin showed no significant changes over time except between days 14 and 21 (mean difference of 0.65, $p<0.0001$).

Wounds allowed to heal by secondary intention

The changes in density between individual time points were statistically significant ($p<0.0001$) except between days 35 and 42.

When comparing wounds allowed to heal by secondary intention to normal skin, the former showed a lower cellular density than the latter at day 7 (mean difference of 0.125). Between days 14 and 84, mean cellular density was higher in wounds allowed to heal by secondary intention then in normal skin. The mean difference was 0.88 at day 14, 0.87 at day 21, 0.63 at day 28, 0.23 at day 35, 0.49 at day 42, 0.56 at day 84 and 0.02 at day 180. These differences were statistically significant ($0<0.0001$) at each time point except at days 7, 35 and 180.

Wounds treated by STSG alone

The changes in cellular density were statistically significant between days 7 and 14 (mean difference of 0.80, $p<0.0001$), days 21 and 28 (mean difference of 0.38, $p=0.0061$) days 42 and 84 (mean difference of 0.34, $p=0.0358$) and days 84 to 180 (mean difference of 0.48, $p=0.0396$).

Wounds treated with STSG alone showed higher levels of cellular density than normal skin throughout the entire study. The mean difference was 0.57 at day 7, 1.47 at day 14, 0.78 at day 21, 0.27 at day 28, 0.31 at day 35, 0.15 at day 42, 0.56 at day 84 and 0.11 at day 180. These differences were statistically significant only at days 7, 14 and 21 ($p<0.0001$).

Wounds treated with STSG were compared to those allowed to heal by secondary intention (at equivalent time points). The mean difference was 0.64 at day 7, 0.04 at day 14, 0.09 at day 21, 0.36 at day 28, 0.09 at day 35, 0.34 at day 42, 0.00 at day 84 and 0.14 at day 180. These differences were statistically significant at days 7 ($p<0.0001$), 28 ($p=0.0137$) and 42 ($p=0.031$).

Wounds treated with SM + STSG

The changes in cellular density between consecutive time post-operative time points were statistically significant between days 14 and 21 (mean difference of 0.76, $p<0.0001$) and days 35 and 42 (mean difference of 0.35, $p=0.0272$).

Wounds treated with SM+STSG were compared to normal skin. The mean difference was 1.82 at day 7, 1.67 at day 14, 0.27 at day 21, 0.13 at day 28, 0.14 at day 35, 0.38 at day 42, 0.08 at day 35 and 0.23 at day 180 These differences were statistically significant at days 7 and 14 ($p<0.0001$).

Wounds treated with SM+STSG showed higher levels of cellular density than wounds allowed to heal by secondary intention at days 7, 14 and 180, and lower levels at other time points. The mean difference was 1.32 at day 7, 0.79 at day 14, 0.60 at day 21, 0.77 at day 28, 0.37 at day 35, 0.11 at

day 42, 0.49 at day 84 and 0.25 at day 180. These measurements were statistically significant ($p<0.0001$ for all except day 84, where $p=0.0293$) at every time point except at days 42 and 180.

Wounds treated with SM+STSG showed higher levels of cellular density than wounds treated with STSG alone at days 7, 14 and 180, and lower levels at other time points. The mean difference was at 0.68 at day 7, 0.21 at day 14, 0.51 at day 21, 0.41 at day 28, 0.45 at day 35, 0.23 at day 42, 0.48 at day 84 and 0.12 at day 180. These differences were statistically significant ($p<0.0001$ for all except day 28, where $p=0.0015$ and day 84 where $p=0.0324$) at each time point except at days 14, 42 and 180.

	Day 7	Day 14	Day 21	Day 28	Day 35	Day 42	Day 84	Day 180
SM+STSG	3.84 (±0.04)	4.16 (±0.14)	3.41 (±0.04)	3.13 (±0.04)	3.05 (±0.05)	3.40 (±0.04)	2.55 (±0.07)	2.67 (±0.07)
STSG alone	3.16 (±0.09)	3.96 (±0.04)	3.92 (±0.03)	3.54 (±0.15)	3.51 (±0.03)	3.17 (±0.04)	3.03 (±0.06)	2.56 (±0.04)
secondary intention	2.51 (±0.03)	3.37 (±0.04)	4.01 (±0.03)	3.90 (±0.03)	3.42 (±0.04)	3.51 (±0.11)	3.03 (±0.7)	2.42 (±0.7)
normal skin	2.64 (±0.06)	2.49 (±0.06)	3.14 (±0.06)	3.27 (±0.06)	3.19 (±0.06)	3.02 (±0.07)	2.47 (±0.13)	2.44 (±0.14)

Table 4.5.9: Mean wound cellar density (score out of 5), where n=108 (36 per wound group) for the 42 day study and n=36 (12 per wound group) for the 180 day study

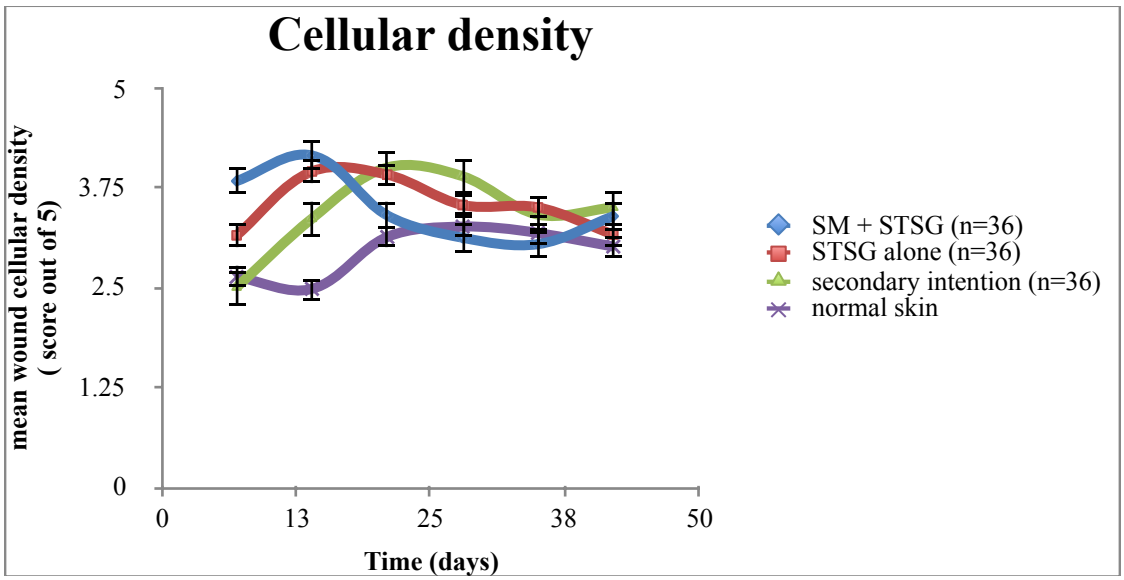

Figure: 4.5.9.1: Mean cellular density versus time (n=108, 36 per wound group) for different reconstructive options in a 42 day study.

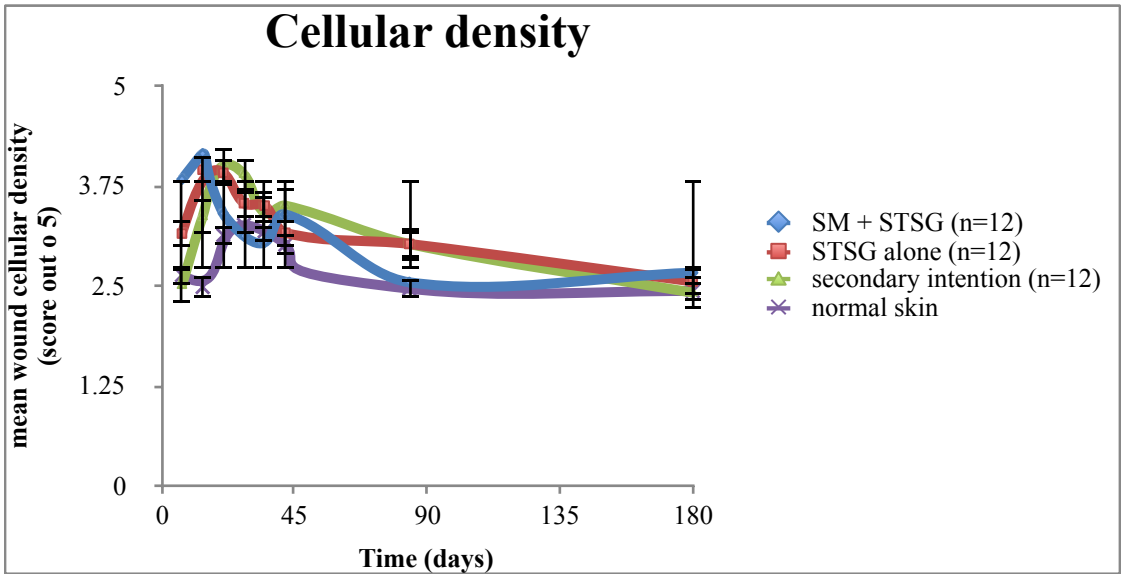

Figure 4.5.9.2: Mean cellular density versus time (n=36, 12 per wound group) for different reconstructive options in a 180 day study.

Interpretations for mean wound cellular density

Wounds treated with SM + STSG showed the highest increase in cellular density over the first 14 days. This then decreased to levels similar to that of normal skin thereafter. This remained at a similar level thereafter. Wounds treated with STSG alone showed a similar increase. This persisted

until day 21 and slowly decreased to levels similar to that of normal skin by 180. Wounds allowed to heal by secondary intention showed a later peak in cellular density at day 21, then followed a similar trajectory to that of wounds treated with STSG alone.

Wound depth and cellular density: Interpretations

Wounds allowed to heal by secondary intention were thicker and showed higher levels of cellular density compared to normal skin at days 7, 14 and 21, but statically no significant difference thereafter. Wounds treated by STSG alone were initially thicker and more cellularly dense than normal skin (up to day 14), but there was no statistically significant difference thereafter. Compared to wounds allowed to heal by secondary intention, wounds treated with STSG alone were less deep yet more dense at day 180. Wounds treated with SM+STSG were deeper than all other treatment modalities at days 7 and 14, but resembled normal skin in terms of wound depth and cellular density for the remainder of the study, while being deeper than wounds treated with STSG alone.

4.5.10 Inflammation

Please see table 4.5.10 and figures 4.5.10.1-2

Normal skin

Cellular density of normal skin showed no statistically significant changes over time.

Wounds allowed to heal by secondary intention

The changes in density between individual time points were all statistically significant ($p<0.0001$ for each, except between days 21 and 28, where $p=0.0004$) except between days 14 and 21.

Wounds allowed to heal by secondary intention showed a higher inflammatory cell density than normal skin throughout the study. These differences were statistically significant ($p<0.0001$ for each time point) between days 7 and 42, except at days 84 and 180.

Wounds treated by STSG alone

The changes in inflammatory cell density were statistically significant between days 14 and 21 (mean difference of 0.49, $p<0.0001$), days 21 and 28 (mean difference of 0.89, $p<0.0001$), days 28 and 35 (mean difference of 1, $p<0.0001$) and days 42 and 84 (mean difference of 0.34, $p=0.0358$). All other differences between consecutive time points were not statistically significant.

Wounds treated with STSG alone showed higher levels of inflammatory cell density than normal skin throughout the entire study. The mean difference was 2.61 at day 7, 2.63 at day 14, 2.12 at day 21, 1.26 at day 28, 0.29 at day 35, 0.16 at day 42, 0.09 at day 84 and 0.07 at day 180. These differences were statistically significant only at days 7, 14, 21 and 28 ($p<0.0001$).

Wounds treated with STSG showed lower density levels in inflammatory cell density than those allowed to heal by secondary intention (at equivalent time points) throughout the entire study, except at day 7. The mean differences were 0.07 at day 7, 0.36 at day 14, 0.8 at day 21, 1.36 at day 28, 1.87 at day 35, 1.56 at day 42, 0.46 at day 84 and 0.07 at day 180. These differences were statistically significant ($p<0.0001$ from days 14 to 42, $p=0.0006$ at day 84), at all time points except at days 7 and 180

Wounds treated with SM + STSG

The changes in inflammatory cell density between consecutive time post-operative time points were statistically significant between days 7 and 14 (mean difference of 0.28, $p=0.0072$), days 21 and 28 (mean difference of 0.79, $p<0.0001$) and days 28 and 35 (mean difference of 0.64, $p<0.0001$).

Wounds treated with SM+STSG showed higher levels of inflammatory cell density when compared to normal skin throughout the study. The mean difference was 1.90 at day 7, 2.21 at day 14, 2.00 at day 21, 1.24 at day 28, 0.64 at day 35, 0.13 at day 42, 0.48 at day 84 and 0.07 at day 180. These differences were all statistically significant ($p<0.0001$ for all except at day 84 where $p=0.0003$) except at days 42 and 180.

Wounds treated with SM+STSG showed lower levels of inflammatory cell density than wounds allowed to heal by secondary intention throughout the study, except at day 180. The mean difference was 0.65 at day 7, 0.78 at day 14, 0.92 at day 21, 1.38 at day 28, 1.52 at day 35, 1.59 at day 42, 0.48 at day 84 and 0.07 at day 180. These measurements were statistically significant ($p<0.0001$) at all time points except at days 84 and 180.

Wounds treated with SM+STSG showed lower levels of inflammatory cell density than wounds treated with STSG alone at each post-operative time point, except at day 35. The mean difference was at 0.71 at day 7, 0.42 at day 14, 0.12 at day 21, 0.02 at day 28, 0.35 at day 35, 0.03 at day 42, 0.02 at day 84 and 0.00 at day 180. These differences were statistically significant ($p<0.0001$) at days 7, 14 and 28 and not statistically significant at the other time points.

	Day 7	Day 14	Day 21	Day 28	Day 35	Day 42	Day 84	Day 180
SM+STSG	2.31 (±0.05)	2.60 (±0.04)	2.41 (±0.09)	1.61 (±0.04)	0.98 (±0.10)	0.47 (±0.09)	0.38 (±0.04)	0.39 (±0.04)
STSG alone	3.02 (±0.05)	3.02 (±0.05	2.53 (±0.04)	1.63 (±0.11)	0.63 (±0.04)	0.50 (±0.03)	0.40 (±0.04)	0.39 (±0.04)
secondary intention	2.96 (±0.05)	3.39 (±0.05)	3.33 (±0.04)	2.99 (±0.04)	2.49 (±0.04)	2.06 (±0.07)	0.86 (±0.06)	0.31 (±0.06)
normal skin	0.41 (±0.07)	0.40 (±0.04)	0.41 (±0.04)	0.38 (±0.04)	0.34 (±0.04)	0.34 (±0.04)	0.31 (±0.08)	0.32 (±0.07)

Table 4.5.10: Mean wound inflammatory cell density (score out of 5), where n=108 (36 per wound group) for the 42 day study and n=36 (12 per wound group) for the 180 day study

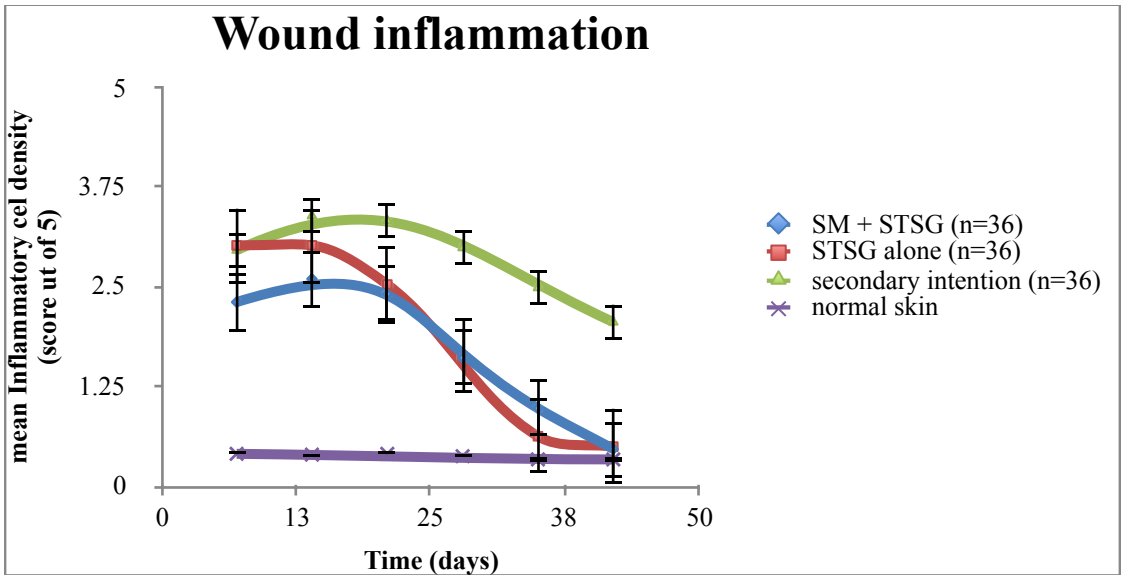

: mean inflammatory cell density versus time (n=108, 36 per wound group) for different reconstructive options in a 42 day study.

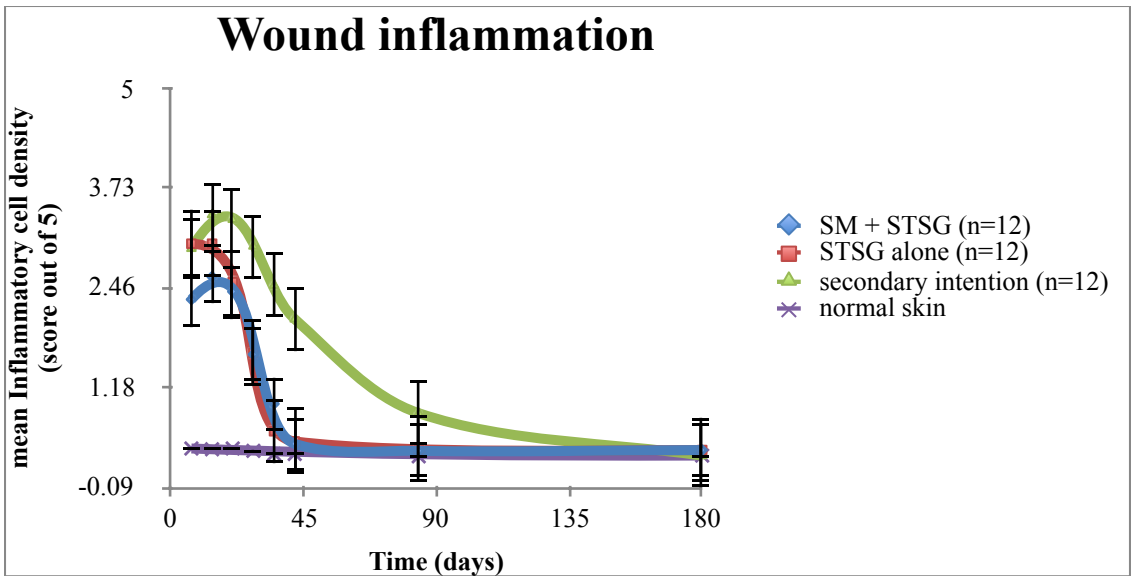

Figure 4.5.10.2: mean inflammatory cell density versus time (n=36, 12 per wound group) for different reconstructive options in a 180 day study.

Interpretations for mean wound inflammatory cell density

Wounds allowed to heal by secondary intention were thicker and showed highest levels of inflammatory cell density, which peaked at days 14 and 21 and declined thereafter. The presence of inflammatory cells persisted to day 180. Wound treated with STSG alone reached their peak inflammatory levels at day 7 and persisted until day 21 before the levels decreased to that of normal skin by day 180. Wounds treated by SM+STSG peaked (to a lower level than wounds treated with STSG alone at day 14. This peak persisted until day 21, and declined on a similar trajectory to that of wounds treated by STSG alone through to day 180. Wounds allowed to heal by secondary intention showed the largest and most persistent inflammatory cell response, followed by wounds treated by STSG alone, followed by those treated with SM+STSG.

4.5.11 Vascular perfusion

Please see table 4.5.11 and figures 4.5.11.1-2

Normal skin

Vascular perfusion of normal skin showed no significant changes over time throughout the entire study.

Wounds allowed to heal by secondary intention

The changes (increases) in vascular perfusion between individual time points were statistically significant ($p<0.0001$) at each post-operative time interval, except between days 7 and 14.

Wounds allowed to heal by secondary intention were compared to normal skin. The mean differences were 19PU at day 7, 7.64PU at day 14, 198.82PU at day 21, 393.93PU at day 28, 494.95PU at day 35, 911.12PU at day 42, 69.46PU at day 84 and 170.32PU at day 180. These differences were statistically significantly ($p<0.0001$) higher for wounds allowed to heal by secondary intention from day 21 onwards.

Wounds treated by STSG alone

The changes in vascular perfusion were statistically significant between each consecutive time point ($p<0.0001$).

Wounds treated with STSG alone showed higher levels of vascular perfusion than normal skin throughout the entire study. This difference increased gradually from day 7 until day 42, and decreased thereafter. The mean difference was 90.14PU at day 7, 133.32PU at day 14, 218.56PU at day 21, 269.41PU at day 28, 732.22PU at day 35, 800.76PU at day 42, 171.83PU at day 84 and 49.21 at day 180. These differences were all statistically significant ($p<0.0001$).

Wounds treated with STSG showed higher levels of vascular perfusion than those allowed to heal by secondary intention (at equivalent time points) between days 7 and 35, and lower levels thereafter. The mean difference was 109.83PU at day 7, 125.72PU at day 14, 218.56PU at day 21, 269.43PU at day 28, 237.57PU at day 35, 110.31PU at day 42, 524.30PU and day 84 and 141PU at day 180. All these differences were statistically significant ($p<0.0001$).

Wounds treated with SM + STSG

The changes in perfusion between consecutive time post-operative time points were statistically significant throughout the study ($p<0.0001$ for each time interval except between day 28 and 35, where $p=0.0025$).

Wounds treated with SM+STSG were compared to normal skin. showed lower levels of vascular perfusion when compared to normal skin at days 7, and higher levels thereafter. Wound vascularity in this wound group increased until day 42, and decreased thereafter, reaching levels similar to that of normal skin. The mean difference was 267.11PU at day 7, 378.30PU at day 14, 624.67PU at day 21 750.64PU at day 28, 780.93PU at day 35, 855.82PU at day 42 147.43PU at day 84 and 8.52PU at day 180. All differences were statistically significant ($p<0.0001$) except at day 180.

Wounds treated with SM+STSG showed increasingly higher levels of vascular perfusion than wounds allowed to heal by secondary intention between days 7 and 35, and lower levels thereafter. The mean difference was 286.10PU at day 7, 370.61PU at day 14, 425.94PU at day 21, 285.9PU at day 35, 55.3PU at day 42, 548.74PU at day 84 and 161.52PU at day 180. These measurements were all statistically significant ($p<0.0001$).

Wounds treated with SM+STSG showed higher levels of vascular perfusion than wounds treated with STSG alone at between days 7 and 42, and lower levels at days 84 and 180. The mean difference was at 176.33PU at day 7, 244.92PU at day 14, 207.31PU at day 21, 82.36PU at day 28,

46.67PU at day 35, 55.18PU at day 42, 24.43PU at day 84 and 20.52PU at day 180. These differences were statistically significant ($p<0.0001$) at each time point except at days 84 and 180.

	Day 7	Day 14	Day 21	Day 28	Day 35	Day 42	Day 84	Day 180
SM+STSG	403.42 (±11.17)	515.413 (±2.11)	760.45 (±2.88)	883.42 (±3.74)	916.91 (±2.45)	993.66 (±7.01)	285.21 (±6.94)	147.87 (±8.81)
STSG alone	227.12 (±3.75)	270.13 (±3.44)	553.12 (±4.82)	796.13 (±3.32)	868.29 (±3.29)	938.56 (±2.79)	309.55 (±5.51)	168.33 (±5.53)
secondary intention	117.41 (±2.89)	144.43 (±2.39)	334.65 (±4.40)	526.74 (±10.05)	631.02 (±4.07)	1048.92 (±14.98)	833.86 (±4.04)	309.33 (±9.03)
normal skin	136.82 (±1.65)	136.34 (±2.31)	136.86 (±1.82)	135.82 (±1.70)	132.88 (±1.79)	136.14 (±2.03)	137.83 (±3.94)	139.38 (±9.58)

Table 4.5.11: Mean wound perfusion (PU), where n=108 (36 per wound group) for the 42 day study and n=36 (12 per wound group) for the 180 day study

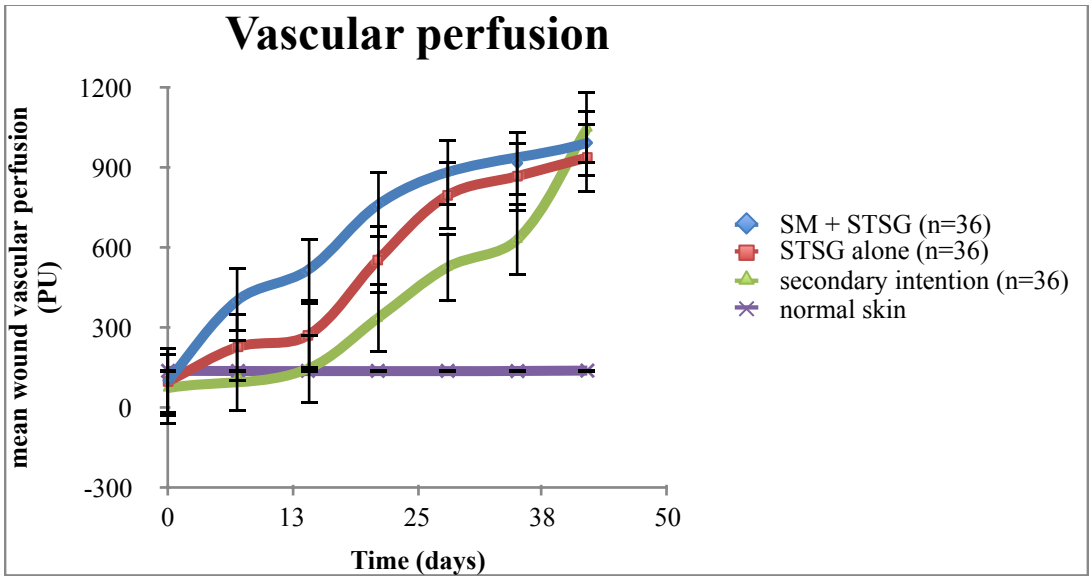

Figure 4.5.11.1: mean wound vascular perfusion versus time (n=108, 36 per wound group) for different reconstructive options in a 42 day study.

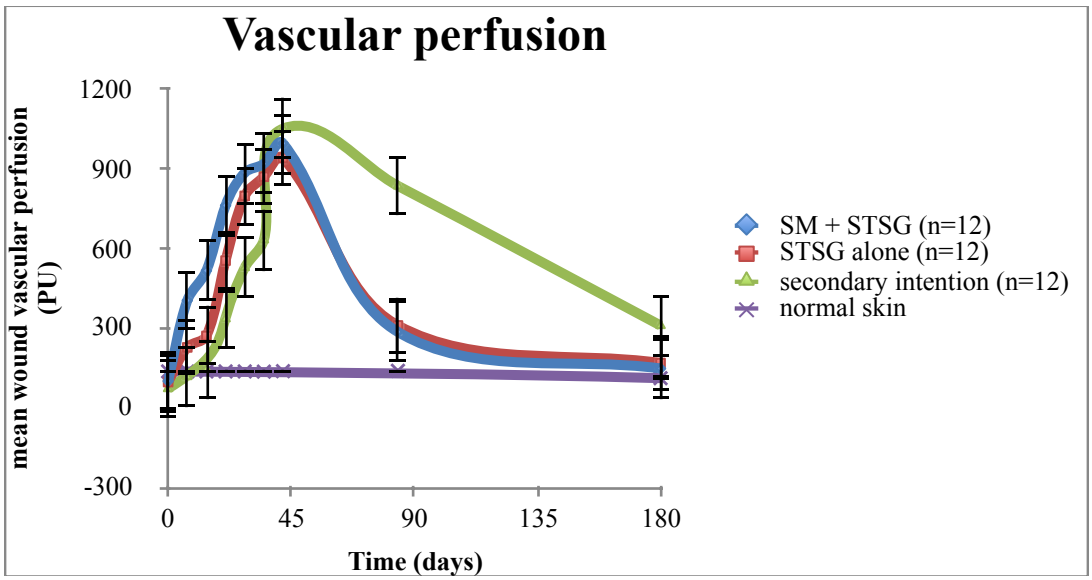

Figure 4.5.11.2: Mean wound vascular perfusion versus time (n=36, 12 per wound group) for different reconstructive options in a 180 day study.

Interpretations for mean wound vascular perfusion

Wounds treated with SM + STSG showed an early neovascularisation, by day 7 with a sharp incline that continued to increase by until day 42. This then gradually decreased over time to match that of normal skin by day 180. Wounds treated with STSG alone showed an increase in vascularity at day 14, peaking at day 42 to similar levels to wounds treated by SM + STSG, then approaching that of normal skin in the long term. Wounds allowed to heal by secondary intention showed a relatively late peak in neovascularisation which declined slowly over time.

4.5.12 Capillary lumen count

Please see table 4.5.12 and figures 4.5.12.1-2

Normal skin

Capillary lumen count of normal skin (measured as tattooed areas) showed little variation over time throughout the study (26/28 comparisons between time points statistically non-significant on

Tukey's multiple comparison test of all time points for all reconstructions).

Wounds allowed to heal by secondary intention

At day 7 the mean capillary lumen count was 2.28 (±0.06), 4.42 (±0.12) at day 14, 5.94 (±0.16) at day 21, 5.07 (±0.13) at day 28, 7.20 (±0.14) at day 35, 6.32 (±0.12) at day 42, 9.13 (±0.27) at day 84 and 10.71 (±0.26) at day 180. The changes in capillary lumen count between individual time points were statistically significant at each post-operative time interval, ($p<0.0001$ at each time interval, except between days 21 and 28, $p=0.0481$, days 35 and 42, $p=0.0481$ and day 84 and 180, $p=0.0006$).

Wounds allowed to heal by secondary intention showed a lower capillary lumen count than normal skin throughout the study. The mean difference was 8.02 and day 7, 5.71 at day 14, 3.92 at day 21, 4.44 at day 28, 3.12 at day 35, 4.23 at day 42, 0.41 at day 84 and 0.03 and day 180. These differences were all statistically significant ($p<0.0001$), except at days 84 and 180.

Wounds treated by STSG alone

The mean difference was 1.4 between days 7 and 14, 3.12 between days 14 and 21, 0.96 between days 21 and 28, 0.00 between days 28 and 35, 1.93 between days 35 and 42, 0.23 between days 42 and 84, and 0.52 between days 84 and 180. These differences were significant between days 7 and 14, days 14 and 21, days 21 and 28, and between days 35 and 42 ($p<0.0001$ for each except between days 21 and 28 where $p=0.027$).

Wounds treated with STSG alone showed lower capillary lumen counts than normal skin between days 7 and 42. This difference decreased gradually from day 7 until day 42. Wounds treated with STSG alone then showed a higher capillary lumen count than that of normal skin. The mean difference was 7.28 at day 7, 5.84 at day 14, 2.48 at day 21, 0.99 at day 28, 1.80 at day 35, 0.12 at day 42, 1.13 at day 84 and 0.06 at day 180. These differences were statistically significant at days 7, 14,

21, 28 and 42 ($p<0.0001$ for all, except $p=0.0178$ at day 28).

Wounds treated with STSG were compared to those allowed to heal by secondary intention. The mean difference was 0.71 at day 7, 0.10 at day 14,1.52 at day 21, 3.42 at day 28, 1.21 at day 35, 4.03 at day 42, 1.13 day 84 and 0.10 at day 180. These differences were statistically significant at days 21, 28, 35 and 42 ($p<0.0001$ for each except at day 35 where $p=0.0003$).

Wounds treated with SM + STSG

The changes in capillary lumen count between consecutive time post-operative time points were statistically significant between days 7 and 14 and between days 14 and 21 ($p<0.0001$ for each time interval).

Wounds treated with SM+STSG showed a lower capillary lumen count when compared to normal skin at days 7 and 14, and higher levels thereafter. The mean difference was 4.15 at day 7 (statistically significant, $p<0.0001$), 2.21 at day 14 (statistically significant, $p<0.0001$), 1.10 at day 21(statistically significant, $p=0.0028$), 1.11 at day 28 (statistically significant, $p=0.0023$), 0.92 at day 35 (statistically significant, p=0,0981), 0.83 at day 42 (not significant), 1.51 at day 84 (statistically significant, $p=0.0031$), and 0.42 at day 180 (not significant).

Wounds treated with SM+STSG showed a higher capillary lumen count than wounds allowed to heal by secondary intention throughout the study. The mean difference was 5.71 at day 7, 3.53 at day 14, 5.11 at day 21, 5.54 at day 28, 3.92 at day 35, 4.91 at day 42, 2.03 at day 84 and 0.42 at day 180. These measurements were all statistically significant ($p<0.0001$), except at day 180.

Wounds treated with SM+STSG showed a higher capillary lumen count than wounds treated with STSG throughout the study. The mean difference was at 3.11 at day 7, 3.62 at day 14, 3.61 at day 21, 2.14 at day 28, 2.76 at day 35, 0.92 at day 42, 0.9 1at day 84 and 0.50 at day 180. These differences were statistically significant ($p<0.0001$) at each time point except at days 42, 84 and 180.

	Day 7	Day 14	Day 21	Day 28	Day 35	Day 42	Day 84	Day 180
SM+STSG	6.02 (±0.10)	7.92 (±0.15)	11.14 (±0.20)	10.55 (±0.16)	11.13 (±0.17)	11.26 (±0.18)	11.03 (±0.25)	11.12 (±0.24)
STSG alone	2.93 (±0.08)	4.34 (±0.19)	7.41 (±)0.13	8.40 (±0.16)	8.48 (±0.14)	10.33 (±0.16)	10.12 (±0.16)	10.61 (±0.13)
secondary intention	2.28 (±0.06)	4.42 (±0.12)	5.94 (±0.16)	5.07 (±0.13)	7.20 (±0.14)	6.32 (±0.12)	9.13 (±0.27)	10.71 (±0.26)
normal skin	10.21 (±0.19)	10.25(± 0.20)	9.97 (±0.19)	9.42 (±0.20)	10.25 (±0.18)	10.42 (±0.20)	9.53 (±0.26)	10.70 (±.25)

Table 4.5.12: Mean capillary lumen count, where n=108 (36 per wound group) for the 42 day study and n=36 (12 per wound group) for the 180 day study

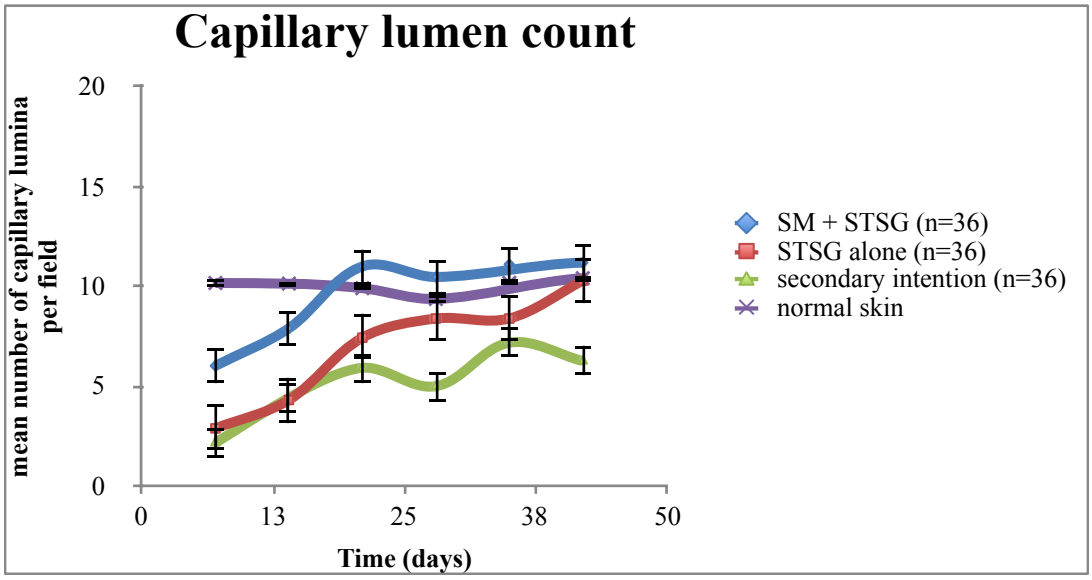

Figure 4.5.12.1: mean capillary lumen count versus time (n=108, 36 per wound group) for different reconstructive options in a 42 day study.

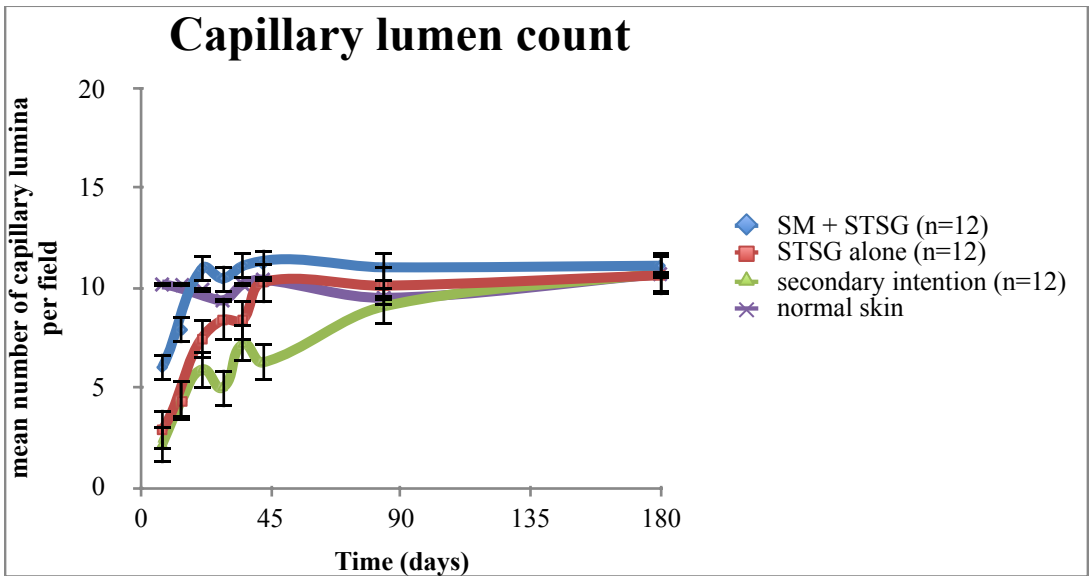

Figure 4.5.12.2: mean capillary lumen count versus time (n=36, 12 per wound group) for different reconstructive options in a 180 day study.

Interpretations for mean capillary lumen count

Wounds treated with SM + STSG showed a sharp increase in capillary formation by day 7 that continued to increase by until day 42. This then gradually decreased over time to approximate that of normal skin by day 180. Wounds treated with STSG alone showed a slightly slower increase in vascularity at peaking at day 42 to levels similar to treated by SM + STSG, then approaching that of normal skin in the long term. Wounds allowed to heal by secondary intention showed a relatively late peak in neovascularisation which increased over time.

4.5.13 von Willebrand factor

Please see table 4.5.13 and figures 4.5.13.1-2

Normal skin

vWF content of normal skin showed no statistically significant changes over time.

Wounds allowed to heal by secondary intention

The mean difference was 0.36 between days 7 and 14 (statistically significant, p=0.0002), 0.23 between days 14 and 21 (not significant), 0.36 between days 21 and 28 (statistically significant, p=0.0002), 0.39 between days 28 and 35 (statistically significant, p<0.0001), 0.19 between days 35 and 42 (not significant), 0.18 between days 42 and 84 (not significant), and 0.09 between days 84 and 180 (not significant).

Wounds allowed to heal by secondary intention showed lower levels of vWF staining than normal skin from throughout the study. The mean difference was 1.91 at day 7, 2.24 at day 14, 1.72 at day 21, 1.62 at day 28, 1.81 at day 35, 1.63 at day 42, 1.06 at day 84 and 1.15 at day 180. These differences were all statistically significant (p<0.0001 at each time point except at day 180 where p=0.0053).

Wounds treated by STSG alone

The mean difference was 0.41 between days 7 and 14, 0.72 between days 14 and 21, 0.44 between days 21 and 28, 0.21 between days 28 and 35, 0.34 between days 35 and 42, 0.22 between days 42 and 84 and 0.11 between days 84 and 180. These differences were significant between days 7 and 14, 14 and 21 and 21 and 28 (p<0.0001).

Wounds treated with STSG alone showed lower levels of vWF staining than normal skin throughout the entire study. The mean difference was 2.03 at day 7, 1.51 at day 14, 0.80 at day 21, 0.72 at day 28, 0.31 at day 35, 0.12 at day 42, 0.01 at day 84 and 0.02 at day 180. These differences were significant at days 7, 14, 21, 28 at 35 (p<0.0001 for each, except at day 28 where p=0.0002 and day 35 where p=0.0286).

Wounds treated with STSG showed higher levels of vWF staining levels compared to those allowed to heal by secondary intention at equivalent time points throughout the study. The mean difference was 0.03 at day 7, 0.41 at day 14, 0.82 at day 21, 0.91 at day 28, 0.75 at day 35, 0.90 at day 42, 0.93

at day 84 and 0.72 at day 180. All these differences were statistically significant ($p<0.0001$ for all time points except day 7, where $p=0.0007$).

Wounds treated with SM + STSG

The changes in vWF staining between consecutive time post-operative time points were statistically significant only between days 7 and 14 (mean difference of 0.4, $p<0.0001$) and days 14 and 21 (mean difference of 0.4, $p<0.00001$).

Wounds treated with SM+STSG showed statistically significant ($p<0.0001$) lower levels of vWF staining when compared to normal skin at day 7 (mean difference of 0.7). All mean differences at other equivalent time points were not statistically significant.

Wounds treated with SM+STSG showed higher levels of vWF staining than wounds allowed to heal by secondary intention throughout the entire study. The mean difference was 1.61 at day 7, 1.75 at day 14, 1.92 at day 21, 1.71 at day 28, 1.24 at day 35, 1.21 at day 42, 1.13 at day 84 and 1.01 at day 180. These differences were statistically significant ($p<0.0001$) at each time point.

Wounds treated with SM+STSG showed higher levels of vWF staining than wounds treated with STSG alone throughout the entire study. The mean difference was at 1.31 at day 7, 1.34 at day 14, 1.04 at day 21, 0.82 at day 28, 0.50 at day 35, 0.41 at day 42, 0.22 at day 84 and 0.44 at day 180. These differences were statistically significant ($p<0.0001$ for all except day 180, where $p=0.0324$) at each time point except at days 84 ($p=0.998$) and 180 ($p=0.0406$).

	Day 7	Day 14	Day 21	Day 28	Day 35	Day 42	Day 84	Day 180
SM+STSG	2.31 (±0.04)	2.72 (±0.05)	3.11 (±0.05)	3.20 (±0.11)	3.21 (±0.05)	3.41 (±0.04)	3.45 (±0.06)	3.52 (±0.06)
STSG alone	1.00 (±0.05)	1.40 (±0.04)	2.12 (±0.05)	2.25 (±0.05)	2.72 (±0.05)	3.02 (±0.04)	3.21 (±0.06)	3.10 (±0.06)
secondary intention	0.62 (±0.04)	1.02 (±0.05)	1.21 (±0.04)	1.60 (±0.05)	2.01 (±0.05)	2.24 (±0.05)	2.36 (±0.06)	2.41 (±0.07)
normal skin	3.00 (±0.08)	2.91 (±0.06)	2.83 (±0.07)	3.12 (±0.06)	3.00 (±0.06)	3.10 (±006)	3.24 (±0.06)	3.14 (±0.11)

Table 4.5.13: Mean vWF staining density (score out of 5)where n=108 (36 per wound group) for the 42 day study and n=36 (12 per wound group) for the 180 day study

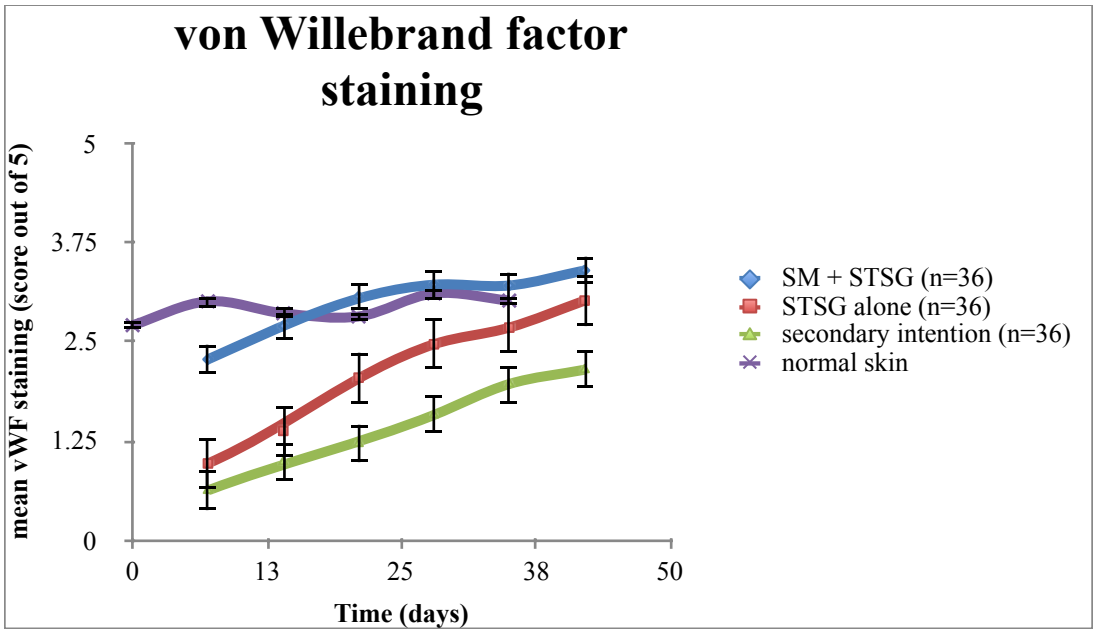

Figure 4.5.13.1: mean von Willebrand staining density versus time (n=108, 36 per wound group) for different reconstructive options in a 42 day study.

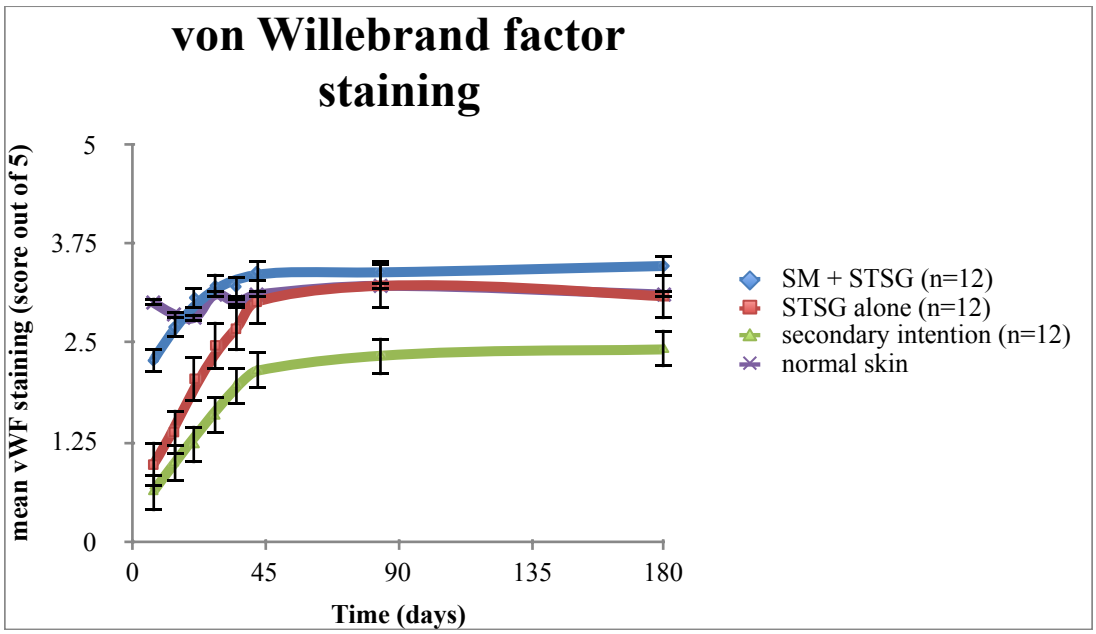

Figure 4.5.13.2: mean von Willebrand staining density versus time (n=36, 12 per wound group) for different reconstructive options in a 180 day study.

Interpretations for mean von Willebrand factor staining density

Wounds treated with SM + STSG showed higher levels of vWF staining at day 7 which continued to increase until day 42, where it plateaud thereafter, at levels similar to that of normal skin by day 180. Wounds treated with STSG alone showed a lesser degree of staining which started later and peaked at day 84 with a small gradual decrease by day 180. Wounds allowed to heal by secondary intention showed vWF staining relatively late with a lower total amount of staining than the other wounds groups throughout the 180 days.

Wound vascularity: Interpretations

Wounds treated with SM+STSG showed the most pronounced vascular response with statistically significant higher levels of wound perfusion, capillary lumen count and vWF staining compared to

wounds treated with STSG alone, and in turn the latter group showed higher levels than wound allowed to heal by secondary intention. There were no significant differences in all these parameters (except for vWF staining) when compared to normal skin at day 180.

4.5.14 Summary of findings

Graft take rate was similar in wounds treated with STSG alone and those treated with SM + STSG. Wounds treated by secondary intention were darker than wounds treated by STSG alone and those treated by SM+STSG by day 42. There were no macroscopic differences between all three wound groups by day 180 (except for wound contraction). No adnexal structures were present in any of the wounds.

Wounds treated by SM+STSG contracted less than those treated by STSG alone, which in turn contracted less than wounds allowed to heal by secondary intention. EDA-FN and α-SMA staining was attenuated in wounds treated by SM+STSG compared with those treated by STSG alone and in those allowed to heal by secondary intention. Levels normalised for all three wound groups towards the end of the study.

Collagen and elastin levels remained lower than those of normal skin for all three wound groups throughout the study before reaching those of normal skin at day 180. It was noted that collagen deposition followed cellular ingress both temporally and spatially.

Wounds treated with SM+STSG initially showed higher neodermal thickness and cellular density, which approached that of normal skin by day 35. Wounds allowed to heal by secondary intention showed lower maximal wound thickness throughout the study but significantly thicker wounds at day 180. Wounds allowed to heal by secondary intention showed the highest levels of inflammation, followed by wounds treated with STSG alone and then by those treated with SM + STSG.

Wounds treated with SM+STSG showed the most pronounced and earliest vascular response with statistically significant higher levels of wound perfusion, capillary lumen count and vWF staining compared to wounds treated with STSG alone, and in turn the latter group showed higher levels than wound allowed to heal by secondary intention. There were no significant differences in all these parameters (except for vWF staining) when compared to normal skin at day 180.

4.6 Conclusions from this study

Wounds treated with SM support long-term STSG survival in the acute full thickness porcine wound (as a single step procedure). As wounds treated with SM + STSG contracted less, and showed lower levels of EDA-FN and α-SMA than those treated with STSG alone, it can be inferred that SM attenuates wound contraction, especially in the earlier phases of wound healing. It may also be concluded that SM stimulates a stronger and earlier angiogenic response, with a deceased inflammatory reaction. Wounds treated with SM + STSG showed very similar parameters to normal skin in the long term.

4.7 Subsequent steps

As SM was proven to support long-term survival of the STSG, and to show some improvement on wounds treated by STSG alone and those allowed to heal by secondary intention, the next logical step would be to compare the behaviour of SM to other commercially available and popular dermal scaffolds currently in use. SM+STSG was compared Matriderm™ and Integra™. Similar parameters were measured. This study is reported in the next section of this chapter.

Chapter 5: Experiment 2: A Comparison of the wound healing properties of Smart Matrix™ with the Commercially Available Dermal Scaffolds Matriderm™ and Integra™.

5.1 Introduction

In the previous section of this chapter, the wound healing properties of Smart Matrix™ and its long term trajectory in the pre-clinical porcine model were characterised. The wound healing properties of Smart Matrix™ with a split thickness skin graft as a single stage procedure was compared with acute wounds allowed to heal by secondary intention and those treated with a split thickness skin graft alone. Wounds treated with SM + STSG exhibited less wound contraction and earlier vascularisation than the other the wound groups, while skin graft take was similar between wounds treated with STSG alone and SM + STSG.

In order to assess its clinical efficiency and its position in the commercial arena, studies were carried out comparing Smart Matrix™ with two commercially available and widely used dermal replacement scaffolds. Integra™ Dermal Replacement Template™, (Integra™). Integra™ life Science is a dermal regeneration template consisting of bovine collagen, chondroitin-6-sulphate and a silastic membrane collagen matrix layer with a silicon oversheet. Matriderm™ (Eurosciences) is a structurally intact matrix of bovine type I collagen with elastin.

5.2 Hypothesis

Acute porcine full thickness wounds treated with Smart Matrix™ and overlying split thickness skin graft as a single stage procedure exhibit a similar wound healing trajectory to similar wounds treated with Matriderm™ and overlying split thickness skin graft as a single stage procedure and those

treated with Integra™ and overlying skin graft and a two stage procedure.

5.3 Aims

The primary objective of this study was to obtain information on the healing trajectories of two commercially available dermal replacement scaffolds, Integra™ and Matriderm™ in order to assess Smart Matrix™'s performance in similar pre-clinical scenarios. The aim was to establish whether Smart Matrix™ is at least non inferior to these dermal replacement scaffolds and whether it offers any clinical advantages over these two established and widely accepted matrices.

5.4 Methods and materials

Please refer to Chapter 3: Methods and Materials for further detail.

The acute porcine full thickness excision wound again was utilised in a 42 day and 180 day study to compare the acute response using the three different scaffolds with overlying split thickness skin grafts. Three circular full-thickness wounds of 4 cm diameter down to muscle fascia were made on either flank of the animal, similar to those described inExperiment 1. Wounds were inspected and re-dressed on post op day 3, 7, 14, 21, 28, 35, 42, 84 and 180. The same observations as the previous studies were carried out in this study. Additionally, scaffold persistence was observed.

5.5 Study outline

For this study, a total of 8 animals were used (and therefore 48 wounds). All animals monitored for a period of 42 days. Of these, half were sacrificed after day 42, while the remaining half were monitored up to day 180 (therefore 24 wounds). The surgical procedures were carried out by the same surgeon (RZA) and senior project licence holder, JFD. Two wounds per animal were treated with SM+STSG, another two wounds by Matriderm™ + STSG (MD+STSG) and another two wounds

by Integra™ + STSG (I+STSG). While Matriderm™ and Smart Matrix™ (after hydration of the scaffold in 0.9% physiological saline) were applied in tandem with the skin graft as a single step procedure at day 0, Integra™ was applied to the wound bed at day 0, and the STSG applied at day 14, after removal of the silicon backing layer, as a two-step procedure. The wounds were randomly assigned. The minimum number of pigs sufficient to yield statistically significant results was used for this study, as per Home Office regulations and project license restrictions.

42 day Study:

Eight pigs were used in the 42 day study with 6 wounds per subject. Forty eight wounds were created with 16 wounds per wound group.
subjects = 8

wounds (n) = 48

Treatment method	**Number of wounds**
Smart Matrix™ + STSG	16
Matriderm™ + STSG	16
Integra™ + STSG	16

Table 5.5.1: Wound treatment distribution in a 42 days study (n=48, 16 per wound group)

180 day Study:

Four pigs were used in the 42 days study with 6 wounds per subject. Twenty four wounds were created with 8 wounds per wound group.

subjects = 4

Wounds (n) = 24

Treatment method	Number of wounds
Smart Matrix™ + STSG	8
Matriderm™ + STSG	8
Integra™ + STSG	8

Table 5.5.2: Wound treatment distribution in a 180 days study (n=24, 8 per wound group)

5.6 Results

5.6.1 Graft take

Please see figure 5.6.1

Wounds treated with Smart Matrix™ and split thickness skin graft.

Of the 16 wounds, 6 showed 100% (of the total wound surface area) graft take, 4 showed 95% graft take, 2 showed 90% graft take, 2 showed 85%, 1 showed 75% and 1 showed 60% graft take. This gives a total of 14 wounds showing more than 80% graft take, and 2 wounds showing less than 80% graft take. No total graft loss occurred in this group.

Wounds treated with Matriderm™ and split thickness skin graft.

Of the 16 wounds, 5 showed 100% graft take, 4 showed 95% graft take, 1 showed 90% graft take, 4 showed 85%, and 2 showed 80% graft take. This gives a total of 16 wounds showing more than 80% graft take. No total graft loss occurred in this group.

Wounds treated with Integra™ and split thickness skin graft.

Of the 16 wounds, 4 showed 100% graft take, 2 showed 95% graft take, 1 showed 90% graft take, 3 showed 85%, 3 showed 80% graft take and 3 showed 75% graft take. This gives a total of 16

wounds showing more than 80% graft take. No total graft loss occurred in this group.

When comparing the three wounds groups, there was no statistically significant difference in graft take.

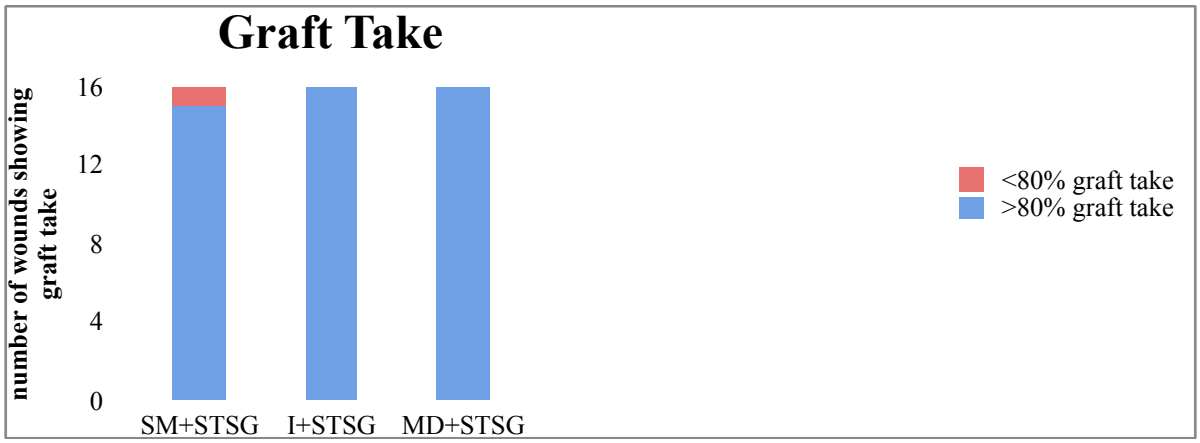

Figure 5.6.1: Wounds showing more than 80% graft take and wounds showing less than 80% graft take for different reconstructive options.

5.6.2 Macroscopic observations

Please see figures 5.6.2.1-3

Wounds treated with Smart Matrix™ and split thickness skin graft

At day 7, all the wounds treated by SM + STSG alone showed a pink vascularised graft adherent to a bed of granulation tissue. At day 14, 6 of the wounds were still moist, while 10 were dry. All wounds were dark pinkish–red in colour. At day 21, all wounds were largely dry with occasional very small patches of moist granulation tissue (less than 10% of wound area, excluding the site of the punch biopsy taken 7 days prior). The dark pink-red colour persisted. At day 35, all wounds in this groups were dry and epithelialised, and slightly paler pink in colour. At day 42, the colour was a much paler pink, resembling that of the surrounding native skin. This remained so until day 180,

when the wounds were completely healed and epthelialised. No adnexae were present at any time point. No infection was observed in any of the wounds at any of the dressing changes or at termination.

Wounds treated with Matriderm™ and split thickness skin graft

At day 7, all the wounds treated by SM + STSG alone showed a pink vascularised graft adherent to a bed of granulation tissue. At day 14, 4 of the wounds were still moist, while 12 were dry. All wounds were dark pinkish–red in colour. At day 21, all wounds were largely dry with occasional moist patches. The wounds in this group became pale pink by day 28, but were still slightly darker than neighbouring native skin at this time point. At day 35, all wounds in this groups were dry and epithelialised, and their colour resembled that of surrounding normal skin. This remained so until day 180, when the wounds were completely healed and epthelialised. No adnexae were present at any time point. No infection was observed in any of the wounds at any of the dressing changes or at termination.

When compared to wounds treated with SM + STSG, wounds treated with MD + STSG showed a very similar macroscopic healing trajectory.

Wounds treated with Integra™™ and split thickness skin graft

At days 7 and 14, all the wounds treated with I + STSG alone showed a dark red (often described as redcurrant jelly red in the literature) wound bed adherent to the overlying dermal matrix and silicon backing. When the backing was peeled off at day 14, the wound beds had a dark red velvet-like texture. At days 21 and 28, the wounds showed a moist pink vascularised graft adherent to a bed of granulation tissue. By day 35, most wounds were dry, with occasional small patches (less than 10%) of granulation tissue. All wounds were dry and epithelialised by day 42. At this time point, the wounds were a slightly darker pink than the surrounding skin. This remained so until day 180,

when the wounds were completely healed and epthelialised. No adnexae were present at any time point. No infection was observed in any of the wounds at any of the dressing changes or at termination.

When compared with wounds treated with SM + STSG, wounds treated with I + STSG, took 14 days longer to become dry and to epithelialise and remained slightly darker in colour.

When compared with wounds treated with MD + STSG, wounds treated with I + STSG, took 14 days longer to become dry and to epithelialise and remained slightly darker in colour.

Macroscopic appearances of the wounds in a 42 day and 180 day study

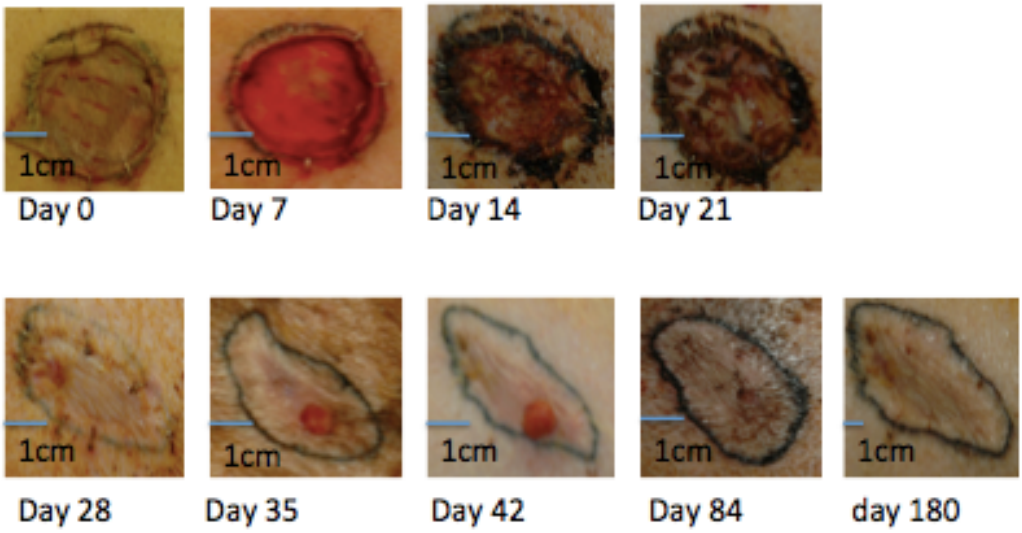

Figure 5.6.2.1: An example of the macroscopic appearances of the full thickness excision wounds treated with Smart Matrix™ + split thickness skin graft in a 42 day and 180 day study.*

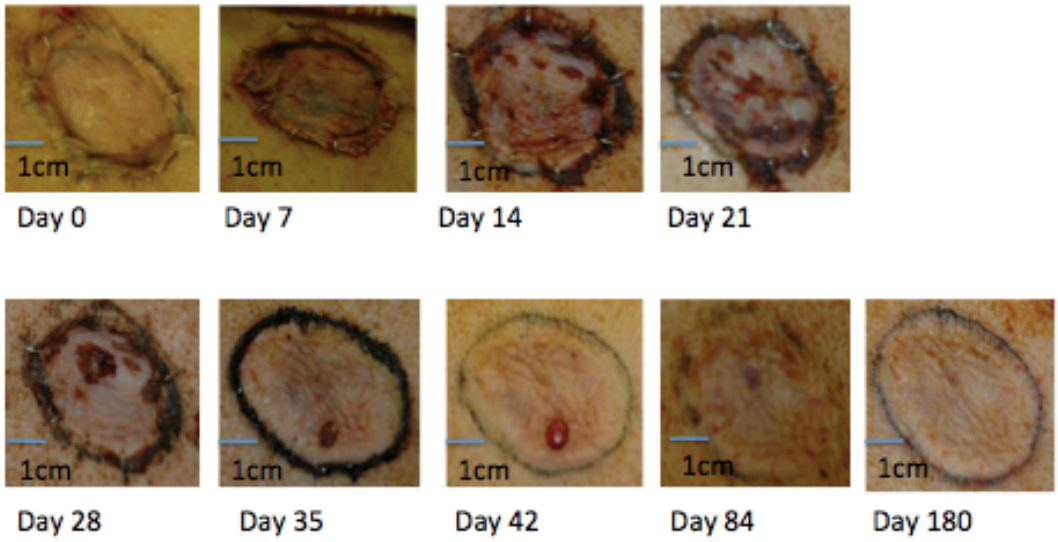

Figure 5.6.2.2: An example of the macroscopic appearances of the full thickness excision wounds treated with Matriderm™ + split thickness skin graft in a 42 day and 180 day study.*

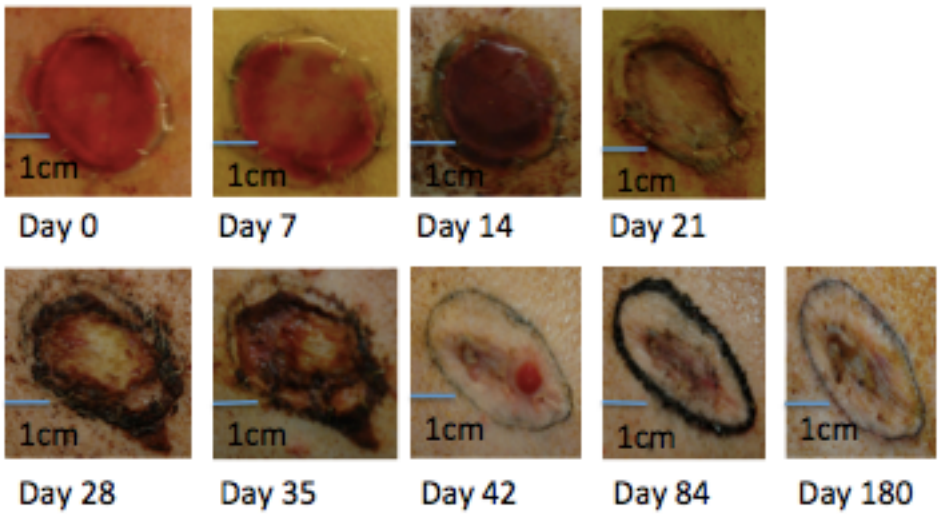

Figure 5.6 2.3: An example of the macroscopic appearances of the full thickness excision wounds treated with Integra™ + split thickness skin graft in a 42 day and 180 day study.*

*Wound area was measured quantitatively using Eykona. For the purpose of this illustration, scale bars have been added to aid interpretation of the images which have been scaled differently (according to camera zoom).

Interpretations of macroscopic wound observations and graft take

Wounds treated with SM + STSG and those treated with MD + STSG followed a very similar healing trajectory, with those treated by MD + STSG approaching the colour of normal skin 7 days earlier. Wounds treated with I + STSG showed a 14 day delay in epithelialisation. The resulting wound colour was slightly darker than the other wound groups and than normal native skin at day 180.

5.6.3 Wound area and contraction

Please see Table 5.6.3 and figures 5.6.3.1-4

Serial wound measurements were taken at each time point using the Eykona camera device. (See Methods and Materials chapter). The tattooed area was measured. This served as a control, to measure pig growth (if at all) and to take this into account when assessing wound contraction. Wound area measurements were calculated as a percentage of the wound area of the tattoo per time point in each pig. All wounds were of identical area measurement at day 0: 12.56cm^2.

Tattooed area

The mean tattoo area showed statistically significant increases ($p<0.0001$) between days 0 and 7 (mean difference of 2.78cm^2), 7 and 14 (mean difference of 2.97cm^2), 14 and 21 (mean difference of 2.11cm^2), 35 and 42 (mean difference of 1.78cm^2, 42 and 84 (mean difference of 4.57cm^2) and 84 and 180 (mean difference of 6.74cm^2).

Wounds treated with Smart Matrix™+ split thickness skin graft

The mean wound area showed a statistically significant decrease in wound area between days 7 and 14 (mean difference of 0.40cm^2, $p<0.0001$). Throughout the remainder of the study, the wound area increased significantly ($p<0.0001$) between consecutive time points. The mean differences were 0.49cm^2 between days 0 and 7, 1.64cm^2 between days 14 and 21, 2.40cm^2 between days 21 and 28, 1.51cm^2 between days 28 and 35, 2.12cm^2 between days 35 and 42, 3.69cm^2 between days 42 and 84 and 5.21cm^2 between days 84 and 180.

When compared to the tattoo, wounds treated with SM + STSG were statistically significantly ($p<0.0001$) smaller at each time point between days 7 and 180. The mean differences were 2.29cm^2 (85% of tattoo area) at day 7, 5.70cm^2 (69% of tattoo area) at day 14, 6.18cm^2 (70% of tattoo area) at day 21, 3.76cm^2 (82% of tattoo area) at day 28, 2.49cm^2 (88% of tattoo area) at day 35, 2.15cm^2 (90% of tattoo area) at day 42, 3.04cm^2 (89% of tattoo area) at day 84 and 4.56cm^2 (87% of tattoo area) at day 180.

Wounds treated with Matriderm™ + split thickness skin graft

A significant decrease occurred between days 7 and 14 (mean difference of 0.61, $p<0.0001$). Between days 14 and 180, significant ($p<0.0001$) increases in wound area occurred. The mean differences were 0.62cm^2 between days 14 and 21, 2.16cm^2 between days 21 and 28, 1.27cm^2 between days 28 and 35, 1.93cm^2 between days 3 and 42, 5.84cm^2 between days 42 and 84 and 4.37cm^2 between days 84 and 180.

When compared to the tattoo, wounds treated with MD + STSG statistically significantly ($p<0.0001$) smaller at each time point between days 7 and 180. The mean differences were 2.38cm^2 (84% of tattoo area) at day 7, 5.96cm^2 (67% of tattoo area) at day 14, 7.46cm^2 (64% of tattoo area) at day 21, 5.53cm^2 (73% of tattoo area) at day 28, 4.55cm^2 (78% of tattoo area) at day 35, 4.4 cm^2 (81% of tattoo area) at day 42, 3.13cm^2 (88% of tattoo area) at day 84 and 5.51cm^2 (84% of tattoo

area) at day 180.

When compared to wounds treated with SM + STSG, wounds treated with MD + STSG showed statistically significantly smaller wound areas at days 14 (mean difference of 0.26cm^2, p=0.0338), 21 (mean difference of 1.28cm^2, p<0.0001), 28 (mean difference of 1.77cm^2, p<0.0001), 35 (mean difference of 2.06cm^2, p<0.0001), and 42 (mean difference of 2.25cm^2, p<0.0001). There were no significant differences in wound area at days 0,7, 84 and 180.

Wounds treated with Integra™ + split thickness skin graft

A significant decrease occurred between days 7 and 14 (mean difference of 1.37cm^2, p<0.0001). Between days 0 to 7 and between consecutive time points between days 14 and 180, significant (p<0.0001) increases in wound area occurred. The mean differences were 1.26cm^2 between days 0 and 7, 0.52cm^2 between days 14 and 21, 1.21cm^2 between days 21 and 28, 2.07cm^2 between days 28 and 35, 1.65cm^2 between days 35 and 42, 4.87cm^2 between days 42 and 84 and 3.71cm^2 between days 84 and 180.

When compared to the tattoo, wounds treated with I + STSG statistically significantly (p<0.0001) smaller at each time point between days 7 and 180. The mean differences were 1.52cm^2 (90% of tattoo area) at day 7, 5.86cm^2 (68% of tattoo area) at day 14, 7.45cm^2 (69% of tattoo area) at day 21, 6.47cm^2 (78% of tattoo area) at day 28, 4.63cm^2 (79% of tattoo area) at day 35, 4.76cm^2 (81% of tattoo area) at day 42, 4.46cm^2 (84% of tattoo area) at day 84 and 7.47cm^2 (78% of tattoo area) at day 180.

When compared to wounds treated with SM + STSG, wounds treated with I + STSG showed a sta-

tistically significantly larger wound area at day 7 (mean difference of 0.77cm^2, p<0.0001). Between days 21 and 180, wounds treated with I + STSG were significantly smaller (p<0.0001) than those treated with SM + STSG. The mean differences were 1.27cm^2 at day 21, 2.71cm^2 at day 28, 2.14cm^2 at day 35, 2.61cm^2 at day 42, 1.43cm^2 at day 84 and 2.93cm^2 at day 180.

When compared to wounds treated with MD + STSG, wounds treated with I + STSG showed a statistically significantly larger wound area at day 7 (mean difference of 0.87cm^2, p<0.0001). At days 21, 42, 84 and 180, wounds treated with I + STSG were significantly smaller (p<0.0001) than those treated with MD + STSG. The mean differences were 0.94cm^2 at day 21, 0.36cm^2 at day 42, 1.33cm^2 at day 84, 2.61cm^2 and 1.99cm^2 at day 180.

	Day 0	Day 7	Day 14	Day 21	Day 28	Day 35	Day 42	Day 84	Day 180
SM+STSG	13 (±0)	13 (±0)	13 (±0.03)	14 (±0.05)	17 (±0.03)	18 (±0.03)	21 (±0.04)	24 (±0.05)	29 (±0.18)
I+STSG	13 (±0)	14 (±0.03)	12 (±0.03)	13 (±0)	14 (±0.11)	16 (±0.03)	18 (±0.04)	23 (±0.07)	26 (±0.04)
MD+STSG	13 (±0)	13 (±0)	12 (±0.03)	13 (±0.04)	15 (±0.04)	16 (±0.02)	18 (±0.03)	24 (±0.05)	28 (±0.06)
normal skin	13 (±0)	15 (±0.14)	18 (±0.09)	20 (±0.07)	21 (±0.04)	21 (±0.06)	23 (±0.11)	27 (±0.14)	34 (±0.10)

Table 5.6.3: Mean wound area (cm^2) where n=48 (16 per wound group) for the 42 day study and n=24 (8 per wound group) for the 180 day study

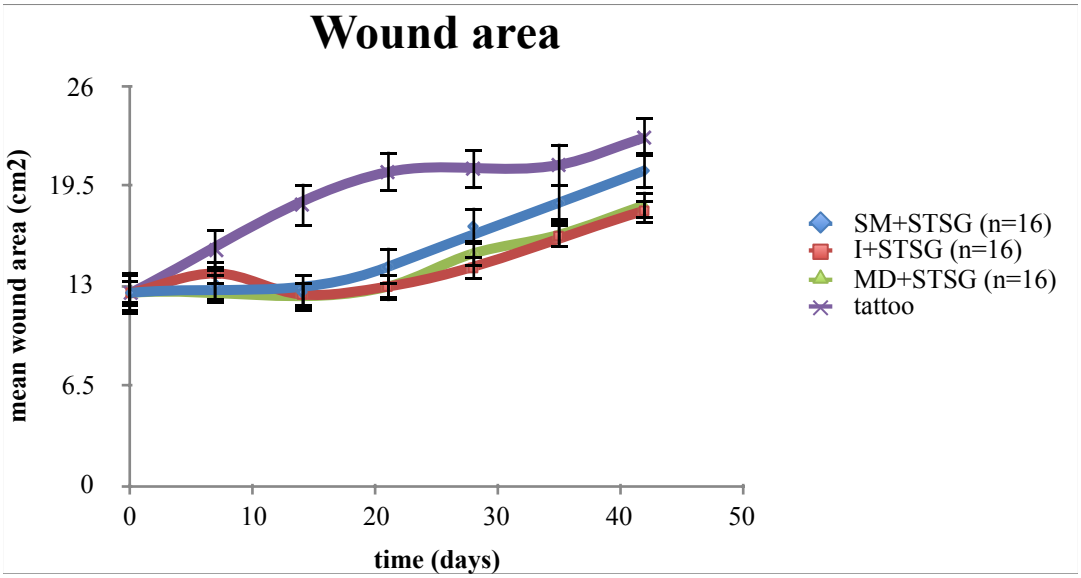

Figure 5.6.3.1:Mean wound area versus time (n=48, 16 per wound group) for different reconstructive options, in a 42 day study.

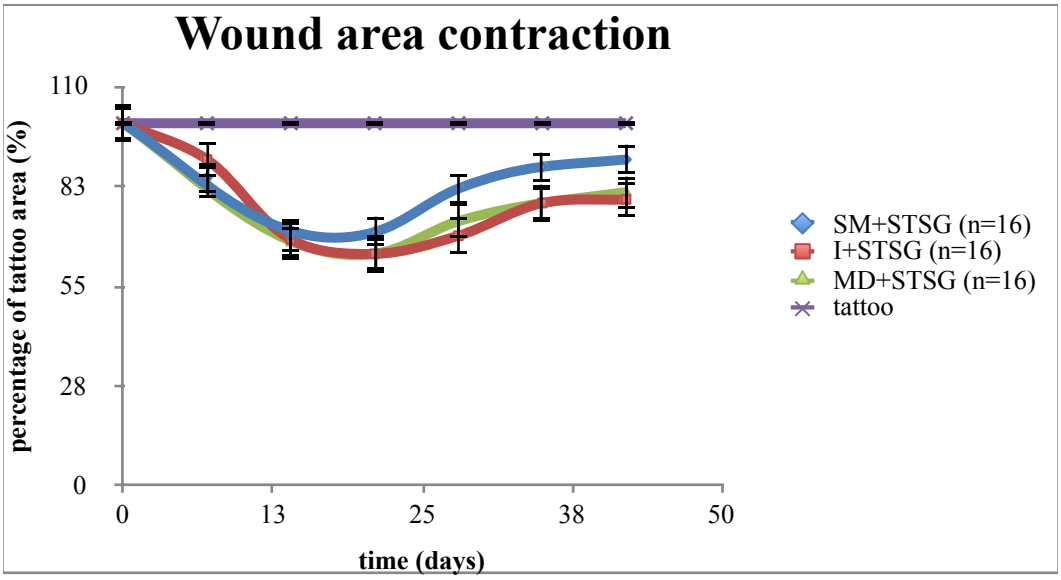

Figure 5.6.3.2: Mean wound area as a percentage of the tattooed area versus time (n=48, 16 per wound group) for different reconstructive options, in a 42 day study.

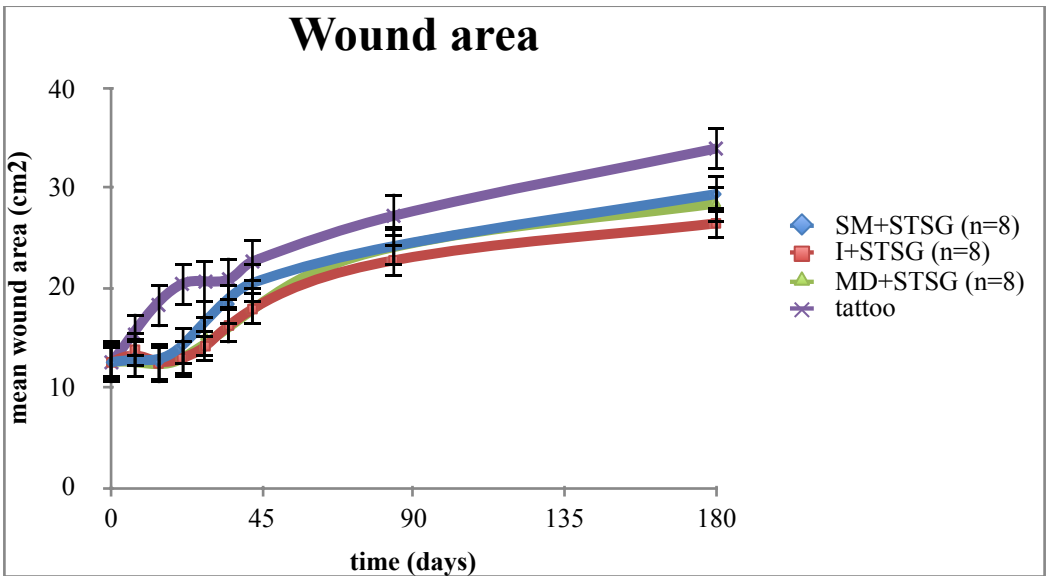

Figure 5.6.3.3: Mean wound area versus time (n=24, 8 per wound group) for different reconstructive options, in a 180 day study.

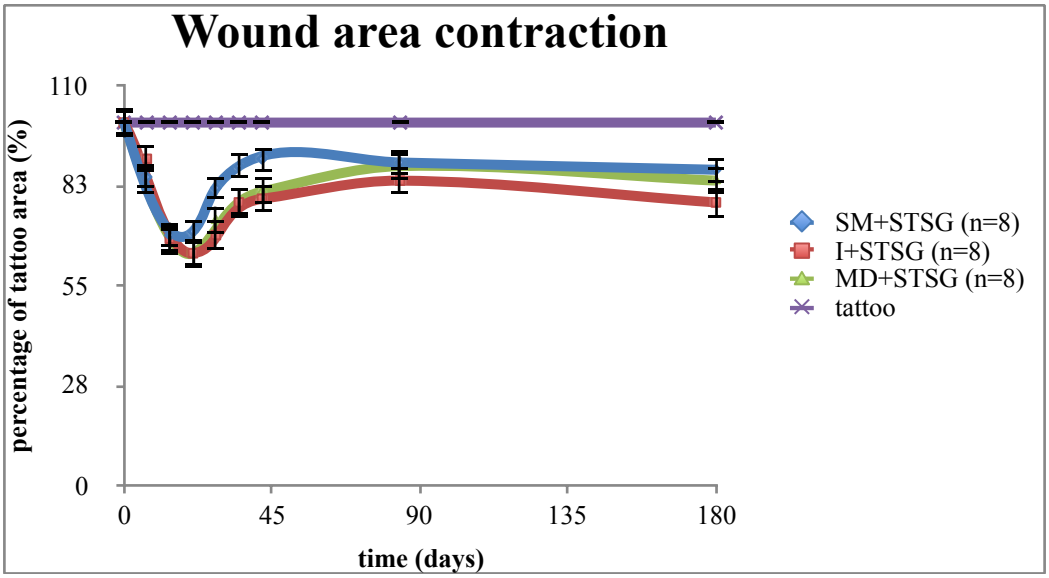

Figure 5.6.3.4: Mean wound area as a percentage of the tattooed area versus time (n=24, 8 per wound group) for different reconstructive options, in a 180 day study.

Interpretations for mean wound area and contraction

The tattooed area increased in size over time. Wounds treated with I+STSG showed the greatest degree of contraction. Wounds treated with SM +STSG and those treated with MD + STSG

showed no significant long-term differences in wound area and contraction. Both these groups were larger than wounds treated with I + STSG, and smaller than the tattooed area. These area differences were all statistically significant ($p<0.0001$).

5.6.4 Extra Domain A-Fibronectin

Please see table 5.6.4 and figures 5.6.4.1-2

Normal skin

The mean EDA-FN staining density of normal skin showed no statistically significant changes over time.

Wounds treated with Smart Matrix™ + split thickness skin graft

The mean EDA-FN staining density showed no statistically significant changes over time. However, a significant gradual decrease occurred between days 28 and 180 (mean difference of 1.42, $p<0.0001$).

When compared to normal skin, wounds treated with SM + STSG showed no statistically significantly different scores of EDA-FN staining density throughout the course of the experiment.

Wounds treated with Matriderm™ + split thickness skin graft

A significantly decrease occurred between days 28 and 35 (mean difference of 1.76, $p=0.0049$).

When compared to normal skin, wounds treated with MD + STSG showed a statistically significantly higher score of EDA-FN density staining at day 14 (mean difference of 1.94, $p=0.03$). There were no other significant differences throughout the rest of the study,

When compared to wounds treated with SM + STSG, wounds treated with MD + STSG showed

statistically significant higher scores of EDA-FN staining density at day 28 (mean difference of 1.71, p=0.0085). There were no significant differences between the two groups throughout the rest of the study.

Wounds treated with Integra™ + split thickness skin graft

There were no statistically significant differences between consecutive time points. A statistically significant (p<0.0001) gradual decrease occurred between days 14 and 180 (mean difference of 2.75).

When compared to normal skin, wounds treated with I + STSG showed significantly higher mean EDA-FN staining density at days 7 (mean difference of 2.09, p=0.0084), 14 (mean difference of 3.01, p<0.0001), 21 (mean difference of 2.67, p<0.0001), 28 (mean difference of 2.9, p<0.0001), and 35 (mean difference of 2.37, p<0.0001).

When compared to wounds treated with SM + STSG, wounds treated with I + STSG, showed significantly higher mean EDA-FN staining density at days 14 (mean difference of 2.29, p<0.0001), 21 (mean difference of 1.72, p=0.0076), 28 (mean difference of 1.65, p=0.0158) 35, (mean difference of 2.48, p<0.0001) and 42 (mean difference of 1.81 p=0.0387). There were no significant differences between the two groups at days 84 and 180.

When compared to wounds treated with MD + STSG, wounds treated with I + STSG showed no statistically significant differences.

	Day 7	Day 14	Day 21	Day 28	Day 35	Day 42	Day 84	Day 180
SM+STSG	1.66 (±0.07)	1.53 (±0.08)	1.58 (±0.08)	1.88 (±0.08)	0.7 (±0.08)	0.42 (±0.07)	0.38 (±0.15)	0.46 (±0.13)
I+STSG	2.93 (±0.08)	3.82 (±0.09)	3.29 (±0.09)	3.52 (±0.08)	3.18 (±0.10)	2.23 (±0.09)	1.08 (±0.15)	1.07 (±0.14)
MD+STSG	2.17 (±0.10)	2.75 (±0.11)	2.29 (±0.08)	3.58 (±0.09)	1.82 (±0.09)	1.64 (±0.10)	0.67 (±0.13)	0.3 (±0.07)
normal skin	0.83 (±0.15)	0.81 (±0.15)	0.63 (±0.14)	0.63 (±0.13)	0.81 (±0.14)	0.48 (±0.11)	0.83 (±0.19)	0.68 (±0.17)

Table 5.6.4: Mean EDA-fibronectin staining density (score out of 5), where n=48 (16 per wound group) for the 42 day study and n=24 (8 per wound group) for the 180 day study

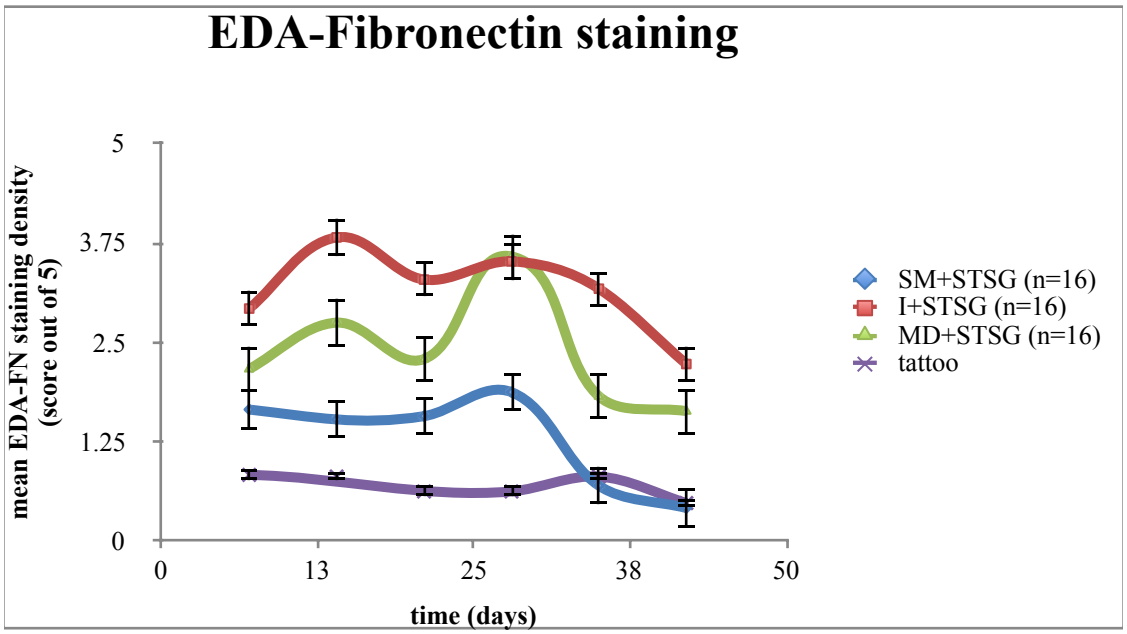

Figure 5.6.4.1: mean EDA-Fibronectin staining density versus time (n=48, 16 per wound group) for different reconstructive options in a 42 day study.

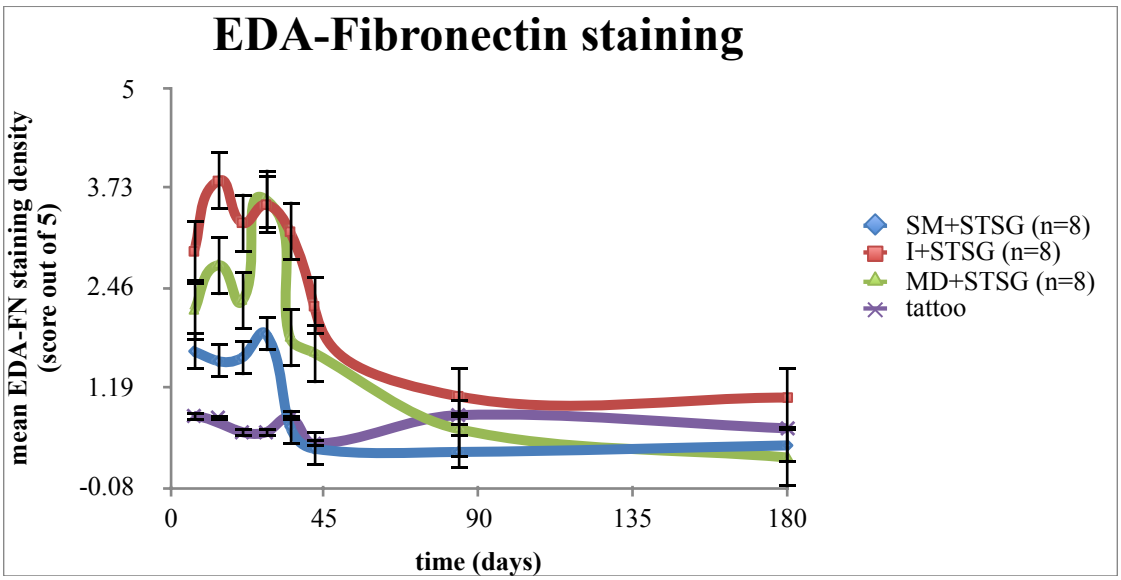

Figure 5.6.4.2: mean EDA-Fibronectin staining density versus time (n=24, 8 per wound group) for different reconstructive options in a 180 day study.

Interpretations for mean EDA-fibronectin staining density

EDA-fibronectin staining was lowest in normal skin (the tattooed area) which showed no significant changes over time. There were no statistically significant differences between normal skin and wounds treated with SM + STSG throughout the study. Wounds treated with MD + STSG and those treated with I + STSG showed no significant differences throughout the study. EDA-FN staining was however significantly higher in these two groups when compared with wounds treated with SM + STSG and in normal skin until day 42. There were no significant long-term differences between all groups.

5.6.5 Alpha-smooth muscle actin

Please see table 5.6.5 and figures 5.6.5.1-2

Normal skin

The mean α-SMA staining density of normal skin showed no statistically significant changes over time.

Wounds treated with Smart Matrix™ + split thickness skin graft

The mean α-SMA staining density in this group showed no statistically significant changes between consecutive time points or over time.

When compared to normal skin, wounds treated with SM + STSG showed no statistically significantly different scores of α-SMA staining density throughout the course of the experiment.

Wounds treated with Matriderm™ + split thickness skin graft

The mean α-SMA staining density in this group showed no statistically significant changes between consecutive time points or over time.

When compared to normal skin, wounds treated with MD + STSG showed statistically significantly higher scores of α-SMA density staining at days 21 (mean difference of 1.32, p=0.0327) and 35 (mean difference of 1.31, p-0.0365).

When compared to wounds treated with SM + STSG, wounds treated with MD + STSG showed statistically significant (p=0.0062) higher scores of α-SMA staining density at day 42 (mean difference of 1.2). There were no significant differences between the two groups throughout the rest of the study.

Wounds treated with Integra™ + split thickness skin graft

There were no statistically significant differences between consecutive time points, except for a significant ($p<0.0001$) decrease between days 35 and 42 (mean difference of 1.55). A statistically significant ($p<0.0001$) increase occurred between days 7 and 35 (mean difference of 3.12) and a statistically significant ($p<0.0001$) decrease occurred between days 42 and 180 (mean difference of 2.3).

When compared to normal skin, wounds treated with I + STSG showed significantly ($p<0.0001$) higher mean α-SMA staining density at days 14 (mean difference of 1.32), 21 (mean difference of 1.78), 28 (mean difference of 2.69), 35 (mean difference of 3.85) and 42 (mean difference of 2.18).

When compared to wounds treated with SM + STSG, wounds treated with I + STSG, showed significantly higher mean α-SMA staining density at days 7 (mean difference of 1.27, $p=0.0019$), 14 (mean difference of 1.12, $p=0.0206$), 21 (mean difference of 1.24, $p=0.0032$), 28 (mean difference of 1.92, $p<0.0001$) 35, (mean difference of 3.5, $p<0.0001$) and 42 (mean difference of 2.24 $p<0.0001$). There were no significant differences between the two groups at days 84 and 180.

When compared to wounds treated with MD + STSG, wounds treated with I + STSG showed a significantly ($p<0.0001$) higher mean α-SMA staining density at day 35 (mean difference of 2.54). There were no other significant differences between the two groups throughout the rest of the experiment.

	Day 7	Day 14	Day 21	Day 28	Day 35	Day 42	Day 84	Day 180
SM+STSG	0.40 (±0.07)	0.45 (±0.07)	1.02 (±0.11)	1.21 (±0.08)	0.79 (±0.11)	0.5 (±0.08)	0.4 (±0.10)	0.42 (±0.09)
I+STSG	1.67 (±0.09)	2.34 (±0.09)	2.26 (±0.09)	3.13 (±0.09)	4.29 (±0.09)	2.74 (±0.08)	1.50 (±0.17)	0.44 (±0.10)
MD+STSG	1.38 (±0.07)	1.56 (±0.08)	1.80 (±0.08)	1.68 (±0.08)	1.75 (±0.09)	1.70 (±0.09)	0.46 (±0.11)	0.38 (±0.10)
normal skin	0.44 (±0.10)	0.52 (±0.11)	0.48 (±0.11)	0.44 (±0.10)	0.44 (±0.10)	0.56 (±0.10)	0.54 (±0.15)	0.63 (±0.18)

Table 5.6.5: Mean alpha smooth muscle actin staining density (score out of 5), where n=48 (16 per wound group) for the 42 day study and n=24 (8 per wound group) for the 180 day study

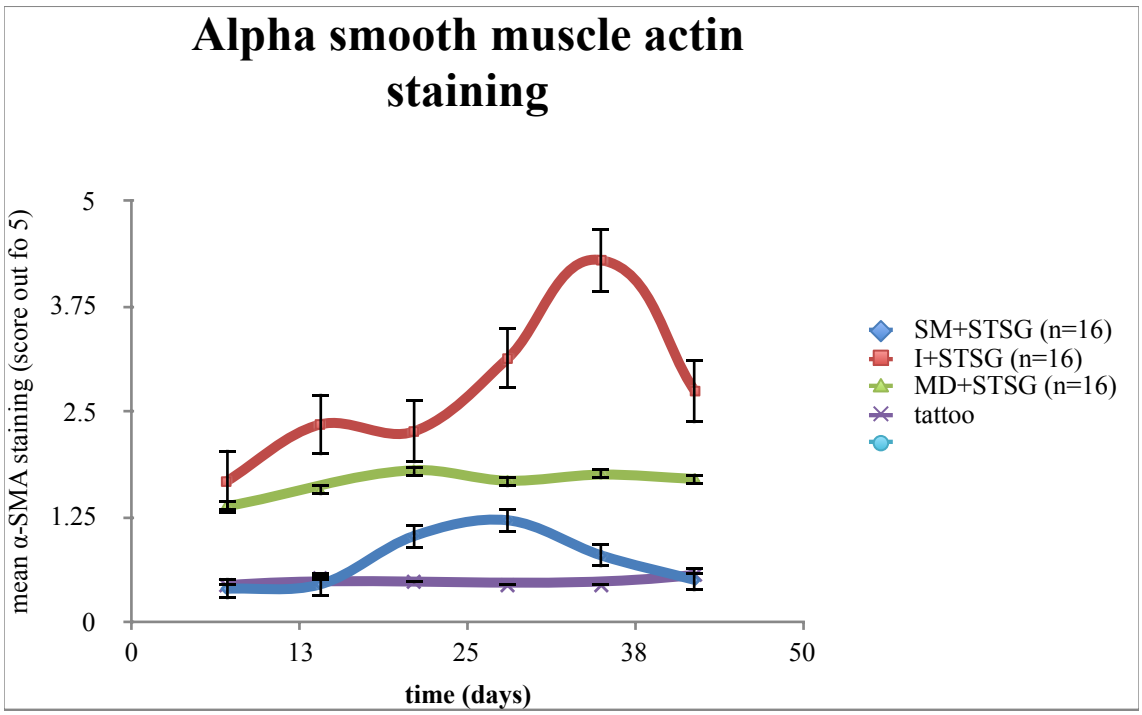

Figure 5.6.5.1: Mean Alpha–Smooth muscle actin staining density versus time (n=48, 16 per wound group) for different reconstructive options in a 42 day study.

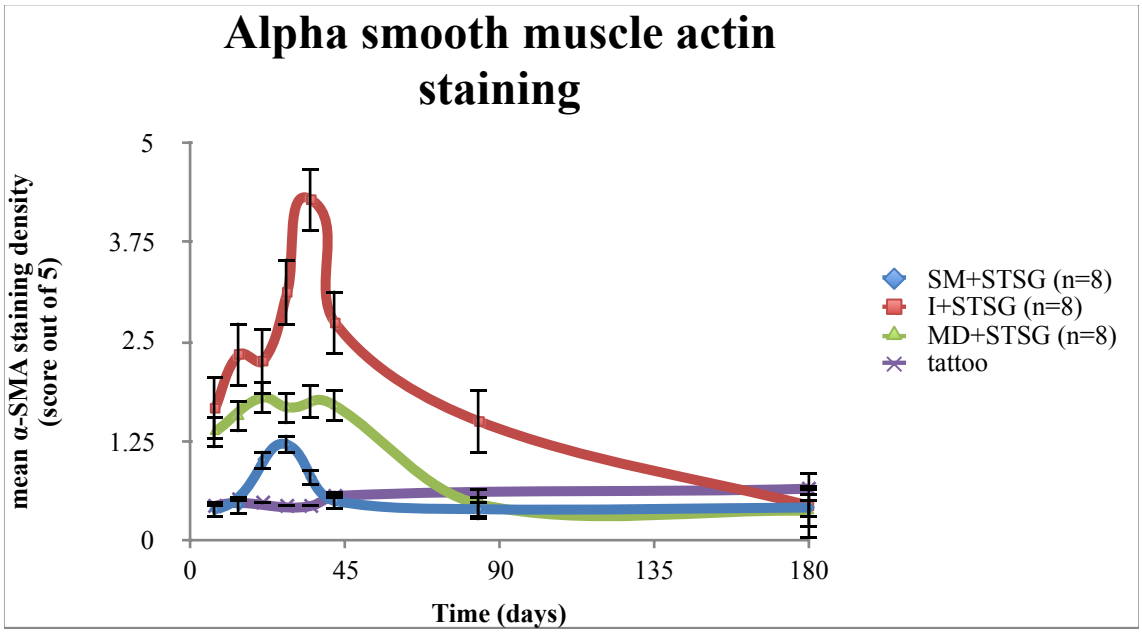

Figure 5.6.5.2: Mean Alpha–Smooth muscle actin staining density versus time (n=24, 8 per wound group) for different reconstructive options in a 180 day study.

Interpretations for mean Alpha Smooth Muscle Actin staining density

Mean α-SMA staining was lowest in normal skin (the tattooed area) which showed no significant changes over time. There were no statistically significant differences between normal skin and wounds treated with SM + STSG throughout the study. Wounds treated with MD + STSG showed no long term significant changes between normal skin and SM + STSG, except from levels in this group being higher at days 21, 35 and 42. Wounds treated with I + STSG showed significantly higher levels than all other wound groups until day 42, especially at day 35. There were no significant differences between all groups by days 84 and 180.

5.6.6 Scaffold presence

Please see figures 5.6.6.1-3

On H+E staining, wounds were observed for the presence of the dermal scaffold. Scaffold persistence was observed, as in the optimal acellular dermal matrix, the scaffold would persist in the wound for a time period sufficient to redirect neodermal tissue formation while being recognised as living tissue, and not persist as a foreign body and its associated immune response (deVries *et al*., 1993). The dermal scaffold was considered to be present if a reddish-orange pattern of structures, dissimilar to cellular and ECM structures was present between the wounds bed and overlying skin graft and parallel to the wound bed was present.

<u>Wounds treated with Smart Matrix™ + split thickness skin graft.</u>

Of the 16 wounds, all showed the presence of the Smart Matrix™ scaffold at days 7, 14 and 21. The dermal scaffold was still present in 5 of the wounds at day 28, 3 wounds at day 35, 1 wound at day 42 and absent in all wounds at days 84 and 180.

<u>Wounds treated with Matriderm™ + split thickness skin graft.</u>

Of the 16 wounds, all showed the presence of the Matriderm™ scaffold at days 7, 14 and 21. The dermal scaffold was still present in 14 of the wounds at day 28, 13 wounds at day 35, 6 wounds at day 42 and absent in all wounds at days 84 and 180.

When compared with wounds treated with SM + STSG, there were no significant differences at days 7,14, 21, 84 and 180. There was a significant difference of 9 wounds ($p<0.0001$) at day 28 and of 10 wounds at day 35 ($p<0.0001$).

Wounds treated with Integra™ + split thickness skin graft.

Of the 16 wounds, all showed the presence of the Integra™ scaffold at days 7, 14, 21, 28, 35 and 42. The dermal scaffold was still present in 12 of the wounds at day 84 and 3 of the wounds at day 180.

When compared with wounds treated with SM + STSG, there were no significant differences at days 7, 14 and 21. There was a significant difference of 11 wounds ($p<0.0001$) at day 28, of 13 wounds at day 35 ($p<0.0001$), of 15 wounds at day 42 ($p<0.0001$), 12 wounds at day 84 ($p<0.0001$) and of 3 wounds at day 180 ($p=0.0435$).

When compared to wounds treated with MD + STSG, wounds treated with I + STSG showed no significant differences at day 7, 14, 21 and 28. There was a significant difference of 3 wounds ($p=0.0435$) at 35, of 10 wounds at day 42 ($p<0.0001$), 12 wounds at day 84 ($p<0.0001$) and of 3 wounds at day 180 ($p=0.0435$).

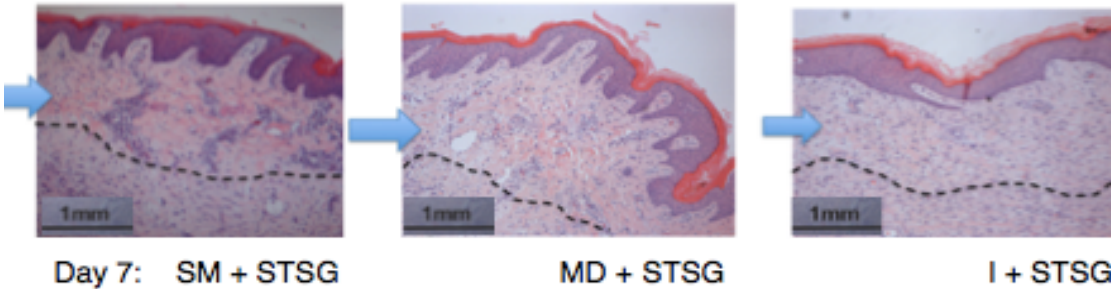

Figure 5.6.6.1: Photographic images showing examples of the presence of the dermal scaffold (blue arrow) on H&E staining at x10 magnification, for different reconstructive options at day 7. The dashed black line shows the interface of the wound bed and dermal scaffold.

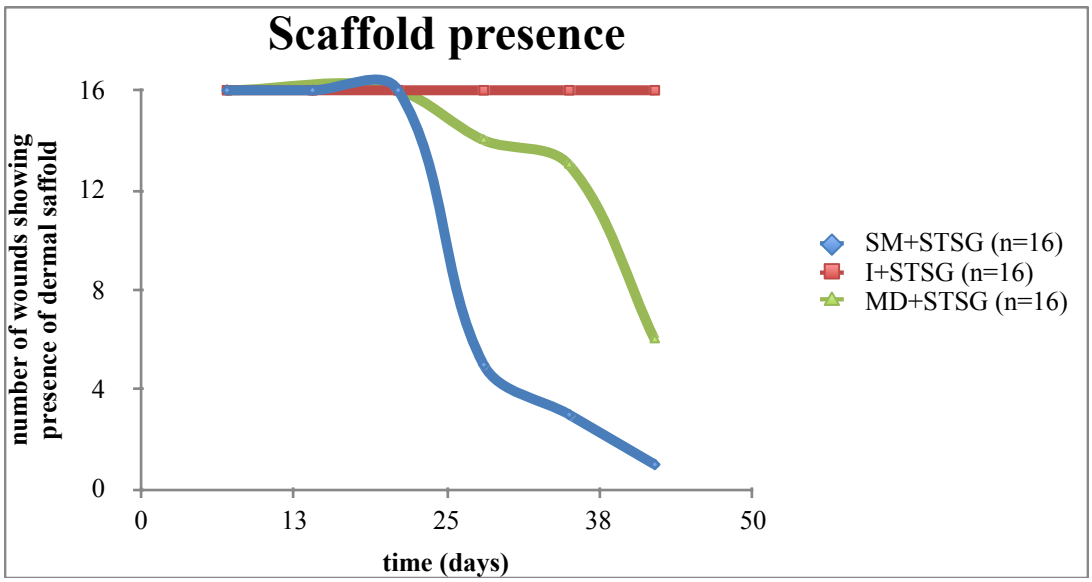

Figure 5.6.6.2: Number of wounds showing scaffold presence versus time (n=48, 16 per wound group) for different reconstructive options in a 42 day study.

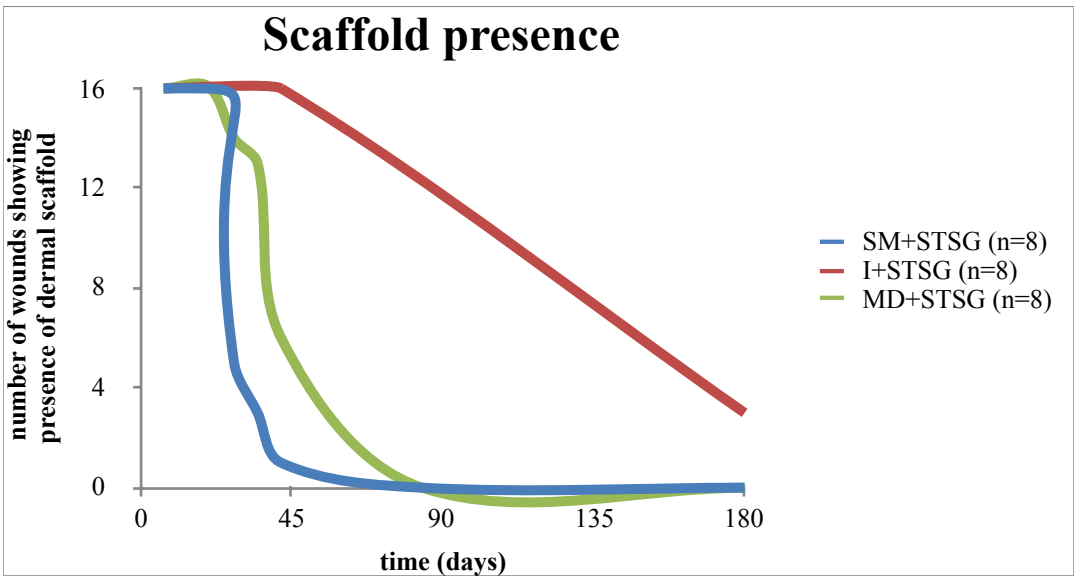

Figure 5.6.6.3: Number of wounds showing scaffold presence versus time (n=24, 8 per wound group) for different reconstructive options in a 180 day study.

Interpretations for scaffold presence

The time for dermal scaffold presence in the wound bed was shortest for wounds treated with SM + STSG, followed by wounds treated with MD + STSG and the longest in wounds treated with I + STSG.

5.6.7 Collagen

Please see table 5.6.7 and figures 5.6.7.1-2

Normal skin

The mean collagen staining density of normal skin showed no statistically significant changes over time.

Wounds treated with Smart Matrix™ + split thickness skin graft

A statistically significant increase occurred between days 7 and 14 (mean difference of 0.67,

p<0.0001) and between days 21 and 28 (mean difference of 0.54, p=0.0039). While no other statistically significant increases occurred between consecutive time points, throughout the course of the study there was a significant increase in elastin staining density. The mean difference between days 28 and 180 was 0.84, p<0.0001).

When compared to normal skin, wounds treated with SM + STSG showed statistically significantly lower scores of collagen staining density at days 7 (mean difference of 2.43, p<0.0001), 14 (mean difference of 1.55, p<0.0001), 21 (mean difference of 1.27, p=0.0003) and 28 (mean difference of 0.67, p=0.0035.) There were no significant differences between the two groups throughout the rest of the study.

Wounds treated with Matriderm™ + split thickness skin graft

Statistically significant increase in collagen staining density occurred between days 7 and 14 (mean difference of 0.54, p=00039) and between days 21 and 28 (mean difference of 1.07, p<0.0001). There were no statistically significant changes between consecutive time points, or throughout the course of the study.

When compared to normal skin wounds treated with MD + STSG showed statistically significant (p<0.0001) lower scores of collagen staining density at days 7 (mean difference of 2.20), 14 (mean difference of 1.45), and 21. There were no significant differences between the two groups throughout the rest of the study.

When comparing wounds treated with MD + STSG to those treated with SM + STSG, there were no statistically significant differences in mean collagen staining density throughout the study.

Wounds treated with Integra™ + split thickness skin graft

A statistically significant increase occurred between days 7 and 14 (mean difference of 0.57, p=0.0012) and between days 21 and 28 (mean difference of 0.67, p<0.0001). While there were no other significant changes between consecutive time points, a significant increase in collagen staining occurred between days 28 and 180 (mean difference of 0.58, p=0.001).

When comparing wounds treated with I + STSG to normal skin, the mean collagen staining density was significantly lower (p<0.0001) at days 7 (mean difference of 2.28), 14 (mean difference of 1.50), and 21 (mean difference of 1.23).

When comparing wounds treated with I + STSG to those treated with SM + STSG, there were no significant difference sin collagen staining over the course of the experiment.

When comparing wounds treated with I + STSG to those treated with MD + STSG, there were no significant differences in collagen staining over the course of the experiment.

	Day 7	Day 14	Day 21	Day 28	Day 35	Day 42	Day 84	Day 180
SM+STSG	1.39 (±0.08)	2.05 (±0.10)	2.50 (±0.11)	3.04 (±0.10)	3.48 (±0.10)	3.85 (±0.07)	3.88 (±0.09)	3.88 (±0.09)
I+STSG	1.53 (±0.08)	2.10 (±0.10)	2.54 (±0.10)	3.21 (±0.10)	3.43 (±0.07)	3.52 (±0.09)	3.48 (±0.14)	3.79 (±0.11)
MD+STSG	1.61 (±0.07)	2.16 (±0.09)	2.32 (±0.08)	3.40 (±0.10)	3.68 (±0.07)	3.64 (±0.08)	3.75 (±0.09)	3.69 (±0.12)
normal skin	3.82 (±0.10)	3.60 (±0.10)	3.77 (±0.10)	3.71 (±0.10)	3.71 (±0.10)	3.46 (±0.14)	3.42 (±0.19)	3.54 (±10.4)

Table 5.6.7: Mean collagen staining density (score out of 5), where n=48 (16 per wound group) for the 42 day study and n=24 (8 per wound group) for the 180 day study

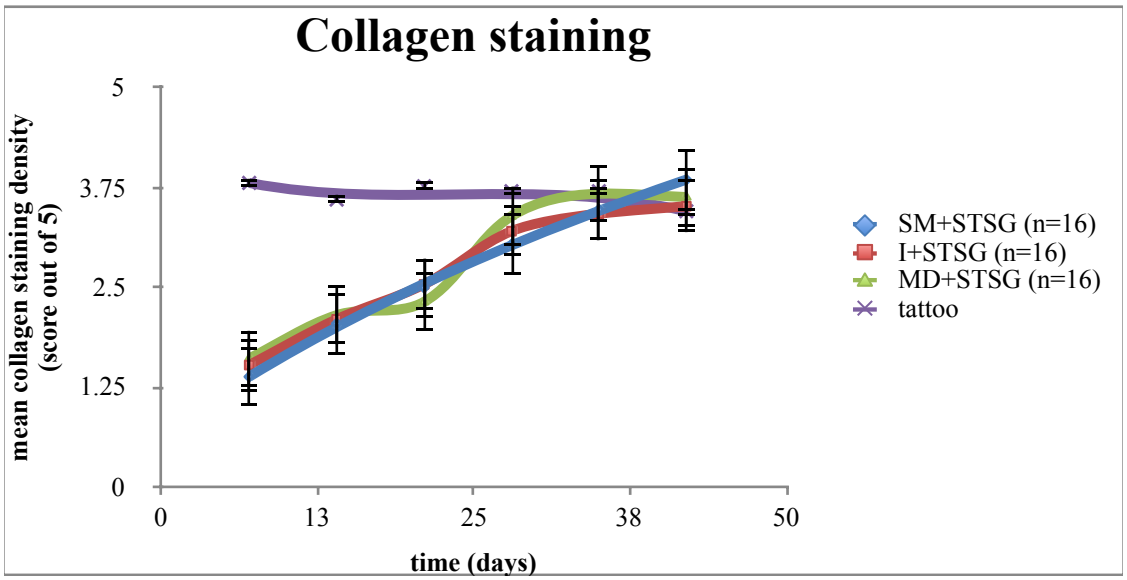

Figure 5.6.7.1: Mean collagen staining density versus time (n=48, 16 per wound group) for different reconstructive options in a 42 day study.

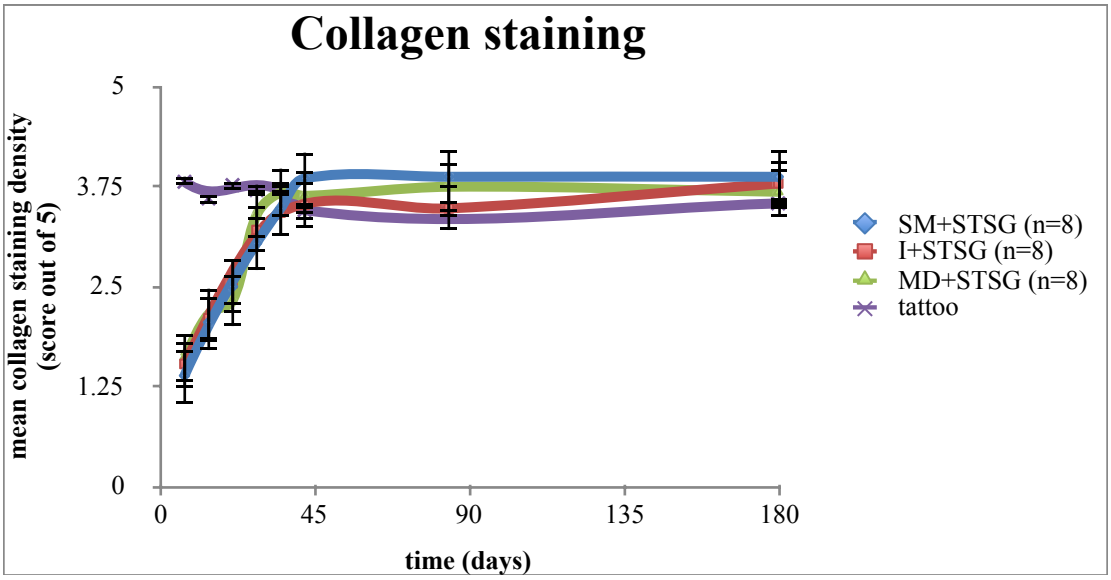

Figure 5.6.7.2: Mean collagen staining density versus time (n=24, 8 per wound group) for different reconstructive options in a 180 day study.

Interpretations for mean collagen staining density

Mean collagen staining density (the tattooed area) showed no significant changes over time. Mean collagen staining density increased over the course of the study for all three wound groups.

Wounds treated with SM + STSG reached collagen levels similar to normal skin by day 35. Wounds treated with MD + STSG reached collagen levels similar to normal skin by day 28. Wounds treated with I + STSG reached collagen levels similar to normal skin by day 28. There were no statistically significant differences between all wound groups in mean collagen staining density. From day 42 onwards, there were no significant differences between all four groups.

5.6.8 Elastin

Please see table 5.6.8 and figures 5.6.8.1-2

Normal skin

The mean elastin staining density of normal skin showed no statistically significant changes over time.

Wounds treated with Smart Matrix™ + split thickness skin graft

Statistically significant increases occurred between days 7 and 14 (mean difference of 0.95, $p<0.0001$) and between days 14 and 21 (mean difference of 0.6, $p=0.007$). While no other statistically significant increases occurred between consecutive time points, throughout the course of the study there was a significant increase in elastin staining density. The mean difference between days 21 and 180 was 0.57, $p=0.0029$.

When compared to normal skin, wounds treated with SM + STSG showed statistically significantly lower scores of elastin staining density at days 7 (mean difference of 1.89, $p<0.0001$), 14 (mean difference of 1.23, $p<0.000$), 21 (mean difference of 0.69, $p=0.0003$) and 28 (mean difference of 0.79, $p<0.0001$.) There were no significant differences between the two groups throughout the rest of the study.

Wounds treated with Matriderm™ + split thickness skin graft

There were no statistically significant changes in elastin staining density between consecutive time points. However, there was a statistically significant increase over the course of the study of 0.89 ($p<0.0001$).

When compared to normal skin wounds treated with MD + STSG showed statistically significant lower score of elastin staining density at day 14 (mean difference of 0.86, $p<0.0001$), and 28 (mean difference of 0.63, $p=0.0182$). There were no significant differences between the two groups throughout the rest of the study.

When comparing wounds treated with MD + STSG to those treated with SM + STSG, there were no statistically significant differences in mean elastin staining density throughout the study.

Wounds treated with Integra™ + split thickness skin graft

The changes between consecutive time post-operative time points were not statistically significant. However, there was a statistically significant ($p<0.0001$) increase in elastin staining over the course of the experiment, with a mean difference of 2.16, ($p<0.0001$) between days 7 and 180.

When comparing wounds treated with I + STSG to normal skin, the mean elastin staining density was significantly lower ($p<0.0001$) at days 7 (a mean difference of1.91), 14 (mean difference of 2.17), 21 (mean difference of 2.17), and day 28 (mean difference of 2.04). Throughout the rest of the study, there were no significant differences.

When comparing wounds treated with I + STSG to those treated with SM + STSG, the mean elastin staining density was significantly ($p<0.0001$) lower at days at day 14 (mean difference of 0.94), day 21 (mean difference of 1.48), 28 (mean difference of 1.25) and 35 (mean difference of 0.69). Throughout the rest of the study, there were no significant differences.

When comparing wounds treated with I + STSG to those treated with MD + STSG, the mean elastin

staining density was significantly ($p<0.0001$) lower at days 7 (mean difference of 1.35), 14 (mean difference of 1.3, 21 (mean difference of 1.69, 28 (mean difference of 1.42) and 35 (mean difference of 0.56, $p=0.0033$).

	Day 7	Day 14	Day 21	Day 28	Day 35	Day 42	Day 84	Day 180
SM+STSG	0.51 (±0.08)	1.46 (±0.07)	2.06 (±0.10)	2.04 (±0.09)	2.22 (±0.10)	2.51 (±0.10)	2.50 (±0.10)	2.63 (±0.10)
I+STSG	0.49 (±0.07)	0.52 (±0.52)	0.58 (±0.58)	0.79 (±0.10)	1.53 (±0.08)	2.04 (±0.10)	2.25 (±0.15)	2.65 (±0.15)
MD+STSG	1.84 (±0.09)	1.82 (±0.10)	2.27 (±0.11)	2.21 (±0.08)	2.59 (±0.07)	2.60 (±0.07)	2.85 (±0.12)	2.75 (±0.12)
normal skin	2.40 (±0.13)	2.69 (±0.13)	2.75 (±0.15)	2.83 (±0.13)	2.38 (±0.14)	2.48 (±0.11)	2.79 (±0.13)	2.96 (±0.22)

Table 5.6.8: Mean elastin staining density (score out of 5), where n=48 (16 per wound group) for the 42 day study and n=24 (8 per wound group) for the 180 day study

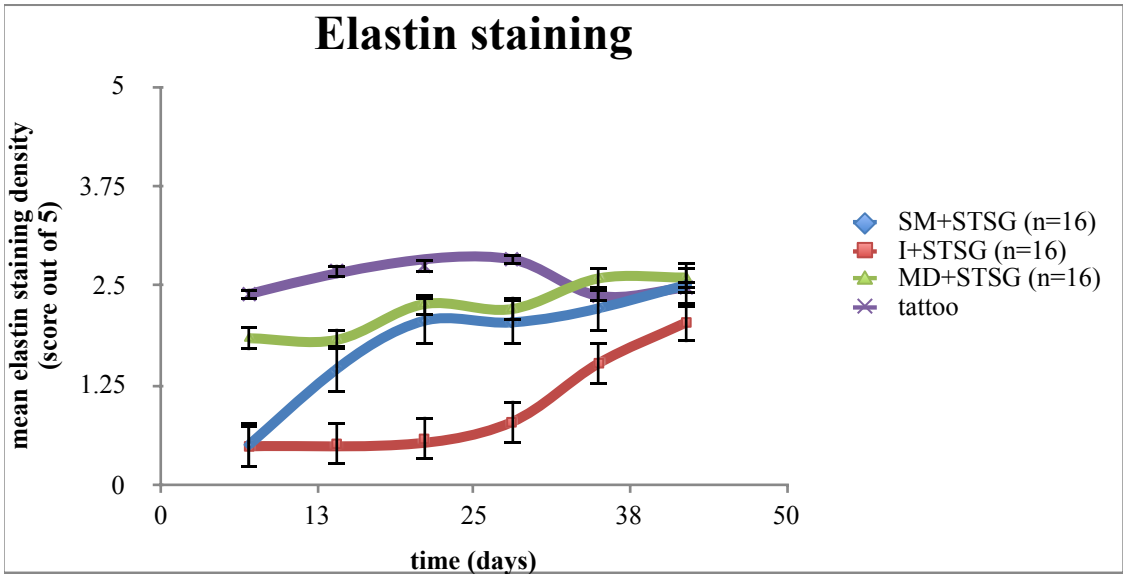

Figure 5.6.8.1: Mean elastin staining density versus time (n=48, 16 per wound group) for different reconstructive options in a 42 day study.

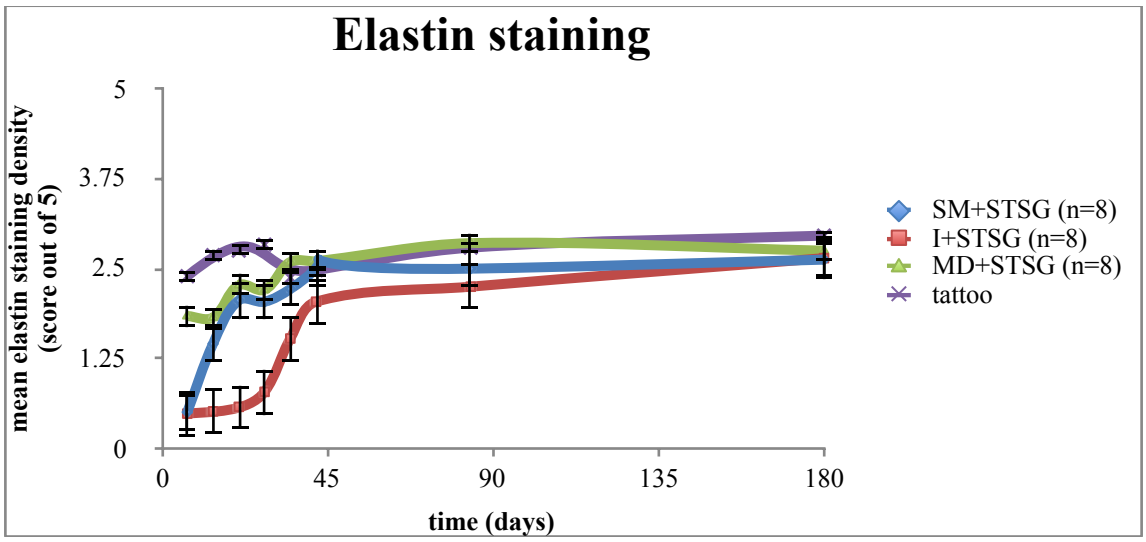

Figure 5.6.8.2: Mean elastin staining density versus time (n=24, 8 per wound group) for different reconstructive options in a 180 day study.

Interpretations for mean elastin staining density

Mean elastin staining density in normal skin (the tattooed area) which showed no significant changes over time. Mean elastin staining density increased over the course of the study for all three wound groups. All three wound groups reached elastin levels similar to normal skin by day 35. There were no statistically significant differences between all wound groups in mean elastin staining density. From day 42 onwards, there were no significant differences between all four groups.

5.6.9 Wound (neodermal) thickness

Please see table 5.6.9 and figures 5.6.9.1-2

Normal skin

The mean thickness of normal skin showed no statistically significant changes throughout the study.

Wounds treated with Smart Matrix™ + split thickness skin graft

The mean thickness of wounds treated with SM + STSG showed statistically significant increases between days 7 and 14, (mean difference of 348.52µm, $p<0.0001$) and between days 14 and 21

(mean difference of 240.02µm, p<0.0001). A statistically significant decrease occurred between days 84 and 180 (mean difference of 220.13µm (p<0.0001).

When compared to normal skin, wounds treated with SM + STSG showed a statistically significant lower wound thickness at day 7 (mean difference of 215.64µm, p<0.0001). Wounds treated with SM + STSG were significantly (p<0.0001) thicker between days 21 and 84. The mean difference at day 21 was 376.24µm, 349.78µm at day 28, 356.32µm at day 35, 291.10µm at day 42 and 204.14µm at day 84.

Wounds treated with Matriderm™ + split thickness skin graft

Statistically significant increases in wound thickness occurred between days 7 and 14 (mean difference of 210.42µm, p<0.0001), days 14 and 21 (mean difference of 253.81µm, p<.0001) and days 21 and 28 (mean difference of 137.65µm, p=0.0142). A statistically significant decrease in wound depth occurred between days 42 and 84 (mean difference of 222.75µm, p<0.0001).

When compared to normal skin, wounds treated with MD + STSG showed a statistically significant lower wound depth at day 7 (mean difference of 200.91µm, p=0.004). Wounds treated with MD + STSG were significantly (p<0.0001) more deep between days 21 and 42. The mean difference at day 21 was 266.52µm, 392.55µm at day 28, 369.42µm at day 35, and 311.31µm at day 42.

When comparing wounds treated with MD + STSG to those treated with SM + STSG, there were no statistically significant differences in thickness throughout the study.

Wounds treated with Integra™ + split thickness skin graft

Statistically significant increases in wound thickness occurred between days 14 and 21 (mean difference of 145.22µm, p=0.0055) and between days 21 and 28 (mean difference of 283.51µm, p<0.0001). A statistically significant decrease in wound thickness occurred between days 42 and 84 (mean difference of 157.53µm, p=0.0388).

When comparing wounds treated with I + STSG to normal skin, the wounds were significantly less thick at days 7 (mean difference of 276.14µm, p<0.0001), and 14 (mean difference of 241.75µm, p=<0.0001). The wounds were significantly thicker at days 28 (mean difference of 178.47µm, p=0.0053), 35 (man difference of 162.81µm, p=0.0243) and at day 42 (mean difference of 253.77µm, p<0.0001).

When comparing wounds treated with I + STSG to those treated with SM + STSG, the mean wound thickness was significantly less at days 14 (mean difference of 375.00µm, p<0.0001), 21 (mean difference of 469.84µm, p<0.0001), 28 (mean difference of 171.42µm, p=0.0002) and 35 (mean difference of 193.61µm, p<0.0001).

When comparing wounds treated with I + STSG to those treated with MD + STSG, the mean wound thickness was significantly (p<0.0001) less at days 14 (mean difference of 251.57µm), 21 (mean difference of 360.11µm), 28 (mean difference of 214.12µm) and 35 (mean difference of 206.73µm).

	Day 7	Day 14	Day 21	Day 28	Day 35	Day 42	Day 84	Day 180
SM+STSG	309.00 (±2.02)	657.54 (±2.40)	897.50 (±2.74)	882.63 (±2.82)	887.98 (±2.34)	820.48 (±1.55)	740.64(±2.96)	520.60(±8.95)
I+STSG	248.48 (±1.74)	282.52 (±4.90)	427.73 (±2.83)	711.27 (±2.06)	694.42 (±2.40)	783.08 (±2.75)	618.06 (±3.40)	526.76 (±3.71)
MD+STSG	323.67 (±2.45)	534.02(±1.90)	787.83 (±2.83)	925.44 (±2.06)	901.08 (±2.40)	840.71 (±2.75)	618.00 (±3.40)	526.76 (±3.71)
normal skin	524.58(±2.94)	524.25 (±4.13)	521.33 (±3.64)	532.9 2(±5.84)	531.67 (±6.61)	529.42 (±3.54)	536.58 (±4.58)	548.83 (±3.93)

Table 5.6.9: Mean neodermal thickness (µ), where n=48 (16 per wound group) for the 42 day study and n=24 (8 per wound group) for the 180 day study

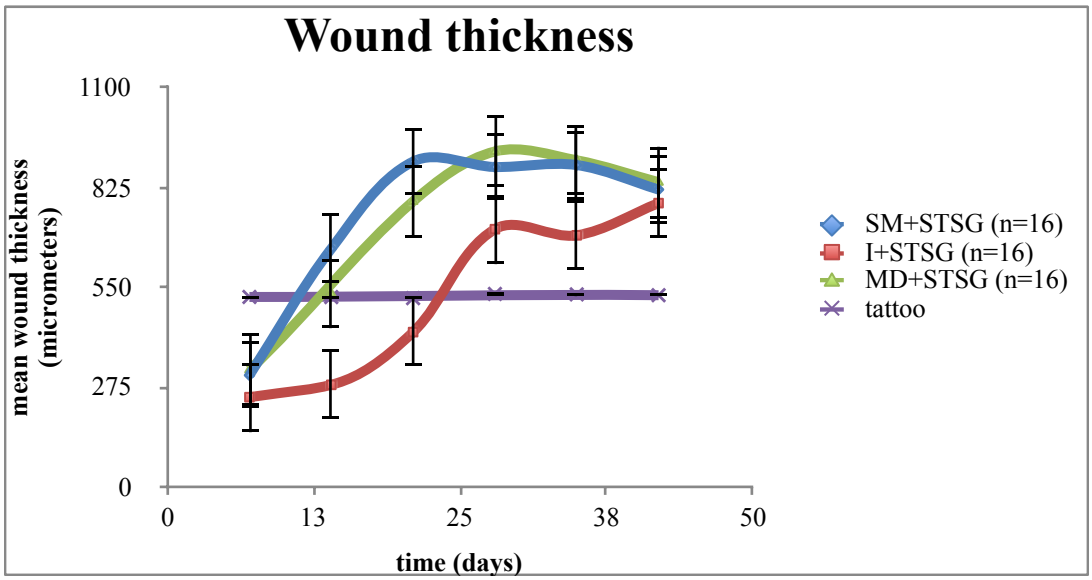

Figure 5.6.9.1: Mean wound thickness versus time (n=48, 16 per wound group) for different reconstructive options in a 42 day study.

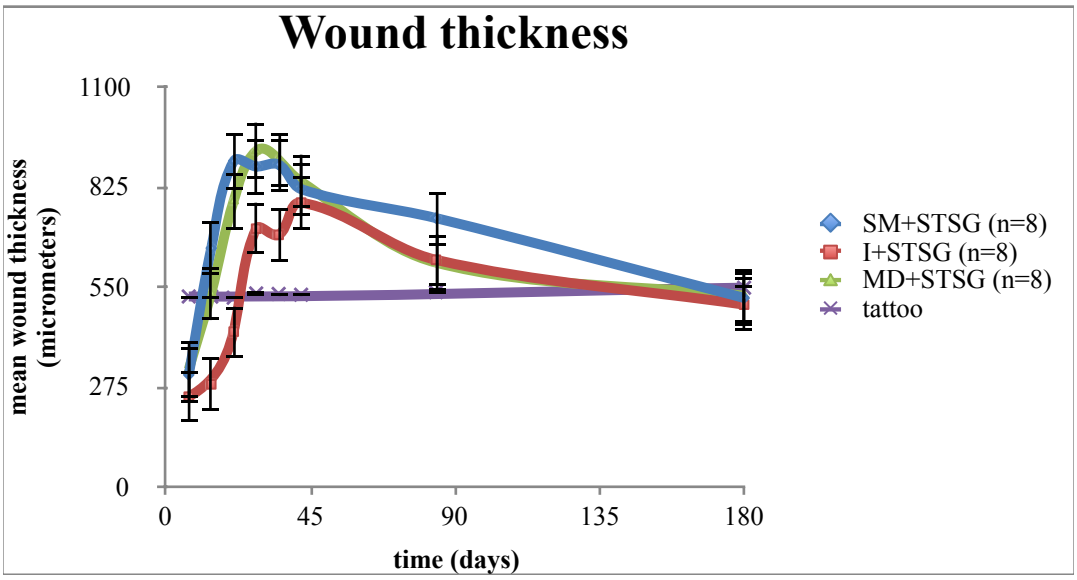

Figure 5.6.9.2: Mean wound thickness versus time (n=24, 8 per wound group) for different reconstructive options in a 180 day study.

Interpretations for mean wound thickness

Mean wound thickness showed no significant change throughout the study in normal skin (the tattooed area). Wounds treated with SM + STSG were less thick than normal skin until day 14 and

thicker until day 84. Wounds treated with MD + STSG were less thick than normal skin at day 7 and thicker from days 21 to 42. There were no significant differences between the two groups thereafter. There were no significant difference in wound thickness between wounds treated with SM + STSG and those treated with MD + STSG. Wounds treated with I + STSG were less thick than normal skin until day 14 and thicker between days 28 and 42. These wounds were less thick than those treated with SM + STSG and those treated with MD+STSG between days 14 and 35. By day 180, there were no significant differences between all four groups.

5.6.10 Cellular density

Please see table 5.6.10 and figures 5.6..10.1-2

Normal skin

The mean cellular density of normal skin showed no statistically significant changes throughout the study.

Wounds treated with Smart Matrix™ + split thickness skin graft

The mean cellular density of wounds treated with SM + STSG showed no statistically significant changes between consecutive time points, except for a statistically significantly decrease from day 21 to day 28 (mean difference of 0.57, p=0.0149). There were no significant differences in mean cellular density over between days 7 and 180.

When compared to normal skin, wounds treated with SM + STSG showed statistically significantly higher scores of cellular density at days 14 (mean difference of 0.77, p=0.01), and 180 (mean difference of 0.92, p=0.0472). There were no significant differences between the two groups throughout the rest of the study.

Wounds treated with Matriderm™ + split thickness skin graft

There were no statistically significant changes in cellular density between consecutive time points. However, there was a statistically significant decrease of 0.84 ($p<0.0001$) between days 14 and 28 and further decreases thereafter. There were no significant differences between the consecutive time points throughout the rest of the study.

When compared to normal skin wounds treated with MD + STSG showed a statistically significantly higher score of cellular density at day 14 (mean difference of 0.86, $p=0.002$), and significantly lower scores at days 35 (mean difference of 0.79, $p=0.0016$), 42 (mean difference of 0.87, $p=0.0007$) and 180 (mean difference of 0.98, $p=0.0184$).

When comparing wounds treated with MD + STSG to those treated with SM + STSG, the former group showed statistically significantly higher scores at days 35 (mean difference of 0.53, $p=0.444$) and 42 (mean difference of 0.63, $p=0.0022$). There were no statistically significant differences in mean cellular density throughout the rest of the study.

Wounds treated with Integra™ + split thickness skin graft

The changes between consecutive time post-operative time points were not statistically significant. However, there was a statistically significant ($p<0.0001$) increase of 1.01 in cellular density between days 7 and 21.

When comparing wounds treated with I + STSG to normal skin, the mean cellular density was significantly lower at days 7 (mean difference of 1.48, $p<0.0001$), and 14 (mean difference of 0.65, $p=0.0495$). Throughout the rest of the study, there were no significant differences.

When comparing wounds treated with I + STSG to those treated with SM + STSG, the mean cellular density was significantly higher at days 7 (mean difference of 1.29, $p<0.0001$), 14 (mean difference of 1.51, $p<0.0001$) and 21 (mean difference of 0.55, $p=0.0263$).

When comparing wounds treated with I + STSG to those treated with MD + STSG, the mean cellular density was significantly lower at days 7 (mean difference of 1.32, $p<0.0001$), and 14 (mean difference of 1.51, $p<0.0001$), and significantly higher at day 42 (mean difference of 0.6, $p=0.0006$) and 180 (mean difference of 0.81, $p=0.0142$).

	Day 7	Day 14	Day 21	Day 28	Day 35	Day 42	Day 84	Day 180
SM+STSG	3.31 (±0.10)	3.68 (±0.09)	3.58 (±0.07)	3.01 (±0.11)	3.11 (±0.10)	3.23 (±0.10)	2.71 (±0.14)	2.58 (±0.10)
I+STSG	2.02 (±0.11)	2.31 (±0.10)	3.03 (±0.11)	3.10 (±0.11)	3.02 (±0.10)	3.20 (±0.08)	3.04 (±0.14)	3.33 (±0.14)
MD+STSG	3.34 (±0.10)	3.82 (±0.07)	3.24 (±0.10)	2.98 (±0.09)	2.58 (±0.08)	2.59 (±0.10)	2.52 (±0.10)	2.52 (±0.17)
normal skin	3.50 (±0.17)	2.96 (±0.16)	3.23 (±0.16)	3.06 (±0.16)	3.38 (±0.15)	3.42 (±0.15)	3.08 (±0.19)	3.50 (±0.19)

Table 5.6.10: Mean wound cellular density (score out of 5), where n=48 (16 per wound group) for the 42 day study and n=24 (8 per wound group) for the 180 day study

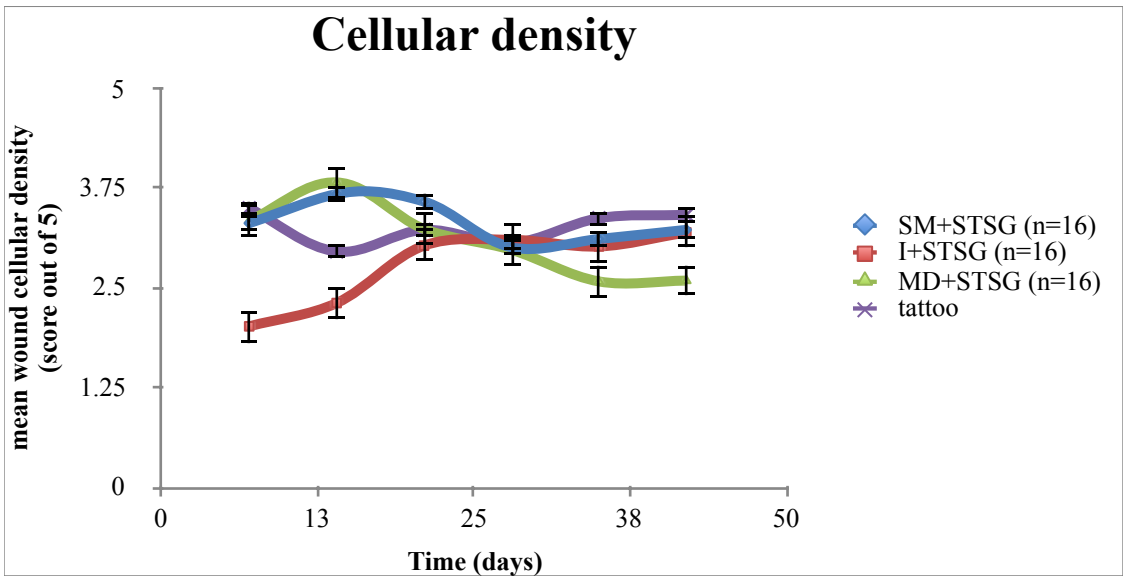

Figure 5.6.10.1: Mean cellular density versus time (n=48, 16 per wound group) for different reconstructive options in a 42 day study.

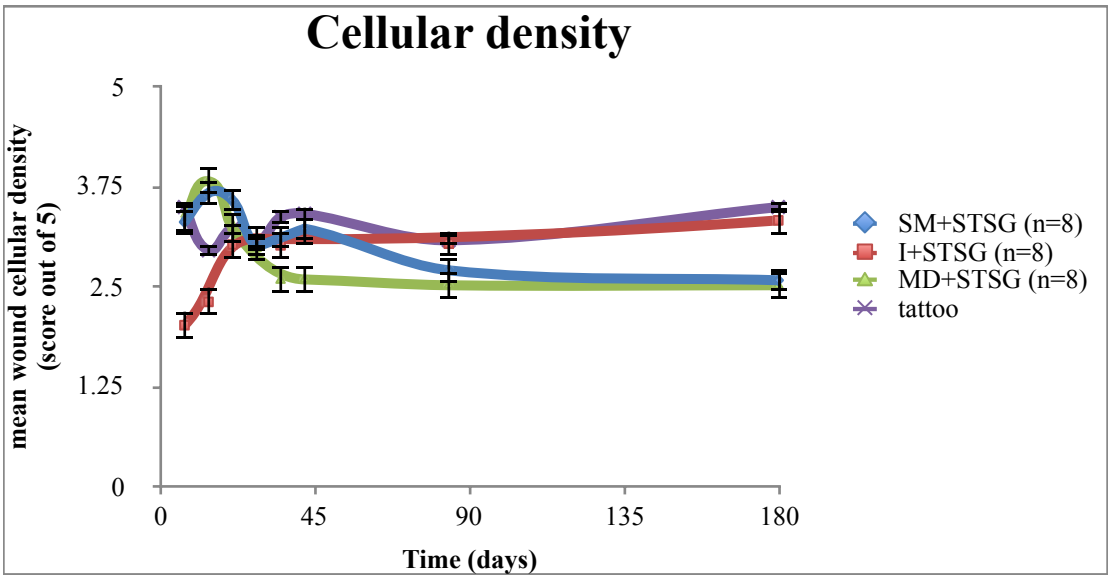

Figure 5.6..10.2 Mean cellular density versus time (n=24, 8 per wound group) for different reconstructive options in a 180 day study.

Interpretations for mean wound cellular density

Mean wound cellular density showed no significant change throughout the study in normal skin (the tattooed area). Wounds treated with SM + STSG showed higher mean cellular density scores than normal skin throughout the study. Wounds treated with MD + STSG showed higher mean cellular

density scores than the former two groups at day 14. There were no significant long-term differences between wounds treated with SM + STSG and MD+STSG after day 42. Wounds treated with I + SSG showed lower mean cellular density levels than normal skin until day 21. There were no significant differences thereafter. At day 180, there were no significant differences between wounds treated with SM + STSG and those treated with MD + STSG. These two wounds groups showed significantly higher levels than wounds treated with I + STSG and normal skin.

5.6.11 Inflammation

Please see table 5.6.11 and figures 5.6.11.1-2

Normal skin

The mean inflammatory cell density of normal skin showed no statistically significant changes over time.

Wounds treated with Smart Matrix™ + split thickness skin graft

The mean inflammatory cell density of wounds treated with SM + STSG showed no statistically significant changes between consecutive time points. There was a statistically significantly decrease from day 14 to day 84 (mean difference of 2.30, $p<0.0001$).

When compared to normal skin, wounds treated with SM + STSG showed statistically significantly higher scores of inflammatory cell density at days 7 (mean difference of 1.77, $p=0.0348$), 14 (mean difference of 2.29, $p=0.0002$) and 21 (mean difference of 1.78, $p=0.0321$). There were no significant differences between the two groups throughout the rest of the study.

Wounds treated with Matriderm™ + split thickness skin graft

There were no statistically significant changes in inflammatory cell density between consecutive time points. However, there was a statistically significant decrease of 1.47 ($p<0.0001$) between days 35 and 42.

When compared to normal skin wounds treated with MD + STSG showed statistically significantly higher scores of inflammatory cell density at days 7 (mean difference of 1.75, $p=0.0409$), 14 (mean difference of 2.48, $p<0.0001$), 21 (mean difference of 2.1, $p=0.0321$) and 35 (mean difference of 1.74, $p=0.0443$). There were no significant differences between the two groups throughout the rest of the study.

When comparing wounds treated with MD + STSG to those treated with SM + STSG, there were no statistically significant differences in mean inflammatory cell density throughout the study.

Wounds treated with Integra™ + split thickness skin graft

The changes between consecutive time post-operative time points were not statistically significant. However, there was a statistically significant ($p<0.0001$) decrease in inflammatory cell density throughout the study when comparing day 7 to days 42 (2.49), 84 (3.08) and 180 (3.49).

When comparing wounds treated with I + STSG to normal skin, the mean inflammatory density was significantly higher at days 7 (a mean difference of 3.66, $p<0.0001$), 14 (mean difference of 2.71), $p<0.0001$), 21 (mean difference of 3.39, <0.0001), day 28 (mean difference of 2.12, $p=0.0016$) and day 35 (mean difference of 1.74, $p=0.0008$). Throughout the rest of the study, there were no significant differences.

When comparing wounds treated with I + STSG to those treated with SM + STSG, the mean inflammatory cell density was significantly higher at days 7 (1.89, $p=0.0002$), and day 21 (1.60, $p=0.0066$). Throughout the rest of the study, there were no significant differences.

When comparing wounds treated with I + STSG to those treated with MD + STSG, the mean inflammatory cell density was significantly higher at day 7 (a mean difference of 1.91, $p<0.00071$). Throughout the rest of the study, there were no significant differences.

	Day 7	Day 14	Day 21	Day 28	Day 35	Day 42	Day 84	Day 180
SM+STSG	2.04 (±0.10)	2.63 (±0.08)	2.15 (±0.11)	1.67 (±0.10)	0.98 (±0.14)	0.66 (±0.19)	0.33 (±0.10)	0.29 (±0.08)
I+STSG	3.93 (±0.09)	3.04 (±0.09)	3.76 (±0.09)	2.49 (±0.07)	2.34 (±0.09)	1.44 (±0.07)	0.85 (±0.15)	0.44 (±0.09)
MD+STSG	2.02 (±0.11)	2.81 (±0.65)	2.48 (±0.08)	2.09 (±0.12)	1.91 (±0.24)	0.44 (±0.07)	0.42 (±0.09)	0.38 (±0.09)
normal skin	0.27 (±0.09)	0.33 (±0.08)	0.38 (±0.09)	0.38 (±0.09)	0.17 (±0.07)	0.33 (±0.09)	0.33 (±0.11)	0.21 (±0.11)

Table 5.6.11: Mean inflammatory cell density (score out of 5), where n=48 (16 per wound group) for the 42 day study and n=24 (8 per wound group) for the 180 day study

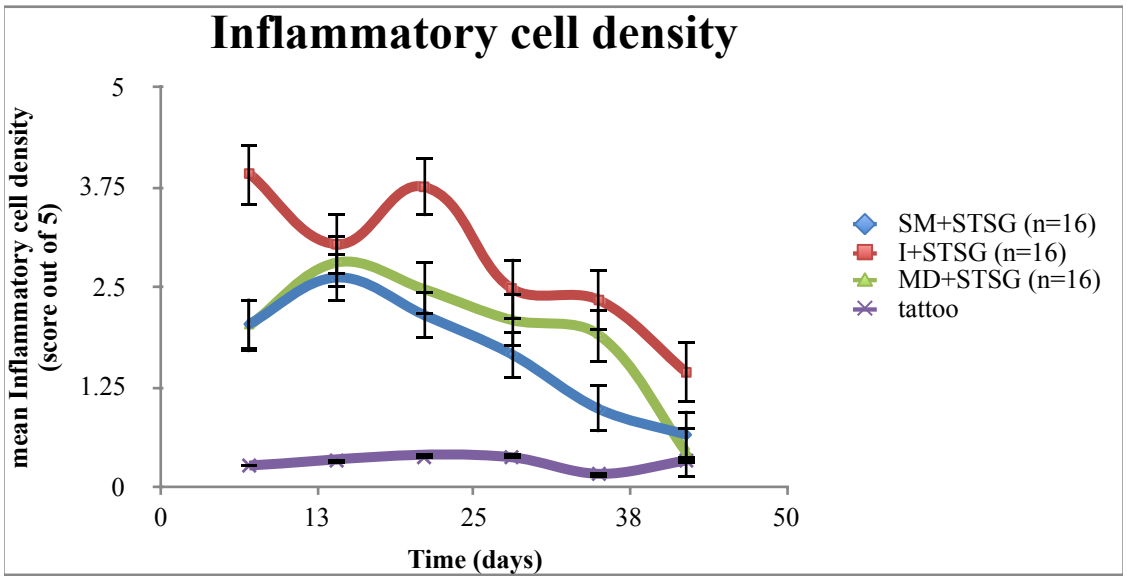

Figure 5.6.11.1: Mean inflammatory cell density versus time (n=48, 16 per wound group) for different reconstructive options in a 42 day study.

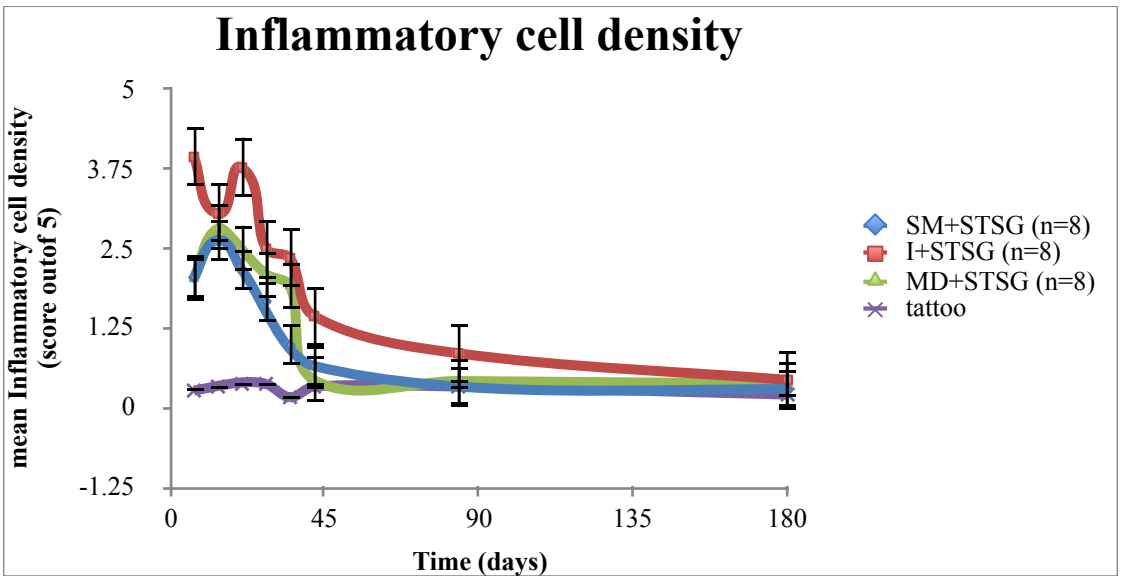

Figure 5.6.11.2: Mean inflammatory cell density versus time (n=24, 8 per wound group) for different reconstructive options in a 180 day study.

Interpretations for mean wound inflammatory cell density

In normal skin, the mean wound inflammatory cell density showed no significant change throughout the study. Wounds treated with SM + STSG showed a consistently (but decreasingly) significantly higher inflammatory cell density than normal skin from day 7 until day 21. Wounds treated with MD + STSG showed a similar trajectory to wounds treated with SM + STSG (there were no significant differences in inflammatory cell density between these two wound groups throughout the study), showing significantly higher inflammatory cell densities between days 7 and 35. Wounds treated with I + STSG showed significantly higher levels of inflammatory cell density than all other groups until day 21, reaching levels similar to normal skin by day 35. From day 35 onwards, all wound groups showed no significant differences to normal skin.

5.6.12 Vascular perfusion

Please see table 5.6.12 and figures 5.6.12.1-2

Normal skin

The vascular perfusion of normal skin showed no statistically significant changes over time.

Wounds treated with Smart Matrix™ + split thickness skin graft

At day 7 the mean vascular perfusion was 426.39PU (±4.08), 485.09PU (±19.63) at day 14, 755.14PU (±37.63) at day 21, 892.65PU (±5.01) at day 28, 920.52PU (±4.21) at day 35, 980.18PU (±5.07) at day 42, 239.61PU (±6.10) at day 84 and 162.24PU (±3.37) at day 180. The mean vascular perfusion of wounds treated with SM + STSG showed statistically significant increases between consecutive time points up to day 42, except between days 28 and 35. There was a mean difference of 58.69PU ($p=0.0041$) between 7 and 14, 270.1PU ($p<0.0001$) between days 14 and 21, and between 137.5PU ($p<0.0001$) between days 21 and 28. There was a significant decrease between days 42 and 84 (mean difference of 740.6PU, $p<0.0001$) and between days 84 and 180 (mean difference of 77.38PU, $p=0.0158$).

When compared to normal skin, wounds treated with SM + STSG showed statistically significantly ($p<0.0001$) higher mean vascular perfusion measurements between days 7 and 42. The differences were 267.82PU at day 7, 327.41PU at day 14, 591.22PU at day 21, 737.00PU at day 28, 753.54PU at day 35 and 817.82PU at day 42.

Wounds treated with Matriderm™ + split thickness skin graft

There was a statistically significant ($p<0.0001$) increase between consecutive time points up to day 28. There was a mean difference of 116.6PU between days 7 and 14, 276.6PU between days 14 and 21, and 104.4PU between days 21 and 28. There was a significant decrease between days 42 and

84 (mean difference of 727.92PU, $p<0.0001$) and between days 84 and 180 (mean difference of 78.14PU, $p=0.0135$). There were no significant differences at days 84 and 180.

When compared to normal skin, wounds treated with MD + STSG showed statistically significantly ($p<0.0001$) higher mean vascular perfusion measurements between days 7 and 42. The differences were 254.13PU at day 7, 371.62PU at day 14, 642.21PU at day 21, 754.65PU at day 28, 772.91PU at day 35 and 804.90PU at day 42. There were no significant differences at days 84 and 180.

When compared to wounds treated with SM + STSG, a statistically significant difference only occurred at day 21, where wounds treated with MD + STSG showed a higher vascular perfusion than those treated with SM + STSG (mean difference of 50.79PU, $p<0.0001$).

Wounds treated with Integra™ + split thickness skin graft

There was a statistically significant increase between consecutive time points between days 2 and 35. There was a mean difference of 57.16PU ($p=0.01$) between days 7 and 14, 233.03PU ($p<0.0001$) between days 14 and 21, 348.12PU ($p<0.0001$) between days 21 and 28, and 66.99PU ($p=0.003$) between days 28 and 35. There were significant ($p<0.0001$) decreases between consecutive time points between days 35 and 180. There was a mean difference of 192.6PU and between days 35 and 42, 186.91PU between days 42 and 84 and 238.95PU between days 84 and 180.

When compared to normal skin, wounds treated with I + STSG showed no statistically significant differences at days 7 and 14. Statistically significant ($p<0.0001$) higher mean vascular perfusion measurements occurred between days 21 and 84. The mean differences were 222.63PU at day 21, 579.31PU at day 28, 634.12PU at day 35, 446.71PU at day 42, and 255.92PU at day 84. There was no statistically significant difference at day 180.

When compared to wounds treated with SM + STSG, wounds treated with I + STSG showed statistically significantly ($p<0.0001$) lower levels of vascular perfusion between days 7 and 84. The

mean differences were 329.92PU at day 7, 331.46PU at day 14, 368.54PU at day 21, 158.02PU at day 28, 118.92PU at day 35,371.11 PU at day 42 and 182.5PU at day 84. There was no statistically significant difference at day 180.

When compared to wounds treated with MD + STSG, wounds treated with I + STSG showed statistically significantly ($p<0.0001$) lower levels of vascular perfusion between days 7 and 42. The mean differences were 316.22PU at day 7, 375.71PU at day 14, 419.34PU at day 21, 175.62PU at day 28, 138.93PU at day 35, and 358.13PU at day 42. At day 84, wounds treated with I + STSG showed statistically significantly ($p<0.0001$) higher vascular perfusion levels than those treated with MD + STSG (mean difference of 177.8PU). There was no statistically significant difference at day 180.

	Day 7	Day 14	Day 21	Day 28	Day 35	Day 42	Day 84	Day 180
SM+STSG	426.39 (±4.08)	485.09 (±19.6)	755.14 (±37.6)	892.65 (±5.01)	920.52 (±4.21)	980.18 (±5.07)	239.61 (±6.10)	162.24 (±3.37)
I+STSG	96.48 (±3.38)	153.64 (±3.83)	386.63 (±4.86)	734.66 (±5.74)	801.64 (±4.90)	609.07 (±4.78)	422.13 (±7.87)	183.25 (±5.31)
MD+STSG	412.68 (±2.82)	529.32 (±4.49)	805.94 (±5.51)	910.29 (±7.72)	940.51 (±3.82)	967.21(±4.24)	244.30 (±16.9)	166.24 (±4.30)
normal skin	158.55 (±2.88)	157.73 (±7.38)	163.98 (±6.09)	155.70 (±4.08)	167.56 (±3.14)	162.34 (±3.50)	166.23 (±5.39)	166.55 (±5.00)

Table 5.6.12: Mean wound vascular perfusion (PU), where n=48 (16 per wound group) for the 42 day study and n=24 (8 per wound group) for the 180 day study

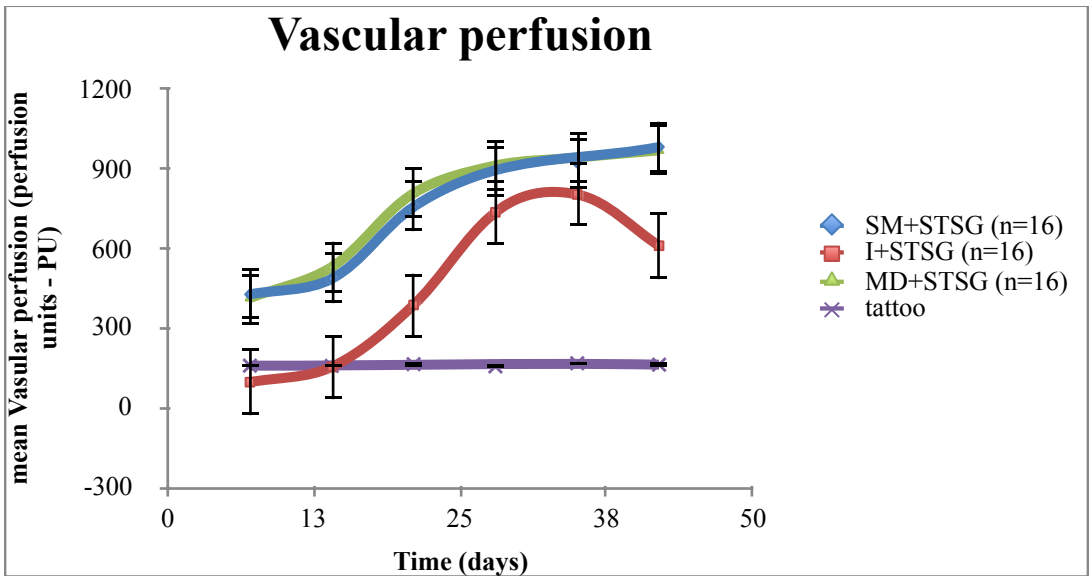

Figure 5.6.12.1: Mean vascular perfusion versus time (n=48, 16 per wound group) for different reconstructive options in a 42 day study.

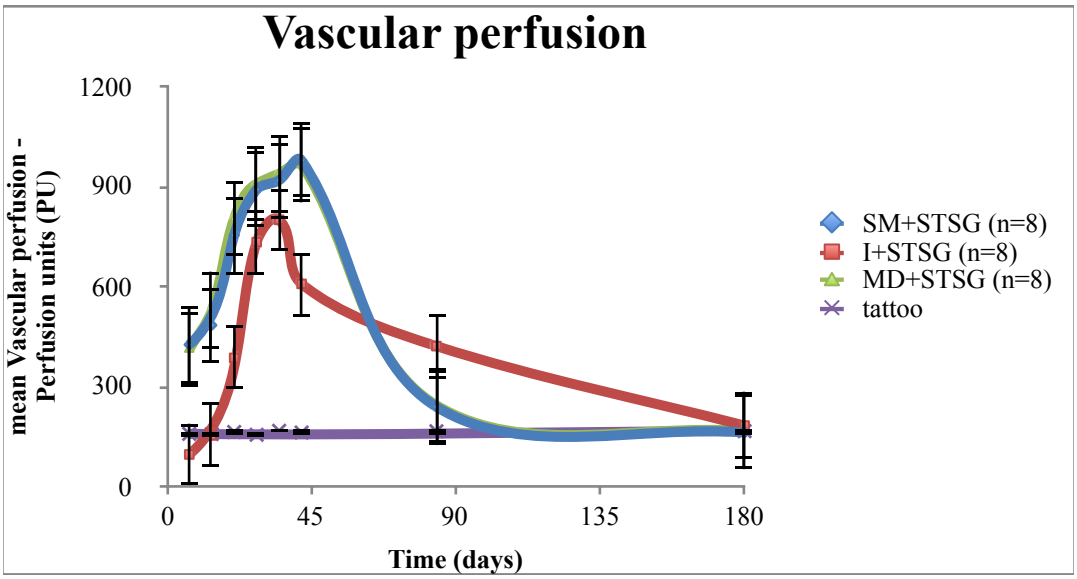

Figure 5.6.12.2: Mean vascular perfusion versus time (n=24, 8 per wound group) for different reconstructive options in a 180 day study.

Interpretations for mean wound vascular perfusion

In normal skin, the mean wound vascular perfusion showed no significant change throughout the study. Wounds treated with SM + STSG and those treated with MD + STSG showed an increase in mean perfusion up to day 35 followed by a decrease over the rest of the study, to reach perfusion

levels similar to that of normal skin after day 42. There were no significant differences between these two wound groups. Wounds treated with I+STSG showed a 14 day delay in reaching peak vascular perfusion levels, which then decreased to levels similar to those of normal skin by day 180. Mean vascular perfusion in this wound groups was significantly lower than the other two wounds groups until day 180. There were no significant differences in all four groups at day 180.

5.6.13 Capillary lumen count

Please see table 5.6.13 and figures 5.6.13.1-2

Normal skin

The mean capillary lumen count of normal skin showed no statistically significant changes over time.

Wounds treated with Smart Matrix™ + split thickness skin graft

The mean capillary lumen count of wounds treated with SM + STSG showed statistically significant increases ($P<0.0001$) between consecutive time points between days 7 and 28. There was a mean difference of 2.73 between days 7 and 14, 1.90 between days 14 and 21 and 2.17 between days 21 and 28. There was a further in significant increase between days 84 and 180 of 1.79.

When compared to normal skin, wounds treated with SM + STSG showed statistically significantly ($p<0.0001$) lower mean capillary lumen counts at days 7 (7.02), 14 (4.60), 21 (2.23) and 180 2.80 ($p=0.0004$).

Wounds treated with Matriderm™ + split thickness skin graft

Statistically significant ($p<0.0001$) increases in mean capillary lumen count occurred between days 14 and 21 (mean difference of 2.00), days 21 and 28 (3.83) and days 35 and 42 (3.20). However, there was a statistically significant increase ($p<0.0001$) throughout the study (8.15).

When compared to normal skin wounds treated with MD + STSG showed statistically significantly ($p<0.0001$) lower mean capillary lumen counts between days 7 and 35. The mean difference was 8.81 at day 7, 9.13 and day 14, 6.63 and day 21, 3.54 at day 28 and 3.46 at day 35. Thereafter, there were no significant differences between the two groups.

When compared to wounds treated with SM + STSG, wounds treated with MD + STSG showed statistically significantly ($p<0.0001$) lower mean capillary lumen counts between days 7 and 35. The mean difference was 1.79 at day 7, 4.5 and day 14, 4.40 and day 21, 2.73 at day 28 and 2.71 at day 35. Thereafter, there were no significant differences between the two groups.

Wounds treated with Integra™ + split thickness skin graft

The changes between consecutive time post-operative time points were statistically significant between days 14 and 42 ($p=0.0009$ between days 14 and 21, $p<0.0001$ for all other measurements).

When comparing wounds treated with I + STSG to normal skin, the mean capillary lumen count was significantly ($p<0.0001$) lower between days 7 and 42. The mean difference was 12 at day 7, 12.04 at day 14, 9.98 at day 21, 7.38 at day 28, 5.33 at day 35 and 2.94 at day 42. Throughout the rest of the study, there were no significant differences.

When comparing wounds treated with I + STSG to those treated with SM + STSG, the mean capillary lumen count was significantly ($p<0.0001$, for all except at day 42, where $p=0.00037$) lower between days 7 and 42. The mean difference was 4.94 at day 7, 7.42 at day 14, 7.75 at day 21, 6.56 at

day 28, 4.58 at day 35 and 1.46 at day 42. At day 180, the mean capillary lumen count was significantly higher ($p<0.0001$) in wounds treated with I + STSG (mean difference of 5.06).

When comparing wounds treated with I + STSG to those treated with MD + STSG, the mean capillary lumen count was significantly ($p<0.0001$) lower between days 7 and 84. The mean difference was 3.15 at day 7, 2.92 at day 14, 3.35 at day 21, 3.83 at day 28, 1.89 at day 35, 1.85 at day 42 and 1.92 at day 84. At day 180 there was no significant difference.

	Day 7	Day 14	Day 21	Day 28	Day 35	Day 42	Day 84	Day 180
SM+STSG	4.94 (±0.14)	7.67 (±0.09)	9.56 (±0.16)	11.73 (±0.09)	12.58 (±0.08)	11.48 (±0.07)	12.33 (±0.12)	10.54 (±0.13)
I+STSG	0 (±0)	0.25 (±0.09)	1.81 (±0.15)	5.17 (±0.15)	8.00 (±0.21)	10.82 (±0.20)	11.16 (±0.38)	15.67 (±4.16)
MD+STSG	3.15 (±0.12)	3.17 (±0.16)	5.17 (±0.15)	9.00 (±0.16)	9.88 (±0.20)	11.88 (±0.22)	13.08 (±0.25)	11.67 (±0.42)
normal skin	11.96 (±0.30)	12.29 (±0.33)	11.79 (±0.35)	12.54 (±0.65)	13.33 (±0.46)	12.98 (±0.52)	12.83 (±0.41)	13.33 (±0.36)

Table 5.6.13: Mean capillary lumen count, where n=48 (16 per wound group) for the 42 day study and n=24 (8 per wound group) for the 180 day study

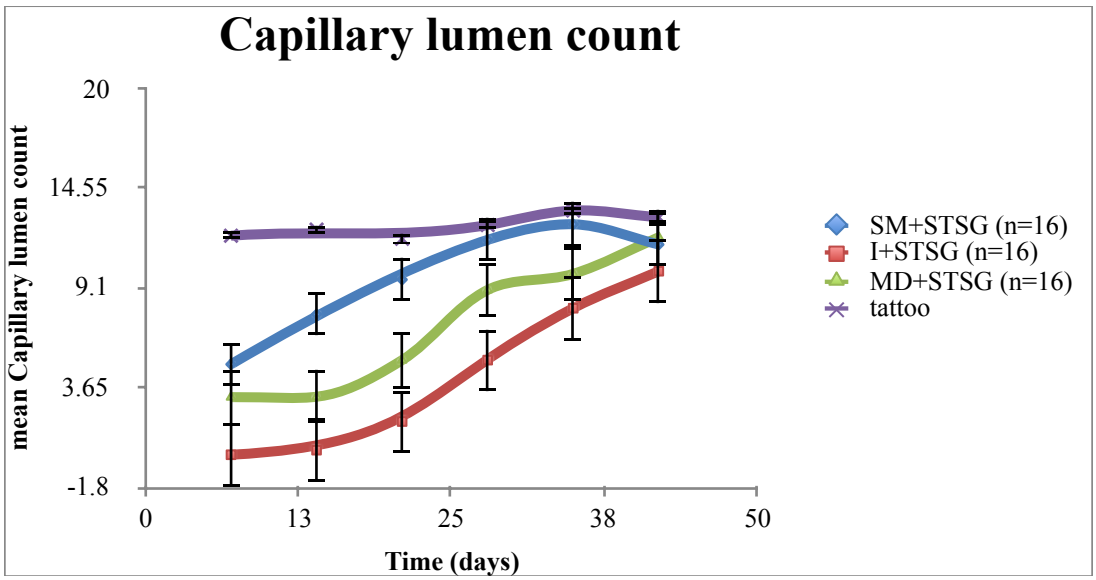

Figure 5.6.13.1: Mean capillary lumen count versus time (n=48, 16 per wound group) for different reconstructive options in a 42 day study.

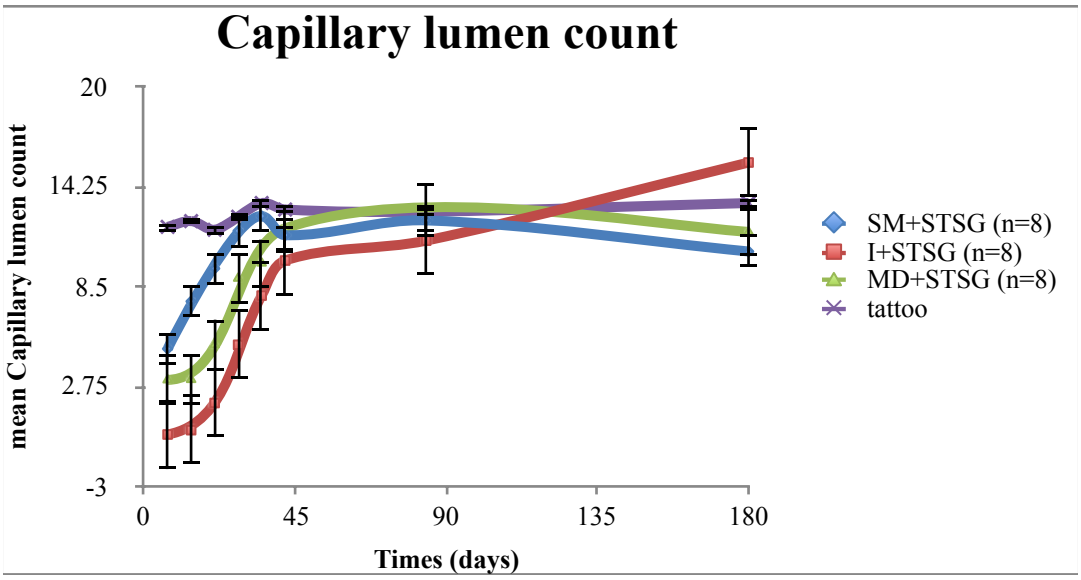

Figure 5.6.13.2: Mean capillary lumen count versus time (n=24, 8 per wound group) for different reconstructive options in a 180 day study.

Interpretations for mean capillary lumen count

In normal skin, the mean capillary lumen count showed no significant change throughout the study. Wounds treated with SM + STSG showed lower mean capillary lumen counts than normal skin at days 7, 14 21 and 180. Those treated with MD + STSG showed lower capillary lumen counts than

normal skin and than wounds treated with SM + STSG between days 7 and 35. Wounds treated with I + STSG showed lower capillary lumen counts than normal skin and wounds treated with SM + STSG up to day 42, and up to day 84 in wounds treated with MD + STSG. There were no significant differences between all wounds groups at day 180, except for wounds treated with SM + STSG which showed significantly lower mean capillary lumen counts than normal skin and wounds treated with I + STSG.

5.6.14 Von Willebrand factor

Please see table 5.6.14 and figures 5.6.14.1-2

Normal skin

vWF content of normal skin showed no statistically significant changes over time.

Wounds treated with Smart Matrix™ + split thickness skin graft

Mean vWF content of wounds treated with SM + STSG showed no statistically significant changes over time. When compared to normal skin, wounds treated with SM + STSG showed no statistically significant changes in vWF staining density.

Wounds treated with Matriderm™ + split thickness skin graft

There were no statistically significant changes in vWF staining between consecutive time points. However, there was a statistically significant increase ($p<0.0001$) in vWF staining throughout the study when comparing day 7 to days 21 (1.66), 28 (1.40), 35 (1.89), 42 (4.94), 84 (1.41) and 180 (1.40).

When compared to normal skin wounds treated with MD + STSG showed statistically significantly

lower levels (mean difference of 1.52, p=0.012) at day 7. The differences throughout the rest of the study were not statistically significant.

When comparing wounds treated with MD + STSG to those treated with SM + STSG, there were no statistically significant differences in mean vWF staining density throughout the study.

Wounds treated with Integra™ + split thickness skin graft

The changes in vWF staining between consecutive time post-operative time points were not statistically significant. However, there was a statistically significant ($p<0.0001$) increase in mean vWF staining density throughout the study when comparing day 7 to days 28 (1.22), 35 (1.80) 42 (3.02), 84 (2.42) and 180 (2.90).

When comparing wounds treated with I + STSG to normal skin, the mean vWF staining density was significantly ($p<0.0001$) lower at days 7 (2.96), 14 (2.37), 21 (1.90), and day 28 (1.66, $p=0.0025$). Throughout the rest of the study, there were no significant differences.

When comparing wounds treated with I + STSG to those treated with SM + STSG, the mean vWF staining density was significantly ($p<0.0001$) lower at days 7 (2.18), 14 (2.5), 21 (2.02), 28 (1.74) and day 35 (1.49, $p=0.0003$). Throughout the rest of the study, there were no significant differences.

When comparing wounds treated with I + STSG to those treated with MD + STSG, the mean vWF staining density was significantly lower at days 7 (1.44, $p=0.0007$), 14 (1.66, $p<0.0001$), 21 (2.29, $p<0.0001$), 28 (1.89, $p<0.0001$) and day 35 (1.53, $p<0.0001$). Throughout the rest of the study, there were no significant differences.

	Day 7	Day 14	Day 21	Day 28	Day 35	Day 42	Day 84	Day 180
SM+STSG	2.44 (±0.14)	3.20 (±0.12)	3.09 (±0.11)	3.21 (±0.11)	3.54 (±0.10)	3.77 (±0.07)	2.67 (±0.09)	2.65 (±0.13)
I+STSG	0.25 (±0.08)	0.69 (±0.08)	1.06 (±0.23)	1.47 (±0.07)	2.05 (±0.23)	2.77 (±0.42)	2.61 (±0.16)	3.15 (±0.15)
MD+STSG	1.69 (±0.09)	2.35 (±0.08)	3.35 (±0.04)	3.09 (±0.09)	3.58 (±0.04)	3.24 (±0.10)	3.10 (±0.06)	3.06 (±0.14)
normal skin	3.21 (±0.15)	3.06 (±0.15)	2.96 (±0.15)	3.13 (±0.15)	3.27 (±0.14)	2.92 (±0.14)	2.79 (±0.23)	3.04 (±0.27)

Table 5.6.14: Mean vWF staining density (score out of 5), where n=48 (16 per wound group) for the 42 day study and n=24 (8 per wound group) for the 180 day study

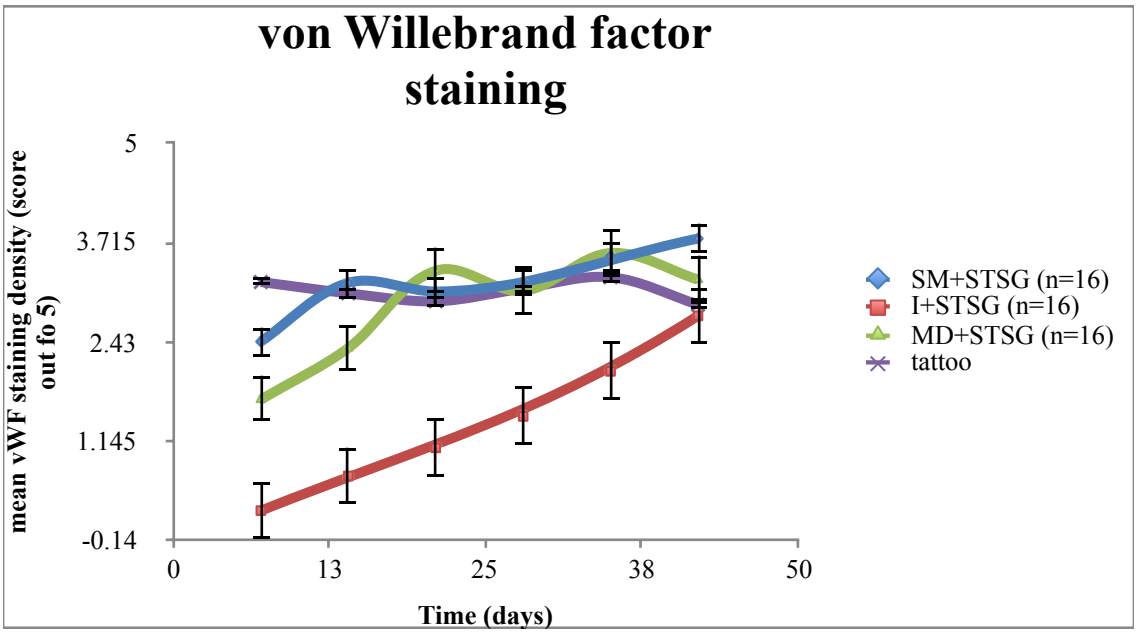

Figure 5.6.14.1: mean von Willebrand staining density versus time (n=48, 16 per wound group) for different reconstructive options in a 42 day study.

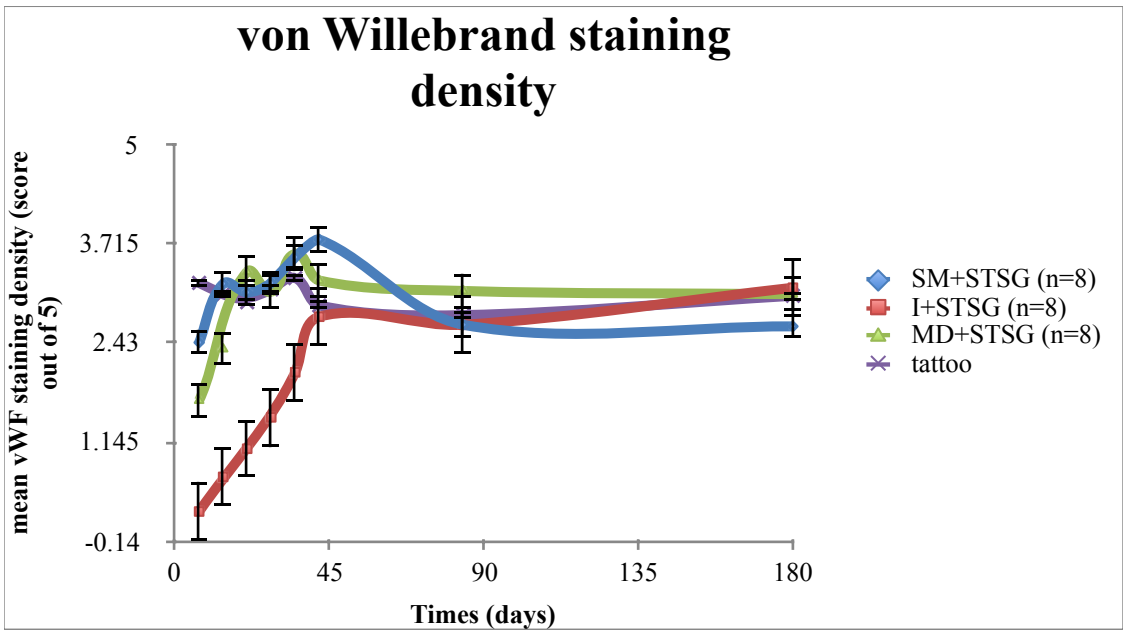

Figure 5.6.14.2: Mean von Willebrand staining density versus time (n=24, 8 per wound group) for different reconstructive options in a 180 day study.

Interpretations for mean von Willebrand factor staining density

In normal skin and in wounds treated with SM + STSG, the mean von Willebrand factor staining density showed no significant change throughout the study. There were no significant differences between these two wound groups throughout the study. Wounds treated with MD + STSG showed lower levels than normal skin at day 7. There were no significant differences between these two groups throughout the rest of the study. There were no significant differences between wounds treated with SM + STSG and those treated with MD + STSG throughout the study. Wounds treated with I + STSG showed lower mean vWF staining densities than normal skin up to day 42, and than the other wound groups up to day 35. Between days 42 and 180, there no significant differences in vWF staining between all four groups.

5.6.15 Summary of findings

Graft take rate was similar in all wound groups. Wounds treated by I + STSG were a darker pink than wounds treated by SM + STSG and MD + STSG. No adnexal structures were present in any

of the wounds.

Wounds treated by SM+STSG and those treated with MD + STSG contracted less than those treated by I +STSG. Wounds treated with SM + STSG and MD + STSG were smaller than the tattooed area. There were no significant differences in wound area and contraction between wounds treated with SM + STSG and those treated with MD + STSG. EDA-FN staining in wounds treated with SM + STSG was similar throughout the study to that of normal skin, while significantly higher in wounds treated with MD + STSG and I + STSG. There were no significant differences in α-SMA staining in normal skin and wounds treated with SM + STSG. Wounds treated with MD + STSG showed higher levels than these groups until day 28, while wounds treated with I + STSG showed the highest levels, which decreased to those of normal skin by day 42. There were no significant long term differences between all groups.

The dermal scaffold persisted from an average of 21 days in wounds treated with SM + STSG, 35 days in those treated with MD + STSG and 84 days in those treated with I + STSG.

Collagen levels increased from the beginning of the study in all wound groups. Wounds treated with MD + STSG and with I + STSG reached collagen staining levels of normal skin by day 28, while those treated with SM + STSG reached normal skin levels by day 35. There were no significant differences between all four groups thereon. Similarly, mean elastin staining density increased over the course of the study for all three wound groups, all reaching levels similar to normal skin by day 35. From day 42 onwards, there were no significant differences between all four groups.

Wounds treated with SM + STSG and those treated with MD + STSG showed peaks in wound thickness by day 21 and a decrease thereafter. Wounds treated with I+STSG showed a delay in peak wound thickness by day 42. AT day 180 all three wound groups showed a similar neodermal thickness to that of normal skin. Wounds treated with SM + STSG and those treated with MD + STSG showed very similar levels of wound cellular density, which were higher than both those of normal skin and wounds treated with I + STSG at the end of the study. Wounds treated with SM +

STSG and those treated with MD + STSG showed similar levels of inflammatory cell density, which approached that of normal skin by ay 28. Wounds treated with I + STSG showed higher levels of inflammation than the other two wound groups but approached that of normal skin by day 35. Wounds treated with SM+STSG showed a very similar trajectory in terms of vascular parameters (perfusion, capillary lumen count and vWF staining) to those treated with MD + STSG. Wounds treated with I + STSG showed a delay until day 42. There were no significant differences between the wound groups and when compared to normal skin at day 180.

5.7 Conclusions from this study

From this study, it can be concluded that acute full thickness porcine wounds treated with SM + STSG show a very similar healing trajectory to those treated with MD + STSG, in terms of wound contraction and vascularity. Vascularity and graft take are delayed in wounds treated with I + STSG. However, the long-term outcome in all parameters for all three wound groups are very similar.

5.8 Subsequent steps

Following this study, the efficacy of SM+STSG in the acute wound was confirmed to be clinically comparable to that of MD+STSG and I+STSG in the acute full thickness excision wound. However, such acute wounds exhibit healthy wound healing properties. The real value of dermal scaffolds and wound healing adjuncts would lie in their ability to expedite and improve the wound healing trajectory of challenging wounds. As revealed through the systematic review described in the introduction chapter, there is much difficulty in obtaining such a predictable and easily reproducible wound healing model to study this. The next section in this chapter describes the evaluation of possible attenuated wound healing porcine model: the partial excision thickness of a full thickness

burn.

Chapter 6: Experiment 3: The porcine attenuated wound healing model – the partial thickness excision of a full thickness burn

6.1 Introduction

Relevant pre-clinical models are imperative to the development of new therapeutic strategies. Synthetic dermal scaffolds have been commercially available for the last two decades. The development of such matrices is dependent upon the simulation of such wounds in the pre-clinical model, and this is where such research is often hampered. As discussed in the introduction chapter, while the biology surrounding chronic and ischaemic wounds in human skin has been elucidated, to date, an easily predictable and reproducible pre-clinical attenuated wound healing model in an animal is not yet available (Seaton *et al.,* 2015).

Currently the gold standard utilises full thickness excision wounds to evaluate experimental materials and advanced therapies (McIntyre *et al.,* 2016, Middlekoop *et al.,* 2004). Acute full thickness wounds without systemic or local compromise and if not of critical size (larger than $2cm^2$ in humans) tend to heal without complication or delay. The healing response in these models is acute and vigorous, and hence, does not fully reflect clinical experience. Challenging wounds demonstrate an inherent imbalance between synthesis and degradation of the extracellular matrix, which leads to an attenuated healing response. There is a real paucity of pre-clinical models simulating this challenging clinical scenario, as it is very difficult to reproduce such a wound model in the pig. Porcine skin is known to heal faster than human skin and with a lower tendency to scarring (Wang *et al.,* 2010).

This means that our ability to simulate or predict the outcome of advances wound healing and reconstruction treatments and biomaterials is very limited. The real value of dermal scaffolds should

lie in their ability to either activate regenerative type healing of chronic wounds or to expedite the healing trajectory in complex wounds, as this would offer significant clinical benefit.

An approach to establishing a more chronic pathology in the pig was devised by extending the acute porcine full thickness wound model using a burn wound.

Prior to this experiment, the method of creation of a full thickness (down to fascia) burn wound in porcine skin was verified and confirmed at the end of previous porcine studies immediately prior to termination of the anaesthetised animal, using the method described below.

6.2 Hypothesis

Partially excising - excision of the necrotic plug, leaving the zone of stasis in situ - a full thickness burn will create a relatively easily reproducible wound model that is representative of some challenging wounds in humans.

6.3 Aim

The aim of this study was to characterise and to exploit the burn injury response - in particular that of the zone of stasis - to create a predictable and reproducible attenuated wound healing model.

6.4 Methods and materials

Please refer to Chapter 3: Methods and materials for further detail.

A partial burn excision defect (see figures 6.4.1-4) was used 24 hours after the burn injury to simulate a challenging wound. An initial characterisation was performed and an evaluation of its behaviour was compared to the gold standard wound healing model, the acute wound: a full thickness excision model (used in the two previous studies in this thesis).

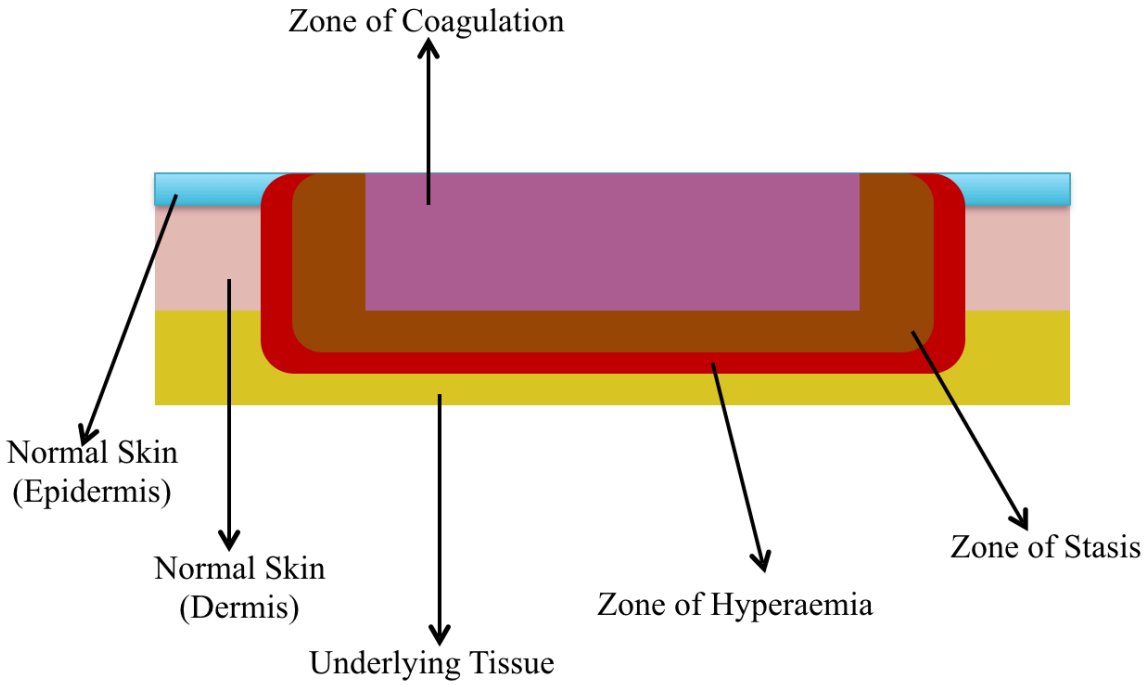

Figure 6.4.1: A schematic diagram showing Jackson's model of zones of a burn injury.

This was created a delayed full-thickness burn wound bed achieved through partial excision. This differs from the conventional surgical treatment for burn wounds, in which the wound is tangentially debrided or excised to healthy bleeding tissue. The delayed wound model excises only the zone of necrosis, leaving the zone of stasis intact, as a wound base. This zone of stasis manifests clinically as an "ischaemic penumbra". Its viability is precarious and often influenced by systemic and local wound factors.

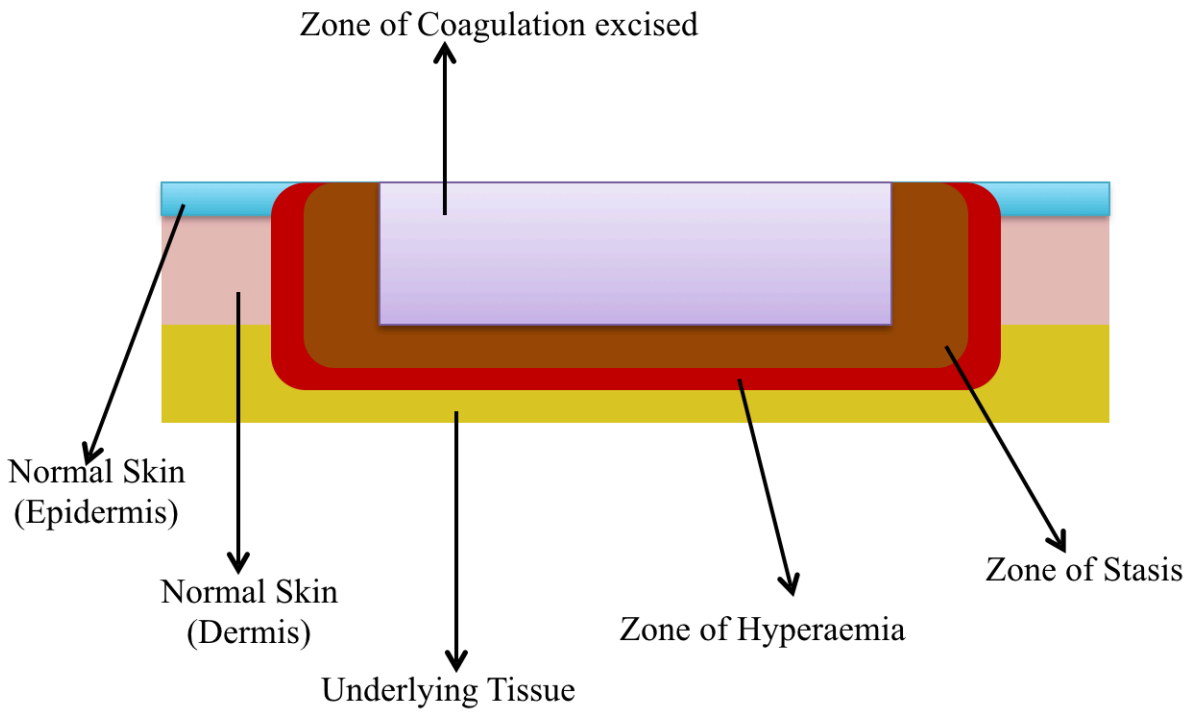

Figure 6.4.2: A schematic diagram showing the partial thickness excision of a full thickness burn model

Full thickness burn wounds, using a cylindrical solid stainless steel metal block with a diameter of 4cm x 3 cm thick, were created on day -1. This was heated in vegetable oil up to 150^{o}C for 120 seconds. 6 wounds were created on each of the pigs' flanks, either burn or control. On day 0 the central zone of necrosis was excised leaving the zone of stasis intact. Split thickness skin grafts were harvested on the same day and inset into the wounds. Animals were monitored for a period of 42 days at 7 day intervals.

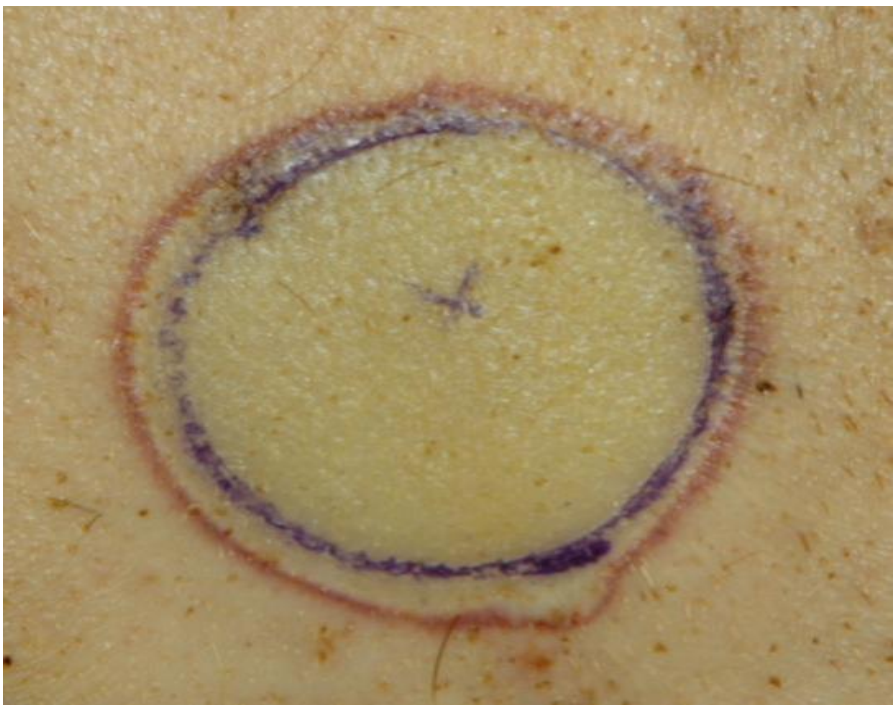

Figure 6.4.3: Day 0: The resulting burn wound one day after the application of the heated cylindrical solid stainless steel metal block

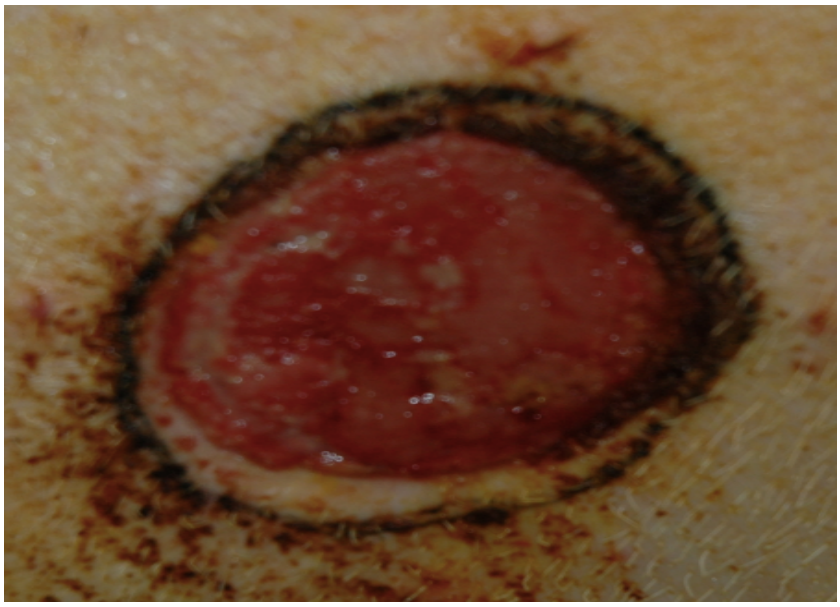

Figure 6.4.4: Day 0: The partial thickness excision of the full thickness burn wound

6.5 Study outline

For this study, a total of 2 animals were used (and therefore 12 wounds). All animals were monitored for a period of 42 days. The surgical procedures were carried out by the same surgeon (RZA) and senior project licence holder, JFD. Three wounds per animal were the partial thickness excision of the full thickness burn, while the other 3 wounds were acute full thickness excision wounds. T The anatomical locations of the different wound types were evenly distributed to reduce positional bias. he minimum number of pigs sufficient to yield statistically significant results was used for this study, as per Home Office regulations and project license restrictions.

<u>42 day Study:</u>

subjects = 2

wounds (n) = 12

Treatment method	**Number of wounds**
Full thickness excision of skin + STSG	6
Partial thickness excision of burn + STSG	6

Table 6.5: Wound treatment distribution in a 42 days study (n=12, 6 per wound group)

Figure 6.5: A schematic diagram showing wound distribution and layout in Pigs A and B

6.6 Results

6.6.1 Graft take

Non-burn wounds (acute full-thickness excision wounds)

All wounds showed graft take of more than 80% of the total wound surface area.

Burn wounds (attenuated wound model)

Of the 6 wounds, 3 showed graft take of more than 80% of the total wound surface area. 3 wounds showed graft take of less than 80% of the total wounds surface area. Of the latter group, one was complete graft loss.

6.6.2 Macroscopic description

Please refer to figures 6.6.2.1-2

Non-burn wounds (acute full-thickness excision wounds)

At day 7 all wounds showed a pink vascularised graft adherent to a bed of granulation tissue. At day 14, 5 of the wounds were still moist, while 3 were dry. The wounds were a dark pinkish–red colour. At day 21, 6 of wounds were dry. The remainder showed small patches of moist granulation tissue. The dark pinkish-red colour persisted. At day 35, all wounds in this groups were dry and epithelialised, but a slightly paler pink. At day 42, the colour was paler. No adnexae were present at any time point. No infection was observed in any of the wounds at any of the dressing changes or at termination.

Burn wounds (attenuated wound model)

At day 7 all wounds showed a dark red-pink wound bed. Pink vascularised graft was adherent to a bed of granulation tissue in the above-mentioned 4 of the wounds. At day 14, all the wounds were still moist. The wounds were dark pinkish–red in colour. At day 21, 6 of the wounds were moist. Those with successful graft take showed small patches of moist granulation tissue. This persisted until day 35. The dark pinkish-red colour persisted until day 42. At day 35, 5 of the wounds were dry and epithelialised, and a slightly paler pink. All wounds were swollen and the wound bed was proud of the surrounding skin between days 7 and 35. At day 42, the colour was paler and the wound bed was level with surrounding skin. Some small (less than 10% wound area) residual patches of moist granulation tissue were still present in those wounds with less than 80% graft take. No adnexal structures or signs of infection were observed in this wound group.

When the burn wounds were compared to the non-burn wounds, the burn wound groups showed a swollen wound bed which stood proud of the skin surface until day 35. Wounds in this group

showed a significantly lower graft survival rate with longer persisting areas of granulation tissue and delayed epithelialisation.

Interpretations of macroscopic wound observations and graft take

The partial-thickness excision wound model treated with split thickness skin graft showed delays in epithelialisation with a higher rate of graft failure and wound bed swelling.

Macroscopic appearances of the wounds in a 42 day study

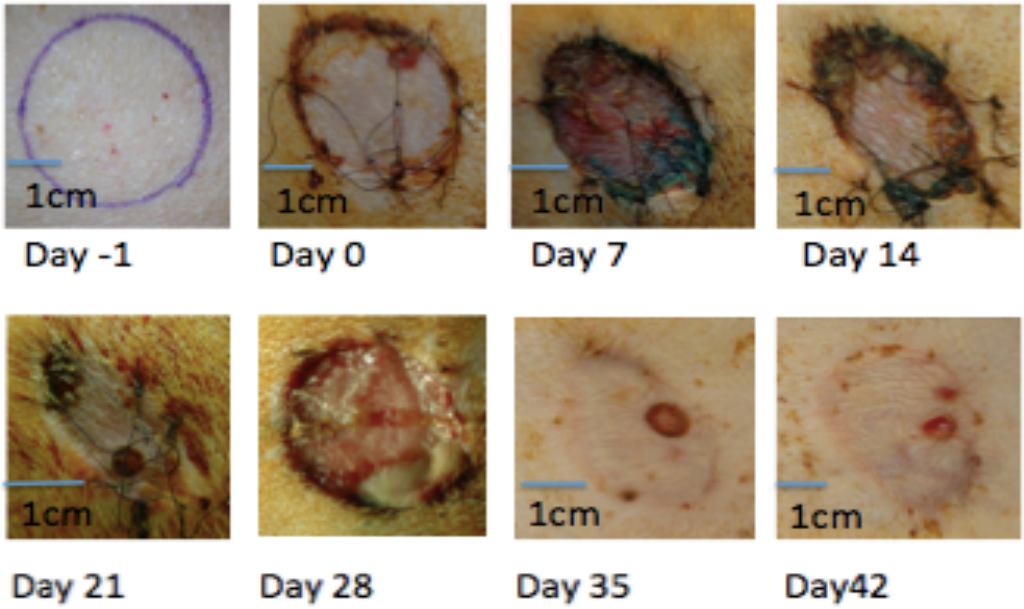

Figure 6.6.2.1:

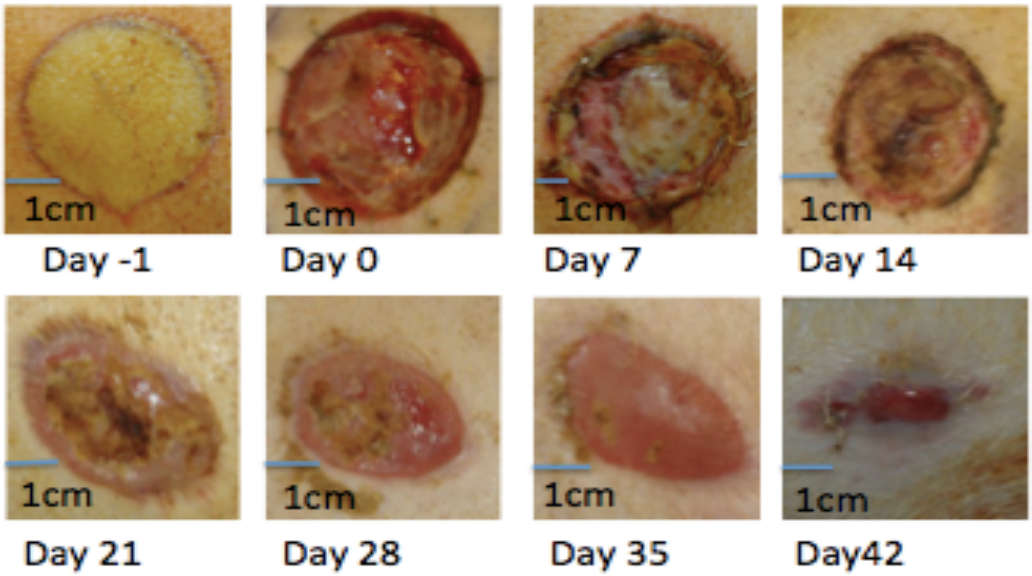

Figure 6.6..2.2: An example of the macroscopic appearances of the full thickness excision wounds (NB) treated with STSG

6.6.3 Wound area and contraction

Please refer to table 6.6.3 and figures 6.6.3.1-2.

Serial wound measurements were taken at each time point using the Eykona camera device. (See Methods and Materials chapter). The tattooed area was measured. This served as a control, to measure pig growth (if at all) and to take this into account when assessing wound contraction. Wound area measurements were calculated as a percentage of the wound area of the tattoo per time point in each pig. All wounds were of identical area measurement at day 0: 12.56 cm^2.

Tattooed area

The mean differences were 2.87cm^2 between days 0 and 7, 3.11cm^2 between days 14 and 21, 6.50cm^2 between days 14 and 21, 4.55cm^2 between days 21 and 28, 0.47cm^2 between days 28 and 35 and 1.27cm^2 between days 35 and 42. The mean tattoo area showed statistically a significant increase between days 14 and 21 ($p<0.0001$) and a significant decrease between days 21 and 28 ($p<0.0001$).

Non-burn wounds (acute full-thickness excision wounds)

The mean differences were 0.49cm^2 between days 0 and 7, 0.29cm^2 between days 7 and 14, 3.12cm^2 between days 14 and 21, 0.63cm^2 between days 21 and 28, 1.66cm^2 between days 28 and 35 and 0.52cm^2 between days 35 and 42 . There were no statistically significant changes in wound area between consecutive time points in this group. A significant decrease in wound area occurred over the course of the study. The mean difference between days 0 and 42 was 5.72cm^2 ($p<0.0001$) occurred between days 7 and 14 (mean difference of 0.61cm^2, $p<0.0001$).

When compared to the tattoo, the mean differences in wound area for the non-burn wounds were 0cm^2 at day 0 (100% of tattoo area), 2.38cm^2 (85% of tattoo area) at day 7, 5.77cm^2 (69% of tattoo area) at day 14, 15.39cm^2 (38% of tattoo area) at day 21, 11.47cm^2 (44% of tattoo area) at day 28, 13.60 cm^2 (35% of tattoo area) at day 35 and 15.39cm^2 (31% of tattoo area) at day 42. These differences were significant ($p<0.0001$) after day 14.

Burn wounds (attenuated wound model)

The mean wound area showed statistically significant increases in wound area between days 0 and 7 (mean difference of 3.54cm^2, $p=0.0153$), days 7 and 14 (mean difference of 4.61cm^2, $p=0.0003$) and days 14 and 21 (mean difference of 9.55cm^2, $p<0.0001$). Throughout the remainder of the study, there were no statistically significant differences in wound area between consecutive time points.

There mean differences were 1.88cm^2 between days 21 and 28, 0.09cm^2 between days 28 and 35 and 1.39cm^2 between days 35 and 42. A statistically significant decrease (mean difference of 4.98cm^2, p=0.0004) occurred between days 21 and 42.

When compared to the tattoo, the mean differences in wound area for the burn wounds were 0 at day 0 (100% of tattoo area), 0.67cm^2 (104% of tattoo area) at day 7, 22.17cm^2 (112% of tattoo area) at day 14, 13.88cm^2 (45% of tattoo area) at day 21, 11.21cm^2 (45% of tattoo area) at day 28, 11.58cm^2 (45% of tattoo area) at day 35 and 15.05cm^2 (32% of tattoo area) at day 42. These differences were significant (p<0.0001) after day 14.

When the burn wounds were compared to the non-burn wounds, the burn wounds showed a larger surface area between days 7 and 42. The mean differences were 0 and day 0, 3.05cm^2 at day 7, 7.95cm^2 at day 14, 1.41cm^2 at day 21, 0.26cm^2 and day 28, 2.01cm^2 at day 35 and 3.92cm^2 at day 42. These differences were statistically significant at days 7 and 14 (p<0.0001).

	Day 0	Day 7	Day 14	Day 21	Day 28	Day 35	Day 42
Burn + STSG	13 (±0)	16 (±0.04)	21 (±0.08)	11 (±0.06)	9 (±0.06)	9 (±0.07)	7 (±0.12)
Non-burn + STSG	13 (±0)	13 (±0.06)	13 (±0.21)	10 (±0.09)	9 (±0.04)	7 (±0.05)	7 (±0.06)
Normal skin	13 (±0)	16 (±0.08)	19 (±0.04)	25 (±0.08)	21 (±0.03)	21 (±0.08)	22 (±0.09)

Table 6.6.3: Mean wound area (cm^2) where n=12 (6 per wound group) for a 42 day study

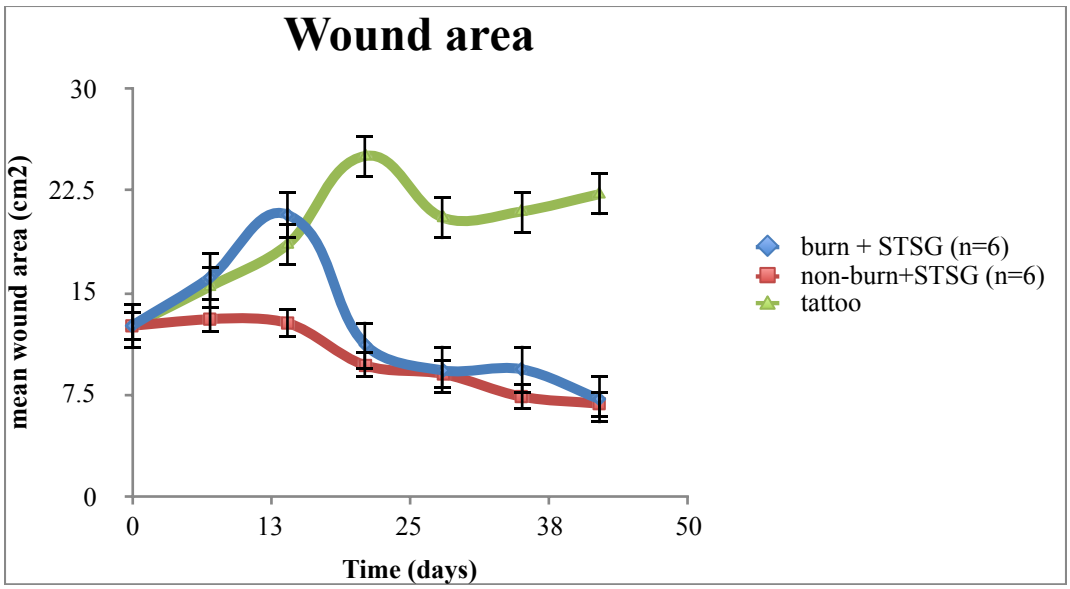

Figure 6.6.3.1: Mean wound area versus time (n=12, 6 per wound group) for the different wounds, in a 42 day study.

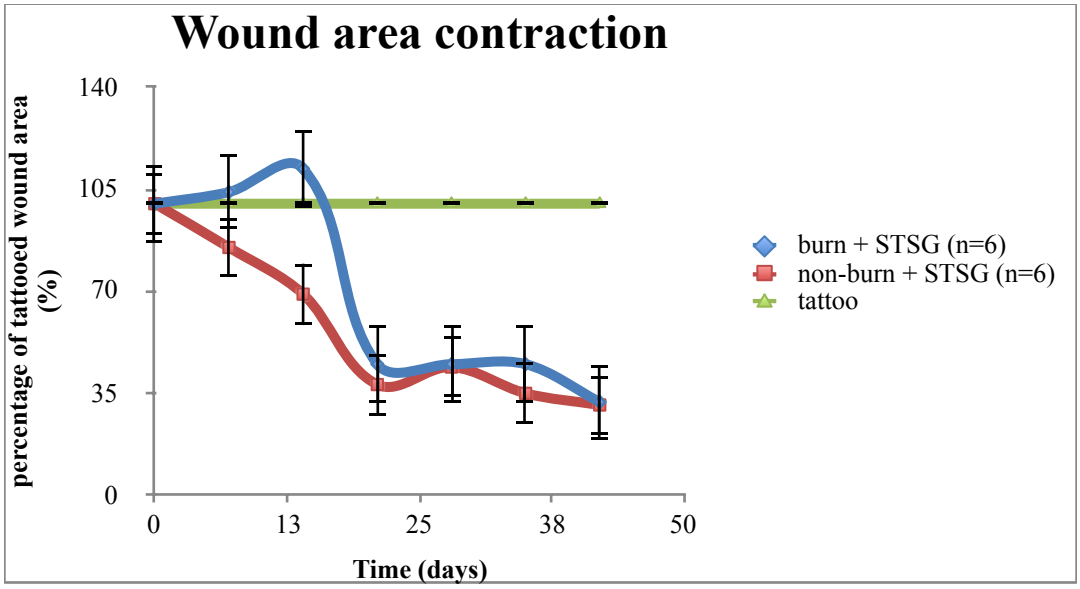

Figure 6.6.3.2: Mean wound area as a percentage of the tattooed area versus time (n=12) for different wounds, in a 42 day study.

Interpretations for mean wound area

Compared to the acute full thickness excision wounds (non-burn wounds), the partial excision burn wounds showed a two week delay in wound contraction, where the burn wound groups were signif-

icantly larger at days 7 and 14. The tattooed are was significantly larger than both wound groups after day 14.

6.6.4 EDA-Fibronectin

Please refer to table 6.6.4 and figure 6.6.4.

Non-burn wounds (acute full-thickness excision wounds)

The mean differences were 0.31 between days 7 and 14, 0.44 between days 14 and 21, 0.31 between days 21 and 28, 0.5 between days 28 and 35 and 0.06 between days 35 and 42. The mean EDA-FN staining density showed no statistically significant changes over time.

Burn wounds (attenuated wound model)

The mean differences were 0.61 between days 7 and 14, 0.53 between days 14 and 21, 0.86 between days 21 and 28, 0.39 between days 28 and 35 and 0.39 between days 35 and 42. The only statistically significant changes between consecutive time points occurred between days 21 and 28 ($p=0.0255$). A statistically significant change increase occurred gradually between days 7 and 28 (mean difference of 1.61, $p<0.0001$).

When the burn wounds were compared to the non-burn wounds, the mean differences were 1.03 at day 7, 0.72 at day 14, 0.64 at day 21, 0.14 and day 28, 1.03 at day 35 and 0.69 at day 42. Non-burn wound showed significantly higher levels of EDA-FN staining at days 7 and 35 ($p<0.0001$).

	Day 7	Day 14	Day 21	Day 28	Day 35	Day 42
Burn + STSG	1.83 (±0.16)	2.44 (±0.15)	2.97 (±0.15)	3.44 (±0.18)	3.83 (±0.15)	3.44 (±0.16)
Non-burn + STSG	2.86 (±0.19)	3.17 (±0.19)	3.61 (±0.16)	3.31 (±0.15)	2.81 (±0.19)	2.75 (±0.23)

Table 6.6.4: Mean EDA-fibronectin staining density (score out 5), where n=12 (6 per wound group) for a 42 day study

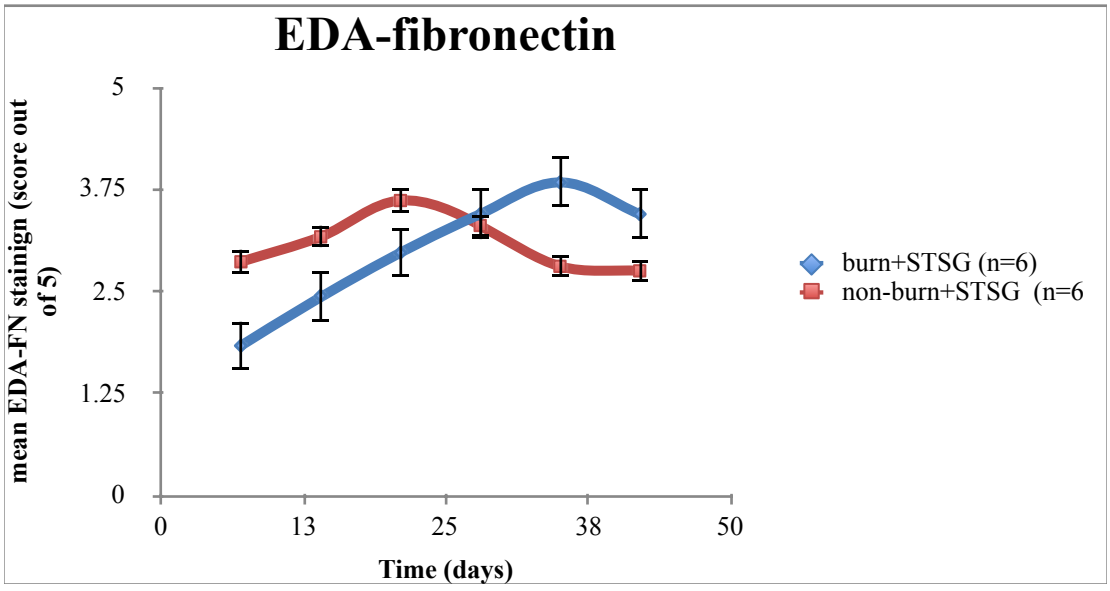

Figure 6.6.4: Mean EDA-Fibronectin staining density versus time (n=12, 6 per wound group) for different wounds in a 42 day study.

Interpretations for mean EDA-Fibronectin staining density

Differences in mean EDA-Fibronectin staining density were not significant between the two wound groups except at days 7 and 35 where EDA-Fibronectin staining density was higher in the acute full thickness excision wounds (non-burn wounds). There was no significant difference at the end of the study by day 42.

6.6.5 Alpha-smooth muscle actin

Please refer totable 6.6.5 and figure 6.6.5.

Non-burn wounds (acute full-thickness excision wounds)

The mean differences were 0.53 between days 7 and 14, 0.42 between days 14 and 21, 0.64 between days 21 and 28, 0.52 between days 28 and 35 and 0.03 between days 35 and 42. There were no statistically significant changes between consecutive or throughout the course of the study.

Burn wounds (attenuated wound model)

The mean differences were 0.22 between days 7 and 14, 0.33 between days 14 and 21, 0.58 between days 21 and 28, 0.03 between days 28 and 35 and 0.11 between days 35 and 42. There were no statistically significant changes between consecutive or throughout the course of the study.

When the burn wounds were compared to the non-burn wounds, the mean differences were 0.08 at day 7, 0.22 at day 14, 0.31 at day 21, 0.92 and day 28, 0.19 at day 35 and 0.33 at day 42. There were no statistically significant differences between the two groups.

	Day 7	Day 14	Day 21	Day 28	Day 35	Day 42
Burn + STSG	2.56 (±0.16)	2.81 (±0.18)	3.14 (±0.17)	3.72 (±0.17)	3.75 (±0.14)	3.86 (±0.16)
Non-burn + STSG	2.56 (±0.11)	3.03 (±0.17)	3.44 (±)0.10	4.08 (±0.08)	3.56 (±0.11)	3.53 (±0.10)

Table 6.6.5: Mean Alpha-Smooth Muscle Actin staining density (score out 5), where n=12 (6 per wound group) for a 42 day study

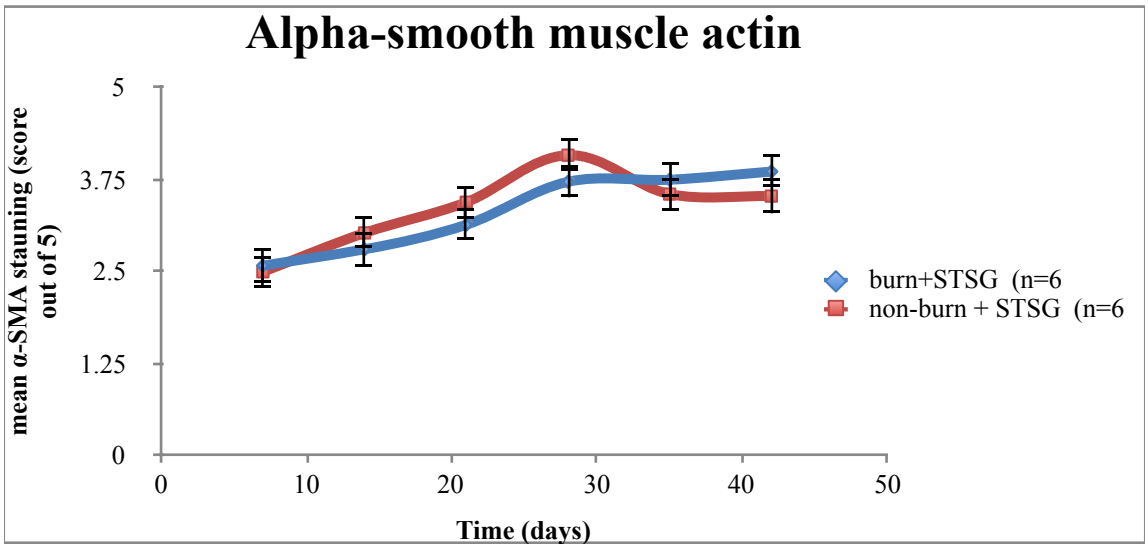

Figure 6.6.5: Mean Alpha–Smooth muscle actin staining density versus time (n=12, 6 per wound group) for the different wounds in a 42 day study.

Interpretations for mean Alpha-Smooth Muscle Actin staining density

Differences in mean Alpha-Smooth Muscle Actin staining were not significant between the two wound groups throughout the study.

6.6.6 Collagen

Please refer to table 6.6.6 and figure 6.6.6

Non-burn wounds (acute full-thickness excision wounds)

The mean differences were 0.28 between days 7 and 14, 0.47 between days 14 and 21, 1.44 between days 21 and 28, 0.08 between days 28 and 35 and 0.28 between days 35 and 42. A statistically significant increase occurred between days 21 and 28 ($p<0.0001$).

Burn wounds (attenuated wound model)

The mean differences were 0.28 between days 7 and 14, 0.31 between days 14 and 21, 0.42 between days 21 and 28, 0.83 between days 28 and 35 and 0.39 between days 35 and 42. A statistically significant increase occurred between days 28 and 35 ($p=0.0038$).

When the burn wounds were compared to the non-burn wounds, the mean differences were 0.36 at day 7, 0.36 at day 14, 0.53 at day 21, 1.56 and day 28, 0.81 at day 35 and 0.69 at day 42. Collagen staining in the non-burn wound group was significantly higher than in the burn group at days 28 ($p<0.0001$), 35 ($p=0.0064$) and 42 ($p=0.0391$).

	Day 7	Day 14	Day 21	Day 28	Day 35	Day 42
Burn + STSG	0.22 (±0.08)	0.50 (±0.13)	0.81 (±0.13)	1.22 (±0.15)	2.06 (±0.15)	2.44 (±0.13)
Non-burn + STSG	0.58 (±0.11)	0.86 (±0.15)	1.33 (±0.16)	2.78 (±0.18)	2.86 (±0.16)	3.14 (±0.17)

Table 6.6.6: Mean collagen staining density (score out 5), where n=12 (6 per wound group) for a 42 day study

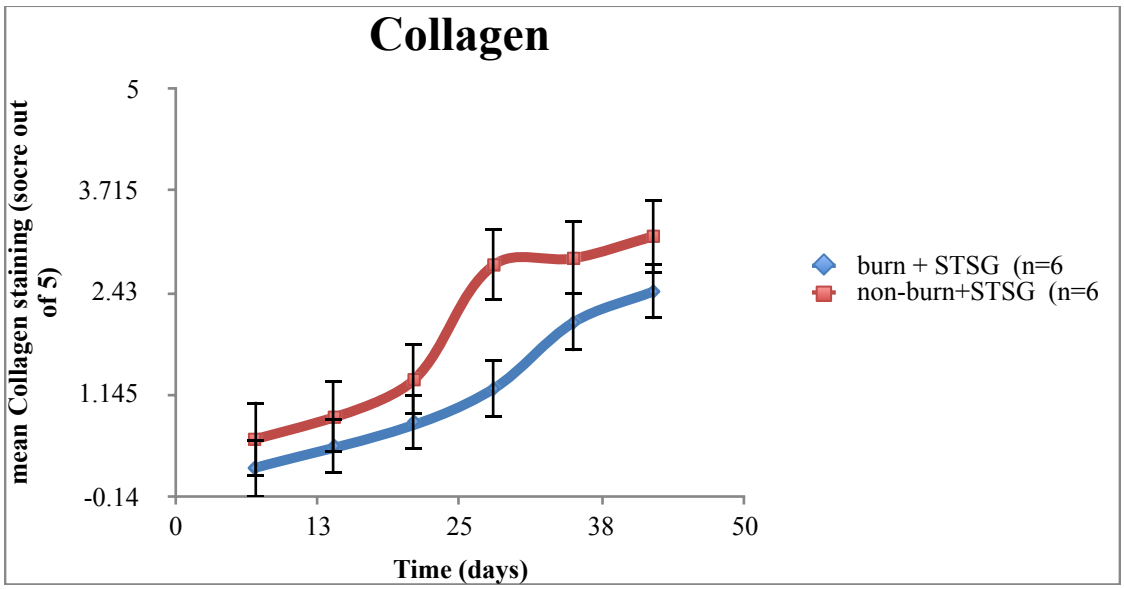

Figure 6.6.6: Mean collagen staining density versus time (n=12) for the different wounds in a 42 day study.

Interpretations for mean collagen staining density

Mean collagen staining density was significantly higher in the acute full thickness excision (non-burn) wounds at days 28, 35 and 42.

6.6.7 Elastin

Please refer to table 6.6.7 and figure 6.6.7

Non-burn wounds (acute full-thickness excision wounds)

The mean differences were 0.03 between days 7 and 14, 1 between days 14 and 21, 0.19 between days 21 and 28, 0.19 between days 28 and 35 and 0 between days 35 and 42. A statistically significant increase occurred between days 14 and 21 (p=0.0001).

Burn wounds (attenuated wound model)

The mean differences were 0.14 between days 7 and 14, 0.33 between days 14 and 21, 0.64 between days 21 and 28, 0.08 between days 28 and 35 and 0.39 between days 35 and 42. There were no statistically significant changes between consecutive time points or throughout the course of the study.

When the burn wounds were compared to the non-burn wounds, the mean differences were 0.39 at day 7, 0.28 at day 14, 0.94 at day 21, 0.5 and day 28, 0.61 at day 35 and 0.22 at day 42. At day 21, the non-burn group showed significantly higher staining levels for elastin than the burn wound group (p=0.0004).

	Day 7	Day 14	Day 21	Day 28	Day 35	Day 42
Burn + STSG	0.25 (±0.08)	0.39 (±0.10)	0.72 (±0.12)	1.36 (±0.14)	1.44 (±0.12)	1.83 (±0.12)
Non-burn + STSG	0.64 (±0.16)	0.67 (±0.16)	1.67 (±0.18)	1.86 (±0.17)	2.06 (±0.17)	2.06 (±0.17)

Table 6.6.7: Mean elastin staining density (score out 5), where n=12 (6 per wound group) for a 42 day study

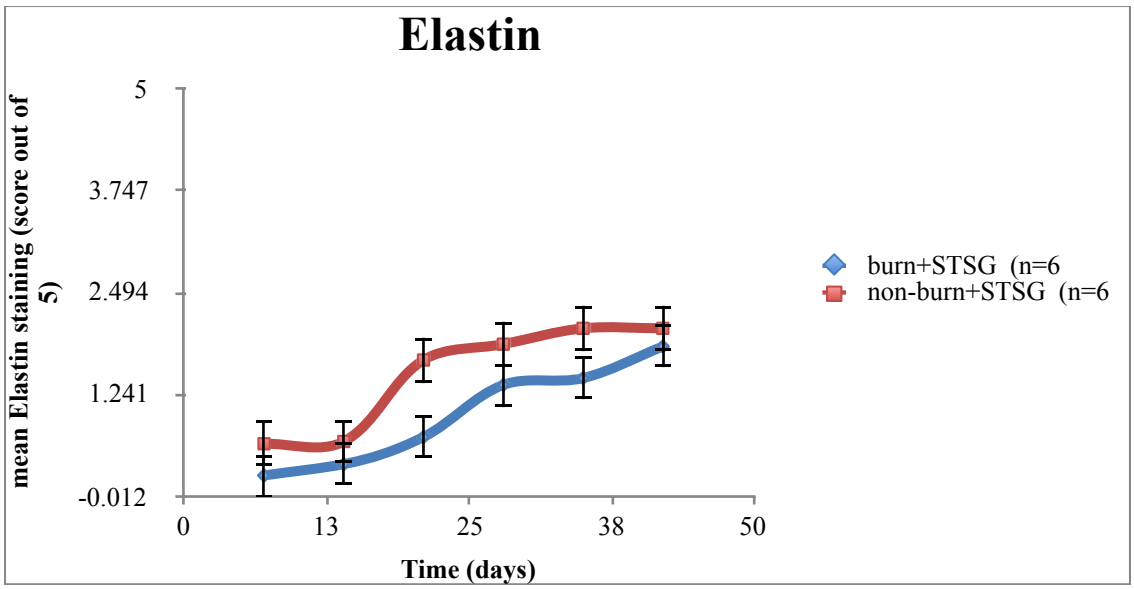

Figure 6.6.7: Mean elastin staining density versus time (n=12) for the different wounds in a 42 day study.

Interpretations for mean elastin staining density

Differences in elastin staining were not significant, except at day 21, when the acute full thickness excision (non-burn) wounds showed significantly higher elastin staining density.

6.6.8 Observations on H&E staining

Please refer to figures 6.6.8.1-8

Non-burn wounds (acute full-thickness excision wounds)

In the full thickness excision wound, deposition of granulation tissue is seen by day 7, with vascular response evident by day 14. This granulation tissue grows outwards from the wound bed without remaining confined to it. The acute wound mounts an early inflammatory response which is sustained until day 28, before it resolves.

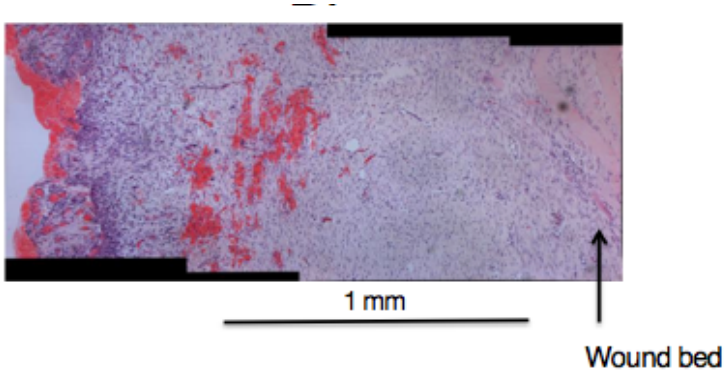

Figure 6.6.8.1: H&E staining (x10 magnification) of the Acute wound healing trajectory at day 7. A vigorous granulate response is seen, already substantial by day 7, growing out from the wound bed.

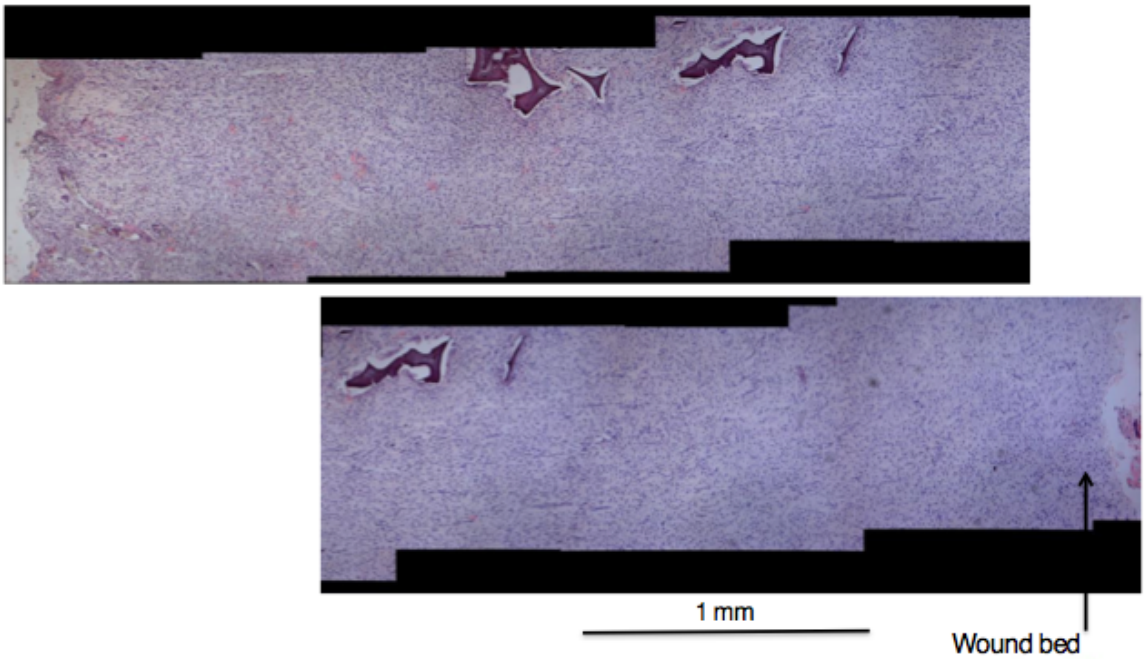

Figure 6.6.8.2: H&E staining (x10 magnification) of the Acute wound healing trajectory at day 14. A mixed neutrophil and fibrovascular infiltrate is seen.

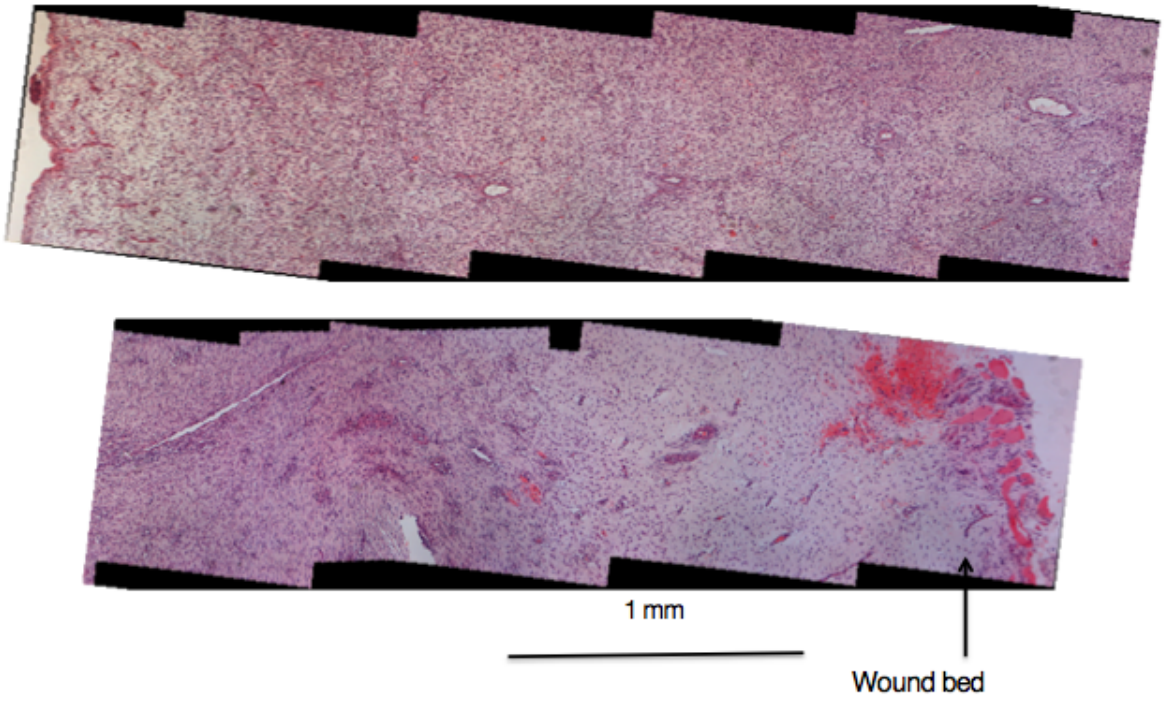

Figure 6.6.8.3: H&E staining (x10 magnification) of the Acute wound healing trajectory at day 28. An inflammatory infiltrate is seen until day 28

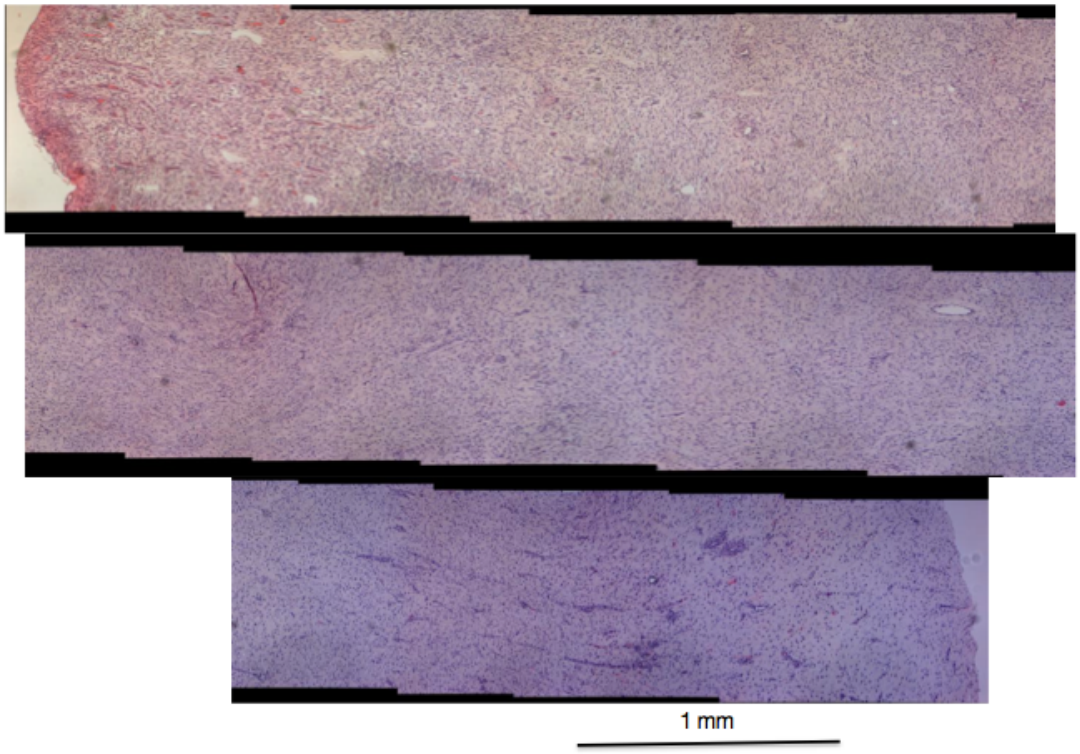

Figure 6.6.8.4: H&E staining (x10 magnification) of the acute wound healing trajectory at day 42.

Burn wounds (attenuated wound model)

The trajectory of the wound healing response of the partial excision burn wound differs somewhat from that of the control full thickness excision wound. Granulation tissue formation is delayed by 14 to 21 days,), and is limited to the wound bed with a higher and delayed inflammatory infiltrate with a disorganised structure. At day 7 the wound bed is a conglomerate of oedematous cells, beginning to show signs of granulation and infiltration at day 14. This becomes extensive by day 21. However, this granulation tissue still remains more or less confined to the wound bed. At day 28 the granulation appears to be more fibrovascular. Maturation continues up until day 42 with signs of inflammation still present

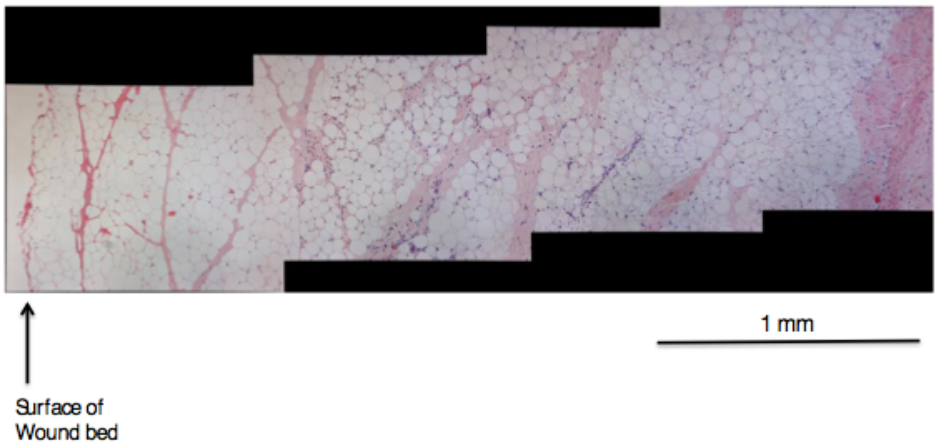

Figure 6.6.8.5: H&E staining (x10 magnification) of the partial excision burn wound model wound healing trajectory at day 7, showing a marked oedematous response.

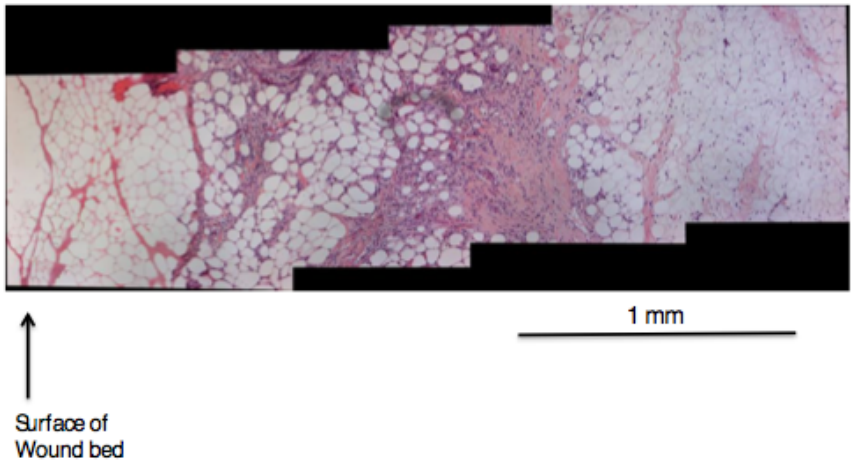

Figure 6.6.8.6: H&E staining (x10 magnification) of the partial excision burn wound model wound healing trajectory at day 14, showing persisting oedema at the wound bed with some coagulation of blood vessels.

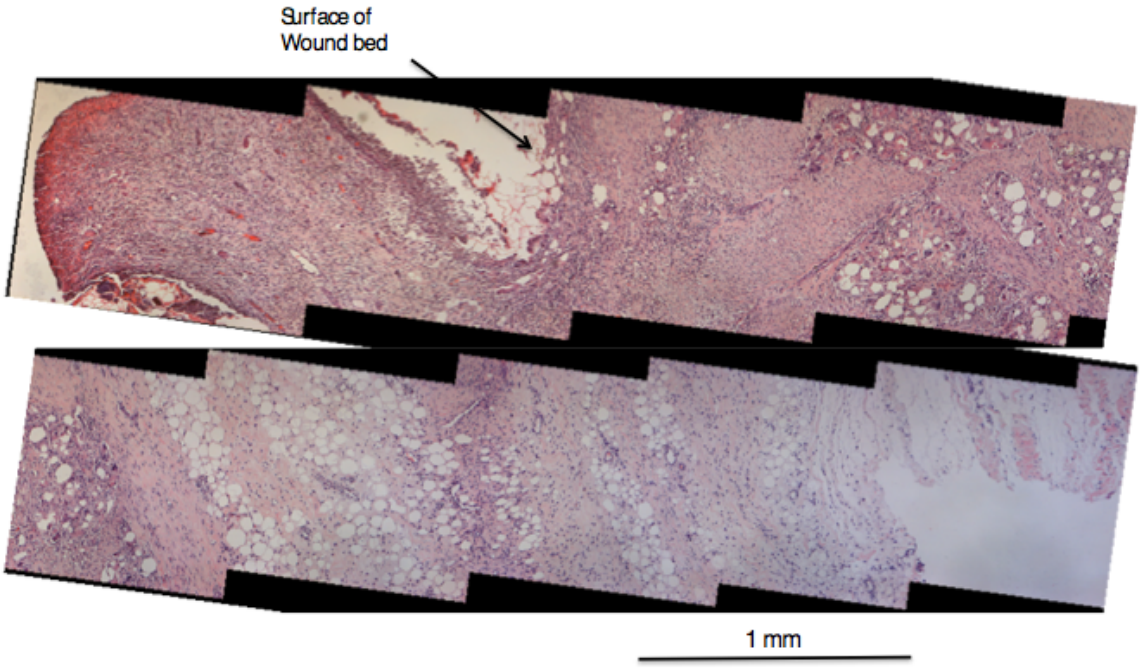

Figure 6.6.8.7: H&E staining (x10 magnification) of the partial excision burn wound model wound healing trajectory at day 28, showing a persisting delayed inflammation with resolution of oedema and granulation tissue formation.

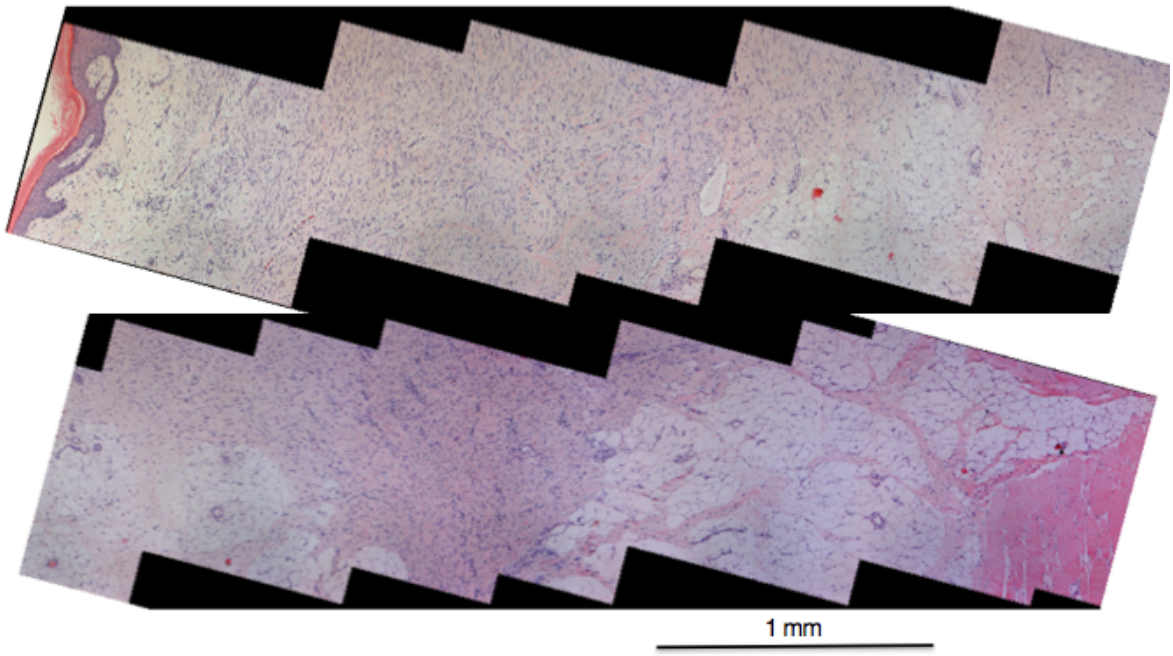

Figure 6.6.8.8: H&E staining (x10 magnification) of the partial excision burn wound model wound healing trajectory at day 42, showing full resolution of oedema and a persisting inflammatory infiltrate.

6.6.9 Wound (neodermal) thickness

Please refer to table 6.6.9 and figure 6.6.9

Non-burn wounds (acute full-thickness excision wounds)

The mean differences were 146.44µm between days 7 and 14, 229.39µm between days 14 and 21, 320.33µm between days 21 and 28, 428v between days 28 and 35 and 562.61µm between days 35 and 42. These increases were statistically significant ($p<0.0001$ for each).

Burn wounds (attenuated wound model)

The mean differences were 45.49µm between days 7 and 14, 183.31µm between days 14 and 21, 255.45µm between days 21 and 28, 96.39µm between days 28 and 35 and 49.72µm between days 35 and 42. These increases were statistically significant ($p<0.0001$ for each).

Throughout the study, the mean thickness of healing tissue from the wound bed was larger in the burn group than in the non-burn group. The mean differences were 199.62µm (±) at day 7, 571.51µm (±) at day 14, 663.89µm (±) at day 21, 811.65µm (±) and day 28, 773.7µm (±) at day 35 and 651.84µm (±) at day 42. These differences were statistically significant ($p<0.0001$ for each).

	Day 7	Day 14	Day 21	Day 28	Day 35	Day 42
Burn + STSG	346.08 (±3.83)	800.89 (±11.4)	984.17 (±4.37)	1239.56 (±7.24)	1355.94 (±3.69)	1286.22 (±13.44)
Non-burn + STSG	146.44 (±4.47)	229.39 (±4.08)	320.33 (±2.46)	428.00 (±22.79)	562.61 (±5.52)	634.44 (±3.82)

Table 6.6.9: Mean neodermal thickness (µm), where n=12 (6 per wound group) for a 42 day study

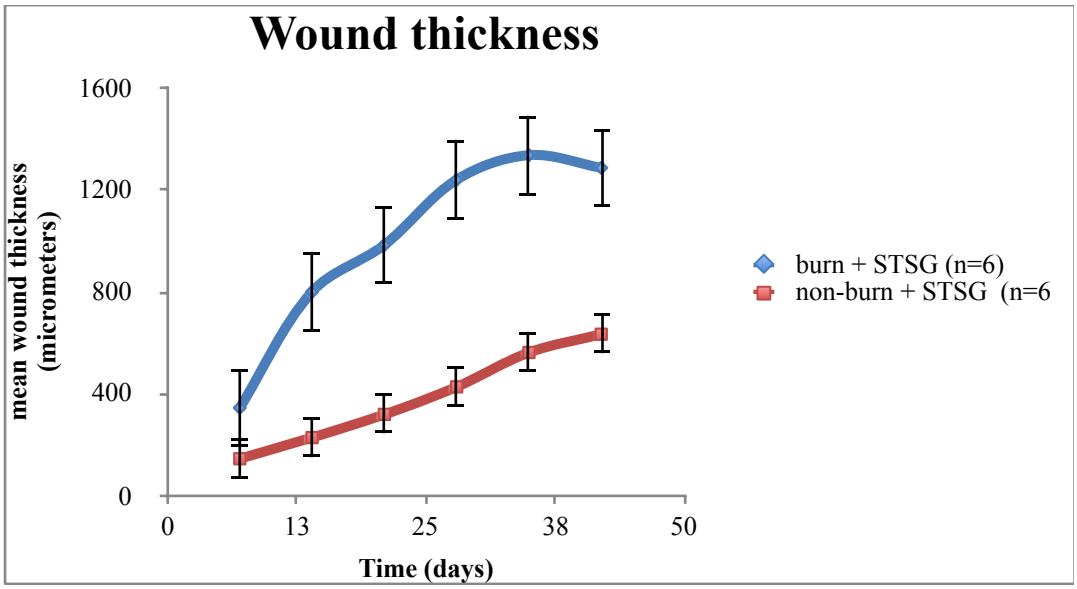

Figure 6.6.9: A graph showing mean wound thickness versus time (n=12, 6 per wound group) for the different wounds in a 42 day study.

Interpretations for mean wound (neodermal) thickness

Throughout the study, the mean thickness of healing tissue from the wound bed was significantly larger in the burn group than in the non-burn group

6.6.10 Cellular density

Please see table 6.6.10 and figure 6.6.10

Non-burn wounds (acute full-thickness excision wounds)

The mean differences were 0.75 between days 7 and 14, 0.39 between days 14 and 21, 0 between days 21 and 28, 0.89 between days 28 and 35 and 1.11 between days 35 and 42. A statistically significant increase in cellular density was seen between days 7 and 21 (mean difference of 1.14,

p<0.0001) and a significant decrease occurred between days 28 and 35 (p=0.0034) and between days 35 and 42 (p=0.0017).

When the burn wounds were compared to the non-burn wounds, the mean differences were 1.31 at day 7, 1.39 at day 14, 0.72 at day 21, 0.22 and day 28, 1.00 at day 35 and 1.61 at day 42. At days 7 (p<0.0001), 35 (p=0.0082) and 42 (p<0.0001) the non-burn wounds were significantly less cellular.

Burn wounds (attenuated wound model)

The mean differences were 0.67 between days 7 and 14, 1.6 between days 14 and 21, 0.50 between days 21 and 28, 0.33 between days 28 and 35 and 0.50 between days 35 and 42. The only significant increase in cellular density between consecutive time points occurred between days 14 and 21 (p=0.0038). The was an overall significant increase over the course of the study (mean difference of 2.05, p<0.0001).

	Day 7	Day 14	Day 21	Day 28	Day 35	Day 42
Burn + STSG	1.17 (±0.13)	1.83 (±0.17)	2.89 (±0.18)	3.39 (±0.25)	3.72 (±0.14)	3.22 (±0.17)
Non-burn + STSG	2.47 (±0.25)	3.22 (±0.17)	3.61 (±0.18)	3.61 (±0.25)	2.72 (±0.14)	1.61 (±0.17)

Table 6.6.10: Mean wound cellular density (score out 5), where n=12 (6 per wound group) for a 42 day study

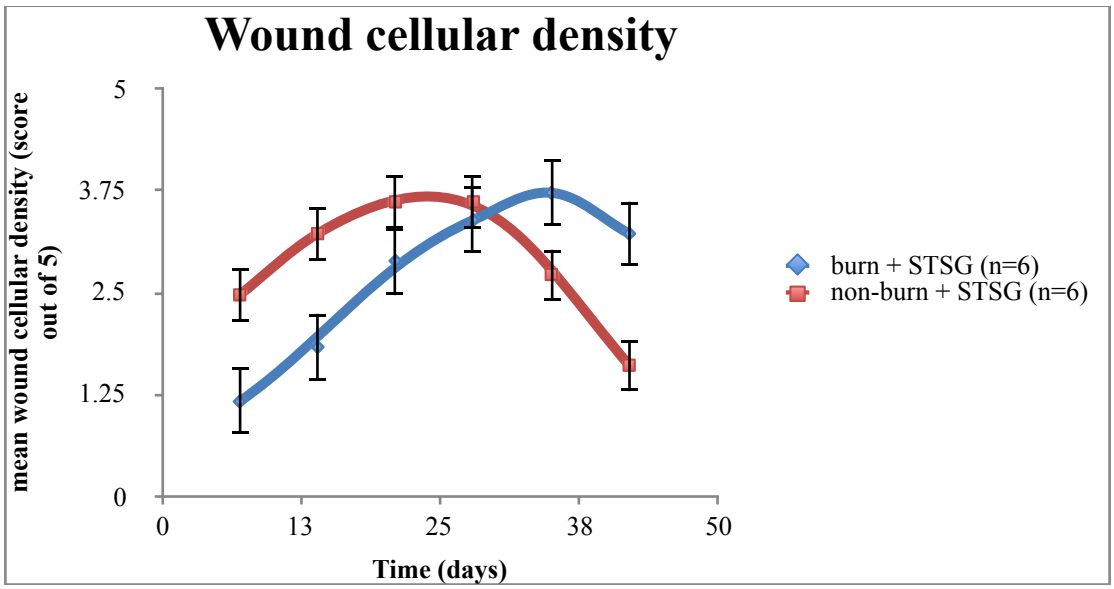

Figure 6.6.10: Mean cellular density versus time (n=12, 6 per wound group) for the different wounds in a 42 day study.

Interpretations for mean wound cellular density

The burn wounds showed a significantly higher cellular density than the non-burn wounds at days 7, 35 and 42.

6.6.11 Inflammation

Please see table 6.6.11 and figure 6.6.11

Non-burn wounds (acute full-thickness excision wounds)

The mean differences were 0.16 between days 7 and 14, 0.22 between days 14 and 21, 0.22 between days 21 and 28, 0.67 between days 28 and 35 and 0.72 between days 35 and 42. No significant changes occurred between consecutive time points, but a significant decrease in inflammatory cell density occurred over the course of the study. (a mean difference of 0.78 between days 7 and 42, p=0.0342).

Burn wounds (attenuated wound model)

The mean differences were 0.31 between days 7 and 14, 1.64 between days 14 and 21, 0.81 between days 21 and 28, 0.08 between days 28 and 35 and 0.58 between days 35 and 42. A significant decrease in inflammatory cell density occurred between days 14 and 21 ($p<0.0001$) and a significant increase occurred between days 21 and 28 ($p=0.0365$). A significant increase occurred over the course of the study (a mean difference of 1.47 between days 7 and 42, $p<0.0001$).

When the burn wounds were compared to the non-burn wounds, the mean differences were 1.81 at day 7, 1.64 at day 14, 0.86 at day 21, 0.28 and day 28, 0.31 at day 35 and 0.44 at day 42. At days 7 ($p<0.0001$), 14, ($p<0.0001$) and 21 ($p=0.0171$) the non-burn wounds showed a significantly higher inflammatory cell density.

	Day 7	Day 14	Day 21	Day 28	Day 35	Day 42
Burn + STSG	1.51 (±0.15)	1.00 (±0.15)	2.64 (±0.23)	3.44 (±0.17)	3.36 (±0.18)	2.78 (±0.17)
Non-burn + STSG	3.11 (±0.18)	3.28 (±0.18)	3.50 (±0.13)	3.72 (±0.13)	3.06 (±0.14)	2.33 (±0.17)

Table 6.6.11: Mean inflammatory cell density (score out 5), where n=12 (6 per wound group) for a 42 day study

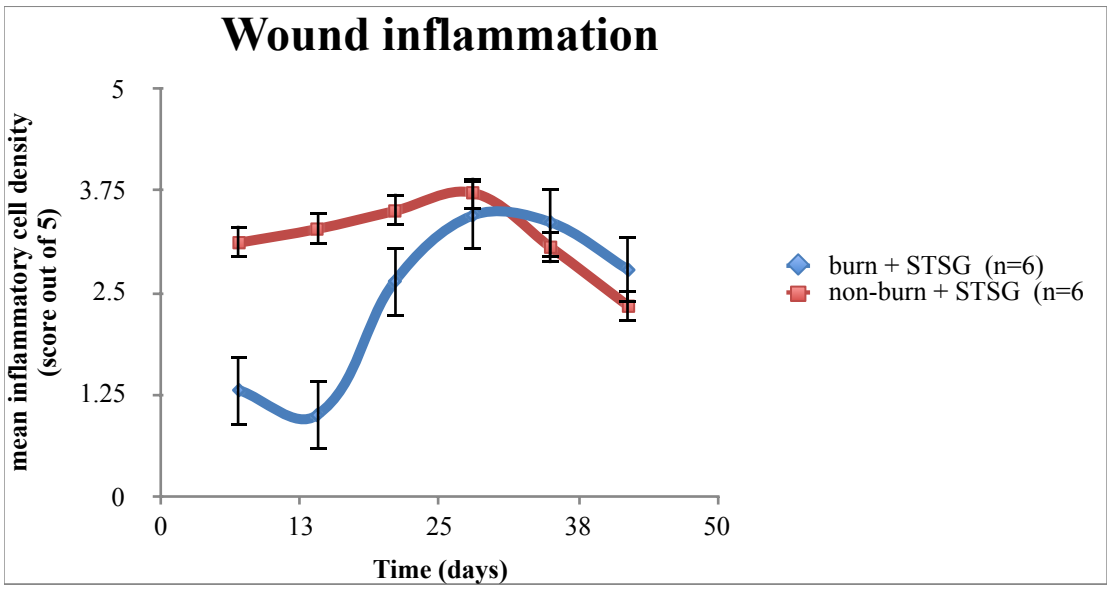

Figure 6.6.11: Mean inflammatory cell density versus time (n=12, 6 per wound group) for the different wounds in a 42 day study.

Interpretations for mean wound inflammatory cell density

The burn wounds showed a lag phase of 21 days for an inflammatory response when compared to the non-burn wounds, as non-burn wounds showed a significantly higher inflammatory cell density than the non-burn wounds at days 7, 14 and 21.

6.6.12 Wound vascular perfusion

please see Table 6.6.12 and figure 6.6.12

Non-burn wounds (acute full-thickness excision wounds)

The mean differences were 98.62PU between days 7 and 14, 106.9PU between days 14 and 21, 258.8PU between days 21 and 28, 89.13PU between days 28 and 35 and 364PU between days 35 and 42. Statistically significant increases in vascular perfusion were seen between each consecutive

time point ($p<0.0001$ for each difference).

Burn wounds (attenuated wound model)

The mean differences were 8.52PU between days 7 and 14, 56.22PU between days 14 and 21, 20.90PU between days 21 and 28, 39.83PU between days 28 and 35 and 9.33PU between days 35 and 42. Significant increases in perfusion between consecutive time points occurred between days 14 and 21 ($p<.0001$) and days 28 and 35 ($p=0.0224$). There was an overall significant increase over the course of the study (mean difference of 117.76, $p<0.0001$).

When the burn wounds were compared to the non-burn wounds, the mean differences were 7.10 at day 7, 114.22 at day 14, 164.94 at day 21, 402.81 and day 28, 452.12 at day 35 and 806.83 at day 42. Non-burn wounds showed significantly higher of levels of vascular perfusion than burn wounds at each time point ($p<0.0001$) except at day 7.

	Day 7	Day 14	Day 21	Day 28	Day 35	Day 42
Burn + STSG	86.02 (±6.12)	77.51 (±8.37)	133.72 (±7.77)	154.62 (±4.89)	194.44 (±5.85)	203.78 (±4.46)
Non-burn + STSG	93.12 (±6.82)	191.73 (±8.86)	298.63 (±6.89)	557.42 (±7.30)	646.55 (±9.51)	1010.58 (±14.34)

Table 6.6.12: Mean wound perfusion (PU), where n=12 (6 per wound group) for a 42 day study

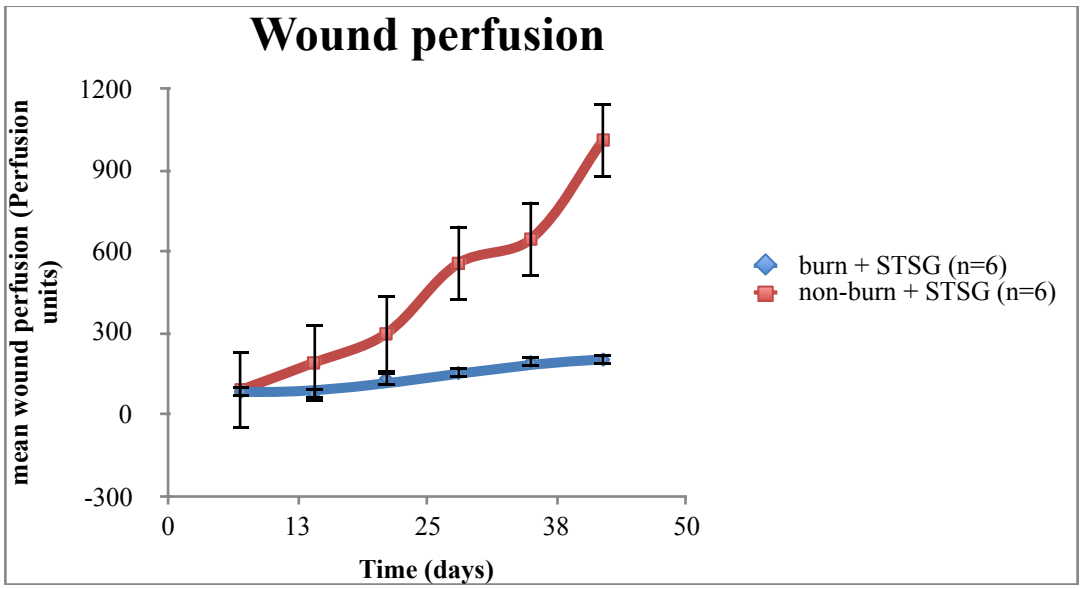

Figure 6.6.12: mean vascular perfusion versus time (n=12, 6 per wound group) for the different wounds in a 42 day study.

Interpretations for mean wound vascular perfusion

The non-burn wound group showed significantly higher of levels of vascular perfusion than burn wounds throughout the study.

6.6.13 Capillary lumen count

Please see table 6.6.13 and figure 6.6.13

Non-burn wounds (acute full-thickness excision wounds)

The mean differences were 1.83 between days 7 and 14, 0.39 between days 14 and 21, 0.72 between days 21 and 28, 0 between days 28 and 35 and 0.94 between days 35 and 42. A statistically significant increase ($p<0.0001$) was seen between days 7 and 14 and over the course of the study (mean difference of 3.89, $p<0.0001$).

Burn wounds (attenuated wound model)

The mean differences were 1.39 between days 7 and 14, 56.22 between days 14 and 21, 20.91 be-

tween days 21 and 28, 39.83 between days 28 and 35 and 9.33 between days 35 and 42. Significant increases in capillary lumen count between consecutive time points occurred between days 7 and 14 (0.0048), 14 and 21 (p=0.0026), 21 and 28 (p=0.0014) and days 28 and 35 (p<0.0001). There was an overall significant increase over the course of the study (mean difference of 7.11, p<0.0001).

When the burn wounds were compared to the non-burn wounds, the mean differences were 4.61 at day 7, 3.22 at day 14, 2.17 at day 21, 1.39 and day 28, 0.44 at day 35 and 0.44 at day 42. Non-burn wounds showed significantly higher of capillary lumen counts than burn wounds at each time point (p<0.0001 at days 7,14 21 and p=0.0048 at day 28) except at days 35 and 42.

	Day 7	Day 14	Day 21	Day 28	Day 35	Day 42
Burn + STSG	0.39 (±0.12)	1.78 (±0.18)	3.22 (±0.17)	4.72 (±0.24)	6.56 (±0.33)	7.52 (±0.27)
Non-burn + STSG	3.17 (±0.27)	5.00 (±0.27)	5.39 (±0.20)	6.11 (±0.32)	6.11 (±0.32)	7.06 (±0.27)

Table 6.6.13: Mean capillary lumen count, where n=12 (6 per wound group) for a 42 day study

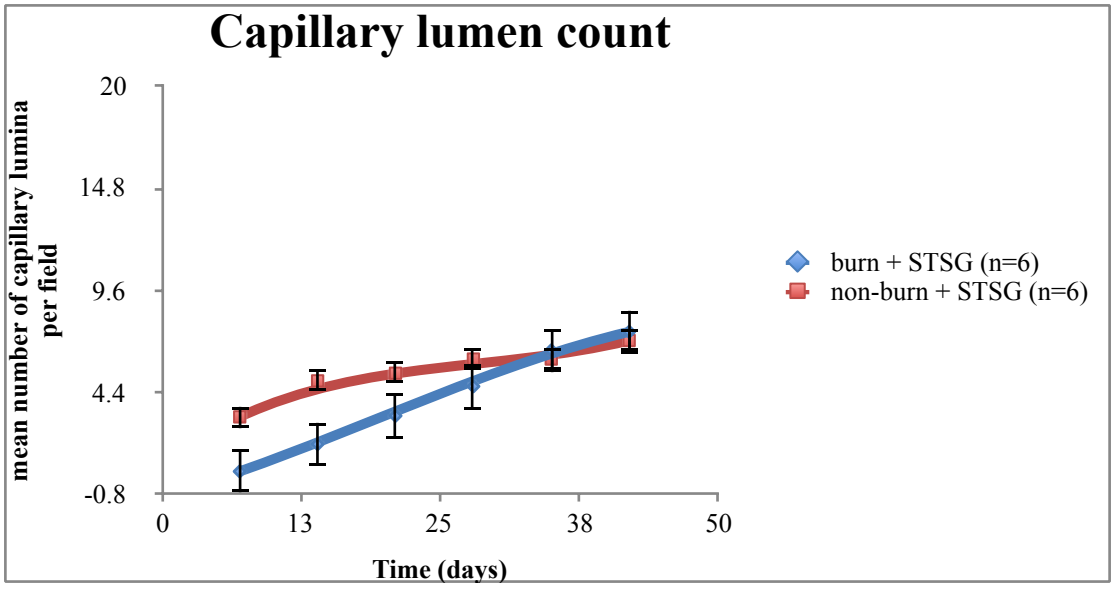

Figure 6.6.13: mean capillary lumen count versus time (n=12, 6 per wound group) for the different wounds in a 42 day study.

Interpretations for mean capillary lumen count

The non-burn wound group showed significantly higher numbers of mean capillary lumen count than burn wounds early in the study. There were no significant differences between the two groups by day 42.

6.6.14 Von Willebrand factor

Please see table 6.6.14 and figure 6.6.14.

Non-burn wounds (acute full-thickness excision wounds)

The mean differences were 0.03 between days 7 and 14, 0.25 between days 14 and 21, 1.03 between days 21 and 28, 0.03 between days 28 and 35 and 0.11 between days 35 and 42. A statistically significant increase was seen between days 21 and 28 ($p=0.0004$). A significant increase occurred over the course of the study (mean difference of 1.42 between days 7 and 42, $p<0.0001$).

Burn wounds (attenuated wound model)

The mean differences were 0.31 between days 7 and 14, 0.89 between days 14 and 21, 0.28 between days 21 and 28, 0.47 between days 28 and 35 and 0.42 between days 35 and 42. A significant increase occurred between days 14 and 21 ($p=0.0046$). There was an overall significant increase over the course of the study (mean difference of 2.36, $p<0.0001$).

When the burn wounds were compared to the non-burn wounds, the mean differences were 1.56 at day 7, 1.28 at day 14, 0.64 at day 21, 1.39 and day 28, 0.94 at day 35 and 0.64 at day 42. Staining for vWF was significantly higher in non-burn wounds at days 7 ($p<0.0001$), 14 ($p<0.0001$), 28 ($p<0.0001$) and 35 ($p=0.0017$).

	Day 7	Day 14	Day 21	Day 28	Day 35	Day 42
Burn + STSG	0.31 (±0.18)	0.61 (±0.16)	1.5 (±0.18)	1.78 (±0.17)	2.25 (±0.17)	2.67 (±0.16)
Non-burn + STSG	1.86 (±0.10)	1.89 (±0.12)	2.14 (±0.16)	3.17 (±0.15)	3.19 (±0.17)	3.31 (±0.14)

Table 6.6.14: Mean vWF staining density (score out 5), where n=12 (6 per wound group) for a 42 day study

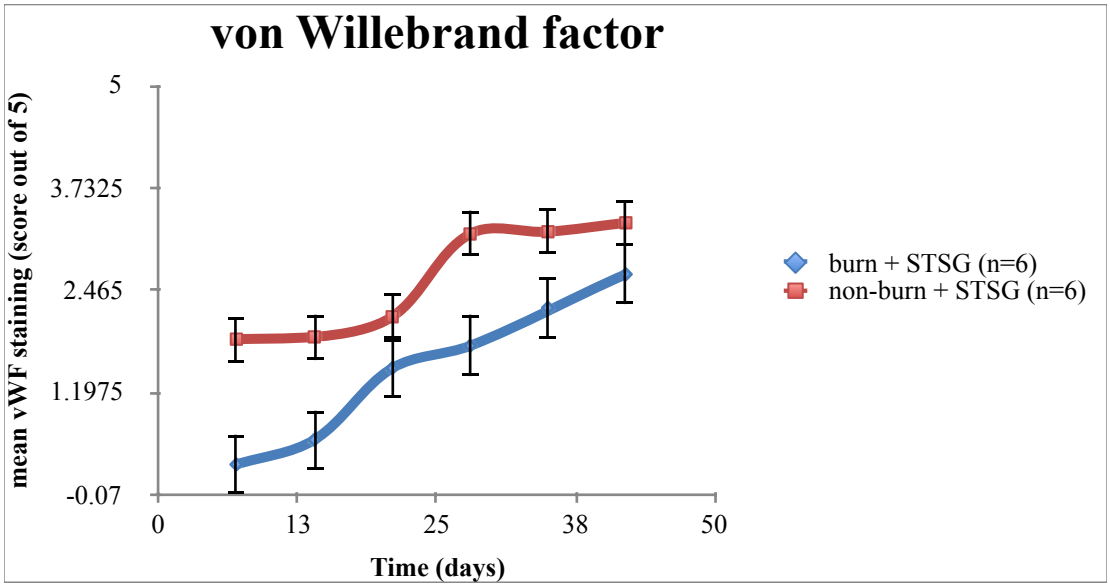

Figure 6.6.14: mean von Willebrand staining density versus time (n=12, 6 per wound group) for the different wounds in a 42 day study.

Interpretations for mean von Willebrand factor staining density

The non-burn wound group showed significantly higher levels of vWF staining than burn wounds

early in the study. There were no significant differences between the two groups by day 42.

6.6.15 Summary of findings

Compared to parallel acute full thickness wounds treated with STSG in the same animals, the delayed partial excision burn wounds showed a 14 day delay in wound contraction.

The acute and attenuated wound healing models showed no significant differences in EDA-FN and α-SMA staining, except at days 14 and 21, where EDA-FN was higher in the burn wound. Collagen and elastin staining were similar in the two wound groups except at day 21 where elastin staining was significantly higher in the acute wound.

Vascular perfusion remained lower in the burn wounds group throughout the study. Capillary lumen counts and vWF staining levels were lower in the burn wounds initially but there were no significant differences at day 42. The partial thickness excision burn wound demonstrated a 21 day delay in the vascular ingress of the wound and new capillary formation, while the acute wound demonstrated a vigorous and relatively rapid initial increase in vascularity.

Burn wounds showed a significantly higher wound depth cellular density, but a lower inflammatory cell infiltrate. Whereas acute wounds gave an expected exudative granulation response, the partial burn excision wound did not produce exudative granulation tissue, but showed a markedly oedematous wound bed with delayed inflammatory infiltration (of 21 days) beneath the wound surface, followed by some fibrovascular granulation tissue ingress after the 14 day delay period. This histological pattern could be called delayed internal granulation to distinguish it from the granulation outwards from the wound bed seen in the acute wound healing response. Additionally, the thickness of the wounds was significantly larger in the partial excision burn.

6.7 Conclusions from this study

From this experiment, it was concluded that the partial thickness excision of a burn wound healing trajectory is characterised by a delayed healing response, with delayed epithelialisation, delayed angiogenesis and prolonged tissue oedema. The partial thickness excision of a full thickness burn wound may be a useful experimental model to differentiate advanced wound treatments, in particular synthetic dermal scaffolds.

6.8 Subsequent steps

Following this study, the partial thickness excision of a burn wound was employed as an attenuated wound healing model to evaluate and compare the wound healing trajectories of different treatment modalities.

Chapter 7: Experiment 4: The evaluation of Smart Matrix™ and split thickness skin graft as a single stage procedure in the attenuated wound healing model.

7.1 Introduction

The previous study showed that the partial excision of a full thickness burn could be a representative and easily reproducible model of attenuated wound healing in mammalian skin. In the next and final experiment in described in this thesis, this model was employed to evaluate the effect Smart Matrix™ and STSG as a single stage procedure and to compare it to different treatment modalities. Matriderm™ with split thickness skin graft as a single stage reconstructive procedure, and split thickness skin grafts alone were compared.

7.2 Hypothesis

Smart Matrix™ supports wound healing in the attenuated wound model.

7.3 Aims

The aim of this experiment was to evaluate and compare the wound healing trajectory of single stage reconstructive procedures using split thickness skin graft alone, Matriderm™ + split thickness skin graft and Smart Matrix™ + split thickness skin graft in the attenuated wound healing model in a 42 day study.

7.4 Methods and materials

Please refer to Chapter 3: Methods and Materials for further detail.

The compromised wound healing model described in the previous chapter was used for this exper-

iment. Three full-thickness burn wounds (in a triangular arrangement) on each of the pigs' flanks were created as described in the previous section on day -1. These wounds were numbered 1- 6. On day 0, the zone of necrosis was excised, leaving the zone of stasis *in situ*.

7.5 Study outline

For this study, a total of 4 animals were used (and therefore 24 wounds). All animals monitored for a period of 42 days. The surgical procedures were carried out by the same surgeon (RZA) and senior project licence holder, JFD. Two wounds per animal were treated with split thickness skin graft alone (STSG alone), two were treated with Matriderm™ and overlying split thickness skin grafting (MD + STSG), and the remaining two were treated with Smart Matrix™ and overlying split thickness skin grafts (SM + STSG). The wound treatment pattern was randomly assigned to the wound numbers. The minimum number of pigs sufficient to yield statistically significant results was used for this study, as per Home Office regulations and project license restrictions.

<u>42 day Study:</u>

subjects = 4

Wounds (n) = 24

Treatment method	**Number of wounds**
Partial thickness excision of burn (burn) + STSG	8
Partial thickness excision of burn (burn) + SM + STSG	8
Partial thickness excision of burn (burn) + MD + STSG	8

Table7.5: Wound treatment distribution in a 42 day study (n=24, 8 per wound group)

7.6 Results

7.6.1 Graft take

Please see figure 7.6.1

Partial excision of full thickness burn wounds treated with split thickness skin graft alone.

Of the 8 wounds, 1 showed 90% graft take, 2 showed 85%, 2 showed 80%, 1 showed 60% and 2 showed 50% graft take. This gives a total of 5 wounds showing more than 80% graft take, and 3 wounds showing less than 80% graft take. No total graft loss occurred in this group.

Partial excision of full thickness burn wounds treated with Smart Matrix™ + split thickness skin graft.

Of the 8 wounds, 2 showed 95% graft take, 1 showed 90% graft take, 3 showed 85% graft take, 1 showed 75% and 1 showed 60% graft take. This gives a total of 6 wounds showing more than 80% graft take, and 2 wounds showing less than 80% graft take. No total graft loss occurred in this group.

Partial excision of full thickness burn wounds treated with Matriderm™ + split thickness skin graft.

Of the 8 wounds, 1 showed 95% graft take, 3 showed 85% graft take, 2 showed 80% graft take and 2 showed 60% graft take. This gives a total of 6 wounds showing more than 80% graft take, and 2 wounds showing less than 80% graft take. No total graft loss occurred in this group (see figure).

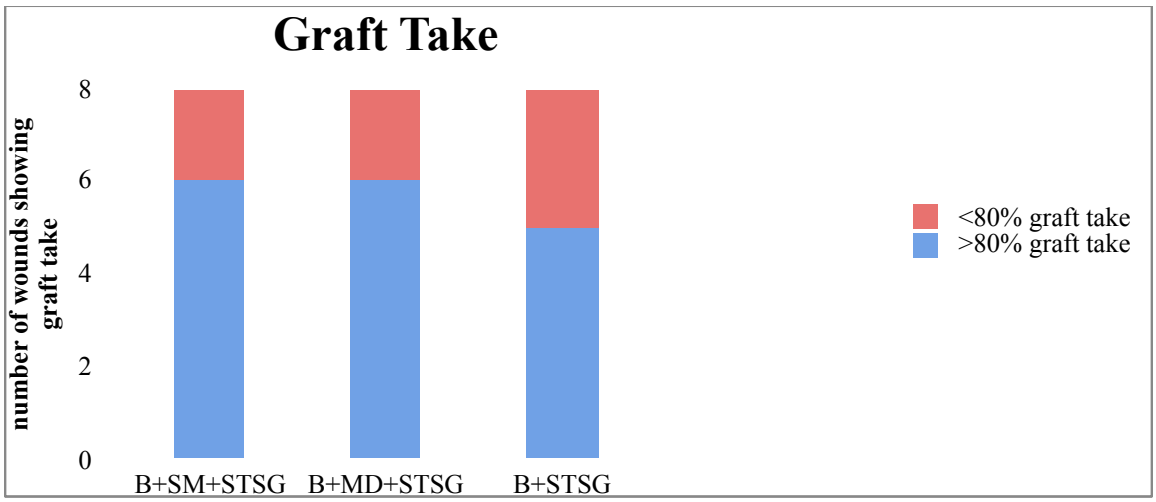

Figure 7.6.1: Wounds showing more than 80% graft take and wounds showing less than 80% graft take (n=24, 8 per wound group) for different reconstructive options.

7.6.2 Macroscopic observations

Please refer to figure 7.6.2.1-3

Partial excision of full thickness burn wounds treated with split thickness skin graft alone.

At day 7 all wounds showed a dark red-pink moist wound bed. Pink vascularised graft was adherent to the wound bed in the above-mentioned percentages. At day 14, all the wounds were still moist and a dark pinkish–red in colour. At day 21, 4 wounds were moist. Those with successful graft take showed only small patches of moist granulation tissue, which persisted until day 35. The dark pinkish-red colour persisted until day 21. At day 21, 3 wounds were dry and epithelialised, and a slightly paler pink. All wounds were swollen and the wound bed was proud of the surrounding skin between days 7 and 35. At day 42, the colour was paler and the wound bed was level with surrounding skin. Some small (less than 10% wound area) residual patches of moist granulation tissue were still present in those wounds with less than 80% graft take. No adnexal structures or signs of infection were observed in this wound group.

Partial excision of full thickness burn wounds treated with Smart Matrix™ + split thickness skin graft.

At day 7 all wounds showed a dark red-pink wound bed of granulation tissue with adherent pink vascularised graft. At day 14, all the wounds were still moist. The wounds were dark pinkish–red in colour. At day 21, 6 wounds were moist. Those with successful graft take showed small patches of moist granulation tissue. This persisted until day 35. The dark pinkish-red colour persisted until day 42. At day 35, 7 wounds were completely dry and epithelialised, and a slightly paler pink. The remaining wound was dry and epithelialised at day 42. All wounds were swollen and the wound bed was proud of the surrounding skin between days 7 and 28. At day 42, the colour was paler and the wound bed was level with surrounding skin. Some small (less than 10% wound area) residual patches of moist granulation tissue were still present in the 2 wounds with less than 80% graft take. No adnexal structures or signs of infection were observed in this wound group.

When compared to wounds treated with STSG alone, wounds treated with SM+ STSG showed earlier signs of epithelialisation and a more successful graft take rate.

Partial excision of full thickness burn wounds treated with Matriderm™ + split thickness skin graft.

At day 7 all wounds showed a dark red-pink wound bed of granulation tissue with adherent pink vascularised graft, with some patches of non-adherent graft, as described above. At day 14, all the wounds were still moist and dark pink–red in colour. At day 21, 6 wounds were still moist and pale pink in colour. Those with successful graft (>80%) take showed very small patches of moist granulation tissue, that persisted until day 35. At day 28, the wounds were pale pink in colour. At day 35, 7 wounds were completely dry and epithelialised. The remaining wound was dry and epithelialised at day 42. All wounds were swollen and the wound bed was proud of the surrounding skin between days 7 and 28. Some small (less than 10% wound area) residual patches of moist granula-

tion tissue were still present in the one of the wounds with less than 80% graft take. No adnexal structures or signs of infection were observed in this wound group.

When compared to wounds treated with STSG alone, wounds treated with SM+ STSG showed earlier signs of epithelialisation and a more successful graft take rate.

When compared to wounds treated with SM+STSG, no macroscopic differences were seen between the two wound groups.

Macroscopic appearances of the wounds in a 42 day study

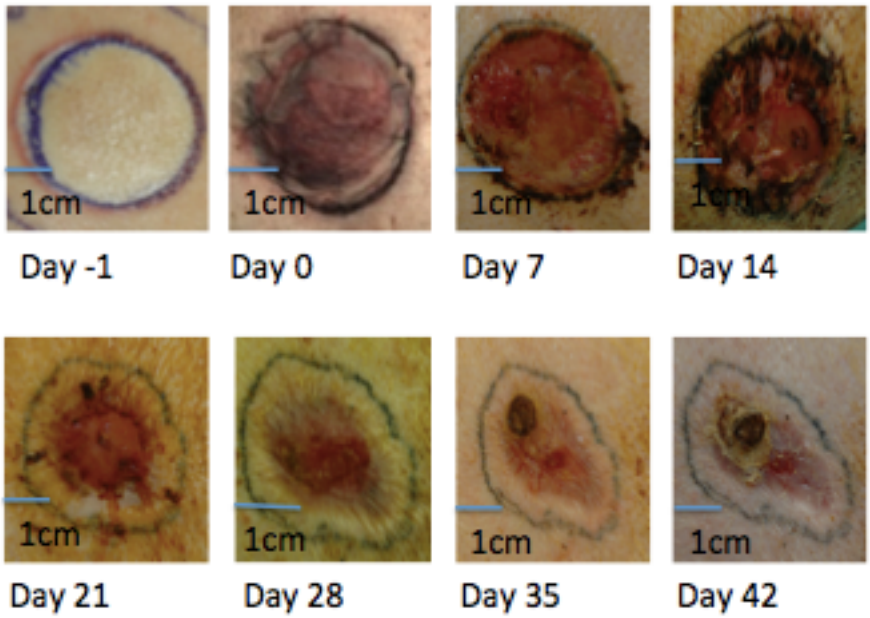

Figure 7.6.2.1: An example of the macroscopic appearances of the attenuated wound model treated with STSG alone

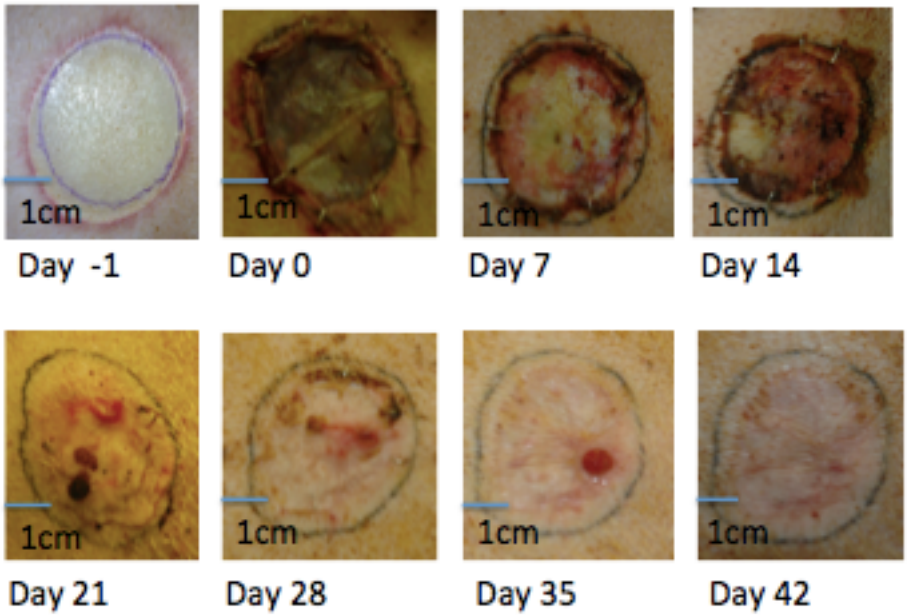

Figure 7.6.2.2: An example of the macroscopic appearances of the attenuated wound model treated with SM + STSG

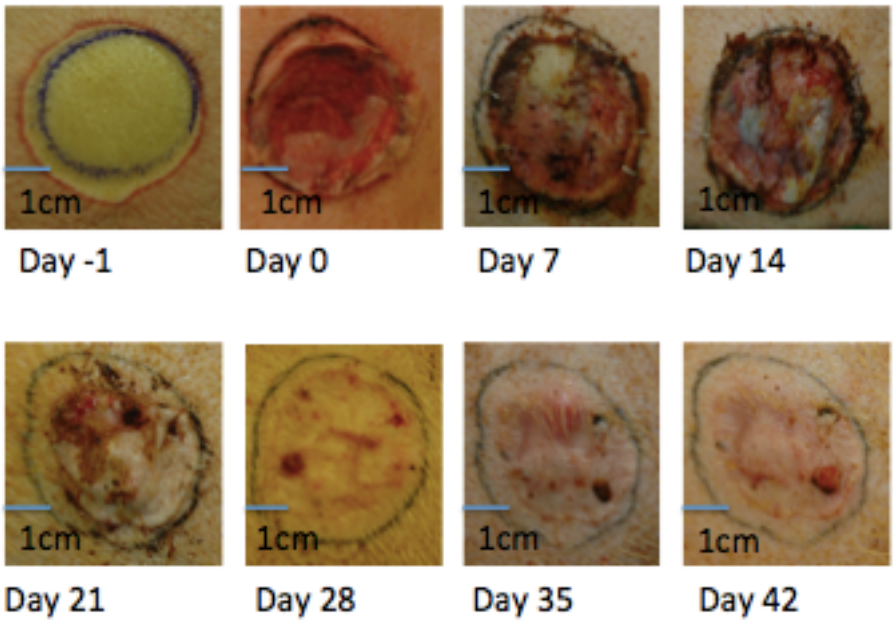

Figure 7.6.2.3: An example of the macroscopic appearances of the attenuated wound model treated with MD + STSG

Interpretations for macroscopic observations and graft take

Wounds treated with MD + STSG and SM + STSG exhibited a similar wound healing trajectory with similar macroscopic features and rates of graft take success and epithelialisation. Wounds treated with STSG alone showed a delay in epithelialisation and a lower rate of successful graft take.

7.6.3 Wound area and contraction

Please see table 7.6.3 and figure 7.6.3.1-2

Serial wound measurements were taken at each time point using the Eykona camera device. (See Methods and Materials chapter). The tattooed area was measured. This served as a control, to measure pig growth (if at all) and to take this into account when assessing wound contraction. Wound area measurements were calculated as a percentage of the wound area of the tattoo per time point in each pig. All wounds were of identical area measurement at day 0: 12.56 cm^2.

Tattooed area

The mean differences were 2.96cm^2 between days 0 and 7, 2.10cm^2 between days 14 and 21, 2.09cm^2 between days 14 and 21, 0.21cm^2 between days 21 and 28, 0.37cm^2 between days 28 and 35 and 1.81cm^2 between days 35 and 42. The mean tattoo area showed statistically significant increases ($p<0.0001$) between days 7 and 14, 14 and 21, 21 and 28 and days 35 and 42.

Partial excision of full thickness burn wounds treated with split thickness skin graft alone.

The wound area differences were statistically significant at between consecutive time points except between days 35 and 42. The mean differences were 5.20cm^2 ($p<0.0001$) between days 0 and 7, 0.55cm^2 ($p=0.0128$) between days 7 and 14 1.28cm^2 ($p<0.0001$) days 14 and 21, 2.18cm^2 ($p<0.00001$) days 21 and 28, 2.22cm^2 ($p<0.0001$) between days 28 and 35 and 0.21cm^2 between days 35 and 42.

When compared to the tattoo, the mean differences in wound area for the burn wounds treated with STSG alone were 0 at day 0 (100% of tattoo area), 2.25cm^2 (113% of tattoo area) at day 7, 1.11cm^2 (93% of tattoo area) at day 14, 1.87cm^2 (79% of tattoo area) at day 21, 4.26cm^2 (68% of tattoo area) at day 28, 6.85cm^2 (61% of tattoo area) at day 35 and 8.88cm^2 (60% of tattoo area) at day 42. These differences were statistically significant ($p<0.0001$), at each time point.

Partial excision of full thickness burn wounds treated with Smart Matrix™ + split thickness skin graft.

The mean wound area showed statistically significant ($p<0.0001$) changes in wound area at all time points. The mean differences were 6.61cm^2 between days 0 and 7, 0.98cm^2 between days 7 and 14 1.36cm^2 days 14 and 21, 1.59cm^2 days 21 and 28, 2.44cm^2 between days 28 and 35 and 0.50cm^2 between days 35 and 42.

When compared to the tattoo, the mean differences in wound area for the burn wounds treated with SM + STSG were 0 at day 0 (100% of tattoo area), 3.65cm^2 (122% of tattoo area) at day 7, 0.14cm^2 (108% of tattoo area) at day 14, 1.94cm^2 (93% of tattoo area) at day 21, 0.56cm^2 (97% of tattoo area) at day 28, 1.52cm^2 (106% of tattoo area) at day 35 and 0.21cm^2 (102% of tattoo area) at day 42. These differences were statistically significant ($p<0.0001$), at days 7, 14 and 21.

When compared to the burn wounds treated with STSG alone, the mean differences in wound area

for the burn wounds treated with SM +STSG were 0cm^2 at day 0, 1.41cm^2 at day 7, 0.97cm^2 at day 14, 0.07cm^2 at day 21, 3.70cm^2 at day 28, 8.37cm^2 at day 35 and 9.09cm^2 at day 42. These differences were statistically significant ($p<0.0001$) at all time points except at day 21.

Partial excision of full thickness burn wounds treated with Matriderm™ + split thickness skin graft.

The mean differences were 5.69cm^2 between days 7 and 14, 0.29cm^2 between days 14 and 21, 3.12cm^2 between days 21 and 28, 0.63cm^2 between days 28 and 35 and 0.52cm^2 between days 35 and 42 . Statistically significant ($p<0.0001$) changes in wound area between consecutive time points occurred for each reading except between days 35 and 42.

When compared to the tattoo, the mean differences in wound area for the burn wounds treated with MD + STSG were 0cm^2 at day 0 (100% of tattoo area), 2.73cm^2 (118% of tattoo area) at day 7, 1.94cm^2 (89% of tattoo area) at day 14, 2.42cm^2 (91% of tattoo area) at day 21, 0.45cm^2 (100% of tattoo area) at day 28, 1.61cm^2 (108% of tattoo area) at day 35 and 0.05cm^2 (99% of tattoo area) at day 42. These differences were significantly different ($p<0.0001$) at days 7, 14, 21 and 35.

When compared to the burn wounds treated with STSG alone, the mean differences in wound area for the burn wounds treated with MD + STSG were 0cm^2 at day 0, 0.49cm^2 at day 7, 0.83cm^2 at day 14, 0.54cm^2 at day 21, 3.81cm^2 at day 28, 8.47cm^2 at day 35 and 8.88cm^2 at day 42. These differences were statistically significant at days 14, 21, 28,35 and 42 ($p<0.0001$,except at day 21, where $p=0.0152$).

When compared to the burn wounds treated with SM + STSG, the mean differences in wound area for the burn wounds treated with MD + STSG were 0cm^2 at day 0, 0.92cm^2 at day 7, 1.80cm^2 at day 14, 0.48cm^2 at day 21, 0.11cm^2 at day 28, 0.1cm^2 at day 35 and 0.21cm^2 at day 42. These differences were statistically significant at days 7 and 14 ($p<0.0001$).

	Day 0	Day 7	Day 14	Day 21	Day 28	Day 35	Day 42
B+SM+STSG	13 (±0)	19 (±0.07)	20 (±0.07)	19 (±0.05)	20 (±0.08)	22 (±0.05)	23 (±0.07)
B+MD+STSG	13 (±0)	18 (±0.06)	16 (±0.06)	18 (±0.07)	20 (±0.08)	23 (±0.05)	22 (±0.08)
B+STSG	13 (±0)	18 (±0.05)	17 (±0.13)	20 (±0.08)	16 (±0.07)	14 (±0.06)	14 (±0.08)
normal skin	13 (±0)	16 (±0.29)	18 (±0.18)	20 (±0.18)	21 (±0.05)	21 (±0.11)	23 (±0.19)

Table 7.6.3: Mean wound area (cm²) where n=24 (8 per wound group) for a 42 day study

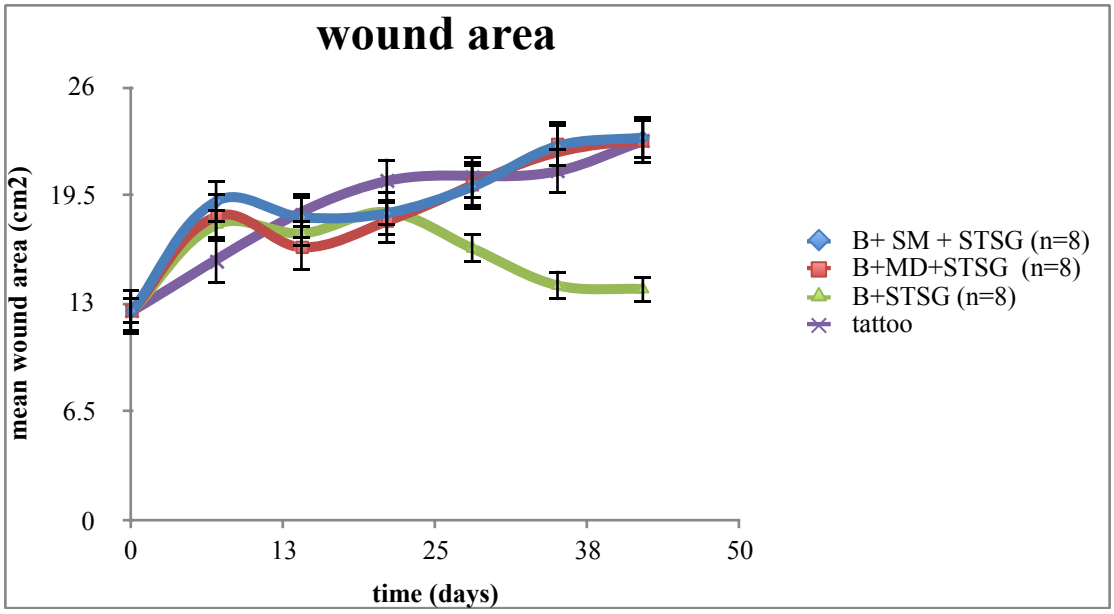

Figure 7.6.3.1: mean wound area versus time (n=24, 8 per wound group) for different reconstructive options for partial thickness burn wounds in a 42 day study.

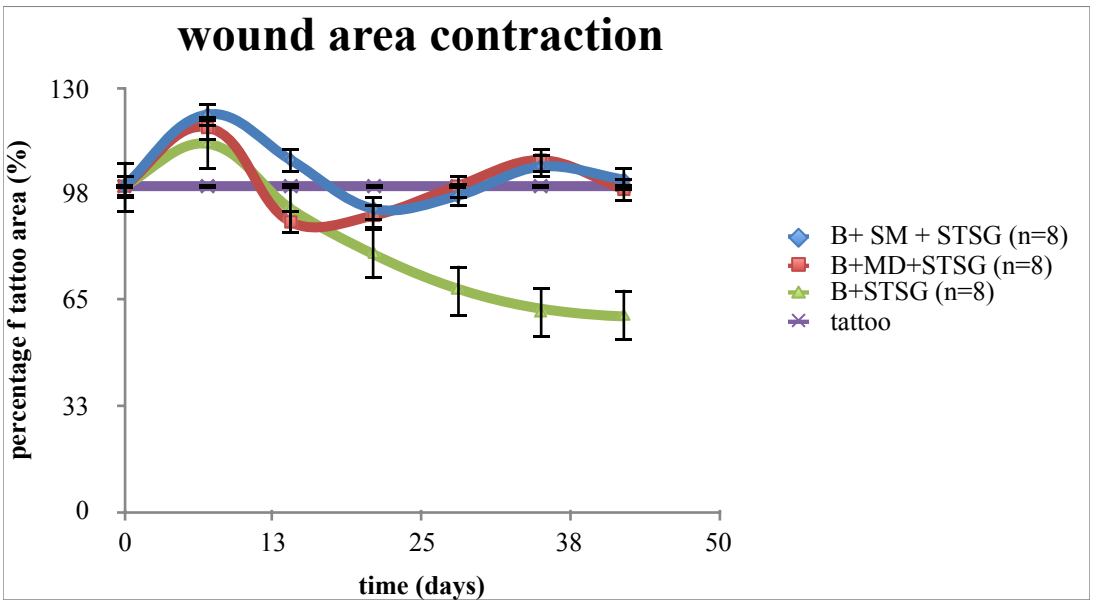

Figure 7.6.3.2: mean wound area as a percentage of the tattooed area versus time (n=24, 8 per wound group) for different reconstructive options for partial thickness burn wounds in a 42 day study.

Interpretations for mean wound area and contraction

Partial thickness excision burn wounds treated with SM + STSG and those threated with MD + STSG showed very similar wound areas to the tattooed area by day 42. The wounds treated with STSG alone showed significantly smaller wound areas than all three other groups.

7.6.4 Extra Domain A – Fibronectin

Please see table 7.6.4 and figure 7.6.4

Tattoo (normal skin)

The mean differences were 0.25 between days 7 and 14, 0.63 between days 14 and 21, 0.50 between days 21 and 28, 0.13 between days 28 and 35 and 0.50 between days 35 and 42. No statistically significant changes occurred throughout the study.

Partial excision of full thickness burn wounds treated with split thickness skin graft alone.

The mean differences were 0.27 between days 7 and 14, 0.07 between days 14 and 21, 0.14 between days 21 and 28, 0.45 between days 28 and 35 and 0.23 between days 35 and 42. The mean EDA-FN staining density showed no statistically significant changes between consecutive time points or over time.

Burn wounds treated with STSG alone showed significantly higher staining density for EDA-FN than the tattoo throughout the study. The mean differences were 3.59 at day 7 ($p<0.0001$), 3.06 at day 14 ($p=0.0004$), 2.37 ($p=0.0409$) at day 21, 2.73 at day 28 ($p=0.0045$), 3.28 at day 35 ($p<0.0001$) and 2.55 at day 42 ($p=0.014$).

Partial excision of full thickness burn wounds treated with Smart Matrix™ + split thickness skin graft.

The mean differences were 0.18 between days 7 and 14, 0.36 between days 14 and 21, 0.80 between days 21 and 28, 0.05 between days 28 and 35 and 0.18 between days 35 and 42. The mean EDA-FN staining density showed no statistically significant changes between consecutive time points or over time.

When the burn wounds treated with SM + STSG were compared to the tattoo, the mean differences were 2.95 at day 7, 2.51 at day 14, 2.25 at day 21, 1.95 and day 28, 2.13 at day 35 and 1.45 at day 42. EDA-FN staining was significantly higher than that of the tattoo at days 7 ($p=0.001$) and 14 ($p=0.0179$).

When the burn wounds treated with SM + STSG were compared to the burn wounds treated with STSG alone, the mean differences were 0.64 at day 7, 0.55 at day 14, 0.11 at day 21, 0.78 and day 28, 1.16 at day 35 and 1.1 at day 42. Burn wounds treated with SM+STSG showed significantly lower levels of EDA-FN staining than those treated with STSG alone at days 35 ($p=0.001$) and 42 ($p=0.0025$).

Partial excision of full thickness burn wounds treated with Matriderm™ + split thickness skin graft.

The mean differences were 0.27 between days 7 and 14, 0.64 between days 14 and 21, 0.01 between days 21 and 28, 0.01 between days 28 and 35 and 0.19 between days 35 and 42. The mean EDA-FN staining density showed no statistically significant changes between consecutive time points or over the course of the study.

When the burn wounds treated with MD + STSG were compared to the tattoo, EDA-FN staining was significantly higher throughout the course of the study. The mean differences were 3.02 at day 7 ($p=0.0006$), 3.04 at day 14 ($p=0.0005$), 3.05 at day 21 ($p=0.0005$), 2.92 at day 28 ($p=0.0012$), 2.88 at day 35 ($p=0.0017$) and 2.35 at day 42 ($p=0.0433$).

When the burn wounds treated with MD + STSG were compared to the burn wounds treated with STSG alone, the mean differences were 0.56 at day 7, 0.02 at day 14, 0.69 at day 21, 0.19 and day 28, 0.41 at day 35 and 0.28 at day 42. There were no significant differences between the two groups over the course of the study.

When the burn wounds treated with MD + STSG were compared to the burn wounds treated with SM + STSG, the mean differences were 0.07 at day 7, 0.53 at day 14, 0.80 at day 21, 0.97 and day 28, 0.75 at day 35 and 0.91 at day 42. EDA-FN staining was significantly higher in burn wounds treated by MD + STSG at day 28 ($p=0.0227$).

	Day 7	Day 14	Day 21	Day 28	Day 35	Day 42
B+SM+STSG	3.20 (±0.09)	3.01 (±0.08)	3.38 (±0.09)	2.58 (±0.14)	2.63 (±0.12)	2.45 (±0.12)
B+MD+STSG	3.27 (±0.09)	3.54 (±0.08)	3.55 (±0.09)	3.54 (±0.06)	3.38 (±0.09)	3.35 (±0.10)
B+STSG	3.82 (±0.08)	3.56 (±0.08)	3.47 (±0.04)	3.35 (±0.10)	3.78 (±0.08)	3.55 (±0.09)
normal skin	0.25 (±0.25)	0.50 (±0.29)	1.13 (±0.43)	3.44 (±0.38)	0.63 (±0.29)	0.50 (±0.41)

Table 7.6.4: Mean EDA-fibronectin staining density (score out 5), where n=24 (8 per wound group) for a 42 day study

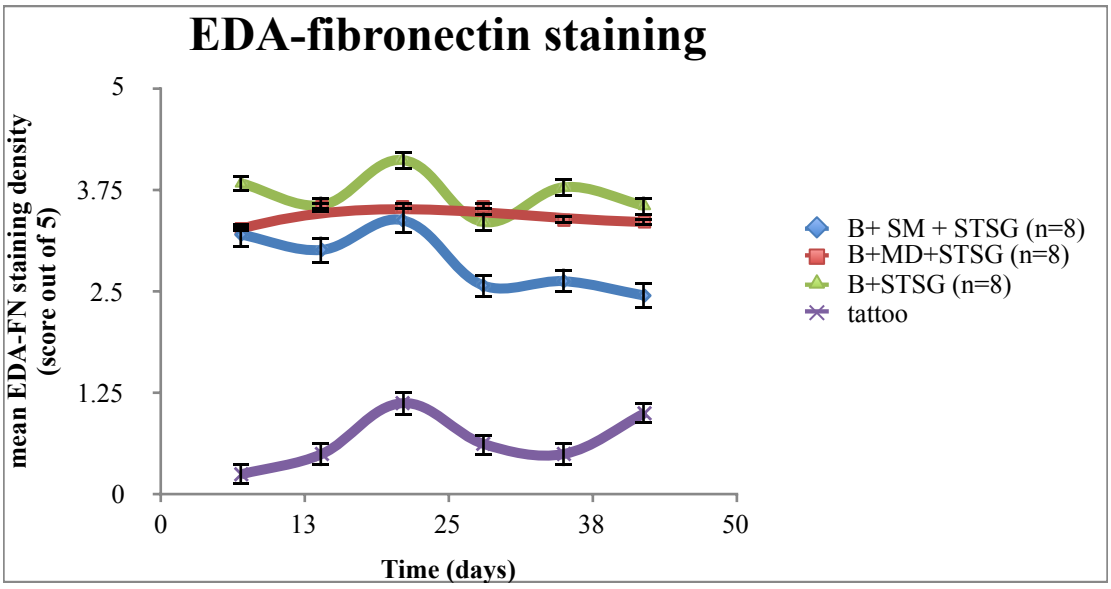

Figure 7.6.4: mean wound EDA – Fibronectin staining density versus time (n=24, 8 per wound group) for different reconstructive options for partial thickness burn wounds in a 42 day study.

Interpretations for mean EDA-Fibronectin staining density

At day 28, the EDA-FN staining density in partial thickness excision of burn wounds treated with SM + STSG was significantly lower than in those treated with MD + STSG. There was no signifi-

cant difference between these groups at day 42. At days 35 and 42 EDA-FN staining density in wounds treated with SM + STSG was significantly lower than in wounds treated with STSG alone. All these wound groups showed significantly higher EDA-FN staining levels than normal skin (the tattooed area).

7.6.5 Alpha-smooth muscle actin

Please refer to table 7.6.5 and figure 7.6.5

Tattoo (normal skin)

The mean differences were 0.13 between days 7 and 14, 0.13 between days 14 and 21, 0 between days 21 and 28, 0.13 between days 28 and 35 and 0.25 between days 35 and 42. No statistically significant changes occurred throughout the study.

Partial excision of full thickness burn wounds treated with split thickness skin graft alone.

The mean differences were 0.02 between days 7 and 14, 0.55 between days 14 and 21, 0.28 between days 21 and 28, 0.23 between days 28 and 35 and 0.5 between days 35 and 42. The mean α-SMA staining density showed no statistically significant changes between consecutive time points or over time.

Burn wounds treated with STSG alone showed higher staining density for α-SMA than the tattoo throughout the study. These differences were significant at days 28 and 42. The mean differences were 2.25 at day 7, 2.37 at day 14, 2.79 at day 2 1, 3.07 and day 28, 2.97 at day 35 and 3.22 at day 42. These differences were significant at days 28 ($p=0.0381$) and 42 ($p=0.0202$).

Partial excision of full thickness burn wounds treated with Smart Matrix™ + split thickness skin

graft.

The mean differences were 0.5 between days 7 and 14, 0.01 between days 14 and 21, 0.72 between days 21 and 28, 0.05 between days 28 and 35 and 0.18 between days 35 and 42. The mean α-SMA staining density showed no statistically significant changes between consecutive time points or over time.

When the burn wounds treated with SM + STSG were compared to the tattoo, the mean differences were 0.61 at day 7, 1.24 at day 14, 1.13 at day 21, 1.84 and day 28, 2.02 at day 35 and 1.59 at day 42. There was no significant difference in α-SMA staining between the two groups over the course of the study.

When the burn wounds treated with SM + STSG were compared to the burn wounds treated with STSG alone, the mean differences were 1.64 at day 7, 1.13 at day 14, 1.67 at day 21, 1.23 and day 28, 0.95 at day 35 and 1.63 at day 42. Burn wounds treated with SM+STSG showed significantly lower levels of α-SMA staining than those treated with STSG alone at days 7 ($p=0.0001$), 21 ($p<0.0001$), 28 ($p=0.0294$) and 42 ($p=0.0001$).

Partial excision of full thickness burn wounds treated with Matriderm™ + split thickness skin graft.

The mean differences were 0.59 between days 7 and 14, 0.13 between days 14 and 21, 0.47 between days 21 and 28, 0.21 between days 28 and 35 and 0.99 between days 35 and 42. The mean α-SMA staining density showed no statistically significant changes between consecutive time points or over the course of the study.

When the burn wounds treated with MD + STSG were compared to the tattoo, the mean differences were 1.15 at day 7, 1.86 at day 14, 1.87 at day 21, 2.33 and day 28, 2.25 at day 35 and 2.99 at day 42. Wounds treated with MD + STSG showed significantly higher mean α-SMA staining density levels throughout the study ($p<0.0001$).

When the burn wounds treated with MD + STSG were compared to the burn wounds treated with

STSG alone, the mean differences were 1.1 at day 7, 0.51 at day 14, 0.93 at day 21, 0.74 and day 28, 0.72 at day 35 and 0.23 at day 42. There were no significant differences between the two groups over the course of the study.

When the burn wounds treated with MD + STSG were compared to the burn wounds treated with SM + STSG, the mean differences were 0.53 at day 7, 0.62 at day 14, 0.74 at day 21, 0.49 and day 28, 0.23 at day 35 and 1.4 at day 42. α-SMA staining was significantly higher in burn wounds treated by MD + STSG at day 42 (p=0.0039).

	Day 7	Day 14	Day 21	Day 28	Day 35	Day 42
B+SM+STSG	0.99 (±0.10)	1.49 (±0.09)	1.50 (±0.07)	2.22 (±0.11)	2.27 (±0.11)	2.09 (±0.10)
B+MD+STSG	1.52 (±)	2.09 (±)	2.24 (±)	2.71 (±)	2.50 (±)	0.62 (±)
B+STSG	2.63 (±0.07)	2.61 (±0.11)	3.17 (±0.07)	3.45 (±0.08)	3.22 (±0.12)	3.10 (±0.63)
normal skin	0.38 (±0.25)	0.25 (±0.13)	0.38 (±0.25)	0.38 (±0.24)	0.25 (±0.24)	0.50 (±0.23)

Table 7.6.5: Mean Alpha Smooth Muscle Actin staining density (score out 5), where n=24 (8 per wound group) for a 42 day study

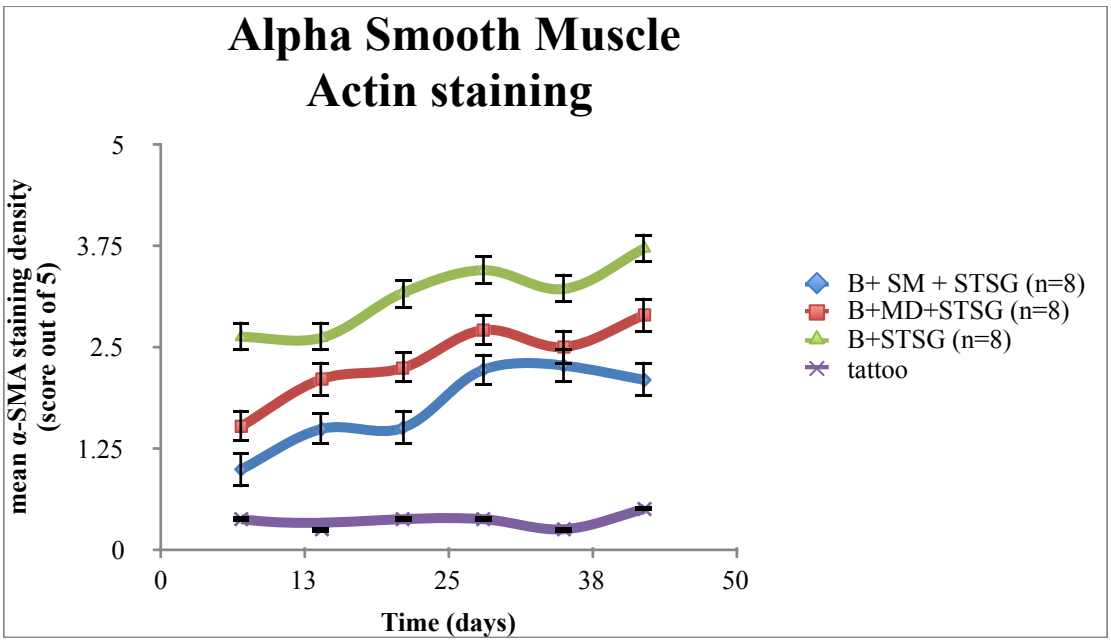

Figure 7.6.5: mean wound Alpha Smooth Muscle Actin staining density versus time (n=24, 8 per wound group) for different reconstructive options for partial thickness burn wounds in a 42 day study.

Interpretations for mean Alpha-Smooth Muscle Actin staining density

For each wound group mean α-SMA staining density showed no significant change throughout the study. Wounds treated with SM + STSG showed no significant differences when compared to normal skin, while mean α-SMA staining density levels were significantly lower than in wounds treated with STSG alone throughout the study and in those treated with MD + STSG at day 42.

7.6.6 Scaffold presence

Please refer to figure 7.6.6

Partial excision of full thickness burn wounds treated with Smart Matrix™ + split thickness skin graft.

Of the 8 wounds, all showed the presence of the Smart Matrix™ scaffold at days 7, 14 and 21. The dermal scaffold was still present in 5 of the wounds at day 28, 3 wounds at day 35 and in 1 wound at day 42.

Partial excision of full thickness burn wounds treated with Matriderm™ + split thickness skin graft.

Of the 8 wounds, all showed the presence of the Matriderm™ scaffold at days 7, 14 and 21. The dermal scaffold was still present in 7 of the wounds at day 28, 6 wounds at day 35 and 5 wounds at day 42.

When compared with wounds treated with SM + STSG, there were no significant differences at days 7,14 and 21. There was a significant difference of 9 wounds ($p<0.0001$) at day 28 and of 10 wounds at day 35 ($p<0.0001$).

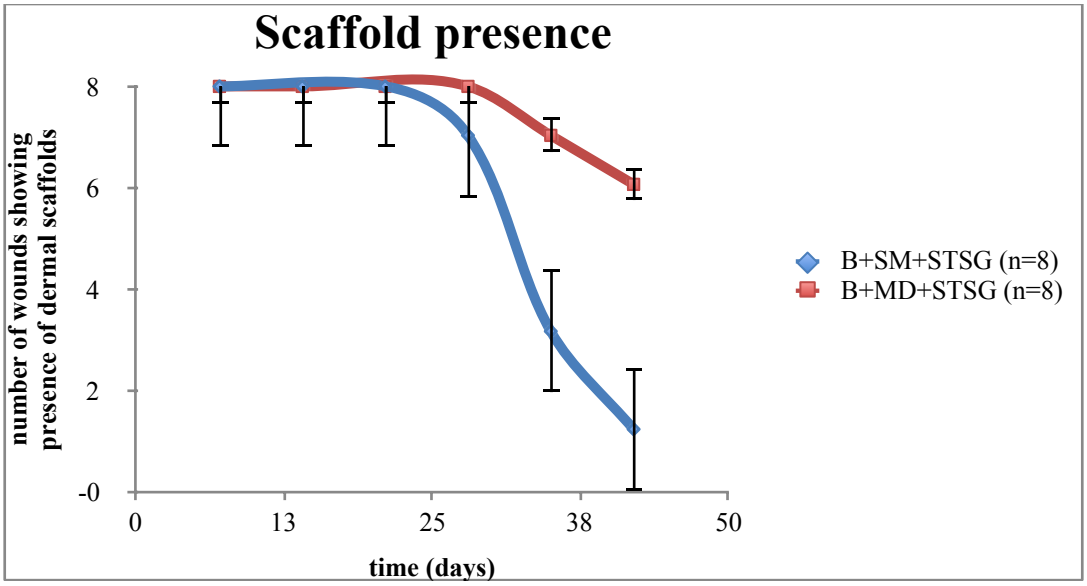

Figure 7.6.6: number of wounds showing scaffold presence versus time (n=16, 8 per wound group) for different reconstructive options in a 42 day study.

Interpretations for scaffold presence

Partial thickness excision of burn wounds treated with MD +STSG showed a longer persistence of the dermal scaffold in the wound bed than those treated with SM + STSG.

7.6.7 Collagen

Please refer to table 7.6.7 and figure 7.6.7

Tattoo (normal skin)

The mean differences were 0.88 between days 7 and 14, 0.5 between days 14 and 21, 0.38 between days 21 and 28, 0 between days 28 and 35 and 0.38 between days 35 and 42. No statistically significant changes occurred throughout the study.

Partial excision of full thickness burn wounds treated with split thickness skin graft alone.

The mean differences were 0.16 between days 7 and 14, 0.06 between days 14 and 21, 0.84 between days 21 and 28, 0.23 between days 28 and 35 and 0.29 between days 35 and 42. The mean collagen staining density showed no statistically significant changes between consecutive time points or over time, except between days 21 and 28 ($p<0.0001$).

Burn wounds treated with STSG alone showed significantly ($p<0.0001$ for the differences at each time point, except at day 42, where $p=0.0087$) lower staining density for collagen than the tattoo throughout the study. The mean differences were 3.95 at day 7, 2.92 at day 14, 3.35 at day 21, 2.14 and day 28, 1.91 at day 35 and 1.24 at day 42.

Partial excision of full thickness burn wounds treated with Smart Matrix™ + split thickness skin graft.

The mean differences were 0.69 between days 7 and 14, 0.01 between days 14 and 21, 0.26 between days 21 and 28, 0.64 between days 28 and 35 and 0.02 between days 35 and 42. The mean collagen staining density showed statistically significant increases between days 7 and 14 and between days 28 and 35 ($p<0.0001$).

When the burn wounds treated with SM + STSG were compared to the tattoo, the mean differences were 3.7 at day 7, 2.14 at day 14, 2.65 at day 21, 2.01 and day 28, 1.38 at day 35 and 1.02 at day 42. Burn wounds treated with SM + STSG showed lower levels of collagen staining at each time point. These differences were significant at each time point (<0.0001 for each difference except at day 35, where $p=0.0013$), except at day 42.

When the burn wounds treated with SM + STSG were compared to the burn wounds treated with STSG alone, the mean differences were 0.25 at day 7, 0.78 at day 14, 0.71 at day 21, 0.13 and day 28, 0.53 at day 35 and 0.22 at day 42. Burn wounds treated with SM+STSG showed lower levels of collagen staining than those treated with STSG alone at each tie point. These differences were significant at days 14 and 21 ($p<0.0001$) and at day 35 ($p=0.0017$).

<u>Partial excision of full thickness burn wounds treated with Matriderm™ + split thickness skin graft.</u>

The mean differences were 1.07 between days 7 and 14, 0.18 between days 14 and 21, 0.06 between days 21 and 28, 0.56 between days 28 and 35 and 0.15 between days 35 and 42. The mean collagen staining density showed significant ($p<0.0001$) increases between days 7 and 14 and between days 28 and 35.

When the burn wounds treated with MD + STSG were compared to the tattoo, the mean differences were 3.93 at day 7, 1.98 at day 14, 2.3 at day 21, 1.87 and day 28, 1.3 at day 35 and 0.78 at day 42. Burn wounds treated with MD + STSG showed lower staining densities of collagen when compared to the tattoo at each time point. These differences were significant ($p<0.0001$ for each reading difference except at day 35 where $p=0.0037$) at each time point except at day 42.

When the burn wounds treated with MD + STSG were compared to the burn wounds treated with STSG alone, the mean differences were 0.02 at day 7, 0.94 at day 14, 1.05 at day 21, 0.27 and day 28, 0.6 at day 35 and 0.46 at day 42. Burn wounds treated with MD + STSG showed higher staining densities of collagen when compared to the burn wounds treated with STSG alone at each time point. These differences were significant at days 14, 21, 35 ($p<0.0001$) and 42 ($p=0.0206$).

When the burn wounds treated with MD + STSG were compared to the burn wounds treated with SM + STSG, the mean differences were 0.23 at day 7, 0.16 at day 14, 0.34 at day 21, 0.15 and day 28, 0.73 at day 35 and 0.24 at day 42. There were no significant differences in collagen staining between these two wound groups throughout the study.

	Day 7	Day 14	Day 21	Day 28	Day 35	Day 42
B+SM+STSG	0.55 (±0.08)	1.24 (±0.08)	1.23 (±0.07)	1.39 (±0.08)	2.13 (±0.12)	2.10 (±0.11)
B+MD+STSG	0.32 (±0.06)	1.40 (±0.07)	1.57 (±0.09)	1.63 (±0.07)	2.20 (±0.11)	2.34 (±0.10)
B+STSG	0.30 (±0.06)	0.46 (±0.06)	0.52 (±0.07)	1.36 (±0.07)	1.59 (±0.07)	1.89 (±0.09)
normal skin	4.25 (±0.14)	3.38 (±0.24)	3.88 (±0.31)	3.50 (±0.29)	3.50 (±0.29)	3.13 (±0.43)

Table 7.6.7: Mean collagen staining density (score out 5), where n=24 (8 per wound group) for a 42 day study

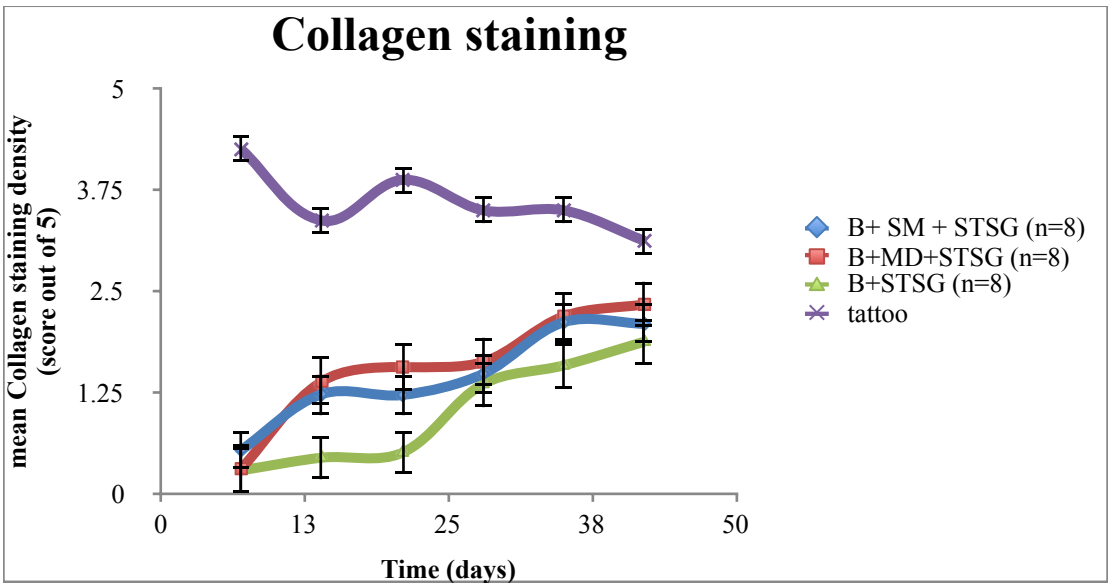

Figure 7.6.7: mean wound collagen staining density versus time (n=24, 8 per wound group) for different reconstructive options for partial thickness burn wounds in a 42 day study.

Interpretations for mean collagen staining density

Mean collagen staining density showed no significant differences between wounds treated with MD + STSG and those treated with SM + STSG. These two wound groups showed significantly higher levels than the wounds treated with STSG alone. All wounds groups showed significantly lower mean collagen staining densities than normal skin (the tattooed area).

7.6.8 Elastin

Please see table 7.6.8 and figure 7.6.8

Tattoo (normal skin)

The mean differences were 0.63 between days 7 and 14, 0.38 between days 14 and 21, 0.13 between days 21 and 28, 0.38 between days 28 and 35 and 0 between days 35 and 42. No statistically

significant changes occurred throughout the study.

Partial excision of full thickness burn wounds treated with split thickness skin graft alone.

The mean differences were 0.06 between days 7 and 14, 0.23 between days 14 and 21, 0.08 between days 21 and 28, 0.18 between days 28 and 35 and 0.45 between days 35 and 42. The mean elastin staining density showed a statistically significant change between days 35 and 42 ($p=0.0468$).

Burn wounds treated with STSG alone showed significantly lower staining density for elastin than the tattoo throughout the study ($p<0.0001$ for each difference except at day 42 where $p=0.0027$). These differences were significant at days 28 and 42. The mean differences were 1.76 at day 7, 2.27 at day 14, 2.42 at day 21, 2.38 and day 28, 1.82 at day 35 and 1.38 at day 42.

Partial excision of full thickness burn wounds treated with Smart Matrix™ + split thickness skin graft.

The mean differences were 0.39 between days 7 and 14, 0.04 between days 14 and 21, 0.42 between days 21 and 28, 0.21 between days 28 and 35 and 0.64 between days 35 and 42. The mean elastin staining density showed no statistically significant changes between consecutive time points except between days 35 and 42 ($p<0.0001$).

When the burn wounds treated with SM + STSG were compared to the tattoo, elastin staining density was higher in the tattoo group at each time point. The mean differences were 1.4 at day 7, 1.64 at day 14, 2.05 at day 21, 0.86 and day 28, 0.93 at day 35 and 0.29 at day 42. These differences were significant at days 7 ($p=0.002$), 14, 21 and 28 ($p<0.0001$).

When the burn wounds treated with SM + STSG were compared to the burn wounds treated with STSG alone, the mean differences were 0.31 at day 7, 0.64 at day 14, 0.36 at day 21, 0.86 and day

28, 0.9 at day 35 and 1.08 at day 42. Burn wounds treated with SM+STSG showed higher levels of elastin staining than those treated with STSG alone throughout the study. These differences were significant ($p<0.0001$) at each time point except at days 7 and 28.

Partial excision of full thickness burn wounds treated with Matriderm™ + split thickness skin graft.

The mean differences were 0.02 between days 7 and 14, 0.15 between days 14 and 21, 0.27 between days 21 and 28, 0.53 between days 28 and 35 and 0.1 between days 35 and 42. The mean elastin staining density showed a statistically significant increase between days 28 and 35 ($p=0.0035$).

When the burn wounds treated with MD + STSG were compared to the tattoo, the mean differences were 0.3 at day 7, 1.32 at day 14, 1.18 at day 21, 1.32 and day 28, 0.42 at day 35 and 0.31 at day 42. Burn wounds treated with MD+ STSG showed lower densities of elastin staining than the tattoo throughout the study. These differences were significant at days 14 ($p<0.0001$), 14 ($p=0.0319$) and 28 ($p=0.0054$).

When the burn wounds treated with MD + STSG were compared to the burn wounds treated with STSG alone, the mean differences were 1.41 at day 7, 1.32 at day 14, 1.24 at day 21, 1.05 and day 28, 1.41 at day 35 and 1.06 at day 42. Burn wounds treated with MD+STSG showed significantly higher ($p<0.0001$) densities of elastin staining than those treated with STSG alone throughout the study

When the burn wounds treated with MD + STSG were compared to the burn wounds treated with SM + STSG, the mean differences were 1.09 at day 7, 0.69 at day 14, 0.88 at day 21, 0.19 and day 28, 0.51 at day 35 and 0.02 at day 42. Elastin staining density was higher in burn wounds treated by MD + STSG at each time point except at day 42. These differences were significant at days 7, 14, 21, 28 ($p<0.0001$) and 35 ($p=0.0071$).

	Day 7	Day 14	Day 21	Day 28	Day 35	Day 42
B+SM+STSG	0.60 (±0.07)	0.99 (±0.11)	0.95 (±0.06)	1.36 (±0.07)	1.57 (±0.09)	2.21 (±0.10)
B+MD+STSG	1.70 (±0.10)	1.68 (±0.12)	1.82 (±0.09)	1.55 (±0.09)	2.08 (±0.10)	2.19 (±0.10)
B+STSG	0.29 (±0.06)	0.35 (±0.06)	0.58 (±0.06)	0.50 (±0.07)	0.68 (±0.08)	1.13 (±0.10)
normal skin	2.00 (±0.41)	2.63 (±0.24)	3.00 (0.41±)	2.88 (±0.13)	2.50 (±0.29)	2.50 (±0.35)

Table 7.6.8: Mean elastin staining density (score out 5), where n=24 (8 per wound group) for a 42 day study

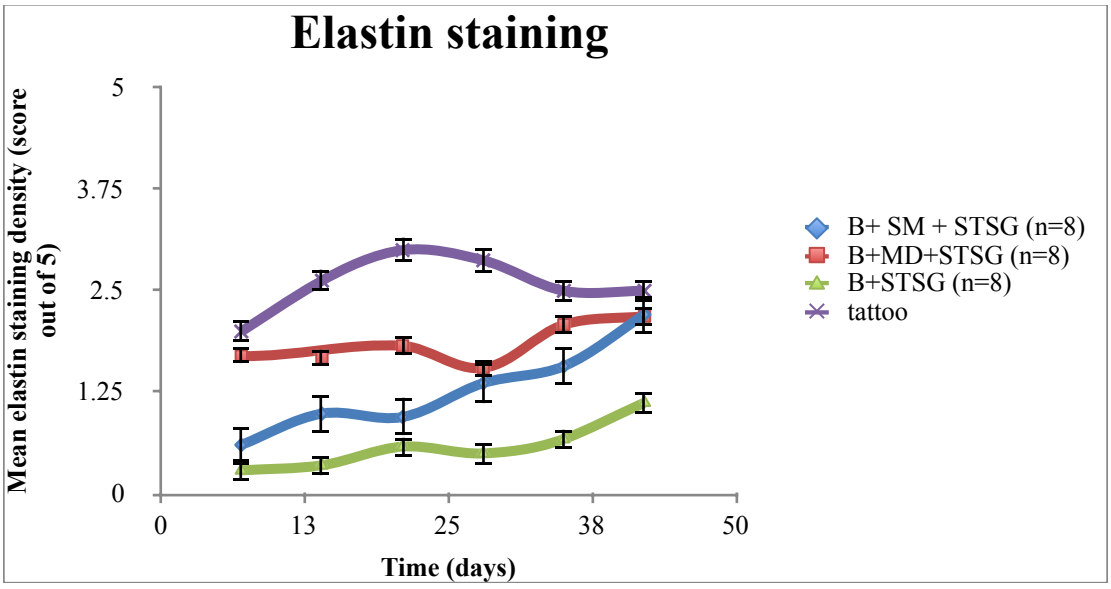

Figure 7.6.8: mean wound elastin staining density versus time (n=24, 8 per wound group) for different reconstructive options for partial thickness burn wounds in a 42 day study.

Interpretations for mean elastin staining density

Mean elastin staining densities showed no long term (day 42) differences between wounds treated

with MD + STSG and those treated with SM + STSG. Mean elastin staining densities were significantly higher in these two wound groups than in wounds treated with STSG alone. Normal skin showed significantly higher elastin staining densities than all three wound groups throughout the study, except at day 42, where there were no significant differences between wounds treated with SM + STSG, MD + STSG and the tattooed area.

7.6.9 Wound (neodermal) thickness

Please see table 7.6.9 and figure 7.6.9

Tattoo (normal skin)

The mean differences were 2.5μm between days 7 and 14, 14.5μm between days 14 and 21, 44μm between days 21 and 28, 15.5μm between days 28 and 35 and 37μm between days 35 and 42. No statistically significant changes occurred throughout the study.

Partial excision of full thickness burn wounds treated with split thickness skin graft alone.

The mean differences were 61.25μm between days 7 and 14, 160.4μm between days 14 and 21, 41.69μm between days 21 and 28, 58.29μm between days 28 and 35 and 165.2μm between days 35 and 42. Each of these changes were statistically significant ($p<0.0001$).

Burn wounds treated with STSG alone were significantly ($p<0.0001$) less thick than the tattoo throughout the study, except at day 35, where the tattoo was slightly less thick (this difference was however not statistically significant). The mean differences were 387.1μm at day 7, 323.4μm at day 14, 148.5μm at day 21, 62.79μm and day 28, 11μm at day 35 and 140.2μm at day 42.

Partial excision of full thickness burn wounds treated with Smart Matrix™ + split thickness skin

graft.

The mean differences were 219.2µm between days 7 and 14, 77.35µm between days 14 and 21, 23.29µm between days 21 and 28, 144.5µm between days 28 and 35 and 165.6µm between days 35 and 42. These increases between consecutive time points were all statistically significant ($p<0.0001$ for each reading except between days 21 and 28, where $p=0.0009$).

When the burn wounds treated with SM + STSG were compared to the tattoo, the tattoo skin was thicker between days 7 and 21 and thinner between days 28 and 42. All these differences were significant, except at day 21. The mean differences were 318.5µm at day 7 ($p<0.0001$), 96.75µm at day 14 ($p<0.0001$), 4.9µm at day 21, 62.4µm ($p=0.0003$) and day 28, 222.4µm at day 35 ($p<0.0001$) and 352.1µm at day 42 ($p<0.0001$).

The burn wounds treated with SM + STSG were significantly ($p<0.0001$) thicker than the burn wounds treated with STSG alone throughout the study. The mean differences were 68.65µm at day 7, 226.6µm at day 14, 143.6µm at day 21, 125.2µm and day 28, 211.4µm at day 35 and 211.8µm at day 42.

Partial excision of full thickness burn wounds treated with Matriderm™ + split thickness skin graft.

The mean differences were 198.3µm between days 7 and 14, 75.33µm between days 14 and 21, 66.48µm between days 21 and 28, 112µm between days 28 and 35 and 160.1µm between days 35 and 42. These increases were statistically significant ($p<0.0001$) between each time point.

When the burn wounds treated with MD + STSG were compared to the tattoo, the tattoo skin was thicker between days 7 and 21 and thinner between days 28 and 42. The mean differences were 315µm at day 7, 114.2µm at day 14, 24.4µm at day 21, 148.9µm and day 28, 213.3µm at day 35 and 337.3µm at day 42. These differences were significant ($p<0.0001$) at each time point except at day 21.

When the burn wounds treated with MD + STSG were compared to the burn wounds treated with STSG alone, the mean differences were 1.41µm at day 7, 1.32µm at day 14, 1.24µm at day 21, 1.05µm and day 28, 1.41µm at day 35 and 1.06µm at day 42. The burn wounds treated with MD + STSG were significantly ($p<0.0001$) thicker than the burn wounds treated with STSG alone throughout the study. The mean differences were 72.06µm at day 7, 20.91µm at day 14, 124.1µm at day 21, 148.9µm and day 28, 362.3µm at day 35 and 197.1µm at day 42.

When the burn wounds treated with MD + STSG were compared to the burn wounds treated with SM + STSG, the mean differences were 3.42µm at day 7, 17.48µm at day 14, 19.5µm at day 21, 23.69µm and day 28, 9.19µm at day 35 and 14.75µm at day 42. These differences were only significant at days 21 (0.0209) and 28 (p=00006).

	Day 7	Day 14	Day 21	Day 28	Day 35	Day 42
B+SM+STSG	241.04 (±2.31)	460.25 (±3.63)	537.60 (±2.33)	560.91 (±3.47)	705.44 (±2.53)	871.06 (±2.12)
B+MD+STSG	244.46 (±1.94)	442.77 (±3.43)	518.11 (±2.31)	594.58 (±2.50)	696.58 (±2.43)	856.31 (±5.35)
B+STSG	172.41 (±2.10)	233.65 (±2.80)	394.02 (±2.45)	435.71 (±8.60)	494.01 (±3.03)	659.23 (±2.60)
normal skin	559.52 (±28.43)	557.03 (±26.61)	542.51 (±8.39)	498.52 (±9.22)	519.00 (±14.74)	591.25 (±12.23)

Table 7.6.9: Mean wound neodermal thickness (µm), where n=24 (8 per wound group) for a 42 day study

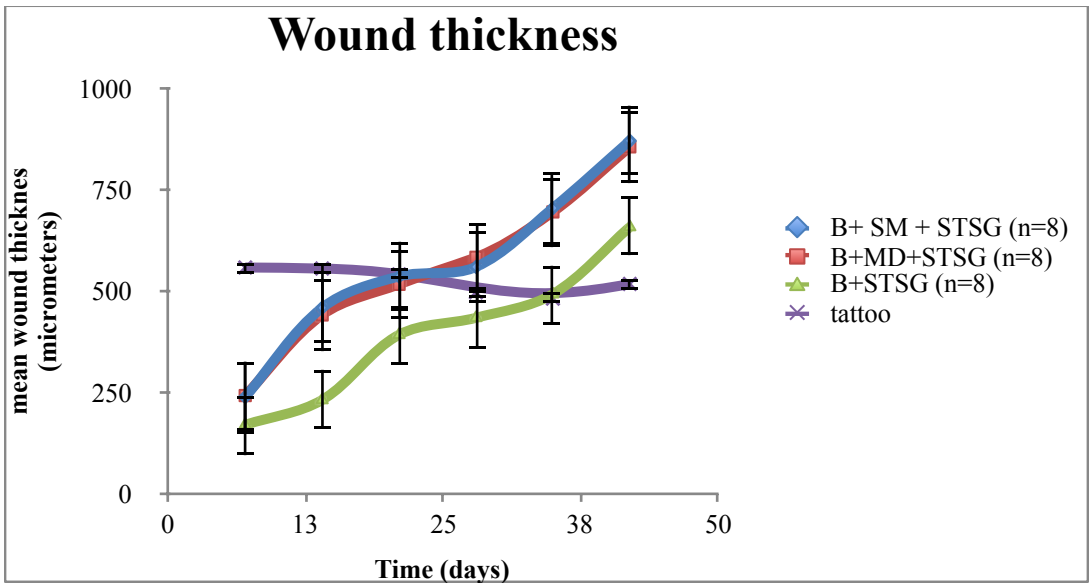

Figure 7.6.9: mean wound thickness (n=24, 8 per wound group) for different reconstructive options for partial thickness burn wounds in a 42 day study.

Interpretations for mean wound thickness

There were no significant differences in the mean thickness of healing tissue from the wound bed in the partial thickness excision of burn wounds treated with MD + STSG and those treated with SM + STSG. Mean wound thickness was significantly larger in these two groups than in those wounds treated with STSG alone throughout the study and than normal skin after day 21.

7.6.10 Cellular density

Please see table 7.6.10 and figure 7.6.10

Tattoo (normal skin)

The mean differences were 0 between days 7 and 14, 0 between days 14 and 21, 0.75 between days 21 and 28, 0.63 between days 28 and 35 and 0.5 between days 35 and 42. No statistically significant

changes occurred throughout the study.

Partial excision of full thickness burn wounds treated with split thickness skin graft alone.

The mean differences were 0.64 between days 7 and 14, 0.24 between days 14 and 21, 0.03 between days 21 and 28, 0.28 between days 28 and 35 and 0.01 between days 35 and 42. No statistically significant changes occurred between consecutive time points or throughout the study.

When compared with the tattoo, the mean differences were 1.3 at day 7, 0.67 at day 14, 0.53 at day 21, 0.25 and day 28, 0.09 at day 35 and 0.6 at day 42. There were no significant differences between the two groups.

Partial excision of full thickness burn wounds treated with Smart Matrix™ + split thickness skin graft.

The mean differences were 0.6 between days 7 and 14, 0.42 between days 14 and 21, 0.15 between days 21 and 28, 0.48 between days 28 and 35 and 0.05 between days 35 and 42. The mean cellular density showed no statistically significant changes between consecutive time points. Over the course of the study (between days 7 and 42), the increase in cellular density was significant (mean difference of 1.97, $p<0.0001$).

When the burn wounds treated with SM + STSG were compared to the tattoo, the mean differences were 1.98 at day 7, 1.38 at day 14, 0.58 at day 21, 0.31 and day 28, 0.17 at day 35 and 0.28 at day 42. There were no significant differences between the two groups at any time point.

When the burn wounds treated with SM + STSG were compared to the burn wounds treated with STSG alone, the mean differences were 0.6 at day 7, 0.7 at day 14, 0.05 at day 21, 0.06 and day 28, 0.26 at day 35 and 0.32 at day 42. There were no significant changes between the two groups at any time point.

Partial excision of full thickness burn wounds treated with Matriderm™ + split thickness skin graft.

The mean differences were 0.79 between days 7 and 14, 0.35 between days 14 and 21, 0.42 between days 21 and 28, 0.51 between days 28 and 35 and 0.21 between days 35 and 42. The mean cellular density showed no statistically significant changes between consecutive time points. Over the course of the study (between days 7 and 42), the increase in cellular density was significant (mean difference of 1.91, $p<0.0001$).

When the burn wounds treated with MD + STSG were compared to the tattoo, the mean differences were 2.09 at day 7, 1.3 at day 14, 0.57 at day 21, 0.22 and day 28, 0.1 at day 35 and 0.19 at day 42. There were no significant differences between the two groups at any time point.

When the burn wounds treated with MD + STSG were compared to the burn wounds treated with STSG alone, the mean differences were 0.79 at day 7, 0.63 at day 14, 0.04 at day 21, 0.03 and day 28, 0.1 at day 35 and 0.42 at day 42. There were no significant differences between the two groups at any time point.

When the burn wounds treated with MD + STSG were compared to the burn wounds treated with SM + STSG, the mean differences were 0.12 at day 7, 0.07 at day 14, 0.01 at day 21, 0.09 and day 28, 0.06 at day 35 and 0.09 at day 42. There were no significant differences between the two groups at any time point.

	Day 7	Day 14	Day 21	Day 28	Day 35	Day 42
B+SM+STSG	1.52 (±0.10)	2.13 (±0.10)	2.54 (±0.13)	2.69 (±0.10)	3.17 (±0.11)	3.22 (±0.09)
B+MD+STSG	1.41 (±0.07)	2.20 (±0.11)	2.55 (±0.07)	2.59 (±0.11)	3.10 (±0.11)	3.31 (±0.10)
B+STSG	2.20 (±0.10)	2.21 (±0)	2.59 (±0.47)	2.63 (±0.10)	2.48 (±0.42)	2.90 (±0.10)
normal skin	3.50 (±0.35)	3.50 (±0.35)	3.15 (±0.31)	2.38 (±0.24)	3.00 (±0)	3.50 (±0.50)

Table 7.6.10: Mean wound cellular density (score out 5), where n=24 (8 per wound group) for a 42 day study

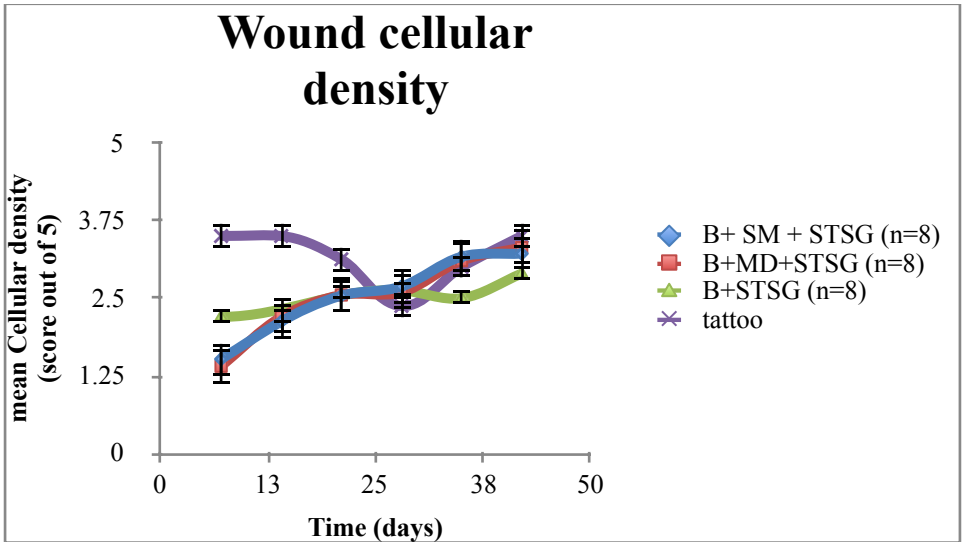

Figure 7.6.10: mean wound cellular density versus time (n=24, 8 per wound group) for different reconstructive options for partial thickness burn wounds in a 42 day study.

Interpretations for mean wound cellular density

Each wound group (excluding the tattoo) showed significantly increases in wound cellular density over the course of the study. There were no significant differences between all four groups.

7.6.11 Inflammation

Please see table 7.6.11 and figure 7.6.11

Tattoo (normal skin)

The mean differences were 0 between days 7 and 14, 0.13 between days 14 and 21, 0.12 between days 21 and 28, 0.25 between days 28 and 35 and 0.13 between days 35 and 42. No statistically significant changes occurred throughout the study.

Partial excision of full thickness burn wounds treated with split thickness skin graft alone.

The mean differences were 0.1 between days 7 and 14, 0.31 between days 14 and 21, 0.56 between days 21 and 28, 0.17 between days 28 and 35 and 0.57 between days 35 and 42. Statistically significant decreases in inflammatory cell density occurred between days 21 and 28 ($p=0.006$) and between days 35 and 42 ($p=0.0043$).

When compared with the tattoo, the mean differences were 2.08 at day 7, 2.19 at day 14, 1.75 at day 21, 1.06 at day 28, 1.15 at day 35 and 0.45 at day 42. Burn wounds treated with STSG alone showed significantly higher levels of inflammatory cell density at days 7, 14 and 21. There were no significant differences between the two groups throughout the remainder of the study.

Partial excision of full thickness burn wounds treated with Smart Matrix™ + split thickness skin graft.

The mean differences were 0.59 between days 7 and 14, 0.52 between days 14 and 21, 0.05 between days 21 and 28, 0.39 between days 28 and 35 and 0.54 between days 35 and 42. Significant decreases occurred between days 7 and 14 ($p=0.0022$), days 14 and 21 ($p=0.0202$) and between days 35 and 42 ($p=0.0112$).

When the burn wounds treated with SM + STSG were compared to the tattoo, the mean differences were 1.21 at day 7, 1.8 at day 14, 1.16 at day 21, 0.98 and day 28, 0.84 at day 35 and 0.18 at day 42. The inflammatory cell density of burn wounds treated with SM + STSG was significantly higher ($p<0.0001$) at day 14. There were no other significant differences between the two groups throughout the rest of the study.

When the burn wounds treated with SM + STSG were compared to the burn wounds treated with

STSG alone, the mean differences were 0.88 at day 7, 0.32 at day 14, 0.44 at day 21, 0.51 and day 28, 0.36 at day 35 and 0.27 at day 42. Burn wounds treated with SM + STSG showed significantly lower levels of inflammatory cell density at days 7 ($p<0.0001$) and 28 ($p=0.0269$). There were no other significant differences between the two groups throughout the rest of the study.

Partial excision of full thickness burn wounds treated with Matriderm™ + split thickness skin graft.

The mean differences were 0.86 between days 7 and 14, 1.28 between days 14 and 21, 0.02 between days 21 and 28, 0.53 between days 28 and 35 and 0.36 between days 35 and 42. The mean inflammatory cell density showed a significant increase between days 7 and 14 ($p<0.0001$) and significant decreases between days 14 and 21 ($p<0.0001$) and days 28 and 35 ($p=0.0151$).

When the burn wounds treated with MD + STSG were compared to the tattoo, the mean differences were 1.26 at day 7, 2.13 at day 14, 1.59 at day 21, 1.49 and day 28, 1.21 at day 35 and 0.72 at day 42. Burn wounds treated with MD+ STSG showed higher densities of inflammatory cell density than the tattoo throughout the study. These differences were significant at days 7 ($p=0.0409$), 14 ($p<0.0001$), 21 ($p=0.008$) and 28 ($p=0.003$).

When the burn wounds treated with MD + STSG were compared to the burn wounds treated with STSG alone, the mean differences were 0.82 at day 7, 0.25 at day 14, 0.16 at day 21, 0.43 and day 28, 0.06 at day 35 and 0.27 at day 42. There were no significant changes between the two groups except at day 7 when burn wounds treated with STSG alone showed significantly ($p<0.0001$) higher levels.

When the burn wounds treated with MD + STSG were compared to the burn wounds treated with SM + STSG, the mean differences were 0.05 at day 7, 0.32 at day 14, 0.44 at day 21, 0.51 and day 28, 0.36 at day 35 and 0.54 at day 42. Significant differences occurred between the two groups at days 28 ($p=0.0269$) and 42 (0.0112), where inflammatory cell density was lower in the burn wounds

treated with SM + STSG.

	Day 7	Day 14	Day 21	Day 28	Day 35	Day 42
B+SM+STSG	1.46 (±0.08)	2.05 (±0.11)	1.53 (±0.09)	1.48 (±0.08)	1.09 (±0.11)	0.55 (±0.08)
B+MD+STSG	1.51 (±0.08)	2.38 (±0.10)	1.97 (±0.09)	1.99 (±0.10)	1.46 (±0.09)	1.09 (±0.11)
B+STSG	2.33 (±0.13)	2.44 (±0.09)	2.13 (±0.11)	1.56 (±0.07)	1.40 (±0.08)	0.82 (±0.07)
normal skin	0.25 (±025)	0.25 (±0.25)	0.38 (±0.25)	0.50 (±0.29)	0.25 (±0.25)	0.38 (±0.24)

Table 7.6.11: Mean inflammatory cell density (score out 5), where n=24 (8 per wound group) for a 42 day study

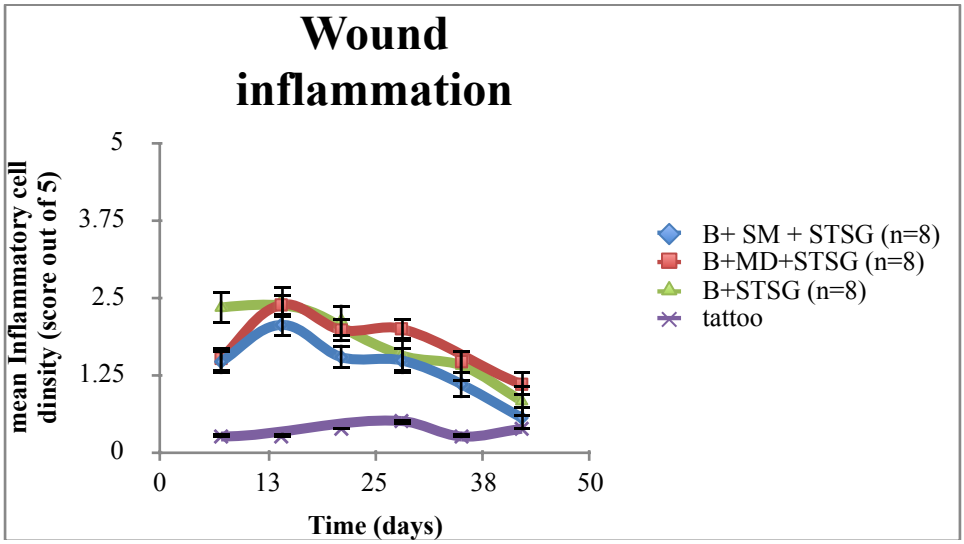

Figure 7.6.11: Mean wound inflammatory cell density versus time (n=24, 8 per wound group) for different reconstructive options for partial thickness burn wounds in a 42 day study.

Interpretations for mean wound inflammatory cell density

Partial thickness excision of burn wounds treated with SM + STSG showed significantly lower lev-

els of inflammatory cell density when compared with wounds treated with MD + STSG at days 28 and 42. There were no significant long-term differences between the tattoo, wounds treated with SM + STSG and those treated with STSG alone at day 42.

7.6.12 Vascular perfusion

Please see table 7.6.12 and figure 7.6.12

Tattoo (normal skin)

The mean differences were 7.8PU between days 7 and 14, 11.8PU between days 14 and 21, 10.28PU between days 21 and 28, 13.58PU between days 28 and 35 and 4.98PU between days 35 and 42. No statistically significant changes occurred throughout the study.

Partial excision of full thickness burn wounds treated with split thickness skin graft alone.

The mean differences were 7.61PU between days 7 and 14, 116.53PU between days 14 and 21, 111.12PU between days 21 and 28, 67.34PU between days 28 and 35 and 171.22PU between days 35 and 42. Statistically significant ($p<0.0001$) increases in vascular perfusion occurred between days 14 and 21, 21 and 28 and 35 and 42.

When compared with the tattoo, the mean differences were 74.14PU at day 7, 58.73PU at day 14, 45.95PU at day 21, 167.20PU at day 28, 221.00PU at day 35 and 392.28PU at day 42. Burn wounds treated with STSG alone showed significantly ($p<0.0001$) higher levels of vascular perfusion at days 28, 35 and 42.

Partial excision of full thickness burn wounds treated with Smart Matrix™ + split thickness skin graft.

The mean differences were 181.31PU between days 7 and 14, 88.72 between days 14 and 21, 213.45PU between days 21 and 28, 36.16PU between days 28 and 35 and 114.86PU between days 35 and 42. Significant increases occurred between days 7 and 14 ($p<0.0001$), days 14 and 21 ($p=0.0025$), days 21 and 28 ($p<0.0001$) and between days 35 and 42 ($p<0.0001$).

When the burn wounds treated with SM + STSG were compared to the tattoo, the mean differences were 29.61PU at day 7, 182.16PU at day 14, 259.14PU at day 21, 482.83PU and day 28, 505.41PU at day 35 and 510.47PU at day 42. The mean vascular perfusion of burn wounds treated with SM + STSG were significantly higher ($p<0.0001$) at each time point except at day 7.

When the burn wounds treated with SM + STSG were compared to the burn wounds treated with STSG alone, the mean differences were 67.14PU at day 7, 240.80PU at day 14, 23.24PU at day 21, 315.62PU and day 28, 254.45PU at day 35 and 228.00PU at day 42. Burn wounds treated with SM + STSG showed significantly ($p<0.0001$) higher levels of vascular perfusion throughout the study except at day 7.

Partial excision of full thickness burn wounds treated with Matriderm™ + split thickness skin graft.

The mean differences were 20.91PU between days 7 and 14, 144.22PU between days 14 and 21, 169.25PU between days 21 and 28, 53.63PU between days 28 and 35 and 66.54PU between days 35 and 42. The mean vascular perfusion showed a significant ($p<0.0001$) increase between days 14 and 21 and days 21 and 28.

When the burn wounds treated with MD + STSG were compared to the tattoo, the mean differences were 65.86PU at day 7, 37.15PU at day 14, 95.21PU at day 21, 274.74PU and day 28, 314.72PU at day 35 and 386.26PU at day 42. Burn wounds treated with MD+ STSG showed higher levels of vascular perfusion than the tattoo at days 21 ($p=0.0207$), 28 ($p<0.0001$), 35 ($p<0.0001$) and 42 ($p<0.0001$).

When the burn wounds treated with MD + STSG were compared to the burn wounds treated with

STSG alone, the mean differences were 8.28PU at day 7, 21.58PU at day 14, 49.26PU at day 21, 107.41PU and day 28, 93.72PU at day 35 and 10.96PU at day 42. Burn wounds treated with MD + STSG showed significantly higher levels of vascular perfusion at days 28 ($p<0.0001$) and 35 ($p=0.0009$).

When the burn wounds treated with MD + STSG were compared to the burn wounds treated with SM + STSG, the mean differences were 58.86PU at day 7, 219.31PU at day 14, 163.92PU at day 21, 208.25PU and day 28, 190.76PU at day 35 and 238.93PU at day 42. Wounds treated with SM + STSG showed significantly ($p<0.0001$) higher levels of vascular perfusion at each time point except at day 7.

	Day 7	Day 14	Day 21	Day 28	Day 35	Day 42
B+SM+STSG	174.18 (±4.86)	308.44 (±6.35)	441.22 (±6.19)	618.71 (±6.54)	667.46 (±8.33)	765.22 (±9.31)
B+MD+STSG	107.41 (±4.58)	118.52 (±4.27)	282.31 (±4.88)	441.27 (±4.53)	461.39 (±7.48)	589.22 (±5.65)
B+STSG	68.91 (±5.42)	88.26 (±6.51)	232.65 (±5.33)	323.63 (±6.57)	389.22 (±3.39)	565.40 (±7.68)
normal skin	144.87 (±5.39)	156.81 (±4.40)	166.96 (±2.87)	143.73 (±6.83)	163.54 (±3.29)	157.55 (±4.75)

Table 7.6.12: Mean vascular perfusion (PU), where n=24 (8 per wound group) for a 42 day study

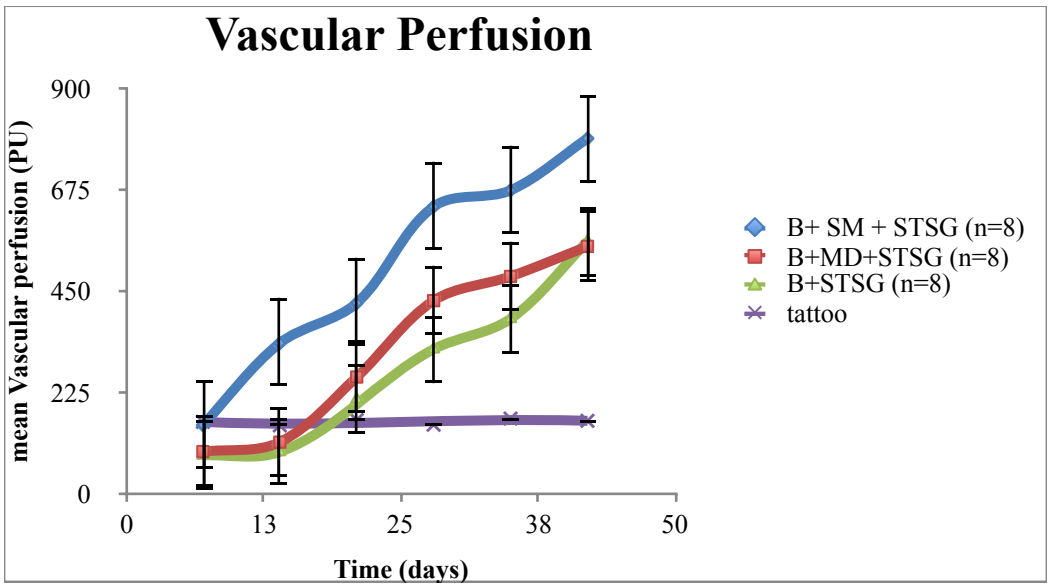

Figure 7.6.12: mean wound vascular perfusion versus time (n=24, 8 per wound group) for different reconstructive options for partial thickness burn wounds in a 42 day study.

Interpretations for mean wound vascular perfusion

Mean vascular perfusion increased for all wound groups over the course of the study. Mean vascular perfusion in the partial thickness burn wounds treated with SM + STSG showed significantly higher levels of vascular perfusion than the other wound groups throughout the study (except at day 7). There were no significant long-term differences between wounds treated with MD + STSG and those treated with STSG alone. At day 42, all wound groups showed significantly higher levels of vascular perfusion than normal skin.

7.6.13 Capillary lumen count

Please see table 7.6.13 and figure 7.6.13

Tattoo (normal skin)

The mean differences were 1.5 between days 7 and 14, 3.5 between days 14 and 21, 0.75 between

days 21 and 28, 1.25 between days 28 and 35 and 0.25 between days 35 and 42. No statistically significant changes occurred throughout the study.

Partial excision of full thickness burn wounds treated with split thickness skin graft alone.

The mean differences were 0.17 between days 7 and 14, 0.94 between days 14 and 21, 1.4 between days 21 and 28, 1.42 between days 28 and 35 and 2.4 between days 35 and 42. No statistically significant changes occurred between consecutive time points. However, a significant ($p<0.0001$) increase (mean difference of 5.98) occurred over the course of the study (between days 7 and 42).

When compared with the tattoo, burn wounds treated with STSG alone showed significantly lower capillary lumen counts than the tattoo throughout the study, except at day 42. The mean differences were 11.73 ($p<0.0001$) at day 7, 13.4 ($p<0.0001$) at day 14, 8.96 ($p=0.0004$) at day 21, 8.31 ($p=0.0019$) at day 28, 8.15 at day 35 ($p=0.0028$) and 6 at day 42.

Partial excision of full thickness burn wounds treated with Smart Matrix™ + split thickness skin graft.

The mean differences were 1.44 between days 7 and 14, 1.25 between days 14 and 21, 2.15 between days 21 and 28, 1.19 between days 28 and 35 and 0.38 between days 35 and 42. No statistically significant changes occurred between consecutive time points. However, a significant ($p<0.0001$) increase (mean difference of 6.4) occurred over the course of the study (between days 7 and 42).

When the burn wounds treated with SM + STSG were compared to the tattoo, the mean differences were 10.48 at day 7, 10.54 at day 14, 5.79 at day 21, 4.4 and day 28, 4.49 at day 35 and 4.33 at day 42. The capillary lumen count of burn wounds treated with SM + STSG was significantly lower ($p<0.0001$) at days 7 and 14. There were no other significant differences between the two groups throughout the rest of the study.

Burn wounds treated with SM + STSG showed higher capillary lumen counts than the burn wounds treated with STSG alone throughout the study. The mean differences were 1.25 at day 7, 2.85 at day 14, 3.17 at day 21, 2.5 and day 28, 3.69 at day 35 and 1.67 at day 42. These differences were significant at days 14 ($p=0.0188$), 21 ($p=0.0033$) and 35 ($p=0.0001$).

Partial excision of full thickness burn wounds treated with Matriderm™ + split thickness skin graft.

The mean differences were 0.4 between days 7 and 14, 0.6 between days 14 and 21, 2.1 between days 21 and 28, 3.17 between days 28 and 35 and 1.71 between days 35 and 42. The mean capillary lumen count showed a significant increase between days 28 and 35 ($p=0.0033$). A significant ($p<0.0001$) increase (mean difference of 7.98) also occurred over the course of the study (between days 7 and 42).

When the burn wounds treated with MD + STSG were compared to the tattoo, the mean differences were 11.75 at day 7, 12.85 at day 14, 8.75 at day 21, 7.4 at day 28, 5.48 at day 35 and 4.02 at day 42. Burn wounds treated with MD+ STSG showed lower capillary lumen counts than the tattoo throughout the study. These differences were significant at days 7 ($p<0.0001$), 14 ($p<0.0001$), 21 ($p=0.0006$) and 28 ($p=0.0147$).

When the burn wounds treated with MD + STSG were compared to the burn wounds treated with STSG alone, the mean differences were 0.02 at day 7, 0.54 at day 14, 0.21 at day 21, 0.92 and day 28, 2.67 at day 35 and 1.98 at day 42. Burn wounds treated with Matriderm™ + STSG showed a significantly higher capillary lumen count at day 35 ($p=0.0471$).

Burn wounds treated with MD + STSG showed lower capillary lumen than those treated with SM + STSG. The mean differences were 1.27 at day 7, 2.31 at day 14, 2.96 at day 21, 3 and day 28, 1.02 at day 35 and 0.31 at day 42. Significant differences occurred between the two groups at days 21 ($p=0.0108$) and 28 (0.0086).

	Day 7	Day 14	Day 21	Day 28	Day 35	Day 42
B+SM+STSG	2.52 (±0.42)	3.96 (±0.44)	5.21 (±0.11)	7.35 (±0.10)	8.54 (±0.11)	8.92(±0.10)
B+MD+STSG	1.25 (±0.15)	1.65 (±0.13)	2.25 (±0.11)	4.35 (±0.26)	7.52 (±0.27)	9.23 (±0.32)
B+STSG	1.22 (±0.06)	1.10 (±0.07)	2.04 (±0.11)	3.44 (±0.10)	4.85 (±0.11)	7.25 (±0.10)
normal skin	13.00 (±0.41)	14.50 (±0.29)	11.00 (±0.71)	11.75 (±1.31)	13.01 (±0.91)	13.25 (±0.48)

Table 7.6.13: Mean capillary lumen count, where n=24 (8 per wound group) for a 42 day study

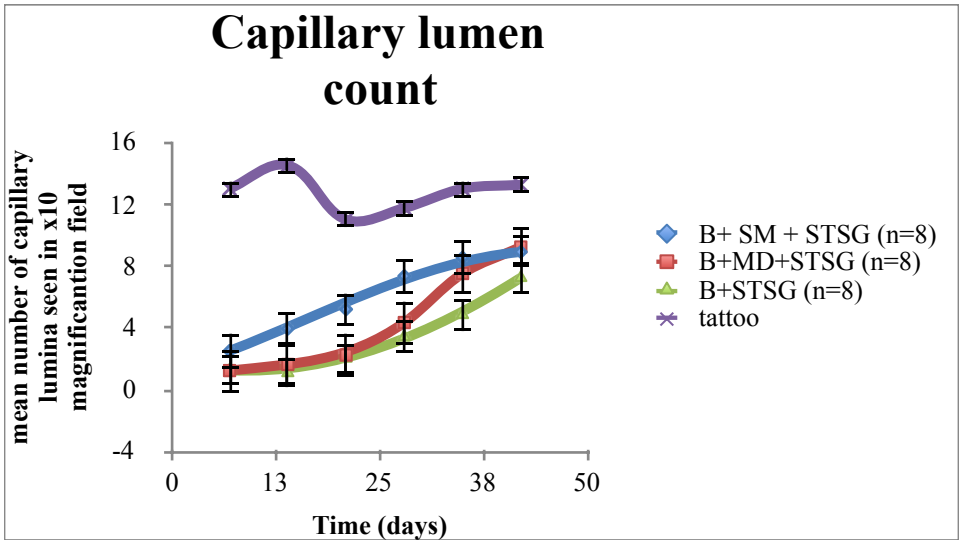

Figure 7.6.13: Mean capillary lumen number per x10 magnification field versus time (n=24, 8 per wound group) for different reconstructive options for partial thickness burn wounds in a 42 day study.

I*nterpretations for mean capillary lumen count*

Mean capillary lumen count increased for all wound groups over the course of the study. At day 42,

wounds treated with MD + STSG and those treated with SM + STSG groups showed significantly higher capillary lumen counts than those treated with STSG alone, and significantly lower counts than normal skin.

7.6.14 Von Willebrand factor

Please see table 7.6.14 and figure 7.6.14

Tattoo (normal skin)

The mean differences were 0 between days 7 and 14, 0 between days 14 and 21, 0.25 between days 21 and 28, 0.88 between days 28 and 35 and 0.75 between days 35 and 42. No statistically significant changes occurred throughout the study.

Partial excision of full thickness burn wounds treated with split thickness skin graft alone.

The mean differences were 0.03 between days 7 and 14, 1.21 between days 14 and 21, 0.06 between days 21 and 28, 0.36 between days 28 and 35 and 0.34 between days 35 and 42. The mean vWF staining density showed a statistically significant increase between days 14 and 21 ($p<0.0001$). A significant ($p=0.0156$) increase (mean difference of 1.28) occurred over the course of the study (between days 7 and 42).

Burn wounds treated with STSG alone showed lower staining density for vWF than the tattoo throughout the study. The mean differences were 2.81 at day 7, 2.84 at day 14, 1.89 at day 21, 0.95 and day 28, 1.833 at day 35 and 0.61 at day 42. These differences were significant ($p<0.0001$) at days 7, 14 and 21.

Partial excision of full thickness burn wounds treated with Smart Matrix™ + split thickness skin graft.

The mean differences were 0.16 between days 7 and 14, 0.21 between days 14 and 21, 0.14 between days 21 and 28, 0.3 between days 28 and 35 and 0.42 between days 35 and 42. The mean vWF staining density showed no statistically significant changes between consecutive time points. However, a statistically significant ($p=0.0156$) increase occurred over the course of the study (mean difference of 1.28).

When the burn wounds treated with SM + STSG were compared to the tattoo, the vWF staining density was higher in the tattoo group at each time point. The mean differences were 0.92 at day 7, 0.09 at day 14, 0.13 at day 21, 0.1 and day 28, 00.41 at day 35 and 0.76 at day 42. These differences were not statistically significant at any time point.

When the burn wounds treated with SM + STSG were compared to those treated with STSG alone, the vWF staining density was higher in the SM + STSG group at each time point. The mean differences were 1.29 at day 7, 1.49 at day 14, 0.49 at day 21, 0.56 and day 28, 0.5 at day 35 and 0.63 at day 42. These differences were significant at days 7 ($p=0.0138$) and 14 ($p=0.0018$).

Partial excision of full thickness burn wounds treated with Matriderm™ + split thickness skin graft.

The mean differences were 1.02 between days 7 and 14, 0.01 between days 14 and 21, 0.16 between days 21 and 28, 0 between days 28 and 35 and 1.64 between days 35 and 42. The mean vWF staining density showed a statistically significant increase between days 35 and 42 ($p=0.0002$). A significant ($p<0.0001$) increase (mean difference of 2.8) occurred over the course of the study (between days 7and 42).

When the burn wounds treated with MD + STSG were compared to the tattoo, the mean differences were 2.28 at day 7, 1.28 at day 14, 1.6 at day 21, 0.39 at day 28, 0.49 at day 35 and 0.78 at day 42. Burn wounds treated with MD+ STSG showed lower densities of vWF staining than the tattoo

throughout the study. These differences were significant ($p<0.0001$) at days 7, 14 and 21.

Burn wounds treated with MD+STSG showed higher densities of vWF staining than those treated with STSG alone throughout the study. The mean differences were 0.53 at day 7, 1.58 at day 14, 0.36 at day 21, 0.46 and day 28, 0.09 at day 35 and 1.38 at day 42. These differences were significant at days 14 ($p=0.0002$) and 42 ($p=0.006$).

When the burn wounds treated with MD + STSG were compared to the burn wounds treated with SM + STSG, the mean differences were 0.92 at day 7, 0.09 at day 14, 0.13 at day 21, 0.1 and day 28, 0.41 at day 35 and 0.76 at day 42. There were no statistically significant differences between the two wound groups throughout the study.

	Day 7	Day 14	Day 21	Day 28	Day 35	Day 42
B+SM+STSG	1.34 (±0.42)	1.89 (±0.44)	2.10 (±0.11)	2.24 (±0.10)	2.54 (±0.14)	3.01 (±0.12)
B+MD+STSG	0.97 (±0.07)	1.99 (±0.11)	1.99 (±0.11)	2.14 (±0.11)	2.14 (±0.13)	2.85 (±0.14)
B+STSG	0.44 (±0.06)	0.41 (±0.07)	1.61 (±0.11)	1.68 (±0.10)	1.21 (±0.11)	0.06 (±0.10)
normal skin	3.25 (±0.48)	3.25 (±0.43)	3.25 (±0.29)	3.50 (±0.56)	2.63 (±0.38)	3.38 (±0.41)

Table 7.6.14: Mean vWF staining density (score out 5), where n=24 (8 per wound group) for a 42 day study

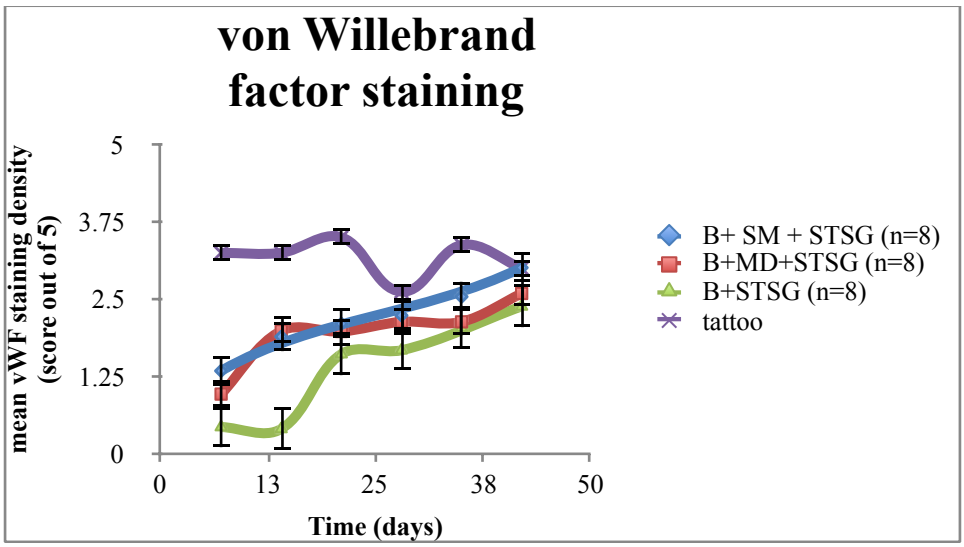

Figure 7.6.14: mean von Willebrand staining density versus time (n=24, 8 per wound group) for different reconstructive options for partial thickness burn wounds in a 42 day study.

Interpretations for mean von Willebrand factor staining density

Mean vWF staining density increased for all wound groups over the course of the study. There were no significant long term differences between wounds treated with SM + STSG and those treated with MD + STSG. At day 42, wounds treated with MD + STSG and those treated with SM + STSG groups showed significantly higher vWF staining densities than those treated with STSG alone, and no significant difference to normal skin.

7.6.15 Summary of findings

Wounds treated with MD + STSG and SM + STSG showed similar macroscopic features and graft take success and epithelialisation. Wounds treated with STSG alone showed a delay in epithelialisation and a lower rate of successful graft take.

Partial thickness excision burn wounds treated with SM + STSG and those treated with MD + STSG showed similar wound areas to each other and to the tattooed area by day 42. The wounds treated with STSG alone contracted more than all three other groups. EDA-FN staining in wounds treated with SM + STSG was similar throughout the study to that of normal skin, while significantly higher in wounds treated with MD + STSG and SM + STSG. EDA-FN staining was highest in wounds treated with STSG alone followed by those treated with MD + STSG and then by those treated with SM + STSG, where levels similar to that of normal skin were reached by day 42, in the latter group. There were no significant differences in α-SMA staining in normal skin and wounds treated with SM + STSG. Wounds treated with MD + STSG showed higher levels than these groups until day 28, while wounds treated with STSG alone showed the highest levels, which persisted until day 42.

The dermal scaffold persisted from an average of 21 days in wounds treated with SM + STSG, 35 days in those treated with MD + STSG and 84 days in those treated with I + STSG.

Matriderm™ scaffolds persisted longer than Smart Matrix™ scaffolds. Of note, when comparing scaffold presence in this study to scaffold presence in the second study described in this thesis, scaffold persistence was longer in the attenuated wound healing model than in the acute wound healing model. The significance of this could not be calculated due to non-matching data sets.

Collagen levels increased from the beginning of the study in all wound groups. Wounds treated with SM + STSG and with MD + STSG showed no significant differences and were both higher than in wounds treated with STSG alone, but lower than in normal skin throughout the study. Mean elastin staining density increased over the course of the study for all three wound groups. Levels were similar in wounds treated with SM + STSG and in those treated with MD + STSG. These two groups reached similar levels to that of normal skin by day 42. Wounds treated with STSG alone showed significantly lower levels throughout the study.

Wounds treated with SM + STSG and those treated with MD + STSG showed similar neodermal

thicknesses which were significantly thicker than wounds treated with STSG alone and normal skin throughout the study. Cellular density increased throughout the study similarly for all three wound groups. There were no significant differences between the wound groups and normal skin at day 42. Inflammatory cell infiltration was lowest in wounds treated with SM + STSG, followed by those treated with MD + STSG and those treated with STSG alone. All wounds showed an inflammatory cell infiltrate similar to normal skin at day 42.

Wounds treated with SM+STSG showed higher initial vascular perfusion than the other wound groups. This however was similar for all wound groups by day 42, and much higher than normal skin. Capillary lumen counts and vWF staining were similar for wounds treated with SM + STSG and those treated with MD + STSG, but bother were higher than in wounds treated with STSG alone and lower than normal skin.

7.7 Conclusions from this study

From this study, it can be concluded that wounds with compromised healing properties treated with SM + STSG follow a very similar would healing trajectory to those treated with MD + STSG. Vascularity and graft take are delayed in wounds treated with STSG alone.

7.8 Subsequent steps

Results from the delayed burn excision model show that biological scaffolds can expedite and enhance wound healing in a compromised wound.

This study was the final experiment carried out for the purpose of research for a PhD. The results of the evidence gained in the *in vivo* pre-clinical setting and that of previous studies pertaining to Smart Matrix™ were subsequently used to design a porcine Good Laboratory Practice study.

Chapter 8: Summary of results

The first two experiments showed that graft take rate in wounds treated with SM+STSG did not differ significantly from those treated with STSG alone, and neither did they differ from wounds treated with MD + STSG and those treated with I + STSG. No adnexal structures were present in any of the wounds.

Wounds treated by SM+STSG contracted less than those treated by STSG alone, which in turn contracted less than wounds allowed to heal by secondary intention. Wounds treated with MD + STSG contracted similarly to those treated with SM + STSG, both contracting significantly less than those treated with I + STSG. EDA-FN and a-SMA staining was attenuated in wounds treated by SM+STSG compared with those treated by STSG alone and those allowed to heal by secondary intention. Wounds treated with MD + STSG showed higher levels of EDA-FN and a-SMA earlier in the study, while wounds treated with I + STSG showed the highest levels, which decreased to those of normal skin by day 42. There were no significant differences thereafter and levels returned to that of normal skin in all wound groups.

Collagen and elastin levels remained lower than those of normal skin for wounds treated with SM + STSG, those treated with STSG alone and those allowed to heal by secondary intention. Collagen levels reached those of normal skin by day 42 in wounds treated with SM + STSG and by day 180 in the other 2 wound groups. Wounds treated with SM + STSG reached collagen and elastin levels similar to those of normal skin 7 days later than wounds treated with MD + STSG (day 35). Collagen deposition followed cellular ingress both temporally and spatially. Elastin levels resembled those of normal skin for these latter 2 wound groups by day 42.

The dermal scaffold persisted from an average of 21 days in wounds treated with SM + STSG, 35 days in those treated with MD + STSG and 84 days in those treated with I + STSG.

Wounds treated with SM+STSG initially showed a thicker neodermis and increased cellular density, which approached that of normal skin by day 35. Wounds allowed to heal by secondary intention showed lower maximal wound thickness throughout the study but significantly thicker wounds at day 180. Wounds allowed to heal by secondary intention showed the highest levels of inflammation, followed by wounds treated with STSG alone and then by those treated with SM + STSG. Wounds treated with SM + STSG and those treated with MD + STSG showed peaks in wound thickness by day 21 and a decrease thereafter. Wounds treated with I+STSG showed a delay in peak wound thickness by day 42. At day 180 all three wound groups showed a similar neodermal thickness to that of normal skin. Wounds treated with SM + STSG and those treated with MD + STSG showed very similar levels of wound cellular density, which were higher than both those of normal skin and wounds treated with I + STSG at the end of the study. Wounds treated with SM + STSG and those treated with MD + STSG showed similar levels of inflammatory cell density, which approached that of normal skin by ay 28. Wounds treated with I + STSG showed higher levels of inflammation than the other two wound groups but approached that of normal skin by day 35.

Wounds treated with SM+STSG showed the most pronounced and earliest vascular response with statistically significant higher levels of wound perfusion, capillary lumen count and vWF staining compared to wounds treated with STSG alone, and in turn the latter group showed higher levels than wound allowed to heal by secondary intention. There were no significant differences in all these parameters (except for vWF staining, which was higher in wounds allowed to heal by secondary intention) when compared to normal skin at day 180. Wounds treated with SM+STSG showed a very similar trajectory in terms of vascular parameters (perfusion, capillary lumen count and vWF staining) to those treated with MD + STSG. Wounds treated with I + STSG showed a delay until day 42. There were no significant differences between the wound groups and when compared to normal skin at day 180.

When compared to parallel acute full thickness wounds treated with STSG in the same animals, the delayed partial excision burn wounds showed a 14 day delay in wound contraction. The acute and attenuated wound healing models showed no significant differences in EDA-FN and a-SMA staining, except at days 14 and 21, where EDA-FN was higher in the burn wound. Collagen and elastin staining were similar in the two wound groups except at day 21 where elastin staining was significantly higher in the acute wound.

Vascular perfusion remained lower in the burn wounds group throughout the study. Capillary lumen counts and vWF staining levels were lower in the burn wounds initially but there were no significant differences at day 42. The partial thickness excision burn wound demonstrated a 21 day delay in the vascular ingress of the wound and new capillary formation, while the acute wound demonstrated a vigorous and relatively rapid initial increase in vascularity. Burn wounds showed a significantly higher wound depths and cellular density, but a lower inflammatory cell infiltrate. Whereas acute wounds gave an expected exudative granulation response, the partial burn excision wound did not produce exudative granulation tissue, but showed a markedly oedematous wound bed with delayed inflammatory infiltration (of 21 days) beneath the wound surface, followed by some fibrovascular granulation tissue ingress after the 14 day delay period. This histological pattern could be called delayed internal granulation to distinguish it from the exudative granulation outwards from the wound bed seen in the acute wound healing response. Additionally, the thickness of the wounds was significantly larger in the partial excision burn.

From this experiment, it was concluded that the partial thickness excision of a burn wound healing trajectory is characterised by a delayed healing response, with delayed epithelialisation, delayed angiogenesis, and prolonged tissue oedema.

When the validated attenuated wound healing model was used to examine the behaviour of Smart Matrix™ + STSG and to compare it with the wound healing trajectory of MD + STSG and STSG

alone, the wounds groups treated with matrices showed similar macroscopic features and graft take success and epithelialisation. Wounds treated with STSG alone showed a delay in epithelialisation and a lower rate of successful graft take. The wounds treated with SM + STSG and those treated with MD + STSG showed similar wound areas to each other and to the tattooed area by day 42. The wounds treated with STSG alone contracted more than all three other groups. EDA-FN staining in wounds treated with SM + STSG was similar throughout the study to that of normal skin, while significantly higher in wounds treated with MD + STSG and I + STSG. EDA-FN staining was highest in wounds treated with STSG alone followed by those treated with MD + STSG and then by those treated with SM + STSG, where levels similar to that of normal skin were reached by day 42, in the latter group. There were no significant differences in α-SMA staining in normal skin and wounds treated with SM + STSG. Wounds treated with MD + STSG showed higher levels than these groups until day 28, while wounds treated with STSG alone showed the highest levels, which persisted until day 42.

The dermal scaffold persisted from an average of 21 days in wounds treated with SM + STSG, 35 days in those treated with MD + STSG and 84 days in those treated with I + STSG. Scaffold persistence was longer in the attenuated wound healing model than in the acute wound healing model. The statistical significance of this could not be calculated due to non-matching data sets.

Collagen levels increased from the beginning of the study in all wound groups. Collagen deposition followed cellular ingress both temporally and spatially. Wounds treated with SM + STSG and with MD + STSG showed no significant differences and were both higher than in wounds treated with STSG alone, but lower than in normal skin throughout the study. Mean elastin staining density increased over the course of the study for all three wound groups. Levels were similar in wounds treated with SM + STSG and in those treated with MD + STSG. These two groups reached similar levels to that of normal skin by day 42. Wounds treated with STSG alone showed significantly

lower levels throughout the study.

Wounds treated with SM + STSG and those treated with MD + STSG showed similar neodermal thicknesses which were significantly thicker than wounds treated with STSG alone and normal skin throughout the study. Cellular density increased throughout the study similarly for all three wound groups. There were no significant differences between the wound groups and normal skin at day 42. Inflammatory cell infiltration was lowest in wounds treated with SM + STSG, followed by those treated with MD + STSG and those treated with STSG alone. All wounds showed an inflammatory cell infiltrate similar to normal skin at day 42.

Wounds treated with SM+STSG showed higher initial vascular perfusion than the other wound groups. This however was similar for all wound groups by day 42, and much higher than normal skin. Capillary lumen counts and vWF staining were similar fro wounds treated with SM + STSG and those treated with MD + STSG, but bother were higher than in wounds treated with STSG alone and lower than normal skin.

Chapter 9: Discussion

These experiments showed that Smart Matrix™ supports the long term survival of a split thickness skin graft when applied as a single step procedure in both simple and challenging cutaneous porcine wound models, with a reduction in wound area contraction and inflammation compared to other wound groups. The partial thickness excision of a full thickness burn in a pig was validated as a useful attenuated wound healing model.

As with all studies, this project has its limitations. The major limitation in these experiments was the use of porcine skin models to simulate human cutaneous wound healing. As highlighted in the literature review, the porcine skin model remains the gold standard as it shares many similarities in hair follicle and blood vessel patterns, collagen and elastin content and wound healing and turnover time that are more similar to humans than the other mammal models (Heinrich *et al*., 1971). Pig skin however only shows a 78% concordance with human skin (Sullivan *et al*., 2001). The porcine dermis and its hair follicles are less vascular with a more sparse hair distribution (Seaton *et al.*, 2015). Differences in the pilosebaceous units are important in that porcine skin lacks eccrine glands on its flanks, having only apocrine glands (Seaton *et al.*, 2015). This factor could have some influence on the interpretation and extrapolation of the results of the experiments described in this thesis, as in humans eccrine sweat glands distributed over the entire body serve as essential sources of keratinocytes during wound epithelialisation (Rittie *et al*., 2013). Additionally, the fibrin used in Smart Matrix fro these experiments was of bovine origin. The potential differences in the mechanism of action of porcine plasmin on fibrin were not taken into account, and may therefore have somehow influenced some results. In Smart Matrix produced for human use, human fibrin from polled blood collection is used. In order to better study scarring potential, it would also have probably been more appropriate to use Red Duroc pigs to establish scarring parameters, as they have a tendency to form hypertrophic scars similar to humans. However, their use was prohibited due to

their increased tendency for malignant hyperthermia, and as these experiments required multiple general anaesthetics, the risks of losing the pigs mid-experiment was too high.

It would have been ideal if the surgeons were blinded to the treatments in question. This was not possible, in this case, as it would have been way too costly to employ another surgeon to carry out these experiments. Additionally, a clinician with sufficient expertise and knowledge in skin grafting procedures and the application of dermal matrices was required to perform these procedures, so most plastic surgery trained doctors would have this prior knowledge. Even if the product names were hidden, they would be immediately recognisable. The author (RZA) is a surgeon with experience in plastic surgery, and hence was familiar with the various products prior to the commencement of the experiments. Her surgical assistant and then supervisor, JFD was familiar with the products through their multiple use in the previous Smart Matrix™ experiments.

During these experiments, many punch biopsies were taken (an 8mm much biopsy was taken at every time point from a circular wound with a 4cm diameter). Although the same amount of these biopsies were taken from all the wounds and from the tattooed area, it is possible that these interfered with the true calculations of wound area and contraction. Also the new wounds then created by these biopsies then healed largely by secondary intention with influence of adjacent tissue. While the surgeons made it a point to take avoid taking biopsies at previous biopsy sites, this tissue might have influenced and somewhat altered true histological findings. The biopsy sites were randomly assigned (informal randomisation) and the first biopsy site was generally taken from the centre of the wound. This would have introduced a sampling bias due to the influence of keratinocyte migration from the wound edges in those biopsies taken more laterally. This could have been mitigated if biopsies were taken at equal distances from the wound edges at each time point, thus decreasing the potential for artefectually skewed results. The sampling schedules were designed following common practices encountered in the medical literature. However, most were not formally validated. Additionally, the use of bipolar diathermy was limited as much as possible, to avoid the

burnt wound bed stimulating a different response. Where possible bleeding was stopped with pressure using a damp gauze. However, on occasion bipolar diathermy was the one resort capable of stemming bleeding.

It wound be helpful in future experiments if the periphery of the wounds was tattooed (about 2mm out of the skin marking) just prior to excision or injury, in order to more easily establish the seams in long term studies and in order to more easily calculate wound area.

It was noted that wound positions altered the macroscopic shape of the wound as the experiments progressed, for example the anterior shoulder wounds took on a more elliptical shape with an oblique direction, while the inferior flank wounds appeared more horizontal and elliptical. This might have influenced the wound area and contraction calculations. In order to mitigate this, the wound treatments were randomly assigned to wound positions. Potential differences in wound behaviour at differing sites on the animal (and difference in skin growth rate between wound locations and tattooed reference location) – in future experiments this could partially be circumvented by retrospectively looking at the distribution of treatment interventions in each wound site to see if there was equity by the end.

The very nature of the pig is that it lives in a relatively unclean environment. While the wounds were meticulously dressed with many layers, and the Orthoplast jacket was waterproof, on some occasions the pigs still managed to get their dressings soiled and some hay still managed to make its way onto the wound bed (though only on 2 occasions). This may or may not have had some influence on the wound healing properties. Of note, no wounds displayed overt signs of infection, and all pigs remained healthy.

When creating the burn wounds in Experiment 3, a method was devised to ensure full thickness burning consistently. However, some inadvertent variability may have occurred due to the ambient temperature in the operating theatre and the pig's core temperature. This method was first verified

at the end of experiment one, using some of the pigs, immediately before sacrifice, and hence may not have been completely representative of the live animal. The various burns created demonstrated the heat needed to create full thickness burn wounds on the pigs' flanks.

In order to reduce inter-observer variability when grading the histology slides, both the author and the scientist carrying out the second reading went through a number of slides to agree on the grading system. It is still however, possible that there remained a degree of inter-observer variability.

In the calculation of capillary lumen count, it is possible that multiple lumina of the same vessel were counted, and that this resulted in an artificially high capillary lumen count. Where this was relatively obvious, for example many lumina close together in one vector, it was accounted for, but other such opportunities may have been missed. In order to mitigate this, capillary lumen count was not the only parameter used to measure for vascularity. It may be argues that the sampling method used for histological analysis somewhat fell short of adequate, as three random areas in the slide were chosen for examination. In some cases, especially in cellular density measurements, due to presence of cell whorls, some measurements may have been artefactually skewed. In future experiments, it might be useful to adopt a systematic approach to picking the areas of the three samples, such as far left, centre and right. Additionally, the sampling validity may be brought into question as it could be argued that more measurements could have been made. The randomisation (of wounds, biopsy sites and histology slide site was done on an informal basis. The use of IT software to generate a less biased randomisation is preferable. Discrete variables were used in this thesis. When reporting summary statistics for such variables, the convention is to report one more decimal place than the number of decimal places measured. This would lead to a sample mean value that does not necessarily appear typical of the other sample measurements, when it could then be argued that the median should be used. However, as parametric tests were used in this thesis (following the assumption of a normally distributed population) the mean was used. This is because one of its im-

portant properties is that it minimises error in the prediction of any one value in sample data set. That is, it is the value that produces the lowest amount of error from all other values in the data set.

The recipient-site response to biologic ECM scaffold materials involves both the innate and acquired immune system and the response is affected by device's raw material composition, among other factors. (Badylak *et al.*, 2008). The fibrin alginate matrix acts as a scaffold for the migration and proliferation of cells involved in wound healing, as well as a reservoir for growth factors and cytokines. Post-wounding angiogenesis relies on fibrinolysis. (Hadjipanayi *et al*., 2015). While the exact mechanisms of this event remain poorly understood, it could be hypothesised that the scaffold's fibrin component is responsible for fibrinolysis-mediated angiogenic disinhibition, as postulated by the *in vitro* study by Hadjipanayi *et al*., in 2015. Hence, the presence of fibrin in the wound bed stimulates an angiogenic response. The outcome of wound healing depends largely on the fibrin structure, such as the thickness of the fibres, the number of branch points, the porosity, and the permeability (Laurens *et al*., 2006). As fibrin persists in the wound as seen through scaffold presence) for 21 days in the acute wound, this would explain why new vessel formation was most marked in the first 21 days. During the angiogenesis process, the fibrin matrix is degraded by endothelial cells. Fibroblasts and endothelial cells adhere to integrin binding motifs in native and denatured collagens, and elastin. These cells migrate into the matrix and proliferate by forming new capillary-like tubes (Staton *et al.,* 2003). This would provide an explanation as to why Matriderm™'s behaviour and that that of Smart Matrix™ were very similar in our experiments. A constituent of Matriderm™ is an elastin peptide motif. This enhances angiogenesis by promoting endothelial cell migration and tubulogenesis through the upregulation of matrix metalloproteinases

(Robinet *et al.*, 2005). Once fibroblasts and endothelial cells invade the fibrin-rich clot in the wound space, the synthesis of a new permanent ECM occurs, hence the new temporary fibrin matrix also promotes granulation tissue formation. These cells are recruited from the tissue adjacent to the wound (Gorodetsky *et al*., 1999) and once they have infiltrated the provisional matrix, they realign to become new vascular structures (angiogenesis). During this process, together with various other cell types, they degrade fibrin through the induction of plasmin activities, metalloproteinases, and the generation of free radicals (Ruoslahti *et al.*, 1996). This provides another explanation as to why Smart Matrix™ shows an early vascular response. Hence the use of a fibrin scaffold is ideal in the circumstances of both acute and especially compromised wound healing, as it provides a stimulus for angiogenesis. This could also explain Smart Matrix™ appears to alter the healing trajectory of the attenuated wound into that of an acute wound, through the fibrin in the matrix stimulating angiogenesis and "kick-starting" the wound healing process.

A key finding in this thesis is that Smart Matrix™ appears to attenuate α-SMA expression. Contractile myofibroblast activity is central to wound healing as it limits the exposed wound area (Li *et al.*, 2011). This is largely dependent on the fibroblast and myofibroblast activation in the granulation tissue of a healing wound. The immune-histological markers for these cells is α-SMA (Darby *et al.,* 1990). As fibrin is the active component in Smart Matrix™, it would be prudent to assume that the fibrin scaffold is responsible for this attenuation. The wounds treated with dermal scaffolds (Smart Matrix™, Matriderm™ and Integra™) contracted less than those treated without scaffolds (STSG alone and those allowed to heal by secondary intention), and wounds treated with Smart Matrix™ contracted less than those treated with the other scaffolds. However, the wounds treated with other scaffolds, STSG alone or allowed to heal by secondary intention did not demonstrate such low levels of α-SMA content. This is a novel finding. Searches in the literature of the influence of fibrin on α-SMA production and on myofibroblast differentiation revealed nothing to con-

tribute to this theory or this finding. However, during haemostasis, (the first occurring component of wound healing), the complement cascade is activated and Complement component C3 induces a prolongation of the fibrin clot (King *et al*., 2015). Tumour necrosis factor–*α* (TNF-*α*) is a potent inflammatory cytokine expressed during the inflammatory phase of wound healing secreted alongside C3 (Esmon 2000). The potent pro- inflammatory cytokines C3 and TNF-α activity are interlinked (Page *et al*., 2018). TNF-α is upregulated, upon encountering the fibrin clot. It contributes to changes in coagulation and C3 induction. Higher TNF-α levels are associated with lower α-SMA expression in human dermal fibroblasts in granulation tissue (Goldberg *et al*., 2007). In 2007 Goldberg *et al* found that this suppression occurs at mRNA level due to antagonistic effect of TNF-α on TGF-*β*1-induced myofibroblast differentiation. (Goldberg *et al.*, 2007). During skin wound repair, fibroblasts transition to myofibroblast under the influences of mechanical stress, cytokines, and an array of ECM molecules, resulting in fibroblast–ECM matrix remodelling and leading to a change in the matrix mechanical tension (Goldberg *et al*., 2007). In view of these findings, it could be proposed that that the prolonged persistence of fibrin in the wound bed induces the sustained upregulation and therefore content of TNF-α, which in turn suppresses α-SMA expression. While fibrin is present in every cutaneous wound and is responsible for inducing homeostasis and releasing the pro-inflammatory cytokines, its presence in the wound bed is usually short lived. As seen in experiments 2 and 4, the scaffold is present in the wound bed for an average of 21 days in the acute wound, and longer in the compromised wound. This longevity of this presence and its slow degradation is attributed to the glutaraldehyde stabilisation. It is this prolonged exposure to what is essentially an organised fibrin clot that acts as a persisting stimulus for TNF-α (together with C3) production which suppresses myofibroblast differentiation and thus α-SMA expression. As seen in experiments 1, 2 and 4, following degradation of the scaffold, α-SMA expression tends to increase again (though to a lesser extent than in other wounds using other scaffolds or STSG alone or secondary intention healing) at days 28 and 35. However, the other wound groups showed that α-SMA

expression is at its most pronounced during the early days of wound healing. Hence, the persisting presence of fibrin during the first 21 days following cutaneous injury is key to suppressing α-SMA expression and reducing wound contraction. To allow for the progression of wound healing, it is also imperative that the fibrin scaffold does not persist for longer, as otherwise the persistent presence of pro-inflammatory cytokines could result in continued TNF-*α* - mediated inflammation and prevent normal matrix deposition. In the normal scenario, TNF-*α* is not present during the re-epithelialisation and ECM reorganisation phases of wound healing (Singer *et al.*, 2009).

The above theory is in keeping with the levels of inflammation shown in wounds treated with SM+STSG. Following degradation of the scaffold in both the acute and the challenging wound, inflammatory cell densities decreased. This would be in keeping with the decreased expression of the pro-inflammatory cytokines following the disappearance of the fibrin clot stimulus. TNF-*α* level quantification studies were not carried out to test this postulated explanation for attenuated α-SMA expression.

It was noted in Experiments 2 and 4 that wounds treated with Smart Matrix™ and with Matriderm™ both demonstrated higher elastin densities. While this can be readily explained in the case of Matriderm™, as elastin is one of its key components, it is not so straightforward with Smart Matrix™. It could be postulated that, as elastin is produced by fibroblasts (Sephel *et al.,* 1986) (not myofibroblasts), as seen through the the attenuation of α-SMA expression, there is probably a larger number of fibroblasts in wounds treated with Smart Matrix™ than in the other wounds, hence allowing for the *de novo* synthesis of elastin.

Yannas *et al* hypothesised that the pore size in a collagen dermal scaffold maybe responsible for the attenuation of wound contraction (Yannas *et al.,* 1980), and the presence of the scaffold within the wound bed physically prevents contraction, as it interrupts the forces of mechanical stress across the wound. Yannas later argued that dermal templates improve skin regeneration by preventing wound

contraction (Yannas *et al.* 2011, Yannas *et al*., 2015). If this theory were extrapolated to all dermal substitutes, this could in part provide an explanation for the decreased contraction seen in wounds treated both by Matriderm™ and Smart Matrix™. This theory is reinforced by the delay observed in wound contraction together with the longer scaffold persistence in the attenuated wound healing models treated with dermal matrices, compared with the wounds treated with STSG alone. Also, it accounts for the lesser degree of wound contraction seen in wounds treated with SM + STSG, compared to those allowed to heal by secondary intention and those treated with STSG alone. Hence the length of time the scaffold is present in the wound is significant if it is to act as a mechanical wound "splint". For fibrin to be effective as a scaffold biomaterial, it must be capable of resisting the forces of contraction for a sufficient amount of time to allow for the new permanent ECM formation. Hence, some from of stabilisation is necessary to reduce the rate of proteolytic degradation, (Mimura *et al*., 2016) particularly by plasmin. The scaffolds are chemically cross-linked (Lee., 2001, Mimura *et al.,* 2016) to achieve this. Glutaraldehyde is used for Smart Matrix™.

While scaffold presence in the wound requires to be long enough to physically attenuate wound contraction to allow for the promotion of angiogenesis, the degradation of the scaffold is an essential component of a rapid constructive remodelling response (Badylak *et al.,* 2008), as *in vivo* and *in vitro* studies have shown that low molecular weight peptides formed during this degradation have chemoattractant potential for several cell types including multipotential progenitor cells and bone-marrow derived cells that participate in the long-term dermal remodelling (Badylak *et al*., 2001). Another advantage of the fibrin–alginate matrix not lingering in the wound is that some longer-lasting dermal scaffolds mount a low grade chronic inflammatory foreign body reaction (Badylak *et al.,* 2008). However, as fibrin undergoes proteolytic degradation "once its job is done" (but rapid break-down is limited by the glutaraldheyde cross-linking), it does not produce a prolonged pro-angiogenic effect and neo-cellularisation stops once the scaffold ceases to be present in the ECM.

Hence, the scars appear flat and pale in the long term. It is evident from observing the behaviour of Matriderm™ and Smart Matrix™ in the attenuated wound healing model that dermal scaffolds persist in the wound bed until new permanent ECM deposition has occurred. This is integral to their ability to aid in the healing of wounds with attenuated healing properties.

Of the products in wide clinical use, the pro-angiogenic properties of Integra™ and Matriderm™, have been attributed to their constituent ECM materials. As postulated by Badylak *et al* the histological integration of each different material is distinct. Vascularisation of the Integra™ sponge structure of 300-500 um thickness takes 14-21 days (as seen in the second experiment). It is only at the point that this superficial tissue is formed that a STSG is typically applied. Although Integra™ collagen has been described as an angiogenic material, its histological effect in the porcine model is to attenuate the innate granulation response. The histological integration response to 1 mm thick Matriderm™ matrix in the same porcine full thickness wound model is also distinct. The material is completely degraded in acute wounds over a period of 35 days. By contrast the fibrin alginate scaffold shows a rapid and dense vascularisation response. Split thickness skin grafting with Smart Matrix™ showed a higher degree of cellular influx and a more rapid rate of angiogenesis at earlier time points, when compared to split thickness skin graft in alone and when compared to Integra™ + STSG, but these parameters were very similar to Matriderm™ + STSG, in the acute wound and in the attenuated wound model.

The long-term survival and stability of wound treated with Smart Matrix™ was evident throughout this thesis through the comparison of the macroscopic and histological observations including collagen and elastin) parameters of the healing skin with normal skin. The long-term studies showed that all parameters approximated that of normal skin by day 180, with the absence of adnexal structures. In keeping with the findings of Philandrianos *et al* in 2012, where 5 different dermal scaf-

folds compared in a long term porcine experiment showed no differences, this was in common for the other dermal scaffolds too (Philandrianos *et al*., 2012).

The ability to employ as dermal scaffold as a one step procedure in both the acute and the attenuated models, as opposed to multi-steps requires less frequent visits to the operating theatre. This in turn is associated with a shorter in-hospital stay, and quicker return to normal activities for the patient. This would prove more cost-effective to the healthcare system and also to the patient and his / her carers. Additionally, the fibrin used in the production of Smart Matrix™ is pharmaceutical grade and is sourced from pooled human blood transfusions. The manufacture process of the raw material is far less costly than that of animal-derived dermal scaffolds. The latter require the rearing, housing and maintenance of the animals followed by sacrifice, harvesting and preparation of the dermis, rendering it acellular and devoid of DNA. This is also advantageous for those religious groups, namely Islam and Judaeism, who oppose the use of porcine derived products and Hindus who oppose the use of bovine-derived products. Conversely, the use of Smart Matrix™ may be met by opposition by Jehovah's witnesses (as the fibrin is derived from human blood products, albeit acellular).

It was noted (but not objectively assessed) by the surgeons using Smart Matrix™ that as a scaffold, it was very easy to handle, both using instruments and using gloved hands. These scaffolds, when their backing is removed, are often notoriously taxing when trying to handle, after they are wetted, especially if they fold over on themselves and need to be unfolded. Smart Matrix™ proved to not tear easily when manipulated, and as it is protein–based, if it folds over, all that is required is for it to be re-immersed in the saline and it unravels alone.

If extrapolated to human clinical scenario, this evidence suggests that Smart Matrix™ may present a novel, non-animal derived dermal replacement scaffold, that may expedite the healing trajectory

of large area wounds that require skin coverage with a skin graft, and may favourably alter the healing trajectory of challenging and indolent wounds and facilitate their healing.

While these studies focussed mainly on the quality of the skin graft and resulting scar *per se* a few other pertinent factors also need to be taken into account.

These experiments highlighted the potential for fibrin to attenuate α-SMA expression production and hence limit the differentiation of fibroblasts into myofibroblasts thereby reducing wound contraction. The exact relationship between fibrin and α-SMA expression needs to be elucidated at a molecular level with further research into the suppressive action and quantification of TNF-α and its relationship to myofibroblast differentiation and wound contraction. The mRNA regulation of α-SMA expression also needs to be elucidated. This phenomenon could be potentially be employed in a variety of other clinical scenarios. It may prove to beneficial to some pathologies that are associated with fibrosis and a high α-SMA content. Dupuytren's contracture is one such fibroproliferative disorder affecting the palmar fascia of the hand, characterised by the increased proliferation and differentiation of fibroblasts to myofibroblasts and accompanied by elevated α-SMA expression. (Krasskova *et al.*, 2019). Hence is probably worth exploring the effect fibrin might have on disease progression or prevention.

Further research into the quality of the healed wound and the properties of the resulting skin may prove useful. So far skin grafted skin lacks adnexae. When used to cover small areas, the provision of a water tight barrier may be sufficient, however, in the case of very large wounds, for example reconstruction following a large burn or resection after necrotising fasciitis, other properties, such as sweating would be immensely beneficial. Further research into improving the reconstructed skin's "function" is needed. The "seam" between innate uninjured skin and the skin graft requires evaluation, as particularly in humans this is often a cause of cosmetic morbidity, in terms of vascular or pigmented raised edges. Additionally, skin grafts were studied over relatively non-mobile ar-

eas of the pig, the flanks) not over dynamic areas such as joints. Further research into the wound healing trajectories of skin undergoing plenty of movement during healing would be beneficial. It would be useful if larger area wounds were examined together with the evaluation of resultant skin with overlying meshed graft. Meshed grafts often require to be used due to a relative paucity donor skin skin available. It tends to produce a "fish net" or snake skin like appearance that is usually considered a cosmetic compromise. The presence of an underlying scaffold may influence the appearance of the resulting new skin. As thinner skin grafts tend to produce less donor site morbidity, studies into the optimal skin graft thickness, ie the thinnest graft possible that would yield the best cosmetic results, would be useful. It would be useful to explore the potential properties of the Smart Matrix™ scaffold in more superficial wounds as wound dressings such as in superficial large area burns and in the potential reduction of morbidity of split thickness skin graft donor sites.

In order to bring Smart Matrix™ to the patient, to help alleviate the suffering associated with large and challenging wounds, a series of steps are necessary. Gaining acceptance into the various national pharmacopeias (such as the British National Formulary, and the US pharmacopeia among others) is an extremely costly multi-process and very arduous task. It is a necessity for any product to undergo a Good Laboratory Practice pre-clinical study, before any human clinical trials can commence. Following the completion of the experiments presented in this thesis, the author was intrinsically involved in the design (but did not carry out any of the experiments or process any of the data) of a GLP study for the *in vivo* evaluation of Smart Matrix™: Safety and Performance of the Smart Matrix™ Wound Repair Scaffold in a Porcine Acute Wound Healing Model. The design involved the creation of four acute full thickness wounds on the pigs to be treated with SM + STSG in a 28 day and 84 day study. In order to plan and design further investigation and trials, the Smart Matrix™ scaffold would require to be classified as a drug or as a medical device, as the steps required for their approval differ quite markedly. At the time of writing (2019), RAFT and SML have

classified Smart Matrix™ as a class III medical device (a medical device with substantial risk). This would require a clinical trial. The author was also intrinsically involved in a design (but did not participate) for a pilot study. In brief, healthy, non-smoker, non-pregnant patients above the age of 18, undergoing wide local full thickness excisions of non-melanomatous skin cancers on their lower limbs were invited to volunteer. This study was limited to a maximum of 7 patients. Non-melanomatous skin cancers (basal cell carcinoma and squamous cell carcinoma) were chosen, as their surgical management (as per the British Association of Dermatology guidelines) dictates an excision of the full thickness of the tumour and the skin to the underlying layer (fascia or fat) with a minimum of a 4mm peripheral margin (Telfer *et al.,* 2008, Motley *et al*., 2009), thus leaving a (usually) circular full thickness skin defect that is too large to be closed primarily (especially as the skin on the lower leg does not usually stretch enough to allow direct closure of such wounds).

To date, no existing dermal replacement scaffold meets all the expectations of an ideal regenerative wound matrix. A very large number of difference matrices are commercially available and others undergoing research. These range from natural biological materials such as autografts, allografts and xenografts,, synthetic materials and composite scaffolds. Traditionally, synthetic matrices have offered excellent predictable control over material and mechanical properties (MacEewan *et al.*, 2017). However, the architecture and some of the regenerative properties are lacking. As Smart Matrix™ uses pharmacological grade fibrin as its major constituent, it combines the advantages of synthetic construction with the positive regenerative attributes of biologic materials.

The preliminary evidence obtained in the third experiment described and validated the partial thickness excision of a full thickness burn model, as a pre-clinical model for some challenging wounds. The zone of stasis in Jackson's burn model (lying between the necrotic plug of burnt issue centrally and the zone of hyperaemia on the outside) is characterised by decreased tissue perfusion , which is potentially salvageable (Hettiarachy *et al*., 2004). Depending on the wound environment, this zone

can either survive or proceed into necrosis. While in the human patient the initial management is resuscitation to increase tissue perfusion to the area, during this experiment, the pig received no systemic management. Hence the zone of stasis remained compromised. The burns were inflicted on day -1, and were excised on day 0 so as not to allow this zone to completely progress to necrosis. This was verified as after the necrotic plug was removed pale but sluggishly bleeding tissue was left *in situ*. The pathophysiology of a burn wound is characterised by a histamine and direct heat mediated reaction leading to rapid oedema formation, due to increased microvascular permeability, vasodilation and increased extravascular osmotic activity (Arturson 1980). Inflammatory cytokines contrite to cell membrane damage partly caused by oxygen-free radicals released from polymorphonuclear leucocytes (Arturson 1980). The development of oedema formation is biphasic. In the first hour during the primary phase the traumatised tissues undergo an abrupt increase in water content while during the second phase a gradual increase in the fluid influx into both burned and surrounding tissues occurs over 12-24 hours (Kaddouri *et al*., 2017). The findings in experiment 3 were consistent with the literature. The compromised wound model showed a higher density of inflammatory cells. Excessive neutrophil infiltration appears to be a common and critical finding in chronic wounds (Zhao *et al*., 2016). In acute simple wounds, the inflammatory infiltrate usually resolves after 14-21 days when infiltrated white cells return to their pre-inflammation numbers (Zhao *et al.*, 2016). In this experiment, the burn wounds showed a lag phase of 21 days for an inflammatory response when compared to the non-burn wounds, as non-burn wounds showed a significantly higher inflammatory cell density than the non-burn wounds at days 7, 14 and 21. However, the inflammation was prolonged until day 35 in the burn wound group. Hence it could be concluded that the wound healing model did simulate chronic wounds both macroscopically and histologically over the course of the experiment. As it subsides, extracellular matrix reconstitution begins, with an accumulation of fibroblasts and to synthesise granulation tissue. Fibroblasts are responsible for ECM (and its constituents) synthesis of this matrix. As discussed above, a relative

increase in fibroblasts (due to less differentiation into myofibroblasts) could provide an explanation as to why the dermal scaffolds appeared to "convert" the challenging wounds into simple wounds in experiment 4. The limiting of inflammation is beneficial as prolonged and exacerbated inflammation impairs wound healing and adversely affects scarring (Qian *et al*., 2016)

Although this model only simulates local pathology, as opposed to a systemic disease, it is characterised by an oedematous and relatively avascular dermal zone, with an inflammatory granulation healing response with the histological characteristic of scar formation. There is no indication from the histological parameters observed that there is a destructive level of wound protease activity in this model however, because the wound bed structure, characterised by oedematous swelling, is preserved during the infiltration of inflammatory granulation tissue and subsequent progression to fibrosis after the two week delay period. This is further confirmed in Experiment 4 by the persistence of the scaffold in this model, longer than in the acute wound healing model. As discussed above, it may be inferred that the scaffold treatments are responsible for activating a healing response in an otherwise delayed internal inflammatory granulation of the zone of stasis. This is indicative that the mechanisms involved in supporting angiogenesis in acute healing stimulate a healing response that must communicate through the wound stasis zone in this delayed model. While this model may indeed prove to be useful as a model for compromised wound healing, it does have its limitations. As seen in this thesis porcine experiments are costly to run, as these involve housing and feeding the pigs, the use of operating theatres and equipment and surgical expertise. While this model is relatively easily reproducible and reliable, there will still be a degree of burn depth discrepancy between wounds and between pigs, due to differences in core temperature and ambient temperature. This may have implications on experiment results if this wound is used as a model for burns. Additionally, such challenging wounds often have many different parameters rendering them indolent to wound healing (as discussed in the literature review). This wound model only provides

one uni-dimensional local modulation, without systemic compromise. It would be useful, as a future step to evaluate this wound model in streptozocin induced diabetic pigs, to more closely simulate clinical scenarios. Additionally, wounds of the area studied in this thesis often heal without sequelae in the human patient. Future experiments should include a small number of larger area wounds on pigs. However, in order to achieve statistical significance of results, more subjects would need to be enrolled into a study, or as described above, more samples wound need to be taken.

To date there exists no pre-clinical model of attenuated wound healing that accurately mirrors that encountered in the clinical scenario. The porcine model remains the gold standard animal model of cutaneous wound healing. Further studies into local and systemic modulation of the partial thickness excision of the porcine full thickness burn wound would be useful in the evaluation of wound healing adjuncts for some challenging wounds.

Chapter 10: Conclusions

From the work described in this thesis, it can be concluded that Smart Matrix™ supports regenerative healing of acute and attenuated full thickness cutaneous wound in the pig.

These pre-clinical results demonstrate that Smart Matrix™ persists in the wound long enough to stimulate a rapid-onset and relatively vigorous angiogenic response, without persisting in the wound long enough to stimulate a foreign body reaction or to cause excessive vascular tissue formation or a raised scar. In pigs, the use of Smart Matrix™ in combination with a split thickness skin graft as a single step procedure results in histological remodelling resembling normal dermis while limiting wound contraction.

Furthermore, the porcine partial thickness excision of a full thickness burn was proven to be an easily reproducible and reliable model for attenuated cutaneous wound healing, using the animal whose skin bears the closest semblance to that of humans. Following the validation described in this thesis, this model can now be employed in the development and evaluation of wound dressings and various other wound healing adjuncts. It could also be used to broaden the understanding of compromised wound healing.

Chapter 11: References

Abdullahi A, Amini-Nik S, Jeschke M. (2014). Animal models in burn research. *Cellular and Molecular Life Science.* 71 (17), p3241-3255.

Ahn C, Mulligan P, Salcido RS. (2008). Smoking-the bane of wound healing: biomedical interventions and social influences. *Advances in Skin and Wound Care.* 21 (5), p227-236.

Ahn S, Mustoe T. (2008). Effects of ischemia on ulcer wound healing: a new model in the rabbit ear. *Annals of Plastic Surgery*. 24 (1), p17-23.

Aksoy M, Vargel I, Canter I, Erk Y, Sargon M, Pinar A, Tezel G. (2002). A new experimental hypertrophic scar model in guinea pigs. *Aesthetic Plastic Surgery*. 26 (5), p388-396.

Allen F, Asnes C, Chang P, Elson E, Lauffenburger D, Wells A. (2002). Epidermal growth factor induces acute matrix contraction and subsequent calpain-modulated relaxation. *Wound Repair and Regeneration.* 10 (1), p67-76.

Alsaad K, Obaidat N, Ghazarian. (2007). Skin adnexal neoplasms--part 1: an approach to tumours of the pilosebaceous unit. *Journal of Clinical Pathology*. 60 (2), p129-144.

Altman D, Bland J. (1995). Statistics notes: the normal distribution. *BMJ*. 310 (6975), p238.

Andrews C, Kempf M, Kimble R, Cuttle L. (2016). Development of a Consistent and Reproducible Porcine Scald Burn Model. *PLoS One*. 11 (9), epub.

Ansell D, Holden K, Hardman M. (2012). Animal models of wound repair: are they cutting it. *Exp erimental Dermatology*. 21 (8), p581-585.

Arbiser J. (1996). Angiogenesis and the skin: a primer. *Journal of the American Academy of Dermatology*. 34 (1), p486-497.

Arnold M, Barbul A. (2006). Nutrition and wound healing. *Plastic and Reconstructive Surgery*. 117 (7Suppl), 42S-58S.

Arturson G. (1980). Pathophysiology of the burn wound. *Annales Chirurgie et Gynaecologicae*. 69 (5), p178-190.

Avci P, Sadasivam M, Gupta A, De Melo W, Huang Y, Yin R, Chandran R, Kumar R, Otufowora A, Nyame T, Hamblin M. (2013). Animal models of skin disease for drug discovery. *Expert Opinions in Drug Discovery*. 8 (3), p331-55.

Ayuk S, Abrahamse H, Houreld N. (2016). The Role of Matrix Metalloproteinases in Diabetic Wound Healing in relation to Photobiomodulation. *Journal of Diabetes Research.* (epub), 2897656.

Badylak S. (2007). The extracellular matrix as a biologic scaffold material. *Biomaterials*. 28 (25), p3587-93.

Badylak S, Valentin J, Ravindra A, McCabe G, Stewart-Akers A. Macrophage phenotype as a determinant of biologic scaffold remodeling. (2008). Macrophage phenotype as a determinant of biologic scaffold remodeling.. *Tissue Engineering Part A*. 14 (11), p1835–1842.

Badylak S, Freytes D, Gilbert T. (2009). Extracellular matrix as a biologic scaffold material: structure and function. *Acta Biomaterial*. 5 (1), p1-13.

Baneyx, G, Baugh L, Vogel V. (2002). Fibronectin extension and unfolding within cell matrix fibrils controlled by cytoskeletal tension. *Proceedings of the National Academy of Science of the United States of America.* 99 (8), p5139-5143.

Bansal R, Ahmad N, Kidwai J. (1980). Alloxan-glucose interaction: Effect on incorporation of14C-leucine into pancreatic islets of rat. *Acta diabetologica latina* . 17 (2), p135-143.

Barber F, Aziz-Jacobo J. (2009). Biomechanical testing of commercially available soft-tissue augmentation materials. *Athroscopy*. 25 (11), p1233-1239.

Barrientos S, Stojadinovic O, Golinko M, Brem H, Tomic-Canic M . (2008). PERSPECTIVE ARTICLE: Growth factors and cytokines in wound healing. *Wound Repair and Regeneration*. 16 (5), p585-601.

Bello Y, Falabella A, Eaglstein W. (2001). Tissue-engineered skin. Current status in wound healing. *American Journal of Clinical Dermatology*. 2 (5), p2305-2313.

Benavides F, Oberyszyn T, VanBuskirk A, Reeve V, Kusewitt D. (2009). The hairless mouse in skin research. *Journal of Dermatological Science*. 53 (1), p10-18.

Bernatchez S, Parks P, Grussing D, Matalas S, Nelson G. (1998). Histological characterization of a delayed wound healing model in pig. *Wound Repair and Regeneration*. 6 (3), p223-33.

Bi H, Jin Y. (2013). Current progress of skin tissue engineering: Seed cells, bioscaffolds, and construction strategies. *Burns Trauma*. 1 (2), p63-72.

Bishop A. (2008). Role of oxygen in wound healing. *Journal of Wound Care*. 17 (9), p399-402.

Blackwood K, McKean R, Canton I, Freeman C, Franklin K, Cole D, Brook I, Farthing P, Rimmer S, Haycock J, Ryan A, MacNeil S. (2008). Development of biodegradable electrospun scaffolds for dermal replacement. *Biomaterials*. 29 (21), p3091-3104.

Bochaton-Piallat M, Gabbiani G, Hinz B. (2016). The myofibroblast in wound healing and fibrosis: answered and unanswered questions. *F1000Research*. 5 (F1000), Rev 752.

Bodnar R, Yates C, Rodgers M, Du X, Wells A. (2009). IP-10 induces dissociation of newly formed blood vessels.. *Journal of Cell Science.* 122 (Pt 12), 2064-77.

Brans T, Dutrieux R, Hoekstra M, Kreis R, du Pont J. (1994). Histopathological evaluation of scalds and contact burns in the pig model. *Burns*. 20 (Suppl 1), S48-51.

Breen A, Mc Redmond G, Dockery P, O'Brien T, Pandit A. (2008). Assessment of wound healing in the alloxan-induced diabetic rabbit ear model. *Journal of Investigative Surgery*. 21 (5), p261-269.

Brenes R, Jadlowiec C, Bear M, Hashim P, Protack C, Li X, Lv W, Collins M, Dardik A. (2102). Toward a mouse model of hind limb ischemia to test therapeutic angiogenesis. *Journal of Vascular Surgery*. 56 (6), p1669-1679.

Brigido S. (2006). The use of an acellular dermal regenerative tissue matrix in the treatment of lower extremity wounds: a prospective 16-week pilot study. *Journal of International Wound Care*. 3 (3), p181-187.

Broughton G, Janis J, Attinger C. (2006). The Basic Science of Wound Healing. *Plastic and Reconstructive Surgery*. 117 (7Suppl), 12S-34S.

Breuing K, Kaplan S, Liu P, Onderdonk A, Eriksson E. (2003). Wound fluid bacterial levels exceed tissue bacterial counts in controlled porcine partial-thickness burn infections. *Plastic and Reconstructive Surgery*. 111 (2), p781-788.

Brown L, Dubin D, Lavigne L, Logan B, Dvorak H, Van de Water L. (1993). Macrophages and fibroblasts express embryonic fibronectins during cutaneous wound healing. *American Journal of-Pathology*. 142 (3), p793-801.

Bryers J. (2008). Medical Biofilms. *Biotechnology and Bioengineering*. 100 (1), p1-18.

Buck M, Houglum K, Chojkier M. (1996). Tumor necrosis factor-alpha inhibits collagen alpha1(I) gene expression and wound healing in a murine model of cachexia. *American Journal of Pathology*. 149 (1), p195-204.

Campos A, Groth A, Branco A. (2008). Assessment and nutritional aspects of wound healing. *Current Opinions in Clinical Nutrition and Metabolic Care.* 11 (3), p281-288.

Capo J, Kokko K, Rizzo M, Adams J, Shamian B, Abernathie B, Melamed E. (2014). The use of skin substitutes in the treatment of the hand and upper extremity. *Hand*. 9 (2), p156-165.

Chadwick S, Heath R, Shah M. (2012). Abnormal pigmentation within cutaneous scars: A complication of wound healing. *Indian Journal of Plastic Surgery*. 45 (2), p403-411.

Chakravarti S, Tam M, Chung A. (1990). The basement membrane glycoprotein entactin promotes cell attachment and binds calcium ions. *The Journal of Biological Chemistry.* 265 (18), p1597-1603.

Chen L, Arbieva Z, Guo S, Marucha P, Mustoe T, and DiPietro L. (2010). Positional differences in the wound transcriptome of skin and oral mucosa. *BMC Genomics*. 11 (1), p471.

Chin K, Anandan S, Koshal K, Gudhajur P. (2013). Current and future developments in the treatment of chronic wounds. *Open Access Surgery*. 6 (1), p43-53.

Christian L, Graham J, Padgett D, Glaser R, Kiecolt-Glaser J. (2006). Stress and wound healing. *Neuroimmunomodulation*. 13 (5), p337-346.

Clark M, Schols J, Benati G, Jackson P, Engfer M, Langer G, Kerry B, Colin D; European Pressure Ulcer Advisory Panel. (2004). Pressure ulcers and nutrition: a new European guideline. *Journal of Wound Care.* 13 (7), p267-272.

Clark R, Lin F, Greiling D, An J, Couchman J. (2004). Fibroblast invasive migration into fibronectin/fibrin gels requires a previously uncharacterized dermatan sulfate-CD44 proteoglycan. *Journal of Investigative Dermatology*. 122 (2), p266-277.

Clark R. (1990). Fibronectin matrix deposition and fibronectin receptor expression in healing and normal skin. *Journal of Investigative Dermatology*. 94 (6 Suppl), 128S-134S.

Compton C, Butler C, Yannas I, Warland G, Orgill D. (1998). Organized skin structure is regenerated in vivo from colla- gen-GAG matrices seeded with autologous keratinocytes. *Journal of Investigative Dermatology*. 110 (6), p908–916.

Converse J, Smahel J, Ballantyne D, Harper A. (1975). Inosculation of vessels of skin graft and host bed: a fortuitous encounter. *British Journal of Plastic Surgery*. 28 (4), p274-282.

Crapo PM, Gilbert TW, Badylak S. (2011). An overview of tissue and whole organ decellularization processes. *Biomaterials.* 32 (12), p3233–3243.

Cuttle L, Kempf M, Phillips G, Mill J, Hayes M, Fraser J, Wang X, Kimble R. (2006). A porcine deep dermal partial thickness burn model with hypertrophic scarring. *Burns*. 32 (7), p806-820.

Dachir S, Cohen M, Kamus-Elimeleh D, Fishbine E, Sahar R, Gez R, Brandeis R, Horwitz V, Kadar T. (2012). Characterization of acute and long-term pathologies of superficial and deep dermal sulfur mustard skin lesions in the hairless guinea pig model. *Wound Repair and Regeneration*. 20 (6), p852-861.

Dai T, Kharkwal G, Tanaka M, Huang Y, Bil de Arce V, Hamblin M. (2011). Animal models of external traumatic wound infections. *Virulence*. 2 (4), p296-315.

Daniel R, Priest D, Wheatley D. (1981). Etiologic factors in pressure sores: an experimental model. *Archives of Physical Medicine and Rehabilitation*. 62 (10), p492-498.

Darby I, Skalli O, Gabbiani G. (1990).Alpha-smooth muscle actin is transiently expressed by myofibroblasts during experimental wound healing. *Laboratory Investigations*. 63(1), p21–29.

Davidson S, Brantley S, Das S. (1991). The effects of ultraviolet radiation on wound healing. *British Journal of Plastic Surgery* . 44 (3), p210-214.

Davidson J. (1998). Animal models for wound repair. *Archives of Dermatological Research*. 290 (1), Suppl:S1-11.

de Almeida T, de Castro Pires T, Monte-Alto-Costa A. (2006). Blockade of glucocorticoid receptors improves cutaneous wound healing in stressed mice. *Experimental Biology and Medicine (Maywood)*. 241 (4), p353-358.

Debeer S, Le Luduec J, Kaiserlian D, Laurent P, Nicolas J, Dubois B, Kanitakis J. (2013). Comparative histology and immunohistochemistry of porcine versus human skin. *European Journal of Dermatol.ogy* 23 (4), p456-466.

Delgado L, Bayon Y, Pandit A, Zeugolis D.. (2015). To cross-link or not to cross-link? Cross-linking associated foreign body response of collagen-based devices. *Tissue Engineering Part B Review*. 21 (3), p298-313.

Demling RH, Desanti L. (1998) Use of Biobrane in the management of scalds. Journal of Burn Care Rehabilitation. 16(3), p329–30.

Demling RH, DeSanti L. Skin, biological properties. 2000. Available at: http://www.burnsurgery.org/Modules/BurnWound%201/sect_I.htm. Accessed June 28, 2019.

Demling RH, DeSanti L. Use of skin substitutes. Available at: http://burnsurgery.org/Modules/BurnWound%201/sect_VIII.htm. Accessed June 28, 2019.

Dieckmann C, Renner R, Milkova L, Simon J. (2010). Regenerative medicine in dermatology: biomaterials, tissue engineering, stem cells, gene transfer and beyond. *Experimental Dermatology*. 19 (8), p697-706.

Dinsdale S. (1974). Decubitus ulcers: role of pressure and friction in causation. *Archives of Phys ical Medicine and Rehabilitation*. 55 (4), p147-152.

Dowsett C, Bielby A, Searle R. (2014). Reconciling increasing wound care demands with available resources. *Journal of Wound Care*. 23 (11), p552-558.

Driskell R, Lichtenberger B, Hoste E, Kretzschmar K, Simons B, Charalambous M, Ferron S, Herault Y, Pavlovic G, Ferguson-Smith A, Watt F. (2013). Distinct fibroblast lineages determine dermal architecture in skin development and repair. *Nature.* 504 (7479), p277-281.

Druecke D, Lamme E, Hermann S, Pieper J, May P, Steinau H, Steinstraesser L. (2004). Modulation of scar tissue formation using different dermal regeneration templates in the treatment of experimental full-thickness wounds. *Wound repair and regeneration*. 12 (5), p518-527.

Dufrane D, van Steenberghe M, Guiot Y, Goebbels R, Saliez A, Gianello P. (2006). Streptozotocin-induced diabetes in large animals (pigs/primates): role of GLUT2 transporter and beta-cell plasticity. *Transplantation*. 81 (1), p36-45.

Dye J, Lawrence L, Linge C, Leach L, Firth J, Clark P. (2004). Distinct patterns of micrrovascular endothelial cell morphology are determined by extracellular matrix composition. *Endothelium.* 11 (3-4), p151-167.

Easterbrook C, Maddern G. (2008). Porcine and bovine surgical products: Jewish, Muslim, and Hindu perspectives. *Archives of Surgery.* 143 (4), p366-270.

Edwards R, Harding K. (2004). Bacteria and wound healing. *Current Opinions in Infectious Diseases*. 17 (2), p91-96.

El-Hamoly T, El-Denshary E, Saad S, El-Ghazaly M. (2015). 3-aminobenzamide, a poly (ADP ribose) polymerase inhibitor, enhances wound healing in whole body gamma irradiated model. *Wound Repair and Regeneration*. 23 (5), p672-684.

Eo H, Lim Y. (2016). Combined Mulberry Leaf and Fruit Extract Improved Early Stage of Cutaneous Wound Healing in High-Fat Diet-Induced Obese Mice. *Journal of Medicinal Food.* 19 (2), p161-169.

Erbatur S, Coban Y, Aydin E. (2012). Comparision of clinical and histopathological results of hyalomatrix usage in adult patients. *International Journal of Burns Trauma*. 2 (2), p118-125.

Esmon C. (2000). The endothelial cell protein C receptor. *Thrombosis and Haemostasis*. 83 (5), p639-643.

Falanga V, Isaacs C, Paquette D, Downing G, Kouttab N, Butmarc J, Badiavas E, Hardin-Young J. (2002). Wounding of bioengineered skin: cellular and molecular aspects after injury. *Journal of Investigative Dermatology*. 119 (3), p653-656.

Ferreira M, Tuma P, Carvalho V, Kamamoto F. (2006). Complex wounds. *Clinics (Sao Paolo)*. 61 (6), p571-578.

Frank S. (2009). The Common Patterns of Nature. *Journal of Evolutionary Biology*. 22 (8), p1563-1585.

Franks P, Morgan P. (2003). Health-related quality of life with chronic leg ulceration. *Expert Review of Pharmacoeconomics and Outcomes Research.* 3 (5), p611-622.

Gaffney P. (1980). Breakdown products of fibrin and fibrinogen: molecular mechanisms and clinical implication. *Journal of Clinical Pathology*. 33 (Suppl 14), p10-17.

Gallant-Behm C, Hildebrand K, Hart D . (2008). The mast cell stabilizer ketotifen prevents development of excessive skin wound contraction and fibrosis in red Duroc pigs. *Wound Repair and Regeneration.* 162 (2), p226-233.

García-Gareta E, Ravindran N, Sharma V, Samizadeh S, Dye J. (2013). A novel multiparameter in vitro model of three-dimensional cell ingress into scaffolds for dermal reconstruction to predict in vivo outcome. *BioResearch (Open Access)*. 2 (6), p412-420.

Ghasemi A, Zahediasl S. (2012). Normality Tests for Statistical Analysis: A Guide for Non-Statisticians. *International Journal of Endocrinology and Metabolism*. 10 (2), p486-489.

Gilliver S, Ashworth J, Ashcroft G. (2007). The hormonal regulation of cutaneous wound healing. *Clinical Dermatology*. 25 (1), p56-62.

Gock H, Murray-Segal L, Salvaris E, Cowan P, D'Apice A. (2004). Allogeneic sensitization is more effective than xenogeneic sensitization in eliciting Gal-mediated skin graft rejection. *Transplantation.* 77(5), p751–753.

Goldberg M, Han Y, Yan C, Shaw M, Garner W. (2007). TNF-α Suppresses α-Smooth Muscle Actin Expression in Human Dermal Fibroblasts: An Implication for Abnormal Wound Healing. *Journal of Investigative Dermatology*. 127 (11), p2645-2655.

Gorodetsky R, Clark R, An J, Gailit J, Levdansky L, Vexler A, Berman E, Marx G. (1999). Fibrin microbeads (FMB) as biodegradable carriers for culturing cells and for accelerating wound healing. *Journal of Investigative Dermatology*. 112 (6), p866-872.

Gosain A, DiPietro L. (2004). Aging and Wound Healing. *World Journal of Surgery*. 28 (3), p321-326.

Gould L, Leong M, Sonstein J, Wilson S. (2005). Optimization and validation of an ischemic wound model. *Wound Repair and Regeneration*. 13 (6), p576-582.

Graham J, Schomacker , Glatter R, Briscoe C, Braue E, Squibb K. (2002). Bioengineering methods employed in the study of wound healing of sulphur mustard burns. *Skin Research and Technol*ogy. 8 (1), p57-69.

Gravvanis A, Lagogiannis G, Delikonstantinou I, Trigkatzi. (2011). The use of Integra™ artificial dermis to minimize donor-site morbidity after suprafascial or subfascial dissection of the radial forearm flap. *Microsurgery*. 31 (6), p502-504.

Greenwood J, Li A, Dearman B, Moore T. (2010). Evaluation of NovoSorb Novel Biodegradable Polymer for the Generation of a Dermal Matrix Part 1: In-vitro Studies. *Wound Practice & Research: Journal of the Australian Wound Management Association*. 18 (1), p14-22.

Grover C, Cameron R, Best S. (2012). Investigating the morphological, mechanical and degradation properties of scaffolds comprising collagen, gelatin and elastin for use in soft tissue engineering. *J journal of the Mechanical Behaviour of Biomedical Materials*. 10 (1), p62-74.

Grüβner A, Nakhleh R , Grüβner A , Tomadze G , Diem P ,Sutherland D. (1993). Streptozotocin-induced diabetes mellitus in pigs. *Hormone and Metabolic Research*. 25 (4), p199-203.

Gu Q, Wang D, Gao Y, Zhou J, Peng R, Cui Y, Xia G, Qing Q, Yang H, Liu J, Zhao M. (2002). Expression of MMP1 in surgical and radiation-impaired wound healing and its effects on the healing process. *Journal of Environmental Pathology Toxicology and Oncology*. 21 (1), p71-78.

Gu J, Iyer V. (2006). PI3K signaling and miRNA expression during the response of quiescent human fibroblasts to distinct proliferative stimuli. *Genome Biology.* 7 (5), R42.

Guerra O, Machin M. (2014). Non-crosslinked porcine-derived acellular dermal matrix for the management of complex ventral abdominal wall hernias: a report of 45 cases. *Hernia*. 18 (1), p71-79.

Guest J, Ayoub N, McIlwraith T, Uchegbu I, Gerrish A, Weidlich D, Vowden K, Vowden P. (2015). Health economic burden that wounds impose on the National Health Service in the UK. *BMJ Open*. 5 (12), e009283.

Guest J, Ayoub N, McIlwraith T, Uchegbu I, Gerrish A, Weidlich D, Vowden K, Vowden P. (2017). Health economic burden that different wound types impose on the UK's National Health Service. *International Wound Journal*. 14 (2), p322-330.

Guo S, Di Pietro L. (2010). Factors Affecting Wound Healing. *Journal of Dental Research*. 89 (3), p219-229.

Guogienė I, Kievišas M, Grigaitė A, Braziulis K, Rimdeika R. (2018). Split-thickness skin grafting: early outcomes of a clinical trial using different graft thickness. *Journal of Wound Care*. 27 (1), p5-13.

Gupta A, Jain G, Raghubir R. (1999). A time course study for the development of an immunocompromised wound model, using hydrocortisone. *Journal of Pharmacological and toxicological methods*. 41 (4), p183-187.

Gurtner G, Werner S, Barrandon Y, Longaker M. (2008). Wound repair and regeneration. *Nature*. 453 (7193), p314-321.

Hadad I, Johnstone B, Brabham J, Blanton M, Rogers P, Fellers C, Solomon J, Merfeld-Clauss S, DesRosiers C, Dynlacht J, Coleman J, March K. (2010). Development of a Porcine Delayed Wound-Healing Model and Its Use in Testing a Novel Cell-Based Therapy. *International Journal of Radiation Oncology, Biology and Physics*. 78 (3), p888-96.

Hadjipanayi E, Kuhn P, Moog P, Bauer A, Kuekrek H, Mirzoyan L, Hummel A, Kirchhoff K, Salgin B, Isenburg S, Dornseifer U, Ninkovic M, Machens H, Schilling A. (2015). The Fibrin Matrix Regulates Angiogenic Responses within the Hemostatic Microenvironment through Biochemical Control. *PLoS One*. 10 (8), e0135618.

Hafner J, Schaad I, Schneider E, Seifert B, Burg G, Cassina P. (2000). Leg ulcers in peripheral arterial disease (arterial leg ulcers): impaired wound healing above the threshold of chronic critical limb ischemia. *Journal of the American Academy of Dermatology*. 43 (6), p1001-8.

Haifei S, Xingang W, Shoucheng W, Zhengwei M, Chuangang Y, Chunmao H. (2015). The effect of collagen-chitosan porous scaffold thickness on dermal regeneration in a one-stage grafting procedure. *Journal of the Mechanical Behaviour of Biomedical Materials*. 29 (1), p114-125.

Halim A, Khoo T, Yussof S. (2010). Biologic and synthetic skin substitutes: An overview. *Indian Journal of Plastic Surgery*. 43 (suppl.), S23-28.

Hall J, Buckley H, Lamb K, Stubbs N, Saramago P, Dumville J, Cullum N. (2014). Point prevalence of complex wounds in a defined United Kingdom population. *Wound Repair and Regeneration.* 2 (6), p694-700.

Han G, Ceilley R. (2017). Chronic Wound Healing: A Review of Current Management and Treatments. *Advanced Therapy*. 34 (3), p599-610.

Hansbrough J, Mozingo D, Kealey G, Davis M, Gidner A, Gentzkow G. (1997). Clinical trials of a biosynthetic temporary skin replacement, Dermagraft-Transitional Covering, compared with cryopreserved human cadaver skin for temporary coverage of excised burn wounds. *Journal of Burn Care and Rehabilitation*. 18 (1), p43-51.

Hansen S, Voigt D, Wiebelhaus P, Paul C. (2001). Using skin replacement products to treat burns and wounds. *Advances in Skin and Wound Care*. 14 (1), p37-44.
Harding K. (2002). Healing chronic wounds. The British Medical Journal. p324, 160.

Hardman M, Ashcroft G. (2008). Estrogen, not intrinsic aging, is the major regulator of delayed human wound healing in the elderly. *Genome Biology*. 9 (5), epub.

Harley B, Kim H, Zaman M, Yannas I, Lauffenburger D, Gibson L. (2008). Microarchitecture of Three-Dimensional Scaffolds Influences Cell Migration Behavior via Junction Interactions. *Biophysical Journal*. 95 (8), p4013-4024.

Harty M, Neff A, King M, Mescher A. (2003). Regeneration or scarring: an immunologic perspective. *Developmental Dynamics*. 226 (2), p268-279.

Harunari N, Zhu K, Armendariz R, Deubner H, Muangman P, Carrougher G, Isik F, Gibran N, Engrav L. (2006). Histology of the thick scar on the female, red Duroc pig: final similarities to human hypertrophic scar. *Burns*. 32 (6), p669-677.

Haslik W, Kamolz L, Nachschlager G, Angel H, Meist G, Frey M. (2007). First experiences with the collagen-elastin matrix Matriderm™ as a dermal substitute in severe burn injuries of the hand. *Burns*. 33 (3), p364-368.

Heinrich W, Lange P, Stirtz T, Iancu C, Heidemann E. (1971). Isolation and characterization of the large cyanogen bromide peptides from the alpha1- and alpha2-chains of pig skin collagen. *FEBS Letters*. 16 (1), p63-67.

Hinz B. (2006). Masters and servants of the force: the role of matrix adhesions in myofibroblast force perception and transmission. *European Journal of Cell Biology*. 85 (3-4), p175-181.

Hirsch T, Spielmann M, Zuhaili B, Koehler T, Fossum M, Steinau H, Yao F, Steinstraesser L, Onderdonk A, Eriksson E. (2008). Enhanced susceptibility to infections in a diabetic wound healing model. *BMC Surgery*. 8 (5), epub.

Ho W. (2002). Skin substitutes: An overview. *Annals of the College of Surgery, Hong Kong*. 6 (1), p106-108.

Hollister S. (2005). Porous scaffold design for tissue engineering. *Nature Materials*. 4 (7), p518-524.

Horch R. E., Kopp J., Kneser U., Beier J., Bach A. D. (2005). Tissue engineering of cultured skin substitutes. *Journal of Cellular and Molecular Medicine.* 9 (3), p592–608

Hopewell J. (1990). The skin: its structure and response to ionizing radiation. *International Journal of Radiation Biololgy*. 57 (4), p751-773.

Huysman E, Mathieu C. (2009). Diabetes and peripheral vascular disease. *Acta Chirurgica Belgica*. 109 (5), p587-594.

Hyodo A, Reger S, Negami S, Kambic H, Reyes E, Browne E. (1995). Evaluation of a pressure sore model using monoplegic pigs. *Plastic and Reconstructive Surgery*. 96 (2), p421-428.

Iozzo R, Schaefer L. (2010). Proteoglycans in health and disease: novel regulatory signaling mechanisms evoked by the small leucine-rich proteoglycans. The FEBS Journal. 277 (19), p3864-3875.

Ito M, Cotsarelis G. (2008). Is the Hair Follicle Necessary for Normal Wound Healing? *Journal of Investigative Dermatology*. 128 (5), p1059-1061.

Jacobi J, Jang J, Sundram U, Dayoub H, Fajardo L, Cooke J. (2002). Nicotine Accelerates Angiogenesis and Wound Healing in Genetically Diabetic Mice. *American Journal of Pathology*. 161 (1), p97-104.

Jansen L, De Caigny P, Guay N, Lineaweaver W, Shokrollahi K. (2013). The evidence base for the acellular dermal matrix AlloDerm: a systematic review. *Annals of Plastic Surgery*. 70 (5), p58-94.

Jaykaran. (2010). How to select appropriate statistical test?. *Journal of Pharmaceutical Negative Results*. 1 (2), p61-63.

Jenkins E, Yip M, Melman L, Frisella M, Matthews B. (2010). Informed consent: cultural and religious issues associated with the use of allogeneic and xenogeneic mesh products. *Journal of the American College of Surgery*. 210 (4), p402-410.

Jost M, Huggett TM, Kari C, Rodeck U. (2001). Matrix-independent survival of human keratinocytes through an EGF receptor/MAPK-kinase-dependent pathway. *Molecular Biology of the Cell.* 12 (5), p1519-1527.

Juhasz I, Kiss B, Lukacs L, Erdei I ,Peter Z, Remenyik E. (2010). Long-Term Followup of Dermal Substitution with Acellular Dermal Implant in Burns and Postburn Scar Corrections. *Dermatology Research and Practice*. (epub) 210150.

Jung Y, Son D, Kwon S, Kim J, Han K. (2013). Experimental pig model of clinically relevant wound healing delay by intrinsic factors. *International Wound Journal*. 10 (3), p295-305.

Kakagia D, Kazakos K, Xarchas K, Karanikas M, Georgiadis G, Tripsiannis G, Manolas C. (2007). Synergistic action of protease-modulating matrix and autologous growth factors in healing of diabetic foot ulcers. A prospective randomized trial. *Journal of Diabetes Complications*. 21 (6), p387-3891.

Kangesu T, Navsaria H, Manek S, Shurey C, Jones C, Fryer P, Leigh I, Green C . (1993). A porcine model using skin graft chambers for studies on cultured keratinocytes. *British Journal of Plastic Surgery* . 46 (3), p393-400.

Karpenko A, Meleca R, Dworkin J, Stachler R. (2003). Cymetra Injection for Unilateral Vocal Fold Paralysis. *Annals of Otology, Rhinology and Laryngology*. 112 (11), p927-934.

Kerrigan C, Zelt R, Thomson J, Diano E. (1986). The pig as an experimental animal in plastic surgery research for the study of skin flaps, myocutaneous flaps and fasciocutaneous flaps. *Laboratory Animal Science*. 36 (4), p408-412.

Khademhosseini A, Langer R. (2007). Microengineered hydrogels for tissue engineering. *Biomaterials*. 28 (34), p5087-5092.

Kim D, Mustoe T, Clark R. (2015). Cutaneous wound healing in aging small mammals: a systematic review. *Wound Repair and Regeneration*. 23 (3), p318-339.

King A. (2012). The use of animal models in diabetes research. *British Journal of Pharmacology*. 166 (3), p877–894.

King R, Tiede C, Simmons K, Fishwick C, Tomlinson D, Ajjan R. (2015). Inhibition of complement C3 and fibrinogen interaction: a potential novel therapeutic target to reduce cardiovascular disease in diabetes.. *Lancet*. 385 (suppl 1), S57.

Kligman L. (1996). The hairless mouse model for photoaging. *Clinical Dermatology*. 14 (2), p183-95.

Kloeters O, Tandara A, Mustoe T. (2007). Hypertrophic scar model in the rabbit ear: a reproducible model for studying scar tissue behavior with new observations on silicone gel sheeting for scar reduction. *Wound Repair and Regeneration*. 15 (Suppl 1), S40-5.

Koenen W, Felcht M, Vockenroth K, Sassmann G, Goerdt S, Faulhaber J. (2010). One−stage reconstruction of deep facial defects with a single layer dermal regeneration template. *Journal of the European Academy of Dermatology and Venereology*. 27 (7), p788-793.

Komarcevic A. (2000). The modern approach to wound treatment. *Medicinski Pregled*. 53 (7), p363-368.

Krassovka J, Borgschulze A, Sahlender B, Lögters T, Windolf J, Grotheer V. (2019). Blue light irradiation and its beneficial effect on Dupuytren's fibroblasts. *Plos One*. 14 (1), e0209833.

Kremer M, Lang E, Berger A. (2000). valuation of dermal-epidermal skin equivalents ('composite-skin') of human keratinocytes in collagen-glycosaminoglycan matrix (Integra™ artificial skin). *British Journal of Plastic Surgery*. 53 (6), p459-455.

Kryger Z, Sisco M, Roy N, Lu L, Rosenberg D, Mustoe T. (2007). Temporal expression of the transforming growth factor-Beta pathway in the rabbit ear model of wound healing and scarring. *J journal of the American College of Surgery.* 205 (1), p78-88.

Kubo M, Van de Water L, Plantefaber L, Mosesson M, Simon M, Tonnesen M, Taichman L, Clark R. (2001). Fibrinogen and fibrin are anti-adhesive for keratinocytes: a mechanism for fibrin eschar slough during wound repair. *Journal of Investigative Dermatology.* 117 (6), p1369-1381.

Kwee B, Mooney D. (2015). Manipulating the intersection of angiogenesis and inflammation. *Annals of Biomedical Engineering*. 43 (3), p628-640.

Kyriakides T, Wulsin D, Skokos E, Fleckman P, Pirrone A, Shipley J, Senior R, Bornstein P. (2009). Mice that lack matrix metalloproteinase-9 display delayed wound healing associated with delayed reepithelization and disordered collagen fibrillogenesis. *Matrix Biology*. 28 (2), p65-73.

Langer A, Rogowski W. (2009). Systematic review of economic evaluations of human cell-derived wound care products for the treatment of venous leg and diabetic foot ulcers. *BMC Health Services Research*. 115 (9), e19591680.

Landsman AS1, Cook J, Cook E, Landsman A, Garrett P, Yoon J, Kirkwood A, Desman E. (2011). A retrospective clinical study of 188 consecutive patients to examine the effectiveness of a biologically active cryopreserved human skin allograft (TheraSkin®) on the treatment of diabetic foot ulcer. *Foot Ankle Spec*. 4 (1), p29-41.

Laurens N, Koolwijk P, de Maat M. (2006). Fibrin structure and wound healing. *Journal of Thromb osis and Haemostasis*. 4 (5), p932-939.

Lawin P, Silverstein P, Still J. (2002). E-Z Derm a porcine heterograft material. *American Journal of Clinical Dermatology*. 3 (7), p507-508.

Lee C, Grodzinsky A, Spector M. (2001). The effects of cross-linking of collagen-glycosaminoglycan scaffolds on compressive stiffness, chondrocyte-mediated contraction, proliferation and biosynthesis. *Biomaterials*. 22 (23), p3145-3154.

Levin F, Turbin R, Langer P. (2011). Acellular Human Dermal Matrix as a Skin Substitute for Reconstruction of Large Periocular Cutaneous Defects. *Ophthalmic Plastic & Reconstructive Surgery*. 27 (1), p44-47.

Li H, Liu J, Xia W. (2001). Establishment and application of experimental animal model for hypertrophic scar. *Zhonghua Zheng Xing Wai Ke Za Zhi*. 17 (5), p276-278.

Li L, Qian Y, Jiang C, Lv Y, Liu W, Zhong L, Cai K, Li S, Yang L. (2012). The use of hyaluronan to regulate protein adsorption and cell infiltration in nanofibrous scaffolds. *Biomaterials*. 23 (12), p3428-3445.

Loh Q, Choong C. (2013). Three-Dimensional Scaffolds for Tissue Engineering Applications: Role of Porosity and Pore Size. *Tissue Engineering Part B Reviews*. 19 (6), p485-502.

Longinotti C. (2014). The use of hyaluronic acid based dressings to treat burns: A review. *Burns Trauma*. 2 (4), p162-168.

Lucas T, Waisman A, Ranjan R, Roes J, Krieg T, Müller W, Roers A, Eming S. (2010). Differential roles of macrophages in diverse phases of skin repair. *Journal of Immunology*. 184 (7), p3964-3977.

Macadam S, Lennox P. (2012). Acellular dermal matrices: Use in reconstructive and aesthetic breast surgery. *Canadian Journal of Plastic Surgery*. 20 (2), p75-89.

MacEwan M, MacEwan S, Kovacs T, Joel Batts J. (2017). What Makes the Optimal Wound Healing Material? A Review of Current Science and Introduction of a Synthetic Nanofabricated Wound Care Scaffold. *Cureus*. 9 (10), e1736.

MacLeod T. M., Sarathchandra P., Williams G., Sanders R., Green C. J. (2004). The diamond CO2 laser as a method of improving the vascularisation of a permanent collagen implant. *Burns*. 30 (7) ,p704–712.

MacLeod T. M., Williams G., Sanders R., Green C. J. (2005). Histological evaluation of Permacol as a subcutaneous implant over a 20-week period in the rat model. *British Journal of Plastic Surgery.* 58 (4), p518–532

MacNeil S. (2007). Progress and opportunities for tissue-engineered skin. *Nature*. 445 (7130), p874-880.

Maeda T, Yamamoto T, Imamura T, Tsuboi R. (2016). Impaired wound healing in bleomycin-induced murine scleroderma: a new model of wound retardation. *Archives of Dermatological Research*. 308 (2), p97-94.

Maklebust J. (1987). Pressure ulcers: etiology and prevention. *Nursing Clinics of North America*. 22 (2), p359-377.

Maldonado A, Cristóbal L, Martín-López J, Mallén M, García-Honduvilla N, Buján J. (2014). A Novel Model of Human Skin Pressure Ulcers in Mice. *Plus One*. 9 (10), e109003.

Mancini R, Quaife. (1962). Histogenesis of experimentally produced keloids. *Journal of Investigative Dermatology*. 38 (1), p143-181.

Marston W, Hanft J, Norwood P, Pollak R. (2003). The efficacy and safety of Dermagraft in improving the healing of chronic diabetic foot ulcers: results of a prospective randomized trial. *Diabetes Care*. 26 (6), p1701-1705.

Martin P. (1997). Wound healing-aiming for perfect skin regeneration. *Science*. 276 (5301), p75-81.

Martin J, Zenilman J, Lazarus G. (2010). Molecular Microbiology: New Dimensions for Cutaneous Biology and Wound Healing. *Journal of Investigative Dermatol.ogy* 130 (1), p38-48.

Matsumoto S. (2010). Islet cell transplantation for Type 1 diabetes. *Journal of Diabetes*. 2 (1), p16-22.

McDaniel J, Browning K. (2014). Smoking, Chronic Wound Healing, and Implications for Evidence-Based Practice. *Journal of the Wound Ostomy and Continence Nurses*. 41 (4), p415-423.

Melendez M, Martinez RR, Dagum A, McClain S, Simon M, Sobanko J, Zimmerman T, Wetterau M, Muller D, Xu X, Singer A, Arora B. (2008). Porcine wound healing in full-thickness skin defects

using Integra™ with and without fibrin glue with keratinocytes. *Canadian Journal of Plastic Surgery*. 16 (3), p147-152.

Mellert J, Hering B, Liu X, Brandhorst D, Brandhorst H, Brendel M, Ernst E, Gramberg D, Bretzel R, Hopt U. (1998). Successful islet auto- and allotransplantation in diabetic pigs. *Transplantation*. 66 (2), p200-204.

Menke N, Ward K, Witten T, Bonchev D, Diegelmann R. (2007). Impaired wound healing. *Clinical Dermatology*. 25 (1), p19-25.

Metcalf D, Bowler P. (2013). Biofilm delays wound healing: A review of the evidence. *Burns Trauma*. 1 (1), p5-12.

Metcalfe A, Ferguson M. (2007). Tissue engineering of replacement skin: the crossroads of biomaterials, wound healing, embryonic development, stem cells and regeneration. *Journal of the Royal Society Interface*. 4 (14), p413–437.

Middelkoop E, van den Bogaerdt A, Lammec E, M.J. Hoekstrab, Brandsmad K, Ulrich A. (2004). Porcine wound models for skin substitution and burn treatment. *Biomaterials*. 25 (9), p1559-1567.

Mitsunaga Junior J, Gragnani A, Ramos M, Ferreira L. (2012). Rat an experimental model for burns: a systematic review. *Acta Cirurgica Brasileira*. 27 (6), p417-423.

Mimura K, Moraes A, Miranda A, Greco R, Ansari T, Sibbons P, Oliani S. (2016). Mechanisms underlying heterologous skin scaffold-mediated tissue remodeling. *Scientific Reports*. 6 (35074)

Min J, Yun I, Lew D, Roh T, W Lee. (2014). The Use of Matriderm™ and Autologous Skin Graft in the Treatment of Full Thickness Skin Defects. *Archive of Plastic Surgery.* 41 (4), p330-336.

Montagna. (1972). The Skin of Non-Human Primates. *The American Zoologist*. 12 (1), p109-124.

Monteiro S, Roque S, de Sá-Calçada D, Sousa N, Correia-Neves M, Cerqueira J. (2015). An efficient chronic unpredictable stress protocol to induce stress-related responses in C57BL/6 mice. *Frontiers in Psychiatry*. 6 (6), epub.

Mordkoff J. (2016). *The Assumption(s) of normality.* Available: http://www2.psychology.uiowa.edu/faculty/mordkoff/GradStats/part%201/I.07%20normal.pdf. Last accessed 19th Nov 2018.

Morel P, Kaufmann D, Matas A, Tzardis P, Field M, Lloveras J, Sutherland D. (1991). Total pancreatectomy in the pig for islet transplantation. Technical alternatives. *Transplantation*. 52 (1), p11-5.

Motley R, Preston P, Lawrence C. (2009). *Multi-progressional guidelines for the management of the patient with primary cutaneous squamous cell carcinoma.* Available: http://www.bad.org.uk/shared/get-file.ashx?id=59&itemtype=document. Last accessed 13th April 2019.

Myers S, Partha V, Soranzo C, Price R, Navsaria H. (2007). Hyalomatrix: a temporary epidermal barrier, hyaluronan delivery, and neodermis induction system for keratinocyte stem cell therapy. *Tissue Engineering*. 13 (1), p2733-2741.

Neumann-Scholz A, Lessee M, Winkler B. (1988). Weiterentwicklung zum Kollagen- Hämostyptikum-Vlies. *Medicamentum Berlin*. 29 (1), p64-65.

Niiyama H, Huang N, Rollins M, Cooke J. (2009). Murine Model of Hindlimb Ischemia. *Journal of Visualized Experiments*. 23, e1036.

Nieswandt B, Varga-Szabo D, Elvers M. (2009). Integrins in platelet activation. *Journal of Thrombosis and Haemostasis*. Suppl (1), p206-209.

Noordenbos J, Doré C, Hansbrough J. (1999). Safety and efficacy of TransCyte for the treatment of partial-thickness burns. *Journal of Burn Care and Rehabilitation.* 20 (4), p275-281.

Norman G. (2010). Likert scales, levels of measurement and the ‘‘laws’’ of statistics. *Advanced Health Science Theory Practicals*. 15 (5), p625-632.

Nunan R, Harding K, Martin P. (2014). Clinical challenges of chronic wounds: searching for an optimal animal model to recapitulate their complexity. *Disease Models and Mechanics.* 7 (11), p1205-1213.

Nuutila K, Siltanen A, Peura M, Bizik J, Kaartinen I, Kuokkanen H, Nieminen T, Harjula A, Aarnio P, Vuola J, Kankuri E. (2012). Human skin transcriptome during superficial cutaneous wound healing. . *Wound Repair and Regeneration*. 20 (6), p830-839.

Ohno S , Hirano S, Tateya I, Kanemaru S, Umeda H, Suehiro A. (2010). Atelocollagen Sponge as a Stem Cell Implantation Scaffold for the Treatment of Scarred Vocal Folds. *Annals of Otology, Rhinology and Laryngology*. 119 (11), p805-810.

Olerud J. (2008). Models for diabetic wound healing and healing into percutaneous devices. *Journal of Biomaterials Science, Polymer Edition*. 19 (8), p1007-1020.

Otene C, Olaitan P, Ogbonaya I, Nnabuko R. (2011). Donor site morbidity following harvest of split thickness skin grafts in South Eastern Nigeria. *Journal of West African College of Surgeons.* 1 (2), p86-96.

Otranto M, Souza-Netto I, Aguila M, Monte-Alto-Costa A. (2009). Male and female rats with severe protein restriction present delayed wound healing. *Applied Physiology Nutrition and Metabolism*. 34 (6), p1023-1031.

Padgett D, Marucha P, Sheridan J. (1998). Restraint stress slows cutaneous wound healing in mice. *Brain Behaviour and Immunity*. 12 (1), p64-73.

Page M,Bester J,Pretorius E. (2018). The inflammatory effects of TNF-α and complement component 3 on coagulation. *Scienctific Reports*. 8 (1), p1812.

Pastar I, Stojadinovic O, Yin N, Ramirez H, Nusbaum A, Sawaya A, Patel S, Laiqua Khalid L, Isseroff R, Tomic-Canic M. (2014). Epithelialization in Wound Healing: A Comprehensive Review. *Adv Wound Care (New Rochelle)*. 3 (7), p445-464.

Peacock E, Madden J, Trier W. (1970). Biologic basis for the treatment of keloids and hypertrophic scars. *Southern Medical Journal*. 63 (7), p755-760.

Peirce S, Skalak T, Rodeheaver G. (2000). Ischemia−reperfusion injury in chronic pressure ulcer formation: A skin model in the rat. *Wound Repair and Regeneration*. 8 (1), p68-76.

Perez R, Davis S. (2008). Relevance of animal models for wound healing. *Wounds*. 20 (1), p3-8.

Philandrianos C,Andrac-Meyer L, Mordon S, Feuerstein J, Sabatier F, Veran J, Magalon G, Casanova D. (2012). Comparison of five dermal substitutes in full-thickness skin wound healing in a porcine model. *Burns*. 38 (6), p820-829.

Posnett J, Franks P. (2008). The burden of chronic wounds in the UK. Nursing Times. 104 (3), p44-45.

Posthauer M. (2012). The role of nutrition in wound care. *Advances in Skin and Wound Care*. 25 (2), p62-63.

Potter M, Linge C, Cussons P, Dye J, Sanders R. (2006). An investigation to optimize angiogenesis within potential dermal replacements. *Plastic and Reconstructive Surgery*. 117 (6), p1876–1885.

Pruitt B, Levine N. (1984). Characteristics and uses of biologic dressings and skin substitutes. *Archives of Surgery.* 119 (3), p312–312.

Pu L, Jackson S, Lachapelle K, Arekat Z, Graham A, Lisbona R, Brassard R, Carpenter S, Symes J. (1994). A persistent hindlimb ischemia model in the rabbit. *Journal of Investigative Surgery*. 7 (1), p49-60.

Qian L, Fourcaudot A, Yamane K, You T, Chan R, Leung KP. (2016). Exacerbated and prolonged inflammation impairs wound healing and increases scarring. *Wound Repair and Regeneration*. 24 (1), p26-34.

Raab G, Klagsbrun M. (1997). Heparin-binding EGF-like growth factor. *Biochimica et Biophisica Acta*. 1333 (3), F179-99.

Raghow R. (1994). The Role of Extracellular-Matrix in Postinflammatory Wound-Healing and Fibrosis. *FASEB J*. 8 (11), p823-831.

Ramos M, Gragnani A, Ferreira L. (2008). Is there an ideal animal model to study hypertrophic scarring? *Journal of Burn Care and Research*. 29 (2), p363-368.

Rittie L, Sachs D, Orringer J, Voorhees J, Fisher G . (2013). Eccrine Sweat Glands are Major Contributors to Reepithelialization of Human Wounds. *The American Journal of Pathology.* 182 (1), p163-171.

Reddy S, El-Haddawi F, Fancourt M, Farrant G, Gilkison W, Henderson N, Kyle S, Mosquera D. (2014). The Incidence and Risk Factors for Lower Limb Skin Graft Failure. *Dermatology Research and Practice*. (2014), epub582080.

Richards A (2002). *Key Notes on Plastic Surgery*. Oxford, UK: Blackwell Science. p27.

Rendell M, Johnson M, Smith D, Finney D, Capp C, Lammers R, Lancaster S. (2002). Skin blood flow response in the rat model of wound healing: expression of vasoactive factors. *The Journal of Surgical Research.* 107 (1), p18-26.

Rivera J, Lozano M, Navarro-Núñez L, Vicente V. (2009). Platelet receptors and signalling in the dynamics of thrombus formation. *Haematologica*. 94 (5), p700-711.

Rheinwald J. G., Green H. (1975) Serial cultivation of strains of human epidermal keratinocytes: the formation of keratinizing colonies from single cells. *Cell* 6 (3), p331–343 .

Richters C, Pirayesh A, Hoeksema H, Kamperdijk E, Kreis R, Dutrieux R, Monstrey S, Hoekstra M. (2008). Development of a dermal matrix from glycerol preserved allogeneic skin. *Cell Tissue Bank*. 9 (4), p309-315.

Rittie L. (2016). Cellular mechanisms of skin repair in humans and other mammals. *Journal of Cell Communication and Signaling*. 10 (2), p103-120.

Rnjak-Kovacina J, Wise S, Li Z, Maitz P, Young C, Wang Y, Weiss A. (2011). Tailoring the porosity and pore size of electrospun synthetic human elastin scaffolds for dermal tissue engineering. *Biomaterials*. 32 (28), p6729-6736.

Roberts A, Heine U, Flanders K, Sporn M. (1990). Transforming growth factor-beta. Major role in regulation of extracellular matrix. *Annals of the New York Academy of Sciences.* 580 (1), 225-32.

Robinet A, Fahem A, Cauchard J, Huet E, Vincent L, Lorimier S, Antonicelli F, Soria C, Crepin M, Hornebeck W, Bellon G. (2005). Elastin-derived peptides enhance angiogenesis by promoting endothelial cell migration and tubulogenesis through upregulation of MT1-MMP. *Journal of Cell Science.* 118 (2), p343-356.

Robinson K. (2003). GLPs and the importance of standard operating procedures. *BioPharm International*. 16 (8), p3-10.

Roy S, Biswas S, Khanna S, Gordillo G, Bergdall V, Green J, Marsh C, Gould L, Sen C. (2009). Characterization of a preclinical model of chronic ischemic wound. *Physiological Genomics*. 37 (3), p211-224.

Rudolph R, Stein R, Pattillo R. (1976). Skin ulcers due to adriamycin. *Cancer*. 38 (3), p1087-1094.

Ruoslahti E. (1996). RGD and other recognition sequences for integrins. *Annual Review Cellular Development Biology*. 12 (1), p697-715.

Ruszczak Z. (2003). Effect of collagen matrices on dermal wound healing. *Advances in Drug Delivery Reviews.* 55 (1), p595–611

Ryssel H, Gazyakan E, Germann G, Ohlbauer M. (2008). The use of Matriderm™ in early excision and simultaneous autologous skin grafting in burns--a pilot study.. *Burns*. 34 (1), p93-97.

Ryssel H, Germann G, Kloeters O, Gazyakan E, Radu C. (2010). Dermal substitution with Matriderm™(®) in burns on the dorsum of the hand. *Burns*. 36 (8), p1248-1253.

Salcido R, Popescu A, Ahn C. (2007). Animal Models in Pressure Ulcer Research. *Journal of Spinal Cord Medicine*. 30 (2), p107-116.

Salem H, Ciba P, Rapoport D, Egana J, Reithmayer K, Kadry M, Machens H, Kruse C. (2009). The influence of pancreas-derived stem cells on scaffold based skin regeneration. *Biomaterials*. 30 (5), p789-796.

Schierle C, De la Garza M, Mustoe T, Galiano R. (2009). Staphylococcal biofilms impair wound healing by delaying reepithelialization in a murine cutaneous wound model. *Wound Repair and Regeneration*. 17 (3), p354-359.

Schilling J. (1976). Wound healing-aiming for perfect skin regeneration. *Surgical Clinics of North America*. 56 (4), p859-874.

Schneider J, Biedermann T, Widmer D, Montano I, Meulia M, Reichmann E, Schiestl C. (2009). Matriderm™ versus Integra™: a comparative experimental study. *Burns*. 35 (1), p51-57.

Seaton M, Hocking A, Gibran N. (2015). Porcine Models of Cutaneous Wound Healing. *ILAR Journal*. 56 (1), p127-138.

Schultz G, Davidson J, Kirsner R, Bornstein P, Herman I. (2011). Dynamic reciprocity in the wound microenvironment. *Wound Repair and Regeneration.* 19 (2), p134-148.

Schurr M,Foster K, Centanni M, Comer A, Wicks A, Gibson A,Thomas-Virnig C, Schlosser S, Lee D. (2009). Phase I/II Clinical Evaluation of StrataGraft: A Consistent, Pathogen-Free Human Skin Substitute. *Journal of Trauma.* 66 (3), p866-874.

Schwentker A, Evans S, Partington M, Johnson B, Koch C, Thom S. (1998). A model of wound healing in chronically radiation-damaged rat skin. *Cancer Letters.* 128 (1), p71-78.

Sen C, Gordillo G, Roy S, Kirsner R, Lambert L, Hunt TK, Gottrup F, Gurtner G, Longaker M. (2009). Human skin wounds: a major and snowballing threat to public health and the economy. *Wound Repair and Regeneration.* 17 (6), p763-771.

Sephel G, Davidson M. (1986). Elastin production in human skin fibroblast cultures and its decline with age. *Journal of Investigative Dermatology*. 86 (3), p279-285.

Seth A, Geringer M, Galiano R, Leung K, Mustoe T, Hong S. (2012). Quantitative comparison and analysis of species-specific wound biofilm virulence using an in vivo, rabbit-ear model. *Journal of the American College of Surgery*. 215 (3), p388-399.

Shahrokhi S, Arno A, Jeschke M. (2014). The use of dermal substitutes in burn surgery: acute phase. *Wound Repair and Regeneration*. 22 (1), p14-22.

Shakespeare P. (2005). The role of skin substitutes in the treatment of burn injuries. *Clinical Dermatology*. 23 (4), p413-418.

Shao H, Yi X, Wells A. (2008). Epidermal growth factor protects fibroblasts from apoptosis via PI3 kinase and Rac signalling pathways. *Wound Repair and Regeneration*. 16 (4), p551-558.

Shevchenko R, James S, James S. (2010). A review of tissue-engineered skin bioconstructs available for skin reconstruction. *Journal of the Royal Society Interface*. 7 (43), p228-258.

Sheu S, Wang W, Fu Y, Lin S, Lei Y, Liao J, Tang N, Kuo T, Yao C. (2014). The pig as an experimental model for mid-dermal burns research. *Burns*. 40 (8), p1679-1688.

Siana J, Rex S, Gottrup F. (1989). The effect of cigarette smoking on wound healing. *Scandinavian Journal of Plastic Reconstructive Surgery and Hand Surgery.* 23 (3), p207-209.

Sibbald B, Roland M. (1998). Understanding controlled trials. Why are randomised controlled trials important?. *BMJ*. 316 (7126), p201.

Simman R, Phavixay L. (2011). Split-Thickness Skin Grafts Remain the Gold Standard for the Closure of Large Acute and Chronic Wounds. *The Journal of the American College of Certified Wound Specialists*. 3 (3), p55-59.

Singer A, Clark R. (1999). Cutaneous wound healing. *New England Journal of Medicine.* 34 (10), p738-746.

Singh N, Armstrong D, Lipsky B. (2005). Preventing foot ulcers in patients with diabetes. *JAMA*. 293 (2), p217-218.

Sisco M, Mustoe T. (2003). Animal models of ischaemic wound healing. Toward an approximation of human chronic cutaneous ulcers in rabbit and rat. *Methods in Molecular Medicine*. 78, p55-65.

Sivak W, Bourne D, Miller M, Manders E. (2016). Simplified Calvarial Reconstruction: Coverage of Bare Skull With GammaGraft Promotes Granulation and Facilitates Skin Grafting. *Journal of Craniofacial Surgery*. 27 (7), p1808-1809.

Sood R, Muffley L, Seaton M, Ga M, Sirimahachaiyakul P, Hocking A, Gibran N. (2015). Dermal Fibroblasts from the Red Duroc Pig Have an Inherently Fibrogenic Phenotype: An In Vitro Model of Fibroproliferative Scarring. *Plastic and Reconsructive Surgery.* 136 (5), p990-1000.

Sorensen J. (2012). Wound healing and infection in surgery: the pathophysiological impact of smoking, smoking cessation, and nicotine replacement therapy: a systematic review. *Annals of Surgery*. 255 (6), p1069-1079.

Soybir O, Gürdal S, Oran E, Tülübaş F, Yüksel M, Akyıldız A, Bilir A, Soybir G. (2012). Delayed cutaneous wound healing in aged rats compared to younger ones. *International Wound Journal*. 9 (5), p478-487.

Spain K. (1915). The relation between the structure of the epidermis of the rat and the guinea pig, and the proliferative power of normal and regenerative of epithelial cels of the same species. *Journal of experimental Medicine*. 21 (3), p193.

Stadler I, Zhang R, Oskoui P, Whittaker M, Lanzafame R. (2004). Development of a simple, noninvasive, clinically relevant model of pressure ulcers in the mouse. *Journal of Investigative Surgery*. 17 (4), p221-227.

Staton C, Brown N, Lewis C. (2003). The role of fibrinogen and related fragments in tumour angiogenesis and metastasis. *Expert Opinions in Biologic Therapies*. 3 (7), p1105-1120.

Steffensen B, Häkkinen L, Larjava H. (2001). Proteolytic events of wound-healing--coordinated interactions among matrix metalloproteinases (MMPs), integrins, and extracellular matrix molecules. *Critical Reviews in Oral Biology and Medicine.* 12 (5), p373-398.

Steed D. (2003). Wound-healing trajectories. *The Surgical Clinics of North America*. 83 (3), p547-555.

Stern R, McPherson M, Longaker M. (1990). Histologic study of artificial skin used in the treatment of full-thickness thermal injury. *Journal of Burn Care and Rehabilitation*. 11 (1), p7-13.

Still J, Glat P, Silverstein P, Griswold J, Mozingo D. (2003). The use of a collagen sponge/living cell composite material to treat donor sites in burn patients. *Burns*. 29 (8), p837-841.

Sullivan T, Eaglstein W, Davis S, Mertz P. (2001). The pig as a model for human wound healing. *Wound Repair and Regeneration*. 9 (2), p66-76.

Suzuki S, Kawai K, Ashoori F, Morimoto N, Nishimura Y, Ikada Y. (2000). Long-term follow-up study of artificial dermis composed of outer silicone layer and inner collagen sponge. *British Journal of Plastic Surgery*. 53 (8), p59-66.

Swaim S, Bradley D, Vaughn D, Powers R, Hoffman C. (1993). The greyhound dog as a model for studying pressure ulcers. *Decubitus*. 6 (2), p32-5, p38-40.

Swift M, Burns A, Gray K, DiPietro L. (2001). Age-related alterations in the inflammatory response to dermal injury. *Journal of Investigative Dermatology*. 117 (5), p1027-1035.

Szkudelski T. (2001). The Mechanism of Alloxan and Streptozotocin Action in B Cells of the Rat Pancreas. *Physiology Research*. 50 (6), p537-546.

Takikawa M, Nakamura S, Nambu M, Sasaki K, Yanagibayashi S, Azuma R, Yamamoto N, Kiyosawa T. (2011). New model of radiation-induced skin ulcer in rats. *Journal of Plastic Surgery and Hand Surgery*. 45 (6), p 258-262.

Tanaka H, Kitoh Y, Kitabayashi N, Matsumura Y, Okayachi H, Nakatsuji Y, Tanaka K, Kubota K, Namba K, Takemura K. (1994). Development of a new delayed healing model of an open skin wound and effects of M-1011G (ointment gauze containing 5% lysozyme hydrochloride) on the model. *Nihon Yakurigaku Zasshi*. 104 (2), p121-131.

Tanihara M, Kajiwara K, Ida K, Suzuki Y, Kamitakahara M, Ogata S. (2008). The biodegradability of poly(Pro-Hyp-Gly) synthetic polypeptide and the promotion of a dermal wound epithelialization using a poly(Pro-Hyp-Gly) sponge. *Journal of Biomedical Material Research*. 85 (1), p133-139.

Telfer N, Colver G, Morton C. (2008). British Association of Dermatologists. Guidelines for the management of basal cell carcinoma. *British Journal of Dermatology*. 159 (1), p35-38.

Tensen C, Flier J, Van Der Raaij-Helmer E, Sampat-Sardjoepersad S, Van Der Schors R, Leurs R, Scheper R, Boorsma D, Willemze R. (1999). Human IP-9: A keratinocyte-derived high affinity CXC-chemokine ligand for the IP-10/Mig receptor (CXCR3). *Journal of Investigative Dermatology.* 112 (5), p716-722.

Theilgaard-Mönch K, Knudsen S, Follin P, Borregaard N. (2004). The transcriptional activation program of human neutrophils in skin lesions supports their important role in wound healing.. *Journal of Immunology*. 172 (12), p7684-7693.

Thomson S, McLennan S, Hennessy A, Boughton P, Bonner J, Zoellner H, Yue D, Twigg S. (2010). A novel primate model of delayed wound healing in diabetes: dysregulation of connective tissue growth factor. *Diabetologia*. 53 (3), p572-583.

Trebaul A, Chan E, Midwood K. (2007). Regulation of fibroblast migration by tenascin-C. *Biochemical Society Transactions*. 35 (4), p695-697.

Tonnesen M, Feng X, Clark R. (2000). Angiogenesis in wound healing. *Journal of Investigative Dermatology.* 5 (1), p40-46.

Troy J, Karlnoski R, Downes K, Brown K,Cruse W, Smith D, Payne W. (2013). The Use of EZ Derm® in Partial-Thickness Burns: An Institutional Review of 157 Patients. *EPlasty*. 13 (1), e14.

Trujillo A, Kesl S, Sherwood J, Wu M,Gould L. (2015). Demonstration of the Rat Ischemic Skin Wound Model. *Journal of Visualized Experiments*. 98 (1), e52637.

Truong A, Kowal-Vern A, Latenser B, Wiley D, Walter R. (2005). Comparison of dermal substitutes in wound healing utilizing a nude mouse model. *Journal of Burns and Wounds (e Plasty)*. 4 (e4), epub.

van der Veen V, van der Wal M, van Leeuwen M, Ulrich M, Middelkoop E. (2010). Biological background of dermal substitutes. *Burns Trauma*. 36 (3), p305-321.

Varga J, Rosenbloom J, Jimenez S. (1987). Transforming growth factor beta (TGF beta) causes a persistent increase in steady-state amounts of type I and type III collagen and fibronectin mRNAs in normal human dermal fibroblasts. *The Biochemical Journal.* 247 (3), p597-604.

Velander P, Theopold C, Hirsch T, Bleiziffer O, Zuhaili B, Fossum M, Hoeller D, Gheerardyn R, Chen M, Visovatti S, Svensson H, Yao F, Eriksson E. (2008). Impaired wound healing in an acute diabetic pig model and the effects of local hyperglycemia. *Wound Repair and Regeneration*. 16 (2), p288-93.

Velander P, Theopold C, Bleiziffer O, Bergmann J, Svensson H, Feng Y, Eriksson E. (2009). Cell suspensions of autologous keratinocytes or autologous fibroblasts accelerate the healing of full thickness skin wounds in a diabetic porcine wound healing model. *Journal of Surgical Research.* 157 (1), p14-20.

Velnar T, Bailey T, Smrkolj V. (2009). The wound healing process: an overview of the cellular and molecular mechanisms. *Journal of International Medical Research*. 37 (5), p1528-1542

Wassermann E, Martijn Van Griensven M, Gstaltner K, Wolfgang Oehlinger W, Schrei K, Redl H . (2009). A chronic pressure ulcer model in the nude mouse. *Wound Repair and Regeneration*. 17 (4), p480-484.

Vitlianova K, Georgieva J, Milanova M, Tzonev S. (2015). Blood pressure control predicts plasma matrix metalloproteinase-9 in diabetes mellitus type II. *Archived of Medical Science*. 11 (1), p85-91.

Volk S, Bohling M. (2013). Comparative wound healing--are the small animal veterinarian's clinical patients an improved translational model for human wound healing research? *Wound Repair and Regeneration*. 21 (3), p372-381.

Wang J, Wan R, Mo Y, Zhang Q, Sherwood L, Chien S. (2010). Creating a long-term diabetic rabbit model. *Experimental Diabetes Research*. 2010 (3), epub289614.

Wei L, Lu Y, He S, Jin X, Zeng L, Zhang S, Chen Y, Tian B, Mai G, Yang G, Zhang J, Wang L, Li H, Markmann J, Cheng J, Deng S. (2011). Induction of diabetes with signs of autoimmunity in primates by the injection of multiple-low-dose streptozotocin. *Biochemical and Biophysical Research Communications*. 412 (2), p373-378.

Werner S, Grose R. (2003). Regulation of wound healing by growth factors and cytokines. *Phsiological Reviews.* 83 (3), p835-870.

Wilson J, Clark J. (2004). Obesity: impediment to postsurgical wound healing. *Advanced Skin Wound Care*. 17 (8), p426-435.

Whitworth K, Lee K, Benne J, Beaton B, Spate L, Murphy S, Samuel M, Mao J, O'Gorman C, Walters E, Murphy C, Driver J, Mileham A, McLaren D, Wells K, Prather R. (2014). Use of the CRISPR/Cas9 System to Produce Genetically Engineered Pigs from In Vitro-Derived Oocytes and Embryos. *Biological Reproduction*. 91 (3), epub.

Woodroof EA. Biobrane: biosynthetic skin prosthesis. In: Wise D, editor. *Burn Wound Coverage*. Boca Raton, Fl: CRC Press; 1984. pp. 1–20.

Woodroof E, Phipps R, Greenwood J, Hickerson W, Herndon D. (2010). The Search for an Ideal Temporary Skin Substitute: AWBAT Plus, a Combination Product Wound Dressing Medical Device. *EPlasty*. 15 (10), e60.

Wynn T. (2008). Cellular and molecular mechanisms of fibrosis. *Journal of Pathology*. 214 (2), p199-210.

Xue M, Jackson C. (2015). Extracellular Matrix Reorganization During Wound Healing and Its Impact on Abnormal Scarring. *Advanced Wound Care (New Rochelle)*. 4 (3), p119-136.

Yan C, Grimm W, Garner W, Qin L, Travis T, Tan N, Han Y. (2010). Epithelial to mesenchymal transition in human skin wound healing is induced by tumor necrosis factor-alpha through bone morphogenic protein-2. *American Journal of Pathology*. 176 (5), p2247-2258.

Yannas I, Burke J, Gordon P, Huang C, Rubenstein R. (1980). Design of an artificial skin. II. Control of chemical composition. *Journal of Biomedical Material Research*. 14 (2) p107–132.

Yannas I, Orgill P, Dennis P, Burke J. (2011). Template for Skin Regeneration. *Plastic and Reconstructive Surgery*. 127 (suppl 1), p60S-70S.

Yannas I, Tzeranis D, So P. (2015). Surface biology of collagen scaffold explains blocking of wound contraction and regeneration of skin and peripheral nerves. *Biomedical Materials.* 11(1), e014106.

Yates C, Bodnar R, Wells A. (2011). Matrix control of scarring. *Cellular and Molecular Life Sciences.* 69 (11), p1871-1881.

Yates C, Whaley D, Wells A. (2012). Transplanted fibroblasts prevents dysfunctional repair in a murine CXCR3-deficient scarring model. *Cell Transplantation*. 21 (5), p919-31.

Zaulyanov L, Kirsner R. (2007). A review of a bi-layered living cell treatment (Apligraf ®) in the treatment of venous leg ulcers and diabetic foot ulcers. *Clinical Interventional Aging.* 2 (1), p93-8.

Zhao J., Hu L., Gong N., Tang Q., Du L. and Chen L. (2015). The effects of macrophage-stimulating protein on the migration, proliferation, and collagen synthesis of skin fibroblasts in vitro and in vivo. *Tissue Engineering.* 21 (5-6), p982-991.

Zhao R, Liang H, Clarke E, Jackson C, Xue M. (2016). Inflammation in Chronic Wounds. *International Journal of Molecular Science*. 17 (12), p2085.

Zhong S, Zhang Y,Lim C. (2010). Tissue scaffolds for skin wound healing and dermal reconstruction. Wiley Interdisciplinary Reviews. *Nanomedicine and Nanobiotechnology.* 2 (5), p510-525.

Zhu K, Engrav L, Tamura R, Cole J, Muangman P, Carrougher G, Gibran N . (2004). Further similarities between cutaneous scarring in the female, red Duroc pig and human hypertrophic scarring . *Burns*. 30 (6), p518-530.